

Development and evaluation of composite insulated beams

Ali Bahadori Jahromi, B.Eng.(Hons), MSc

*A thesis submitted to Napier University in partial fulfilment of the
requirements for the Degree of
DOCTOR OF PHILOSOPHY*

School of the Built Environment
Napier University
Edinburgh, Scotland, UK
(March 2006)

Abstract

Thesis title: Development and evaluation of Composite Insulated Beams

Degree: Doctor of Philosophy (PhD)

Author: Ali Bahadori-Jahromi

Date: March 2006

The worldwide demand for wood has doubled in the last 30 years to approximately 3.5 billion m³ per annum, driven by the increase in world population and improvements in general living standards. Forest product industries previously relied on an inexhaustible supply of high quality log to produce large volumes of fine sawn timber, but now old growth timber is a declining resource. The reduced supply of good quality timber coupled with the increased demand for structural wood products led to the development of Engineered Wood Products (EWP), which include Glued laminated timber (Glulam), Parallel Strand Lumber (PSL), Laminated Strand Lumber (LSL), Laminated Veneer Lumber (LVL), Oriented Strand Board (OSB), Plywood, Structural insulated panels (SIP) and wooden I-beams all used in the construction industry.

This research describes the fabrication and investigation of new engineered wood products called Composite Insulated Beams (CIB). The CIBs were tested to determine their structural performance, long term durability, thermal and dynamic behaviors. CIBs combine the efficiency of sandwich panels with existing engineered wood products to produce new, competitive and cost effective EWP with improved structural value and durability. The CIBs consist of a composite frame with I or rectangular cross-sections. Each frame is constructed by bonding at least two webs to the top and bottom flanges. The interior of a frame could be filled with a material which would enhance thermal properties, structural performance and long term durability of the beam.

Three combinations of materials were used in beam frame construction, timber-flanges with OSB-webs, timber-flanges with plywood-webs, LVL-flanges with plywood-webs. Five different beam designs have been manufactured in each of the three material combinations and all were then tested to determine their engineering properties. The differences among the designs are number of webs, which vary from

two to four, and connection methods between the webs and flanges. Four different connection methods were used including tongue and groove, lamination, recessed and a combination of tongue and groove together with lamination. Moreover, the structural performance of I-beams, Glulam beams and LVL beams was also investigated to provide comparison for CIB performance.

Variations of material properties were viewed as an important factor affecting ultimate bending and shear capacity of a beam even when all beams were made from one grade of timber, so elements of such beams were statistically sorted by their stiffness to create uniform performance. LVL box I-beams and box I-beams can be used instead of solid timber sections or Glulam, because additional webs significantly enhanced the structural performance of CIBs and they maintain the high strength to weight ratio.

A parametric study based on Eurocode 5 was developed to explore effects of variations in beam geometry and materials on permissible spans of CIBs, I-beams and solid timber joists together with their governing design criteria. The study showed that for identical loading conditions CIBs can offer longer spans than I-beams and lower beam depths for similar spans. Results varied with CIB profile.

Experiments also showed that using injected polyurethane as infill not only enhanced the thermal resistance of beams, but also improved their long term durability and bearing capacity. The infill also reduces the weakening effect of a web-opening on shear strength. Investigation of the CIB's dynamic performance showed that using infill improves the damping ratio of the beams. It also demonstrated that there is a direct relation between support stiffness and the natural frequency of CIBs.

Author's declaration

This thesis is submitted to Napier University for the degree of Doctor of Philosophy. No portion of the work referred to in this thesis has been submitted in support of an application for another degree or qualification in this or any other University. I declare that, unless otherwise stated in the text, the contents of this thesis are the results of my own work conducted under the guidance of my supervisors.

Work published and/or presented in advance of the thesis, as well as citations of this work in the technical literature, are listed below.

1. **Bahadori Jahromi , A., Kermani, A., Zhang, B., Harte, A., Walford, B., Bayne, K. and Turner, J.** Influence of geometrical profiles on the structural properties of engineered composite timber beams.
Proceedings of the Institution of Civil Engineers (ICE). Journal of Buildings & Structures. In print 2006
2. **Bahadori Jahromi, A., Zhang, B., Harte, A., Walford, B., Bayne, K. and Turner, J.** Investigating the structural performance of multi-web I-beams.
Journal of the Institute of Wood Science. In print 2006
3. **Bahadori Jahromi, A., Kermani, A., Zhang, B., and Reid, D.** A parametric evaluation of multi-webbed composite joists based on Eurocode 5.
Journal of the Institute of Wood Science. In print 2006
4. **Bahadori Jahromi , A., Kermani, A. and Zhang, B..** Parametric study of multi-webbed composite timber joists, pp.421-429. IN - *Proceedings of the Second PRoBE Conference, Glasgow Caledonian University, Glasgow, 16-17 November 2005.* Glasgow: Glasgow Caledonian University. ISBN 1-903661-82-X
5. **Bahadori Jahromi , A..** Composite insulated beams (CIBs).
Innovation and research focus, (61) May 2005: Available at:
<http://www.innovationandresearchfocus.org.uk>

Acknowledgements

I would like to offer my thanks for the support and guidance provided by my supervisors, Professor Abdy Kermani of Napier University, Edinburgh and Professor Nenad Bicanic, of the University of Glasgow.

I would like to acknowledge the Royal Academy of Engineering for a Global Research Award of £3500 and the Royal Society of Edinburgh for the award of the J.M. Lessells Engineering Travel Scholarship of £7500, which together funded 7 months research work at SCION Research Center in New Zealand from August 2003 to February 2004. I thank all those people involved who gave their valuable time to help me fulfill the objectives of my study and to make the project a great success; Dr Bryan Walford, Mr. John Turner, Mrs. Karen Bayne and Charles McIntosh.

Thanks also to Professor Robin MacKenzie and Dr David Reid for departmental assistance and support on a number of occasions during my study in the School of the Built Environment (SBE) in Napier University. I very much appreciate the help and suggestions given throughout the course of this work by Dr. Ben (Binsheng) Zhang and Dr. Bill McKenzie. Thanks are also due to Ron Hunter, Stephan Paterson, Jack Laidlaw, Alan Barber and Willie Lang for their expedient and proficient technical assistance, and to the University for the use of laboratory facilities.

My deepest gratitude goes to Dr David Cumming for his friendship, encouragement, guidance and support. Without his mentorship, constructive criticism, ongoing feedback and genuine kindness in good and bad times this work would have been unachievable.

Finally I would like to thank my wife, Christina for her support, patience and understanding as well as my parents Rahim and Effat and my sisters Leila and Ladan. Their love and faith in me gave me strength to keep up with the enormous amount of work and inspired me to complete it.

Table of contents

Abstract	i
Author’s declaration	iii
Acknowledgements	iv
Table of contents	v
List of figures	xi
List of tables	xv
List of symbols	xvii
List of Acronyms	xxii
Glossary of terms	xxiv
CHAPTER 1: INTRODUCTION	1
1.1 General	1
1.2 Definition of engineered wood products.....	2
1.2.1 Prospects for engineered wood products.....	2
1.3 General advantages of engineered wood products.....	2
1.4 Overall disadvantage of engineered wood products	3
1.5 The Composite Insulated Beam concept.....	3
1.5.1 Definition of a Composite Insulated Beam (CIB).....	4
1.5.2 Geometrical configuration	4
1.6 Research objectives.....	4
1.7 Outline of the thesis	6
CHAPTER 2: A REVIEW OF LITERATURE ON ENGINEERED WOOD PRODUCTS	10
2.1 Engineered wood products	10
2.2 Types of Engineered wood products.....	10
2.2.1 Timber replacements and sheathing board products.....	10
2.2.2 Combined products	10
2.3 Timber Replacements and sheathing board products.....	11
2.3.1 Timber replacement- structural composite lumber	12
2.3.1.1 Laminated veneer lumber.....	12
2.3.1.1.1 Manufacturing process.....	13
2.3.1.1.2 Advantages of LVL.....	13
2.3.1.1.3 Disadvantages of LVL	14
2.3.1.2 Parallel strand lumber	14
2.3.1.2.1 Manufacturing process	14
2.3.1.2.2 Advantages of PSL.....	15
2.3.1.2.3 Disadvantages of PSL	15
2.3.1.3 Laminated strand lumber.....	15
2.3.1.3.1 LSL manufacturing process	15
2.3.1.3.2 Advantages of LSL	16
2.3.1.3.3 Disadvantages of LSL.....	16
2.3.2 Timber replacement: glued laminated timber	16
2.3.2.1 Manufacturing of Glued Laminated Timber	16
2.3.2.2 Glulam advantages	17
2.3.2.3 Area of concern	18
2.3.2.4 Application.....	18
2.3.3 Sheathing board - Plywood.....	18
2.3.3.1 Manufacturing process	19
2.3.4 Oriented strand board.....	19
2.3.4.1 Manufacturing process	19

2.3.4.2	Difference between OSB and Wafer-Board.....	19
2.3.5	Plywood or OSB or Wafer board.....	20
2.4	Types of combined products.....	20
2.4.1	Combined products: wood-based I-beam.....	21
2.4.1.1	I-beam materials.....	21
2.4.1.2	Manufacturing process.....	21
2.4.1.3	Advantages compared to sawn timber.....	21
2.4.1.4	Disadvantages compared to sawn timber.....	22
2.4.2	Combined products: sandwich insulated panels (SIP).....	22
2.4.2.1	Advantages of sandwich insulated panels (SIP).....	23
2.4.2.2	Area of concern with regard to sandwich insulated panels (SIP).....	23
2.5	Composite Insulated Beam.....	23
2.5.1	Cross section of the composite insulated beam.....	23
2.5.2	Possible CIB advantages.....	24
2.5.3	Potential use.....	25
2.5.4	Design Methods.....	25
2.5.4.1	Web Joint.....	25
2.5.4.2	Veneer direction in plywood web.....	26
2.6	Summary and conclusions.....	27
	CHAPTER 3: MANUFACTURING AND FABRICATION PROCEDURES.....	28
3.1	Introduction.....	28
3.2	Manufacturing the CIBs: stage one.....	28
3.2.1	Manufacturing the compression samples.....	28
3.2.2	Manufacturing the beams for shear tests.....	29
3.2.3	Problems arising during the manufacturing processes.....	29
3.3	Manufacturing the CIBs : stage two.....	30
3.3.1	Fabricating the CIBs.....	32
3.3.2	Selecting and testing the CIB components.....	35
3.3.2.1	Selecting the timber flanges.....	35
3.3.2.2	Matching the timber flanges.....	35
3.3.2.3	Testing and grouping the timber flanges.....	36
3.3.2.4	Selecting the LVL flanges.....	37
3.3.2.5	Testing and preparing the webs.....	39
3.3.2.6	Machining the flanges.....	40
3.3.3	Assembling process.....	42
3.3.3.1	Double I-Beams and LVL Double I-Beam.....	43
3.3.3.2	Box Beam.....	45
3.3.3.3	Boxed I-Beams.....	46
3.3.3.4	Recessed Beams.....	48
3.3.3.5	Boxed double I-beams.....	48
3.3.4	I, Double I, Recess, Box, Box I and Box double I-beam.....	48
3.4	Sorting and numbering the beams after manufacturing.....	49
3.4.1	Sorting and assigning the ID number to the timber flange beams.....	49
3.4.1.2	Assigning the ID number for the beams with LVL flanges.....	54
3.5	MoE variation between the timber and LVL.....	55
3.6	Moisture content of the beams.....	55
3.7	Using the injected polyurethane.....	57
3.7.1	Advantages of injected polyurethane over polystyrene sheets.....	58
3.8	Weighing the beams.....	58
3.9	Measuring the density of the timber and LVL flanges.....	59

3.10 Manufacturing procedure: stage three.....	61
3.10.1 Web and flange materials.....	61
3.10.2 Adhesive.....	61
3.10.3 Testing and grouping the timber flanges according to their stiffness.....	62
3.11 Chapter summary and conclusions.....	65
Chapter 4: Testing procedures	67
4.1 Structural tests of CIBs	68
4.1.1 General features of the beams.....	69
4.1.2 Describing the testing scheme- stage one	69
4.1.3 Testing the short beams.....	70
4.1.1.1 Stiffness tests, three-point-bending.....	72
4.1.1.2 Shear strength and stiffness tests, four-point-bending.....	72
4.1.1.3 Testing the beams that contained web-openings.....	74
4.1.1.4 Compression / Bearing tests.....	77
4.1.1.5 Pull out test.....	78
4.1.1.5.1 Making the pull-out test apparatus.....	79
4.1.1.5.2 Description of the pull-out test.....	80
4.1.2 Testing the long beams	80
4.1.2.1 Long span bending tests-three-point-bending.....	82
4.1.2.2 Determination of shear modulus - method one.....	83
4.1.2.3 Determination of shear modulus - method two.....	85
4.1.2.4 Long span bending tests, four-point-bending.....	86
4.2 Durability/Weathering tests	87
4.2.1 Test specimens	87
4.2.2 Testing equipment.....	87
4.2.2.1 Treatment tank	88
4.2.2.2 Steaming treatment.....	89
4.2.2.3 Kiln drying	90
4.2.2.4 Freezer.....	91
4.2.3 Durability test procedures	92
4.3 Describing the testing schemes, stage two.....	94
4.4 Full scale testing.....	97
4.5 Methods of loading	97
4.6 Summary and conclusion	99
CHAPTER 5: INFLUENCE OF GEOMETRICAL PROFILES ON THE STRUCTURAL PERFORMANCE OF ENGINEERED COMPOSITE TIMBER BEAMS.....	101
5.1 Introduction.....	101
5.2 Background	101
5.3 Manufacture of engineered beams	104
5.3.1 Geometric properties of the beams	104
5.3.2 Material properties	104
5.3.3 Matching components for the beams	107
5.3.4 Plywood webs	107
5.4 Testing procedure.....	108
5.5 Shear stress, shear factor and deflection equations.....	108
5.5.1 Distribution of shear stress.....	110
5.5.2 Shear factor	113
5.5.3 Deformation of the beam	118
5.5.3.1 Derivation of the deflection equation for four point bending	118
5.5.3.2 Derivation of the deflection equation for three point bending.....	121

5.6 Discussion of Results	123
5.6.1 Determination of E and G	123
5.6.2 Failure modes and ultimate strength	128
5.6.3 Prediction of the failure mode	136
5.7 Chapter summary and conclusions	139
CHAPTER 6: INVESTIGATING THE STRUCTURAL PERFORMANCE OF MULTI-WEB I- BEAMS	141
6.1 Introduction	141
6.2. Background	141
6.3. Description of the light composite beams	143
6.4. Testing procedure	143
6.4.1 Effect of the circular web-opening	143
6.4.2 Bearing capacity tests	145
6.4.3 Pulling test	146
6.5 Finite element modelling	148
6.5.1 Anisotropic nature of wood	148
6.5.2 Modelling the bearing and pulling test	150
6.5.2.1 <i>Explaining the assumptions</i>	150
6.5.2.2 <i>Computational modelling</i>	151
6.5.3 Results of the finite element analysis	153
6.6 Buckling of the plywood web	157
6.6.1 Plywood web subjected to compression load	157
6.6.2 Geometric properties	157
6.6.3 Slenderness	158
6.6.4 Compressive instability factors	159
6.6.5 Assessment of the lateral compressive buckling of the plywood web	160
6.7 Discussion of the results	162
6.7.1 Effect of the web opening	162
6.7.2 Bearing capacity of the beams	170
6.7.3 Failure modes	172
6.7.4 Pulling resistance	174
6.8 Summary and conclusions	177
CHAPTER 7: DEVELOPMENT OF THE PARAMETRIC MODEL TO ASSESS THE PERFORMANCE OF THE CIB BASED ON EUROCODES	178
7.1 Introduction	178
7.2 Eurocodes	178
7.2.1 National title page, foreword and Annex	179
7.2.2 Status of Eurocodes in UK	179
7.2.3 EN1995 Eurocode 5: Design of timber structures	179
7.3 Design model based on Eurocode 5	180
7.3.1 Geometric properties	181
7.3.2 Basic variables	182
7.3.3 Characteristic properties	184
7.3.3.1 <i>Characteristic material properties of timber</i>	184
7.3.3.2 <i>Characteristic material properties of OSB</i>	185
7.3.4 Design material properties	186
7.3.4.1 <i>Design material properties of timber</i>	186
7.3.4.2 <i>Design material properties of OSB</i>	187
7.3.5 Characteristic loads and deformations	188
7.3.6 Design loads and stresses	190

7.3.7 Ultimate limit state design (ULS)	193
7.3.8 Serviceability limit state design (SLS).....	198
7.3.8.1 Static deflection (Design deformation)	199
7.3.8.2 Vibration-Option A	201
7.3.8.3 Vibration-Option B	204
7.3.9 Outcome of the design procedures	206
7.4 Maximum permissible span	206
7.5 Reduction of inconvenient floor vibration	209
7.6 Summary and conclusions	211
CHAPTER 8: PARAMETRIC EVALUATION OF MULTI-WEBBED COMPOSITE JOISTS	
BASED ON EUROCODE 5	212
8.1 Introduction	212
8.2. Parametric study	213
8.2.1 Ultimate limit states design (ULS).....	214
8.2.2 Serviceability limit state design (SLS).....	215
8.2.4 Assumptions	216
8.2.5 Characteristic values of the material properties	216
8.3 Lateral buckling factor	216
8.4. Discussion of the results	217
8.4.1 Controlling criteria under the ULS conditions.....	230
8.4.2 Critical criteria under the SLS conditions.....	231
8.4.3 Comparison of options A and B regarding the permissible span.....	231
8.4.4. Influence of material variation	242
8.4.5. Effect of geometric variation	242
8.4.6. Lateral stability and geometric configurations.....	244
8.5 Beam depth	246
8.6 Summary and conclusions	248
CHAPTER 9: PERFORMANCE OF BEAMS WITH INFILL OF POLYURETHANE	
(COMPOSITE INSULATED BEAMS, CIB).....	250
9.1 Introduction	250
9.2 Effect of the infill on structural performance.....	251
9.2.1 Bearing capacity and infill materials.....	251
9.2.2 Infill material and stiffness	253
9.2.3 Effect of a web opening in beams with and without infill	255
9.3 Durability	262
9.3.1 Durability testing procedures	262
9.3.2 Discussion of durability results.....	263
9.3.2.1 <i>Explanation of different durability performance</i>	268
9.3.2.2 <i>Explanation of reduction in ultimate load capacity</i>	268
9.4 Thermal performance CIBs.....	272
9.4.1 Thermal transmittance.....	272
9.4.2 Effect of the foam on thermal properties	276
9.5 Composite insulated beams with OSB webs	277
9.6 Dynamic performance of the beam	284
9.6.1 Experimental bending vibration of a beam	284
9.6.2 Theoretical bending vibration of the beam	289
9.6.2.1 <i>Natural frequency</i>	289
9.6.2.2 <i>Damping factor, force and ratio</i>	293
9.7 Chapter summary and conclusions.....	294
CHAPTER 10 CONCLUSIONS AND RECOMMENDATIONS	298

10.1 Introduction	298
10.2 Engineered wood products	298
10.3 Fabrication process	298
10.4 Testing procedures	299
10.5 Geometrical variability and structural performance	300
10.6 Investigating the structural performance of multi-webbed I-beams	300
10.7 Analytical model to assess the beams based on EC5	301
10.8 Parametric evaluation of CIBs, I-beams and solid timber joists	302
10.9 Effect of infill on performance of CIBs	303
10.9.1 Structural performance of the plywood webbed beams	303
10.9.2 Durability of the plywood webbed beams	304
10.9.3 Thermal performance of plywood webbed beams	305
10.9.4 Structural performance of OSB webbed beams	305
10.9.5 Dynamic performance of the OSB webbed beams	305
10.10 Potential applications of findings:	306
10.10 Recommendations for future research	307
10.10.1 Effects of long term loading	307
10.10.2 Flooring system studies	307
10.10.3 Evaluation of the fire resistance of CIBs	307
10.10.4 Environmental issues regarding CIBs	308
REFERENCES	309
APPENDICES	I
Appendix A: Material properties of CIB beams	II
Appendix B: Effect of the foam on CIB beams	XLI

List of figures

Figure 1.1 Various CIB configuration	4
Figure 2.1 Wood fibre used more efficiently when is converted to the engineered wood product.....	12
Figure 2.2 LVL manufacturing process	13
Figure 2.3 Tapered glue laminated timber	17
Figure 2.4 Cross-sectional profiles of test beams	24
Figure 2.5 Connecting the webs - tongue and groove method.....	26
Figure 3.1 Shows variation of initial CIB designs	29
Figure 3.2 Composite insulated beam profiles.....	31
Figure 3.3 Different web-flange connections.....	32
Figure 3.4 Planer-moulder machine.....	34
Figure 3.5 Double ended tenon-maker, machining the plywood webs.....	34
Figure 3.6 Colour-coded flanges after machining, ready for assembly	37
Figure 3.7 Testing material properties of the 3ply-plywood.....	40
Figure 3.8 Machining different flange profiles	41
Figure 3.9 Fabricating the Double I-beam	43
Figure 3.10 Pneumatic press clamp (Taylor clamp)	44
Figure 3.11 Clamping system used for long I-beams and Double I-beams.....	45
Figure 3.12.Laminated press for short Boxed profiles.....	46
Figure 3.13 Modified Glulam press had been used for fabrication of the Boxed beams	46
Figure 3.14 Distribution of MoE among different CIB profiles after final matching	52
Figure 3.15 Distribution of the moisture content for top and bottom timber flanges	56
Figure 3.16 Distribution of the moisture content for top and bottom LVL flanges...	57
Figure 3.17 Average weight per meter length for the profiles without infill.....	59
Figure 3.18 Average weight per meter length for the profiles with infill.....	59
Figure 3.19 Density of the timber flanges before and after oven drying	60
Figure 3.20. The correlation between modulus of elasticity and density	61
Figure 3.21 Distribution of MoE for C16 and C24 timber	62
Figure 3.22 Using roller press to assemble the Double and I-beam	64
Figure 4.1 Testing procedures for evaluating the short span beams (2100 mm).....	71
Figure 4.2 Non destructive testing procedure for short beams under three point bending.....	73
Figure 4.3 Test arrangement for measuring load-deflection and shear strength under four-point-bending	74
Figure 4.4 Test arrangement of the CIBs with a web opening	76
Figure 4.5 Test apparatus for compression test.....	78
Figure 4.6 Test rig for pulling test	80
Figure 4.7 Shows the testing program which was developed to assess the long beams *M.L-D: Measuring load-deflection	81
Figure 4.8 (a) Test arrangement to measure the load-deflection of the beam subjected to three-point-bending.....	82
Figure 4.8 (b) Three points load test rig to measure load-deflection of filled boxed I-Beam over a 4.5m span	82
Figure 4.9 Test arrangement and measurement of MoE in bending.....	83
Figure 4.10(A) Test method to determine the apparent MoE over 1450mm span	84
Figure 4.10(B) LVL section subjected to three-point-bending over a 1450mm span	85
Figure 4.11 Test methods to measure E_{app} over 1.45, 2.10, 3.00 and 4.00 m spans ..	86

Figure 4.12 Test method to measure load-deflection relative to supports	87
Figure 4.13 Treatment tank used for durability test.....	89
Figure 4.14 Exposing the beams to steam and at 100 °C.....	90
Figure 4.15 Durability tests- Box beams inside the kiln.....	91
Figure 4.16 Kiln temperatures during the six cycles.....	91
Figure 4.17 Test rig for long span beams undergoing four-point-bending.....	96
Figure 4.18 Test method for long span beams – Three-point-bending test	97
Figure 5.1. Cross-sectional profiles of test beams	103
Figure 5.2 Test arrangement for short span beams	109
Figure 5.3 Test arrangement for long span beams	109
Figure 5.4 Typical beams tested over 2.1m and 4.35m span	110
Figure 5.5 calculation of shear stress as a function of y for the flange and webs....	112
Figure 5.6 Distribution of shear stress in flange and web areas of a double I-beam	112
Figure 5.7 Actual loading (P) and dummy loading (R) on four point simply supported beam	119
Figure 5.8 Actual loading (P) on three point simply supported beam	122
Figure 5.9 Modulus of elasticity vs span for three-point bending	124
Figure 5.10 E and G values for different combinations	127
Figure 5.11 Failure modes for various beams under four-point bending over 2.1 m span	129
Figure 5.12 Load-deflection relationships for short beams of varied profiles under four-point bending.....	130
Figure 5.12 (Continued) Load-deflection relationships for short beams of varied profiles under four-point bending	131
Figure 5.13 Load-deflection curves for long span beams of varied profiles under four-point bending.....	132
Figure 5.13 (Continued) Load-deflection curves for long span beams of varied profiles under four-point bending.	133
Figure 6.1 Cross section of the beams, made with timber/ LVL flanges and plywood webs	142
Figure 6.2. Test arrangement for measuring maximum loading capacity of the beams	144
Figure 6.3 Four points bending tests, boxed I-Beam and double I-beam with web opening	145
Figure 6.4. Test arrangement for measuring maximum bearing capacity of the beams	145
Figure 6.5. Failure of the double I-beam (top) and recessed beam (bottom) under compression load.....	146
Figure 6.6 Testing apparatus for tension pulling test.....	148
Figure 6.7 Grain angle θ and Ring angle ϕ	151
Figure 6.8 Timber is cut from different areas of the log.....	151
Figure 6.9 Distribution of the maximum principal stress on timber flange under compression	154
Figure 6.9 Distribution of the maximum principal stress on timber flange under compression (Cont.)	155
Figure 6.9 Distribution of the maximum principal stress on timber flange under compression (Cont.)	156
Figure 6.10 Plywood web under compression load	157
Figure 6.11 Load deflection graphs for different circular web openings.....	164

Figure 6.11 Load deflection graphs for different circular web openings.....	165
Figure 6.12 Beams with circular web opening before and after failure.....	166
Figure 6.12 Beams with circular web opening before and after failure (Cont.)	167
Figure 6.13 Buckling load limit corresponding to plywood web height	174
Figure 7.1 Cross section of the model design, double I-beam.....	181
Figure 7.2 Double I-beam cross section modeled by LUSAS software to obtain the torsional constant, I_{tor}	184
Figure 7.3 Components of the deflection (Reproduced from Eurocode 5).....	199
Figure 7.4 Procedure for identifying the maximum permissible span of the profile.....	207
Figure 8.1 Engineered joists used in flooring systems: (a) I-beam, (b) Double I-beam, (c) Box beam, (d) Box I-beam.	214
Figure 8.2 Permissible spans for engineered joists with C16 flanges and Plywood webs, based on different design criteria	220
Figure 8.3 Permissible spans for engineered joists with C24 flanges and Plywood webs, based on different design criteria	222
Figure 8.4 Permissible spans for engineered joists with C16 flanges and OSB webs, based on different design criteria	224
Figure 8.5 Permissible spans for engineered joists with C24 flanges and OSB webs, based on different design criteria	226
Figure 8.6 Permissible spans for solid timber joists based on different design criteria	229
Figure 8.7 Permissible span and lateral buckling factor for engineered joists with C16 timber flanges.....	245
Figure 8.8 - Permissible span and lateral buckling factor for C16 solid timber joists	245
Figure 9.1 Traditional box and I-beams.....	252
Figure 9.2 Filled box I-beam before and after compression test.....	253
Figure 9.3 Test arrangement for measuring maximum loading capacity of the beams	255
Figure 9.4 Mode of failure in the double I-beam with various sizes of web opening	260
Figure 9.5 Modelling the beam	260
Figure 9.6 Maximum principal stresses in an empty double I-beam with 152mm web opening.....	261
Figure 9.7 Measuring load deflection and shear capacity of short beam under four point bending.....	264
Figure 9.8 Comparing the load deflection of the box beams without and with foam at the end of different cycles	266
Figure 9.9 Box beam failed under four point bending test after exposure to 6 cycles of accelerated weathering conditions.	270
Figure 9.10 Box beam with infill is failed under four point bending after exposure to 6 accelerated weathering cycles	271
Figure 9.11 Thermal transmittance of box I-beam without insulation.....	274
Figure 9.12 Thermal transmittance of box I-beam with insulation.....	275
Figure 9.13(A) Comparison between the CIB made of C16 timber flanges without and with infill	279
Figure 9.13(B) Comparison between the CIB made with C24 timber flanges without and with infill	280
Figure 9.14 Test arrangement and failure mode	282
Figure 9.15 Failure in an I-beam.....	282

Figure 9.16 Evaluating natural frequency and damping ratio of a beam.....	285
Figure 9.17 Demonstration of dynamic characteristic for the Double I-beam 825 without infill.....	286

List of tables

Table 3.1 Statistical method for sorting and numbering the beams.....	51
Table 3.2 Comparing the MoE of the LVL and NZ timber	55
Table 3.3 Distribution of the moisture content after assembling the beam	56
Table 3.4. Foam density in different profiles.....	59
Table 3.5 Density of the timber and LVL flanges before and after oven drying.....	60
Table 3.6. Comparing the MoE of the C16 and C24 timber.....	63
Table 4.1 Time table and sequence of Cycles 1 to 6	93
Table 5.1. Summary of material properties	106
Table 5.2. Testing combinations for calculating E and G.....	125
Table 5.3. Shear factor, sectional area and second moment of area of the beams.....	126
Table 5.4. Comparison of elastic modulus for the timber flanges and the fabricated beams	128
Table 5.5 Mechanical properties of short span beams.....	134
Table 5.6. Mechanical properties of long span beams.....	135
Table 6.1 Elastic parameters and Poisson ratio for Sitka Spruce at 12% moisture content.....	152
Table 6.2 Mechanical properties of the beam components for FE analysis	152
Table 6.3 Bending test results for beams with web openings.....	163
Table 6.4 Effect of a circular web opening in load/deflection of short span beams..	169
Table 6.5 Average bearing capacity and flange tensile and shear stresses per unit load	171
Table 6.6 Buckling limit load and corresponding tensile and shear ratios	173
Table 6.7 Maximum pulling resistance and flange and web stresses	176
Table 7.1 Serviceability limit state criteria	198
Table 7.2 - Permissible span for Double I-beam of 300mm depth with OSB web and C16 timber flange	208
Table 7.3 Comparison between the vibration criteria of C16 and C24 Double I-beams	209
Table 7.4 Effect of m and n_{40} on value of v and v_d	210
Table 8.1 Permissible spans of box I-beams with C16 timber flanges and plywood webs	218
Table 8.2 Permissible spans of C16 solid timber joists	228
Table 8.3 Design permissible spans for different profiles	233
Table 8.4 Enhancement of permissible span due to material variations.....	243
Table 8.5 Enhancement of permissible span due to geometric variations.....	243
Table 9.1 - Average maximum bearing capacity of the different designs with and without infill material.	252
Table 9.2 Effect of infill on load deflection of the long span beams with LVL flanges	254
Table 9.3 Result of destructive tests for beams of 4.35m span.....	255
Table 9.4 Effect of infill on performance of beams with various sizes of web opening	257
Table.9.5 Effect of the accelerated ageing method on structural performance of the box beams	264
Table.9.5 Effect of the accelerated ageing method on structural performance of the box beams	265
Table 9.6 Average results for the beams without and with infill.....	267
Table 9.7 Moisture content of the box beam before and after testing	269

Table 9.8 Average moisture content and percentage difference before and after the durability tests.....	270
Table 9.9 The U value of the beam cross-section without and with foam.....	276
Table 9.10 Limiting U-value standards (W/m ² K).....	276
Table 9.11 Average results of structural tests over a 4.35m span.....	278
Table 9.12 Effect of the foam on stiffness of the beam.....	283
Table 9.13 Natural frequency and damping ratio of the beams without and with infill	287
Table 9.14 Average dynamic characteristic of the beam without and with infill	288
Table 9.15 Lowest five frequency factors, $\lambda_i L$ for a single span beam	290
Table 9.16 Effect of the support condition on dynamic characteristics of I-beams ..	292

List of symbols

Roman characters

A	Cross-section area (m^2 or mm^2)
<i>a</i>	Deflection of the timber floor under unit point load (mm/kN)
a	Distance between the supports and the load head (mm or m)
<i>a_d</i>	Deflection of the timber floor under unit point load (mm/kN)
A_{Flange}	Cross area of the timber flanges, (mm^2)
A_{osb}	Cross-section area of the OSB webs (mm^2)
A_s	Projected area of the test specimen (m^2)
A_{timber}	Area of the flange (mm^2)
b	Breadth of the flange (mm)
B	Floor breadth (mm)
B_{c/t,f}	Axial compression and tension in the timber flanges due to bending
b_w	Breadth of the webs (mm)
b_{wEqu}	Equivalent breadth of the web (mm)
C	A damping factor
C_⊥	Compression perpendicular to the timber grain (bearing)
C_∥	Compression parallel to the OSB/Plywood panel length
C_{b,f}	Compression in the extreme fibres of the timber flanges due to bending
C_{b,w}	Compression in the extreme fibres of the OSB/ Plywood web due to bending
C_C	Critical damping factor
D	Density of specimen which is obtained from experimental work (kg/m^3)
E	Young modulus of a beam (N/m^2) or (N/mm^2)
E_{0,mean,P5}	Mean characteristic elastic modulus of P5 particleboard, (N/mm^2)
E_{0,mean,timber}	Mean characteristic elastic modulus of timber, parallel to the grain, (N/mm^2)
E_{0.05}	5 percentile characteristic value of modulus of elasticity (N/mm^2)
E_{0.95}	95 percentile characteristic value of modulus of elasticity (N/mm^2)
EI_{joist}	Flexural rigidity of the floor joist about an axis perpendicular to the beam direction (y-axis in this case) in N mm^2

E_L, E_T, E_R	Young's moduli in L, T and R directions
ν_{ij}	Poisson's ratio for transverse strain in the j-direction
$E_{m,0,mean,OSB}$	Mean characteristic elastic modulus of OSB web (N/mm ²)
E_{mean}	Mean characteristic value of modulus of elasticity (N/mm ²)
$E_{Plywood}$	Young's modulus of the plywood (N/mm ²)
E_{Timber}	Young's modulus of the timber (N/mm ²)
f	Natural frequency (Hz)
$f_{c,0,k}$	Characteristic compressive strength, parallel to the grain (N/mm ²)
$f_{c,90,k}$	Characteristic compressive strength, perpendicular to the grain (N/mm ²)
f_{mk}	Characteristic bending strength (N/mm ²)
$f_{t,0,k}$	Characteristic tensile strength, parallel to the grain (N/mm ²)
$f_{t,90,k}$	Characteristic tensile strength, perpendicular to the grain (N/mm ²)
G	Shear modulus (N/mm ²)
G_k	Characteristic value of linearly distributed permanent action of the floor (kN/m)
g_k	Total permanent action (kN/m ²)
g_{k1}	Permanent action (kN/ m ²)
g_{mjoist}	Permanent action of Double I-beam (kN/m ²)
G_{RT}, G_{LT}, G_{LR}	Shear moduli in the R-T, L-T and L-R planes
H0, H76, H102, H152	Hole or opening diameter and the following number indicates the diameter of the circular opening (mm)
h	Depth of the joist (mm)
$h_{f,c}$ or $h_{f,t}$	Compressive or tensile flange depth (mm)
h_w	Clear distance between flanges (mm)
I	Second moment of area about the strong axis (m ⁴ or mm ⁴)
I_{tor}	Torsional constant (mm ⁴)
$K_{3PF,4350}$	Load /deflection result under 3 point bending test for the beam with infill over 4350mm span
$K_{3PF,4350}/K_{3P,4350}$	Ratio of the load deflection filled/empty under 3 point bending
$K_{3PNF,4350}$	Load /deflection result under 3 point bending test for the beam without infill over 4350mm span

K_{4PF,4350}	Load /deflection result under 4 point bending test for the beam with infill over 4350mm span
K_{4PF,4350}/K_{4P,4350}	Ratio of the load deflection filled/empty under 4 point bending
K_{4PNF,4350}	Load /deflection result under 4 point bending test for the beam without infill over 4350mm span
k_c	Thermal conductivity of the specimen (W/m K°)
k_{C0}, k_{C2}, k_{C4} and k_{C6}	Load over deflection value tested under four-point arrangement at the end of cycles 0, 2, 4 and 6
k_h	Depth factor for rectangular solid timber section with characteristic density of $\rho_k < 700 \text{ kg/m}^3$
k_{mod}	Modification factor for duration of load and moisture content
K_{NF, H 76}/K_{NF,H 0}, K_{NF, H 102}/K_{NF,H 0} and K_{NF, H 152}/K_{NF,H 0}	Load deflection ratio
K_{NF,4500} K_{NF,3000} K_{NF,2100} K_{NF,1450}	Load over deflection value for the beam without foam with a span of 4500, 3000, 2100 and 1450mm tested under three point bending arrangement (kN/mm)
K_{NF,H 0}	Load/deflection value before creating a web opening
K_{NF,H 76}, K_{NF,H 102}, K_{NF,H 152}	Value of the load/deflection after creating web openings of 76, 102 and 152 mm diameter
l	Bearing length l (mm)
L	Floor or beam span, L (mm) or (m)
LS_b	Lateral stability when subjected to bending
M	Moisture content (%)
m_{imposed}	Weight per area for floor (kg/m ²)
m_{joist}	Weight per area for Double I-beam (kg/m ²)
n	Young's modulus ratio of OSB to timber $n = E_{m,0,mean,OSB} / E_{0,mean,timber}$
P_{max}	Maximum loading capacity (kN) or (N)
P-Δ	Curve for the three-point bending N/mm or kN/mm
Q_{Flange}	First moment of the area for flange (mm ³ or m ³)
Q_k	Characteristic value of linearly distributed variable action of the floor (kN/m)
q_k	Variable action (kN/m ²)
Q_s	Heat flow through the test specimen (Watts)

Q_{web}	First moment of the area for web (mm^3 or m^3)
r	Radius of gyration of section (mm)
R_t	Thermal resistance of specimen (m^2K/W)
s	Spacing of the joists (mm)
S_p	Panel shear in the OSB/Plywood web
S_R	Planar (rolling) shear in the OSB/Plywood web
t	Thickness of P5 particleboard (mm)
$T_{b,f}$	Tension in the extreme fibres of the timber flanges due to bending
$T_{b,w}$	Tension in the extreme fibres of the OSB/Plywood web due to bending
t_C	Cold side air temperature (K°)
t_H	Warm side air temperature Kelvin (K°)
U_F	Thermal transmittance of the beam with foam ($W/m^2 k^\circ$)
U_{NF}	Thermal transmittance of the beam without foam ($W/m^2 k^\circ$)
U_s :	Thermal transmittance ($W/m^2 k^\circ$)
v_d	Design limit for unit impulse velocity ($m/Nsec^2$)
v	Unit impulse velocity response in ($m/Nsec^2$)
W/m	Weight per meter length (kg/m)
w_c	Pre-camber (mm)
w_{creep}	Creep deflection (mm)
$W_{Double\ I-beam}$	Weight per meter length for Double I-beam (kg/m)
w_{fin}	Final deflection (mm)
$w_{g,k,max}$	Maximum characteristic deflection (mm)
w_{inst}	Instantaneous deflection (mm)
$w_{net,fin}$	Net final deflection (mm)
$w_{q,k,max}$	Maximum characteristic deflection due to the variable load (mm)

Greek characters

α or φ	Shear factors
ζ	Damping ratio which is the ratio between the damping factor, C , and critical damping, C_C
ρ	Density of the beam (kg/m^3)
λ	Factor depending on support condition

ω	Natural frequency (rad/s)
Δ	Total deflection of the beam (mm)
Δ_1	Deflection of the beam as a result of the bending moment (mm)
γ_m	Partial factor for material properties for ultimate limit states
Δh_w	Glued embedded length of the web into the flanges (mm)
Δ_{max}	Deflection at maximum load (mm)
σ	Bending, compression or tensile stress (N/mm ²)
τ	Shear stress (N/mm ²)
Δ_2	Deflection of the beam caused by the shear force (mm)
ρ_{OSB}	Density of the OSB (kg/m ³)
ρ_{timber}	Density of the timber flange (kg/m ³)

List of Acronyms

APA	The Engineered Wood Association
ASTM	American Society for Testing and Materials
BS	British Standards
BS EN	British Standard European Standard (Europäische Norm)
CEN	European Committee for Standardisation
CIB	Composite insulated beam
EC0	Eurocode Basis of structural design
EC1	Eurocode Actions on structures
EC5	Eurocode 5 design of timber structures
EFDD	Enhanced frequency domain decomposition
EOTA	European Organisation for Technical Approvals
EWP	Engineered wood products
FDD	Frequency domain decomposition
FRP	Fibre reinforced polymers
Glulam	Glued laminated lumber
HS	Hole size
LSL	Laminated strand lumber
LVL	Laminated veneer lumber
M.L-D	Measuring load-deflection
MDF	Medium density fibreboard
MoE	Modulus of elasticity
NF	No foam or without infill material (empty)
NSBs	National standards bodies
OSB	Oriented strand board
PSL	Parallel strand lumber
PVA	Glue polyvinyl acetates
SCL	Structural composite lumber
SIP	Structural insulated panels
SLS	Serviceability limit state design
SSI	Stochastic subspace identification,
StDev	Standard deviation
TJM	Trus Joist MacMillan

TRADA	Timber Research and Development Association
ULS	Ultimate limit state design
UNECE	United Nations Economic Commission for Europe

Glossary of terms

Box Double I-beams comprise a double I-beam with two additional webs which are laminated to both sides to create the box cross section.

Box I-beams are composite beams with a box shaped cross-section where top and bottom flanges are connected via three webs with middle web grooved and side webs laminated to the flanges.

Double I-beams are composite beam with an I shaped cross section where top and bottom flanges are connected via two webs grooved into the flanges.

LVL box double I-beams are box double I-beams fabricated with LVL flanges.

LVL box I-beams are box I-beams fabricated with LVL flanges.

LVL Double I-beams are double I-beams fabricated with LVL flanges.

Recessed beams are composite beams with a box cross-section where top and bottom flanges are connected via two webs which is recessed within the flanges.

SCION is a Crown Research Institute in New Zealand with a shared vision of developing sustainable biomaterials for future generations. Formerly known as Forest Research, Scion is focused on applying a deep knowledge of plantation forestry, wood and fibre to the development of new biomaterials from renewable plant resources.

CHAPTER 1: INTRODUCTION

1.1 General

Not many materials used in our daily life are sustainable products. Wood is one of the few sustainable materials, because it can be re-grown after being harvested under careful forestry management.

Timber is the only construction material to have a positive effect on the environment, because of the trees' ability to absorb carbon dioxide and release oxygen (Canadian wood council, 2000). The research conducted by ATHENA Sustainable Materials Institute on behalf of the Canadian wood council to assess the environmental effects of using wood, sheet metal and concrete for residential construction shows wood has the least detrimental impact (APA Engineered Wood Handbook 2002).

Timber frame construction is a very attractive solution as it meets market demands for improved efficiency, better cost control, faster construction, better quality and performance, together with minimising environmental damage (Grantham ,Enjily, 2003).

The efficiency of timber and timber products is recognised more than at any other time; this is reflected by relaxation of the building regulations for combustible construction. In England and Wales timber frames can now rise up to 7 floors (TRADA 2001). The Building Research Establishment recently accomplished full scale tests on a multi-storey, six floor, timber frame construction. The project provides technical research data in response to increasing market demand for timber frame buildings (Grantham, Enjily 2003).

However solid timber is limited structurally by the number of naturally occurring defects including knots, slope of grain, compression wood, and shake (Mckenzie 2000, Kermani 1999). In addition, wood properties in timber are not distributed evenly (Steffen et al 1997, Dahlbom et al 2000 and Bengtsson 2000). One ideal solution to overcome these problems is to develop secondary products from timber in which defects are either eliminated or dispersed randomly and which in addition

possess more consistent properties compared to timber. In consequence, one of the five major research areas which are suggested by WoodWisdom-Net is focused on Third Generation engineered wood products (WoodWisdom-Net 2005).

1.2 Definition of engineered wood products

What are engineered wood products?

Engineered wood products by definition consist of large group of wood products which are either made by bonding the chips, flakes, strands and veneer together, or fabricated by combining two or more woods and wood products to form the new product. These products in general have better material properties and structural performance compares to the original sawn timber. In other words any wood product which obtains some of its structural properties from more than natural wood fibre or sawn timber is an engineered wood product. Adhesives or fasteners or a combination of both are common features of engineered wood products. *“Structural engineered wood products are “engineered” by virtue of possessing structural properties that are confirmed by methods other than simple visual grading” (Hiles 2002).*

1.2.1 Prospects for engineered wood products

The United Nations Economic Commission for Europe (UNECE, 2003) in its comprehensive report suggests that engineered wood products continue to innovate in their design and applications. Furthermore engineered wood products are considered as part of the solution to the “Sound use of wood” policy. This report mentions that EWPs have a bright future and it has provided the wood industry with a much-needed boost.

Demands for engineered wood products are predicted to grow to twenty times in the next decade, meanwhile manufacturers in Europe and America regularly report a 100% sales increase in a year (Leicester 2000).

1.3 General advantages of engineered wood products

Engineered wood products (EWPs) significantly increase sawmill detritus recovery by using the resources more efficiently and also provide high quality products for end-users. A main advantage of EWPs is that they are more stable and offer greater structural strength, dimensional stability and long term performance than conventional

wood products. Further more EWPs are more uniform and consistent than solid sawn timber. This is mainly achieved by dispersing or eliminating the natural defects which are inherent within the timber. For instance strength variability of structural composite lumber (SCL) is 10% while this for mechanically stress graded timber is 20 % and it reaches to 35% for visually graded timber (Lam and Prion 2003). In contrast, engineered wood products have predictable performance and they are gaining popularity with both architects and design engineers. In addition EWPs are considered more environmentally friendly than the conventional wood products. (UNECE, 2003).

1.4 Overall disadvantage of engineered wood products

Engineered wood products in general are more expensive than solid sawn timber, they may cost up to two-three times that of the equivalent timber (Advanced Building, 2002).

Engineered wood products, excluding span rated plywood and oriented strand board (OSB), are proprietary and not necessarily compatible (Smulski 1997). Currently most manufacturers provide their own designing tables.

1.5 The Composite Insulated Beam concept

The study of behaviour of sandwich panels, together with studies of the advantages and limitations of engineered wood and wood products, led to development of a new type of engineered wood product. This new concept, termed a Composite Insulated Beam (CIB) (Kermani and Bahadori-Jahromi, 2003), was developed during the course of this research at Napier University. The award of an international travel scholarship from Royal Society of Edinburgh and a Global Research Award from the Royal Academy of Engineering facilitated a seven months comprehensive experimental project involving fabricating and testing of 200 CIBs at the New Zealand, SCION Research Centre. In July 2004, the Napier University CIB Concept Team was awarded a £200,000 Scottish Enterprise grant toward further research on structural, fire and acoustic performance of CIBs as well as exploring the possibility of using home grown timber (Sitka Spruce) for CIB construction (Scottish Enterprise 2004).

1.5.1 Definition of a Composite Insulated Beam (CIB)

The current design of CIB has a rectangular, or I-shaped, profile. These profiles consist of at least two webs which can be made with OSB or plywood and at least two flanges which are glued or mechanically connected to the webs. Flanges can be made out of solid timber or laminated veneer lumber (LVL). The beam-frame creates a volume, which can be filled with Polystyrene sheet or injected Polyurethane to improve insulation property.

1.5.2 Geometrical configuration

Typical examples of CIB configurations are shown in figure 1.1. The current research considered the use of oriented strand board (OSB) or plywood as a web materials and timber or LVL as flange material. Polystyrene sheets or injected polyurethane was studied as infill material. However other combinations may be considered in future. SYLVIC R15 which is a Resorcinol formaldehyde resin with liquid hardener SYLVIC L5 was used for bonding the wood based components.

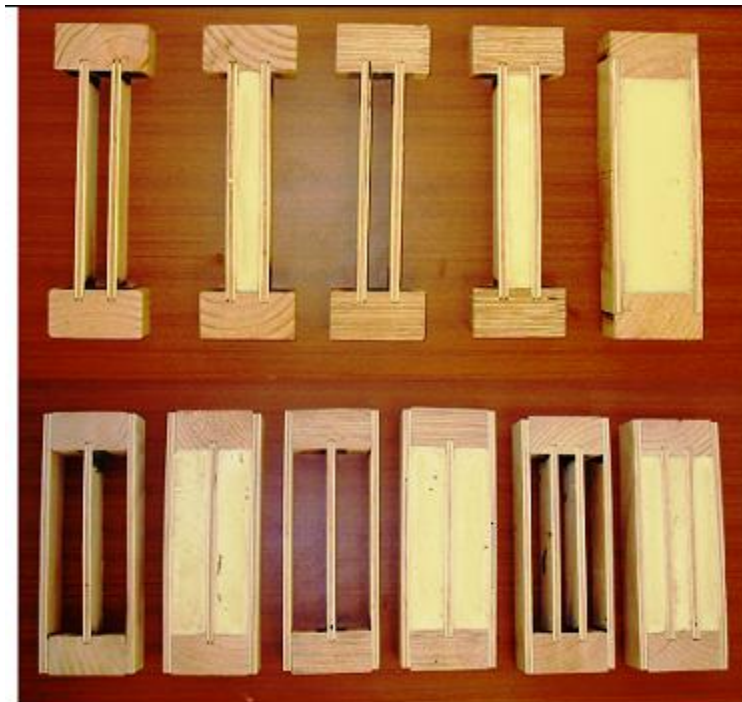


Figure 1.1 Various CIB configuration

1.6 Research objectives

The primary goal of this research is to evaluate the performance of newly designed composite insulated beams.

The research report concentrates initially on the design and manufacture of the various CIB profiles. This is followed by descriptions of comprehensive experimental tests carried out on full scale beams.

Key objectives considered vital for the successful completion of this research are summarised as follows:

1. Reviewing the existing engineered wood products in the market in terms of manufacturing and performance
2. Developing, designing and manufacturing the new engineered wood products (CIB) with various profiles
3. Investigating the structural performance of the manufactured beams by subjecting them to a series of non-destructive and destructive tests in order to:
 - Examine the influence of various web flange connection mechanisms and web numbers on the structural performance of the CIBs
 - Determine the effects of two different types of filling material on structural behaviour of CIBs with different cross-sections
 - Examine the effect of two different webs and two flange materials on structural performance of the beams
 - Investigate effects of a circular service hole placed on the webs in causing reduction of stiffness and strength of the beams with and without infill materials
4. Perform comparative structural testing to evaluate the existing engineered wood products against CIBs
5. Evaluate long term durability of the beams which could demonstrate viability of the design components
6. Assess the vibrational performance of the CIB beams
7. Analyse and discuss the experimental data

8. Develop a parametric based model for analysis and simulation of the structural behaviour of the flooring system which is designed with different CIB beams
9. Compare and evaluate performance of CIBs against that of plywood or OSB webs
10. Evaluate the viability and performance of CIB beams for use in a variety of structural situations

1.7 Outline of the thesis

The following sections summarise the structure of the thesis from chapter two onwards based on the aforementioned objectives.

Chapter 2: A review of literature on engineered wood products

This chapter presents a review of the existing engineered wood products in the market and explains the fabrication method, application, advantages and disadvantages of each product. This leads to descriptions of Composite Insulated Beams, their potential applications, and their possible advantages.

Chapter 3 : Manufacturing and fabrication process

This chapter describes the manufacture of CIB beams and addresses several issues related to manufacturing. CIB beams for this study were manufactured in three stages. Phase one briefly describes the initial experimental work undertaken in Napier University and then follows the practical work in New Zealand, Scion Research Centre (NZ Scion) while the last stage describes experiments at Napier University. In phase one CIBs were fabricated by creating SIP Panels with polystyrene cores and using OSB faces as web elements together with timber as flange material.

Phase two, manufacturing in NZ Scion, describes fabricating various profiles of CIBs with and without infill material. Plywood was used as webs and solid timber and Laminated Veneer Lumber (LVL) were used as flanges, while injected polyurethane was used as infill material. Overall 200 full-scale beams were fabricated.

Phase three, explains the fabricating process conducted at Napier University as part of the on going Proof of Concept research. In this stage timber graded C16 and C24 was used as flange material while OSB/3 was employed for the webs.

Chapter 4 : Testing procedure

This chapter describe the structural testing procedure which is carried on CIB beams, I-Beam, Glulam and LVL beams. This is followed by describing the durability testing procedure. Series of non-destructive and destructive tests were also conducted to evaluate the structural properties of the Beams, while durability tests revealed the structural performance of the beams before and after exposure to extreme weather conditions.

Chapter 5 : Influence of the geometrical profiles on the structural properties of composite timber beams

Experiments are described, which were designed to test the strength and deformation characteristics of lightweight timber composite beams manufactured with six different cross-sectional profiles. There are also comparisons with readily available laminated veneer lumber (LVL) and glued-laminated (Glulam) beams. A study was conducted to provide a comparison of the beam designs and to determine possible effects of cross-sectional configuration and connection details on the structural properties of the beams. Also described is the model which was used to achieve an even distribution of material properties in each different profile.

The most efficient profile in terms of structural performance and ease of manufacturing procedures was identified. The influence of shear deflection on the total deflection of the I-beams, Box beams, Double I-beam, Box I-beam and on solid sections of LVL and Glulam beams is discussed.

Chapter 6 : The structural performance of multi-webs-I-beams

This chapter presents accounts of extensive laboratory testing carried out to determine the effect of circular web-openings on the load/deflection and the shear capacity of different profiles. This is followed by determination of the maximum bearing capacity of each design. A new testing method developed to evaluate the tension resistance of the flange/web connection in single and Double I-beams is fully described.

The effect of increasing the diameter of the web-opening was investigated to ascertain whether it reduced maximum loading capacity and stiffness of beams with different cross-sections. The study also shows the effect of additional webs on structural performance of the I-beam in term of shear, bearing and pulling capacity. Furthermore

the direct relation of tension stress perpendicular to the grain direction of the flange with pulling resistance is demonstrated.

Chapter 7 : Development of a parametric model based on Eurocodes to assess the performance of CIBs

This study starts with a descriptive discussion on Eurocodes, as all the designs and calculations are based on Eurocodes. This is followed by a description of the analytical model which was developed to assess CIBs used in flooring systems. The permissible span of the double I beam was evaluated by applying this model. Moreover, it is explained that this model can be used to predict the permissible span of any CIB profile. The described model was used in the parametric study conducted in chapter eight. This study also provides a straight forward solution to avoid excessive vibration in designing light timber flooring systems.

Chapter 8: A parametric evaluation of multi-webbed composite joists based on Eurocode 5

An original parametric model for CIB flooring systems was developed based on that described in chapter seven. The new parametric model meets the requirements of Eurocode 5 and its UK National Annex. Vibration criteria in the design codes may significantly reduce the permissible span of the joists for domestic construction. This author investigated the influence of vibration criteria in designing a CIB timber flooring system and compared its behaviour to that of a traditional timber floor. This study also demonstrates effects of geometrical and material properties on enhancement of permissible CIB spans. Furthermore, the influence of lateral support on the vibration characteristics of each profile was evaluated and discussed. The aim of the study was to predict the permissible span of different profiles with fixed beam depth; however, the results can also be used to assess effects of geometrical and material variability on reduction of beam depth necessary for a fixed span.

Chapter 9: Effect of the infill on performance of CIB beams

The author investigated effects of injected rigid polyurethane foam on the structural performance, long term durability and thermal properties of CIBs made from plywood webs and timber or LVL flanges. The work was extended to evaluate the structural

performance and dynamic behaviour of CIBs made from OSB webs and C16 or C24 timber flanges. Structural performance of the empty and filled beams was examined with regard to bending, shear and bearing capacities. Accelerated ageing methods were also employed to study the long-term durability of CIBs. Thermal properties were evaluated by simulating the empty and filled beams which were exposed to outdoor conditions from one side and indoor conditions from the other. Experimental methods along with a computational package were used to examine the dynamic behaviour of CIBs and to analyse the results.

Outcome of this study revealed the effect of the foam on the structural and dynamic performance of CIBs. Satisfactory alternative web materials were identified for use in CIB manufacture.

Chapter 10 : Conclusions and recommendation for future research

This Chapter draws together the conclusions of the preceding chapters and provides a summary of conclusions from the whole research process. This is followed by suggestions for the logical continuation and development of the work described in this thesis.

CHAPTER 2: A REVIEW OF LITERATURE ON ENGINEERED WOOD PRODUCTS

This chapter introduces the various engineered wood products (EWP), along with their applications, advantages and disadvantages. Thereafter is an introduction to a new type of EWP which is identified as a composite insulated beam (CIB).

2.1 Engineered wood products

Engineered wood products are developed in response to the concern over forest depletion and harvesting restrictions on old-grown timber in addition to the increasing demand for higher quality timber products. The idea is to create higher performance products and or add value to the existing materials available to be utilised. For instance small-diameter trees or low-grade trees could be used as a raw material for EWP.

2.2 Types of Engineered wood products

All the engineered wood products follow one fundamental concept which is maximizing the strength and stiffness and minimizing the waste by bonding the wood base material together, or bonding it with other materials.

The engineered wood products could be classified in two major groups:

- Timber replacements and sheathing board products
- Combined products

2.2.1 Timber replacements and sheathing board products

This group mainly utilize the raw material to create new products by bonding the timber or wood elements like veneers, chips, flaks and strands to manufacture products like laminated veneer lumber, parallel strand lumber, laminated strand lumber and oriented strand board.

2.2.2 Combined products

The second group of EWP are created by using the first group of EWP in novel structural designs. This is achieved by combining EWP with each other or some times

with other materials and adopting them into the innovative design. I-beam and structural insulated panel (SIP) can be mentioned as good examples of this group. I-Beam is a combination of solid wood or LVL flanges with OSB or plywood webs assembled in “I” profile; whereas structural insulated panel is a sandwich panel which is constructed by bonding the Polystyrene foam core between two layers of OSB or plywood board. This adoption of wood products provides the foundation for market growth (Fell 2002) .

The first group generally requires high capital investment, whereas the second group requires medium or low capital investment. However, both groups are designed to use more of the available wood resources and decrease waste by providing new products based on previously unutilised scraps of the original timber.

2.3 Timber Replacements and sheathing board products

In this section variety of timber replacements and sheathing products are introduced and the manufacturing process, advantages and disadvantages of each are reviewed. However out of five different sheathing products only two, plywood and OSB, are discussed, since those two products have been used mainly for structural purposes.

Timber Replacements

- **Structural composite lumber (SCL)**
 1. Laminated veneer lumber (LVL)
 2. Parallel strand lumber (PSL)
 3. Laminated strand lumber (LSL)
- **Glue laminated timber**

Sheathing boards

4. Plywood
5. Cellulosic fibreboard (MDF)
6. Hardboard
7. Particleboard
8. Oriented strand board (OSB)

2.3.1 Timber replacement- structural composite lumber

Structural composite lumber (SCL) is a general term which is given currently to three types of engineered wood products: laminated veneer lumber (LVL), parallel strand lumber (PSL) and laminated strand lumber (LSL). These products are manufactured out of veneer or strand or small wood elements bonded together with structural adhesive. Wood grain in these products is aligned along the length to optimise its structural performance.

These products are an alternative to solid sawn timber and could be used as a support beam, header, joist or as columns.

These products offer better utilization of the wood fibre in comparison to sawn timber (Figure 2.1).

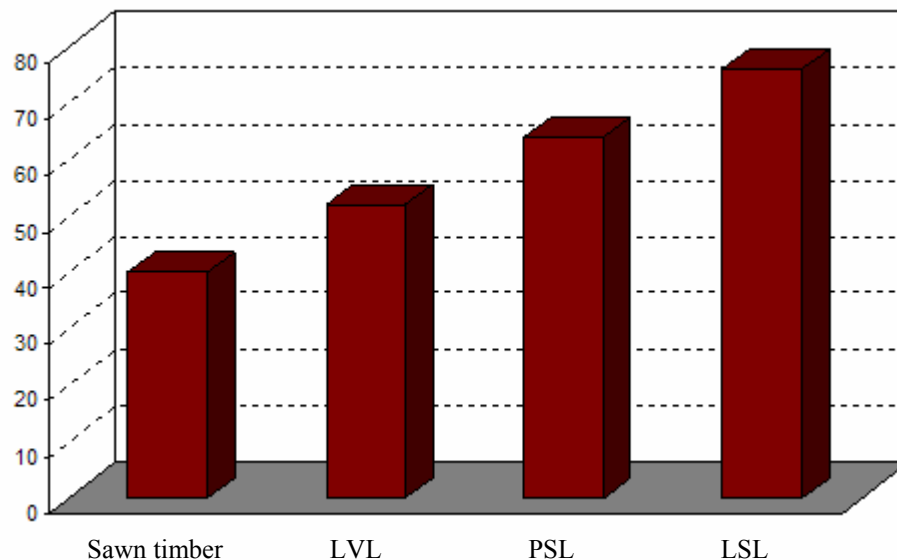


Figure 2.1 Wood fibre used more efficiently when is converted to the engineered wood product (Reproduced from Nelson 1997)

2.3.1.1 Laminated veneer lumber

Laminated veneer lumber (LVL) was the first SCL product which was commercially produced in the early 1960s; however, prior to that time LVL had been produced during the second world war in Europe and United States for making aeroplane propellers (Forest products laboratory, 1987).

2.3.1.1.1 Manufacturing process

LVL is currently manufactured in Finland, New Zealand and the USA. In general, the process is started by debarking the logs and then soaking them in the hot water for 24 hours. This is followed by peeling the log to veneers typically 3 to 4mm thick. Veneers are dried and graded according to their stiffness and strength while passing through an Ultrasonic-Veneer-Tester* machine. Veneers are coated by structural adhesive and piled so that low grade veneer is placed in the centre while high grade veneers are positioned on top and bottom. Then the veneers enter a hot press where they are shaped into a solid panel (Figure 2.2).

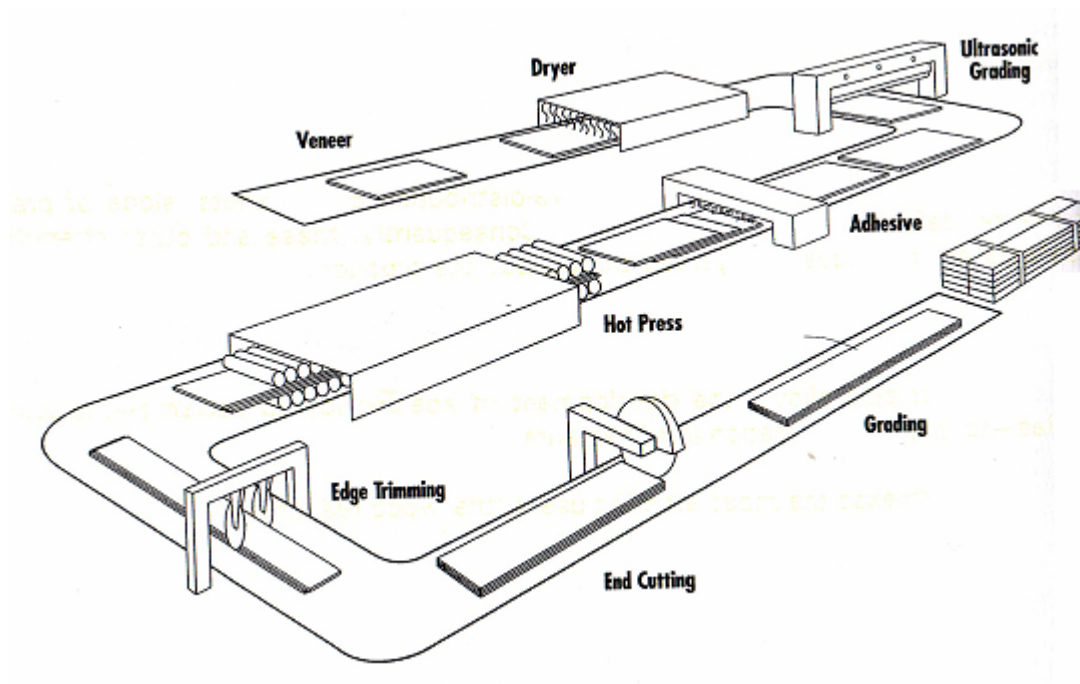


Figure 2.2 LVL manufacturing process

(Figure obtained from Nelson 1997)

An *ultrasonic veneer tester determines the physical properties of dry veneer sheets by repetitively measuring ultrasonic stress wave propagation time as the veneer under test moves through the machine at production line speeds.

2.3.1.1.2 Advantages of LVL

Predictability of performance, large range of available sizes, dimensional consistency, dimensional stability and easy treatability are the main advantages of LVL over timber logs. Moreover, the use of veneers in LVL fabrication redistributes and

overcomes the natural timber defects like knots, slope of grain which often occur in logs.

The coefficient of variation in strength and stiffness for LVL only varies from 10 to 15 while it reaches 25 to 40 for solid sawn timber.

2.3.1.1.3 Disadvantages of LVL

There is a limitation on the size of log that could be used for the peeling process and some wood species are unsuitable for peeling. Compared to PSL and LSL, the pressing procedure does not improve the strength and stiffness significantly by increasing the density of the veneers. Finally, laminated veneer lumber is susceptible to copping across the width if stored improperly.

2.3.1.2 Parallel strand lumber

The EWP known as parallel strand lumber or PSL is the result of years of research (1971-1987) by Derek Barnes, Mark Churchland and Walter Schilling in MacMillan Bloedel Ltd. of Vancouver, Canada. After MacMillan Bloedel's and Trus Joist formed a joint venture in 1991, the technology transferred to Trus Joist MacMillan (TJM) for its management. At present PSL is produced at plants in Vancouver, British Columbia, Canada; Colbert, Georgia and Buchanan, West Virginia in the United States.

2.3.1.2.1 Manufacturing process

This process is similar to that for LVL: logs are rotary peeled into veneer sheets with 2 to 3mm thickness. The veneers are then chipped to thin strands, which have lengths up to 2400 mm and are approximately 18 mm wide. Strands are coated with structural glue and pass through a continuous rotary belt press to build a mat of highly consistent density. An adhesive is cured by microwaves. Using this method it is possible to manufacture larger cross-sections than for LVL.

Veneers for PSL are mainly obtained from sapwood, which has higher strength compare to heartwood. Currently Douglas-fir, Western hemlock, Southern Pine and Yellow-Poplar have been used as raw materials for PSL.

2.3.1.2.2 Advantages of PSL

Parallel strand lumber has all the advantages of LVL, however unlike LVL it is not possible to assemble the strand's base on their strength and stiffness. As an alternative PSL strength is enhanced by raising the level of density of the strands.

Acceptance of preservative and fire retardant in PSL is even better than LVL. In addition the percentage of fibre utilization in PSL is higher than in LVL and this could be enhanced by running the PSL and LVL plants at one site.

2.3.1.2.3 Disadvantages of PSL

The disadvantages are similar to those of LVL. PSL products are limited to peelable logs. In comparison to solid sawn lumber and glued laminated timber, PSL products are heavier and harsher to saws and drills. Furthermore connection must be made with metal plates and bolts instead of nails.

Parallel strand lumber, like LVL, is considered as high capital technology; and it requires a stable production process.

2.3.1.3 Laminated strand lumber

Laminated strand lumber (LSL) is the newest engineered wood product which is commercially produced. The product was developed by Trus Joist MacMillan in the USA during the early 1990s (ECO link 2001) .

To some extent, there is similarity between LSL and OSB technology; the main difference is length of the strand in LSL, which reaches 30 cm. This greater length is the principal reason for LSL's flexural strength.

2.3.1.3.1 LSL manufacturing process

Logs of Aspen and Poplar are cut into strands up to 30 cm long and 3 cm wide. Dried strands are oriented parallel to the panel length during mat formation, which takes better advantage of the wood's natural strength. Strands are monitored and undesirable strands are separated in advance and used as fuel for the manufacturing process. The rest of the strands enter a revolving drum where adhesive is sprayed on them. A polymeric diphenylmethane diisocyanate has been used as bonding for the

strands. Adhesive curing occurs while the panel passes through a stationary steam injection press. Panels are manufactured in 2.4×10.7-14.7 m sizes with 25 to 100 mm thickness.

2.3.1.3.2 Advantages of LSL

LSL enjoys all the advantages of LVL and PSL, but unlike them, LSL is not limited by availability of peel-able logs and by log size; raw material for LSL could be obtained from various species, from small logs and from crooked logs. Some 76% of the wood fibre is used, which is nearly double the amount utilised in solid sawn timber.

Strategic layering procedure and increasing density of strands enhances the strength and limits copping potential.

2.31.3.3 Disadvantages of LSL

The dimensional stability of LSL is not as good as LVL and PSL. The higher density of the LSL wood fibre in comparison to LVL and PSL make it more susceptible to swelling with changes in moisture content and so LSL can not be used where moisture content exceeds 19% RH (Product approval.1996). Moreover, laminated strand lumber like LVL and PSL requires high capital investment.

2.3.2 Timber replacement: glued laminated timber

Modern Glulam was introduced to market around 100 years ago. Kari Fridrich Otto Hetzer, a German carpenter, invented and presented his technical breakthrough, Glulam with a 43 m span, in 1910 at the world exposition in Brussels (SNCCBLC 2004).

2.3.2.1 Manufacturing of Glued Laminated Timber

Glued laminated timber (Glulam) is one of the oldest engineered wood products that is used in a variety of structural and architectural applications. It is manufactured by bonding suitably selected and prepared timber elements to form a straight or curved member. The grain of a timber element is aligned along its length. Timber elements could be assembled so that high grade members were positioned on the top and

bottom which are exposed to maximum compression and tension stress in bending, whereas lower grade members fill the core area (BS EN 386-2001) .

Lengths of the Glulam can be manufactured, which are longer than the timber elements that are commercially available. Longer elements of Glulam are produced by using a finger jointing technique. BS 5291:1984 provides specific details on manufacturing the finger joint.

Phenol-Resorcinol-Formaldehyde is the most widely used adhesive for Glulam and further information on its use is provided in BS EN 301, 1992.

Glulam could have two different assembly methods, horizontal and vertical, but generally it is installed so that applied load is perpendicular to the wider face. If the Glulam is placed in position so that applied load is parallel to the wide face it is considered as a vertically laminated assembly.

2.3.2.2 Glulam advantages

Glulam could easily be manufactured in curved shapes which are generally expensive in other materials. It can also be fabricated in a wide range of sizes and shapes. For example, it is possible to obtain a 30 meter span with straight Glulam and up to 150 meter spans in Glulam arches (Yeh 2002). Glulam could even be created in a tapered configuration. Figure 2.3 shows four different configurations for tapered Glulam.

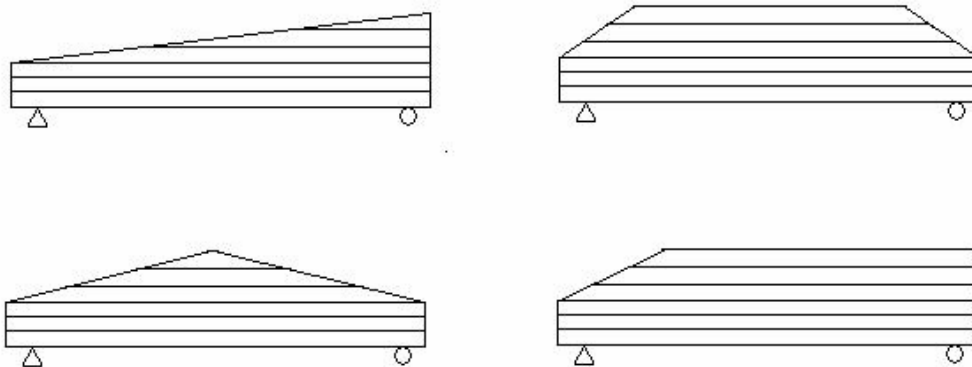


Figure 2.3 Tapered glue laminated timber

The lamination process disperses the natural wood defects randomly. This result in better structural properties compared to the same size structure in solid sawn timber.

Yeh (2002) states that coefficient of variation for the modulus of elasticity of Glulam is 10% which is much lower than that for timber, which is between 20% and 35%.

2.3.2.3 Area of concern

The surface of Glulam sustains cracks around the glue lines when Glulam has been exposed to rain and sun in bridge constructions. The cracks occur because of the variation of drying and moistening of the timber surface, and they happen even when the Glulam has been surface coated. A washboard structure occurs as result of the disintegration caused by ultra-violet rays. As a result water and moisture can penetrate the surface, which makes the timber vulnerable to rot and fungi attacks as well as reducing the strength and stiffness of the construction (Danish Technological Institute 1999).

2.3.2.4 Application

Glulam is used for headers, beams, girders, columns, bridges and for heavy trusses. It is also frequently used where the structure of a building is left uncovered as an architectural feature. Glue laminated timber has a reputation for being employed in remarkable designs with soaring open spaces (e.g. roofs of swimming pools and sport centres).

2.3.3 Sheathing board - Plywood

Plywood is a panel product which is made out of an odd number of veneer layers bonded together with structural adhesive. Veneers are aligned so that the grain of adjoining plies is placed at right angles.

The first structural plywood was fabricated by the Portland Manufacturing Company in 1905. Plywood manufactured between 1905 and the mid 1930's had a delamination problem, since the producer used non-waterproof adhesive. The invention of a waterproof adhesive, Phenol-formaldehyde, during the Second World War solved the delamination problem.

2.3.3.1 Manufacturing process

Currently, lower grade peeler logs are used in the plywood industry, since higher grade (large diameter) logs are sent to the sawmills. A peelable log is immersed in hot water or exposed to steam to ease the peeling procedure and also to reduce the veneer breakage. The log is peeled to veneers and transferred to a clipping station, which sizes the veneers and removes the defects. Veneers are visually graded and dried to 5% RH. Dried veneers are coated with adhesive and assembled before entering the hot press. An average pressure of 100 to 200 psi and high temperature (300° F) is applied to the assembled veneers to bond them together and cure the adhesive.

2.3.4 Oriented strand board

Oriented strand board (OSB) also known as wafer-board is made of wood fibres and chips, which are oriented crosswise and lengthwise in layers and bonded together with structural adhesive.

A structural panel called wafer board was developed by Dr James d'Arcy Clark in 1954; however, the current OSB board was not presented until 1982 (Lowood,1997).

2.3.4.1 Manufacturing process

In board OSB and wafer-board manufacturing the process starts by heating the debarked log in the soaking pool. Then logs are sliced into strands and dried. The dried strands or wafers are mixed with adhesive and wax and shaped into thick loose pads. These pads enter into the large heated press to form the panel and cure the adhesive.

2.3.4.2 Difference between OSB and Wafer-Board

Even though both products have a similar principle but they differ in arrangement of the flakes. Oriented strand boards are made of long narrow strands. These strands are aligned in layers, so that the grain of the strands is parallel to each other while they form a right-angle with the adjoining layers in a similar way to plywood panels. In contrast, strands in wafer-board have non-directional alignment with a random orientation.

2.3.5 Plywood or OSB or Wafer board

1. Long term deflection or creep

Laufenberg, et al., (1999) investigated the long-term deflection or creep behaviour, for plywood, OSB and wafer-board, which are exposed to constant 85% RH and cyclic 50% to 85% RH environments for a period of six months. His test results showed that the creep increased from Plywood to OSB and from OSB to wafer board.

2. Linear expansion of Plywood and OSB

The average expansion of plywood in the grain and transverse directions is around 0.06 to 0.08% whereas in OSB the expansion is 0.16 % to 0.23%. This might cause a problem if OSB panels were adjusted tightly and buckling occurs when they get wet (H.Spelter 1997).

3. Structural performance

- **Modulus of elasticity**

Plywood stiffness is significantly higher than that of OSB. However, plywood stiffness is more variable in compression to OSB (Spelter 1997).

- **Shear value**

Fisette (1997) states that OSB has double the shear value through its thickness when compared to the same thickness of plywood.

- **Pullout resistance of Plywood and oriented strand board**

The nail and screw withdrawal strength of plywood and oriented strand board was tested by (Chui, Craft 2002) who concluded that Plywood and OSB have almost similar pullout resistance for the same size of fastener.

2.4 Types of combined products

Out of numbers of combined products which are available in market place, I-Beams and structural insulated panels are most well known. There follows discussion of manufacturing processes, advantages and disadvantages of the two combined products, which represent this group:

1. I-beam or I-joist
2. Structural insulated panels (SIPs)

2.4.1 Combined products: wood-based I-beam

Wooden I-joists or wooden I-beams were first introduced in the 1920s; however, the concept of using a panel product as a web with solid timber as flanges did not develop until the 1940s, when research was conducted into the use of box and I-shaped airframe designs in wooden aeroplanes (Nelson 1997) , but the product was not commercialised until 1968. Then Trus Joist Corporation introduced their proprietary product to the market. Today many companies manufacture the I-beam across the world, because I-beams can be used for various applications, but they are principally used as a replacement for sawn timber floor joists.

2.4.1.1 I-beam materials

I-beam flanges can be made out of machine graded or visually graded solid sawn timber, or from laminated timber and laminated veneer lumber. Webs are usually prepared from plywood or oriented strand board. However in the past I-beams were manufactured using hardboard, particleboard and wood fibre board webs (Hilson and Rodd 1984), (Clinch and Halligan 1989), (Sandberg and Stehr 1997).

2.4.1.2 Manufacturing process

The I-beam production process is started by cutting sawn timber or LVL to the flange width. If it is necessary flanges could be finger-jointed and then grooved along the length of the beam. Parallel to this procedure, plywood or OSB board is cut to the web size and a wedge shape is machined along the plywood edges. Adhesive is applied inside the flange groove prior to the assembly process. Flange and web arrive at the assembly machine where the web is fitted in the flange grooves and all is pressed together. The product is sized to the desired length and passes through the oven for immediate curing or is stored in the curing room.

2.4.1.3 Advantages compared to sawn timber

Less material is used in a compound I-beam than in an equivalent sawn timber beam designed to achieve similar performance. Furthermore an I-beam offers better strength to weight ratio in comparison to sawn timber and it is not limited in length and size. Finally, research has shown that the creep behaviour of OSB webbed I-beams is the same as that of sawn timber (ASTM 1993).

2.4.1.4 Disadvantages compared to sawn timber

Web stiffeners required, especially on bearing locations in order to prevent a bearing failure. I-beams have low torsion resistance and maximum of three members is the workable limit. Lateral restraint is also required to prevent rotation of top and bottom flanges.

A compound wooden I-beam is vulnerable to fire because webs are thinner and flange dimension is small compared to a sawn timber equivalent beam (Nelson 1997).

A parametric study, which is described in chapter 7, showed that I-beams are more susceptible to vibrational problems in comparison to the solid sawn timber. For the same reason 'TRADA Timber I-joist, 2003' suggested that the deflection limit should be reduced from $L/333$ to $L/360$.

Cold bridging is another concern about I-beams. 'Timber I-Joist, 2003' reported that running an I-beam through the header joists on the outside of a timber frame can cause cold bridging.

Unlike a solid timber joist, no notching or cutting of the timber flange is permitted for a compound I-beam (Timber I-joist 2003).

2.4.2 Combined products: sandwich insulated panels (SIP)

Sandwich insulated panels are relatively simple structural components, which generally consist of two facings, that are relatively thin and of high strength, enclosing a core of rather thick, light material with adequate stiffness in a direction normal to the faces of the panel (Morley 2000). Many alternative forms of sandwich construction can be obtained by combining different facing and core materials. The facings may be steel, aluminium, wood or even concrete, whereas the core may be made of cork, balsa wood, rubber, solid plastic, rigid foam material or even paper.

Sandwich panels have been used for building refrigerated storage, automobiles and ships since 1960.

2.4.2.1 Advantages of sandwich insulated panels (SIP)

Construction with SIP panel offers better thermal performance in comparison to timber frame construction and it has been proved to be more energy efficient. Ease of construction and fast installation can be mentioned as another advantages of sandwich panels (Koschade 2002).

2.4.2.2 Area of concern with regard to sandwich insulated panels (SIP)

Poor fabrication during the gluing, pressing or curing process may cause delamination between the core and face materials.

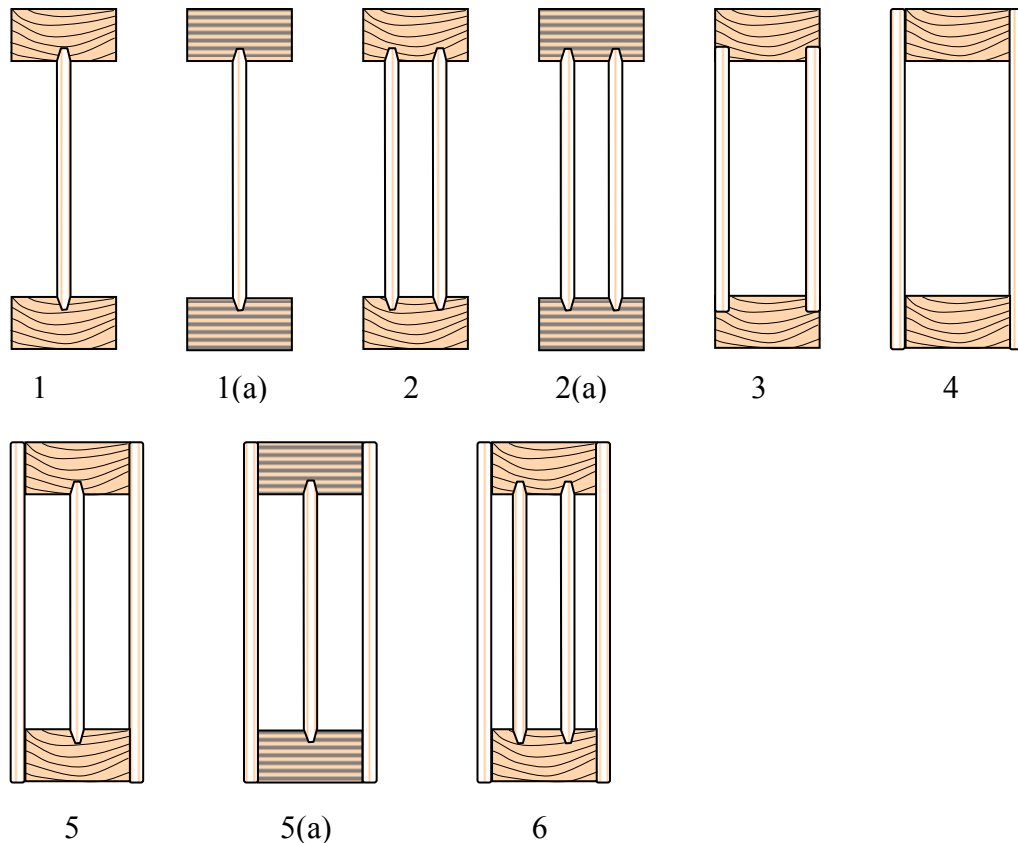
Consumer energy information mentions that insects and rodent can cause a problem, for in a few cases insects and rodent tunnelled throughout the SIPs; however, this can be avoided by using insecticides on the panels (EREC 2004).

2.5 Composite Insulated Beam

The composite insulated beam is a new concept in engineered wood products. The idea of the CIB is to combine the efficiency of a sandwich panel with that of existing EWPs, to produce new, competitive and cost-effective EWPs with improved structural qualities and long-term durability. CIB beams consist of a composite frame with 'I' or rectangular cross sections. A beam frame is constructed by bonding at least two webs to the top and bottom flanges. Inside, the beam frame may be filled with, for example, injected polyurethane, to enhance the structural performance and long term durability of the beam, as well as providing sound insulation. (Bahadori-Jahromi 2005)

2.5.1 Cross section of the composite insulated beam

Composite insulated beams could be also be described as multi-web composite beams or timber beams, since the cross-section of the beams consists of two, three or even four webs, which are connected to the top and bottom flanges. Double I-beam, recessed beam and box beam are terms used where the beam has two webs in its cross-section, whereas the terms boxed I-beam and boxed double I-beam stand for beams, which have three and four webs in their cross sectional profile, see (Figure 2.4). Further details about the manufacturing process are given in chapter 3.



Beams with timber flanges:

- (1) I-beam; (2) Double I-beam; (3) Recessed beam;
 (4) Box beam; (5) Boxed I-beam; (6) Boxed double I-beam.

Beams with LVL flanges:

- (1a) LVL I-beam; (2a) LVL Double I-beam; (5a) LVL Boxed I-beam

Figure 2.4 Cross-sectional profiles of test beams

2.5.2 Possible CIB advantages

CIBs could possess several advantages in comparison with similar cross-sections lacking infill material, or with existing light composite beams, and even with EWPs.

Some of these CIB characteristics are summarised below:

- Lightweight and can be handled easily
- Good thermal and sound insulation characteristics
- Superior load capacity than comparable sized solid timber or engineered timber products
- Excellent dimensional stability
- Resists shrinkage, warping and splitting

- More efficient than solid timber or engineered timber products for large spans and loads
- Unlike I-Joist and Box Beams they are not susceptible to shear buckling and web stiffeners are not required.
- In combination with Glulam as its flanges, CIBs can be constructed as a curved beam or an arched bridge or arched frame.

2.5.3 Potential use

CIBs possess substantial stiffness and strength combined with ease of fabrication, lower costs and comparatively lightweight so they can be substituted competitively for existing engineered products such as: Glulam, LVL, LSL, I-beams and box beams. They can be utilized as: main structural members such as trimmer beams, header beams, columns and posts. Moreover, CIBs can be used in straight or curved profile long span frameworks such as portal frames, roof trusses and in particular in bridge construction.

2.5.4 Design Methods

By design composite insulated beams (CIB) are assembled so that the beam components take best advantage of their material properties. Fabricating the beam into the “I” or “rectangular” section by combining timber or LVL flanges with plywood or OSB webs provides a high degree of structural efficiency. In general, flanges are designed to provide the bending capacity while webs carry the shear forces.

2.5.4.1 Web Joint

Webs generally connect to each other by using the tongue and groove joint method shown in Figure 2.5; however, there are other methods such as scarf joints. Specification of this design for plywood was available some years ago. In research by Chui on the strength of OSB scarf joints it was found that the optimum joint strength could be obtained when the scarf slope is about 1 to 7. (Chui 2000)

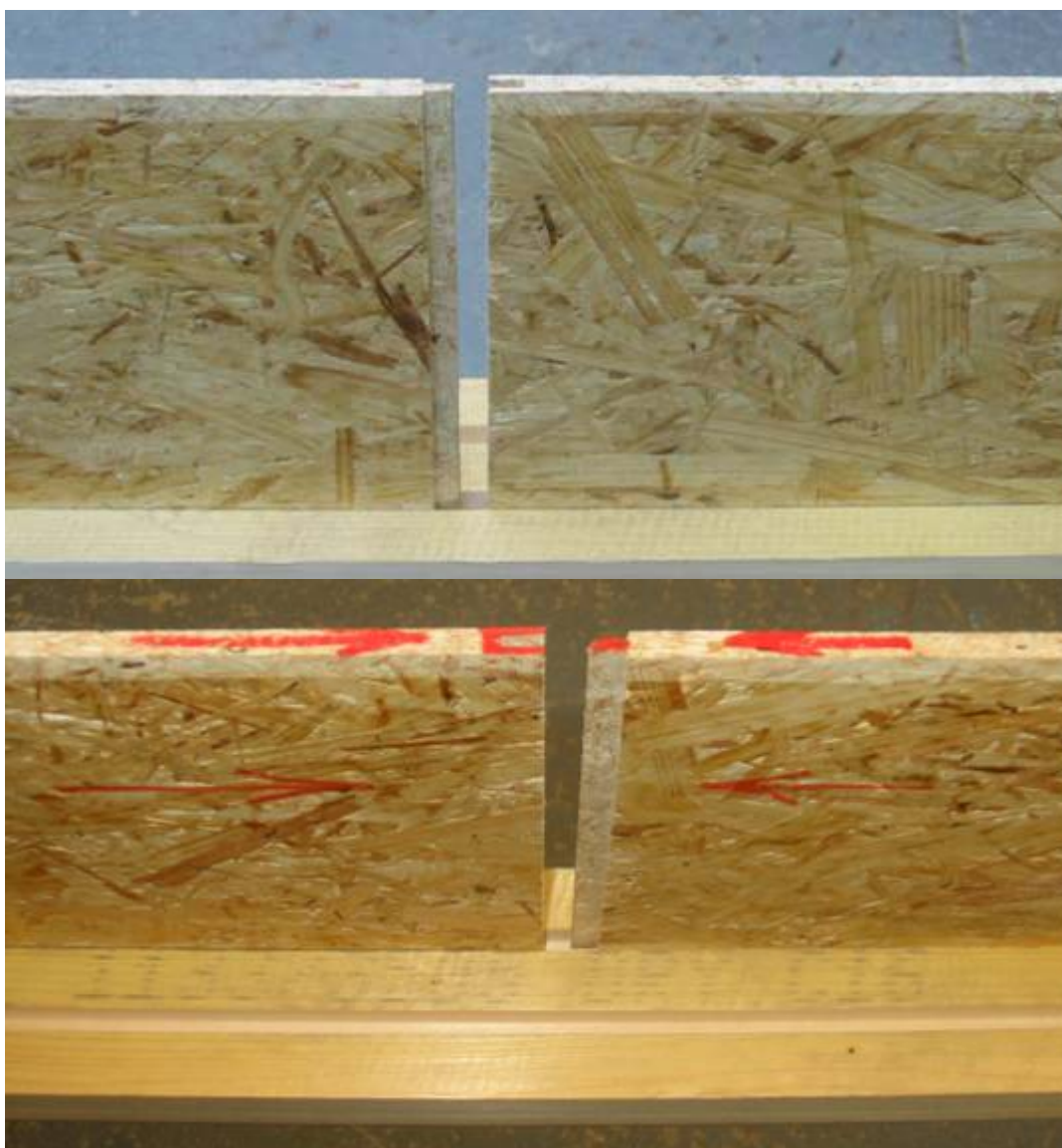


Figure 2.5 Connecting the webs - tongue and groove method

2.5.4.2 Veneer direction in plywood web

The influence of plywood veneer orientation on performance of I-beams and box beams was first investigated by (Lewis... et al. 1943, and Lewis... et al. 1944 a,b). That research concluded that box beam webs with 45° veneers assembly were more efficient in carrying the shear stresses than veneer oriented at 0 or 90°. Further studies showed that veneer assemblies parallel or perpendicular had about the same shear strength.

Fawcett and Sack, 1977 investigated the effects of web-ply orientation on structural performance. Their studies concluded that web crippling performance improves by

increasing number of plies perpendicular to the beam axis. Even though this result is in contrary to previous work (Lewis... et al. 1944), but most of the manufacturers place the plywood web so that the major ply is perpendicular to the flange grain direction (Leichti... et al. 1990).

Kermani, 1996 examined influence of grain direction on in-plane strength of plywood. His studies concluded that when the face grain direction is parallel (0°) with the direction of the applied load then in-plane bending, tensile and compressive strength attain their maximum value.

2.6 Summary and conclusions

This chapter briefly described the grounds for developing engineered wood products (EWPs) and continued with an introductory literature review concerning existing engineered wood products. There are two main categories of EWP, namely timber replacements and combined products. Different EWPs were reviewed: their advantages and disadvantages for engineering were discussed together with their manufacturing processes. There followed an introduction to the concept of composite insulated beams (CIB) and various cross-sections were described. The possible advantages and potential uses of CIBs were described. Key points in the chapter follow:

- Engineered wood products were developed in response to limitations on harvesting old growth timber and increasing demand for higher quality timber products.
- Timber replacement products demand high capital investment, but combined products require low or medium capital investment.
- Composite Insulated Beams are new engineered wood products, which can be defined as being combined products.
- CIBs were developed by combining the structural and thermal efficiency of sandwich panels with that of existing engineered wood products.

CHAPTER 3: MANUFACTURING AND FABRICATION PROCEDURES

3.1 Introduction

This chapter describes the manufacturing process for the composite insulated beams (CIB) and addresses several related manufacturing problems. The manufacturing process was carried out in three stages as follows:

- Primary work conducted in Napier University
- Major work conducted in New Zealand SCION Research Centre
- Closing work conducted in Napier University

In the primary stage, CIB were fabricated by employing SIP Panels with a polystyrene core, OSB faces as web elements and lastly timber as flange material.

Stage two, the main work, concerned the manufacture of CIB and was undertaken in New Zealand SCION Research Institute. In that stage two hundred beams with and without infill material were fabricated. Plywood was used as web material, whereas timber and laminated veneer lumber (LVL) were used as flange materials, while injected polyurethane was used as infill. The author did most of the manufacturing, with technical support, not only to understand the possible difficulties and problems, but also to ensure high quality uniform products. This was achieved after completing intensive training with various testing machines and wood processing equipment in NZ SCION Research Centre. Stage three at Napier concerned the manufacture of CIBs which were made using OSB webs with C16 and C24 timber flanges.

3.2 Manufacturing the CIBs: stage one

Two types of samples were fabricated; first, the samples for bearing or compression tests are described and second, those for shear tests. The following sections describe the fabrication procedures and dimensional details of the samples.

3.2.1 Manufacturing the compression samples

It was decided to fabricate the CIB by using structural insulated panels (SIPs) as web elements together with timber grade C24 as flange material. The eight different profiles considered are shown in Figure 3.1. The bearing test samples were 290 mm high and 300mm long, while width of the SIP governed the dimensions of flanges.

Structural insulated panels had OSB faces 11mm wide and 120mm thick overall. Flanges for designs A, C, E and G had widths of 98, 160, 98 and 120 mm respectively, but all were 45mm thick. Profiles without infill material, polystyrene, also had similar dimensions. Two types of adhesive were used; MOR AD E656-060 bonded the infill foam to the timber flanges, whereas PVA glue linked OSB faces to timber flanges.

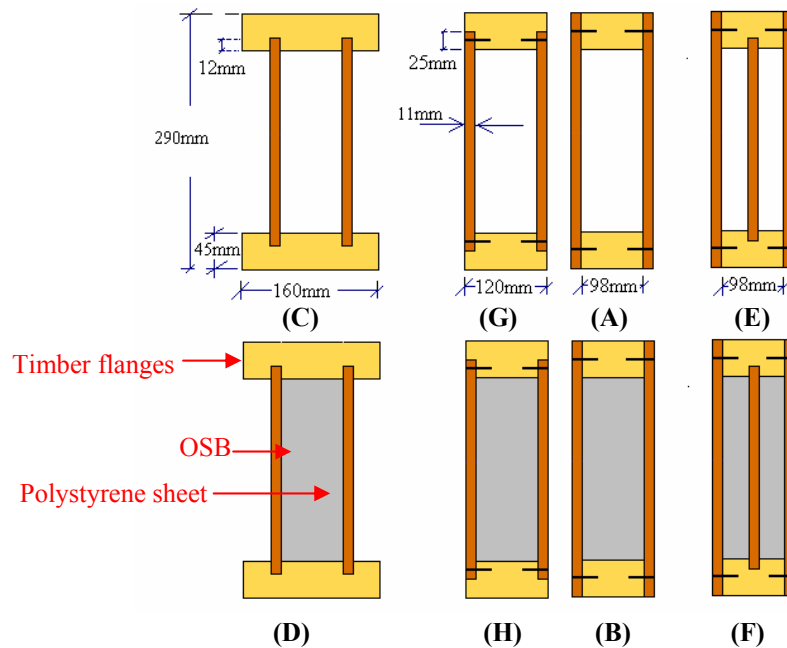


Figure 3.1 Shows variation of initial CIB designs

3.2.2 Manufacturing the beams for shear tests

Sixteen CIBs in four designs were fabricated to be 2300mm long and 290 mm high. Each design was replicated 3 times with infill and once without infill material, the cross-sectional dimensions of all the beams were identical to the compression samples. A table-rotor was used to groove the timber flanges and a circular saw was used to cut the web and flange components into the required sizes.

3.2.3 Problems arising during the manufacturing processes

1. Applying two types of adhesive makes the manufacturing process difficult time consuming and complicated.

2. Using prefabricated SIPs limited the connections between the web and flanges to rectangular tongue and groove rather than the typical trapezoid shape, because it is not possible for the available tenon-machine to taper the prefabricated panels.
3. When the timber flanges had slight bends along their length, it was difficult to assemble the components properly.
4. Using a fastener adds to the total material cost and slows assembly processes. Furthermore, industry is not in favour of using fasteners in timber products. (Ranai 2003)
5. It was not possible to control temperature and humidity variation in the stock room nor during the fabrication and testing procedures applied to CIBs.
6. Moisture content of the components was not measured due to lack of facilities.

3.3 Manufacturing the CIBs : stage two

The sixteen different beam designs shown in Figure 3.2 were considered for manufacturing. All of the designs were 290mm high. Designs 1, 2, 3, 4, 5, 10, 11 and 12 are 88 mm wide but designs 6, 7, 8, 9, 13, 14, 15 and 16 are 106 mm wide. Three-ply plywood was used as web material, while timber and LVL were used as flange materials. Designs 1, 3, 5, 6, 7, 9, 10, 12, 13, 14 and 16 were manufactured with timber flanges but designs 2, 4, 8, 11 and 15 were made with LVL flanges as shown in Figure 3.2. Injected polyurethane was employed as filling material for designs 10, 11, 12, 13, 14, 15 and 16.

Four types of connections were used for joining webs to flanges.

- Laminated connections were employed in designs 6 and 13 shown in Figure 3.3(a).
- Tongue and groove connections were used in designs 1, 2, 3, 4, 10 and 11 shown in Figure 3.3 (b).
- Combinations of laminated and tongue and groove connection were used in designs 7, 8, 9, 14, 15 and 16 shown in Figure 3.3(c).
- Recessed connections were employed in designs 5 and 12 shown in Figure 3.3(d).

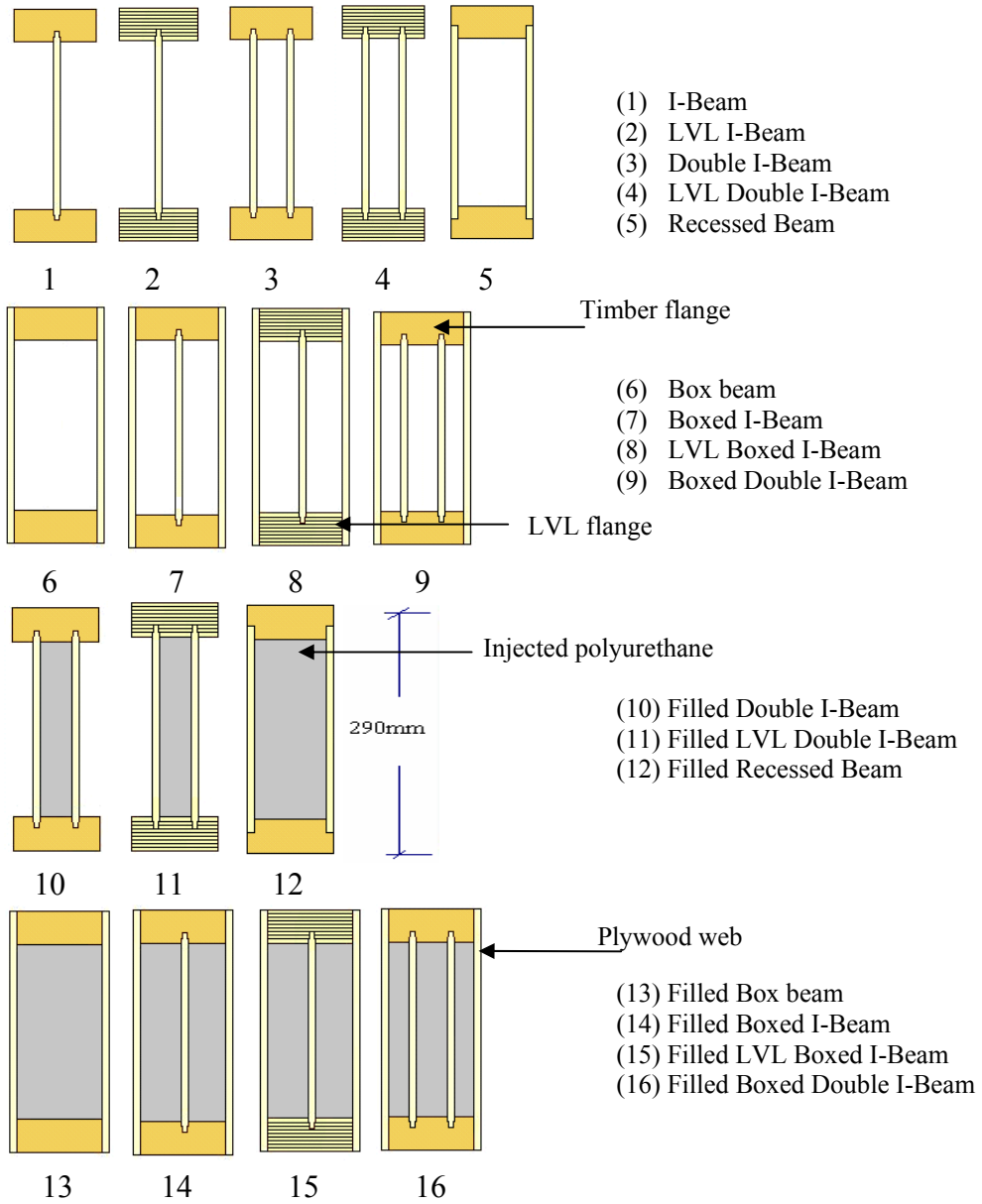
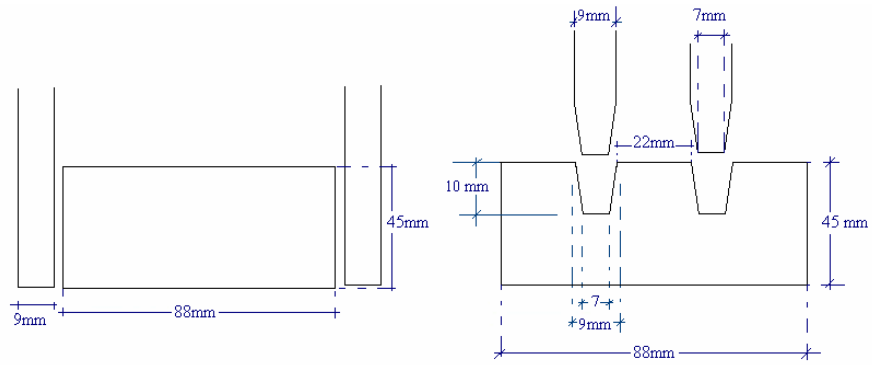
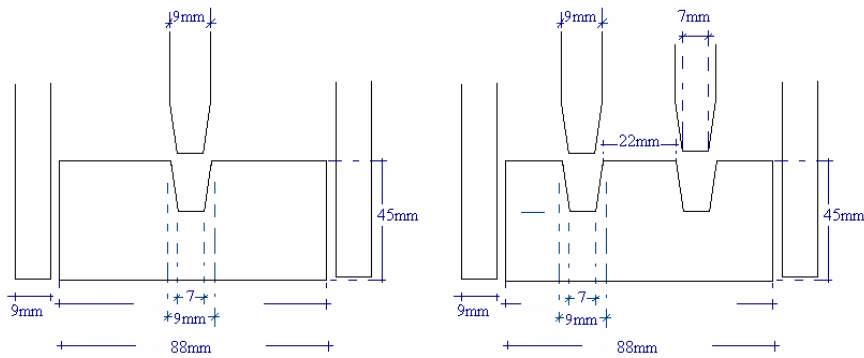


Figure 3.2 Composite insulated beam profiles

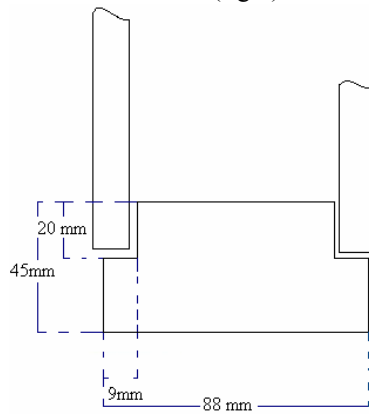


(a) Laminated connection- Box beam

(b) Tongue and groove connection-Double I-beam



(c) Combination of laminated and tongue and groove connection, Boxed I-beam (Left) , Boxed double I-beam (right)



(d) Recessed connection –Recessed beam

Figure 3.3 Different web-flange connections

3.3.1 Fabricating the CIBs

Each CIB beam has three different components, a web of plywood, flanges of timber/LVL and infill material, namely injected polyurethane. The bond between timber/LVL flanges and plywood webs was provided by Resorcinol Formaldehyde adhesive (ORICA Adhesives and Resins, 2002). The manufacturing process could be described in three stages as follows:

- Preparing the components of the beam

- Testing the material properties of each individual component before manufacturing
- Assembling the CIBs

Equipment used to prepare and assemble the components of the CIBs

- Planer-Moulder* (Figure 3.4)
- Radial arm cross-cut circular saw and table saw
- Double ended tenon-maker (Figure 3.5)
- Pneumatic press or Taylor clamp
- Lamination clamping jig
- G clamps
- Weighing scale
- Pneumatic impact wrench
- Torque wrench
- Electronic load cell
- Moisture meter**
- Humidity sensor (electronic hygrometer)
- Pneumatic Brad-Nail gun
- Roller glue-spreader

***Planer-Moulder**

This machine could planed all four sides of a board in one pass, and also could produce various profiles by changing the cutting knives.

****Timber moisture meter**

This timber moisture meter indicates the moisture content of wood over the range from +7 to +35% . The accuracy of readings was $\pm 3\%$.

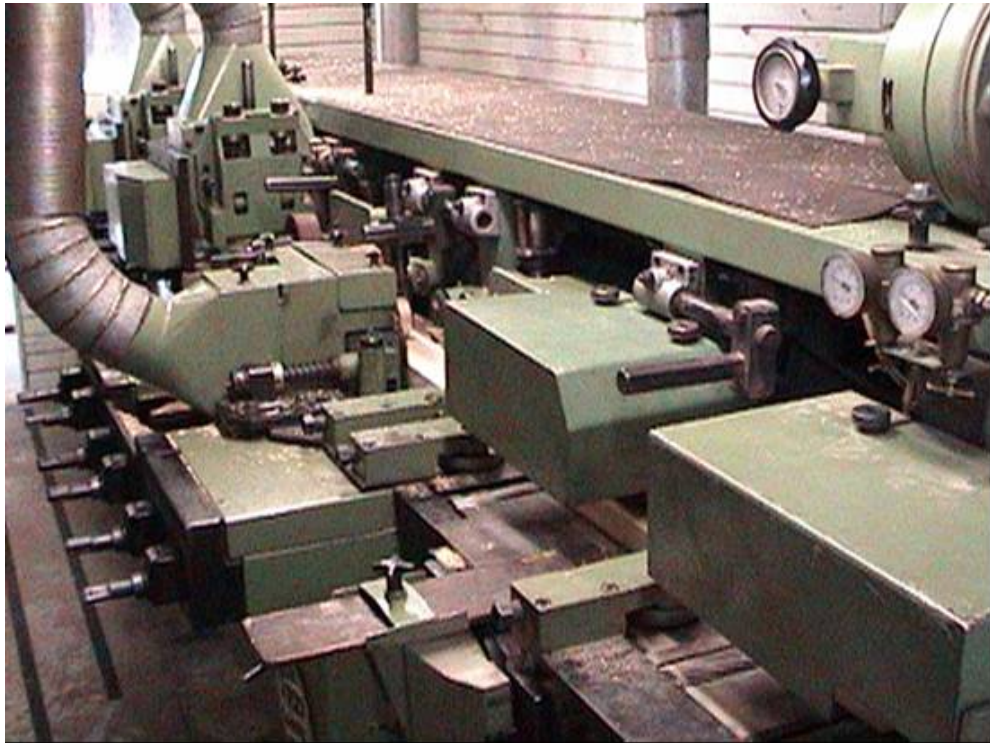


Figure 3.4 Planer-moulder machine

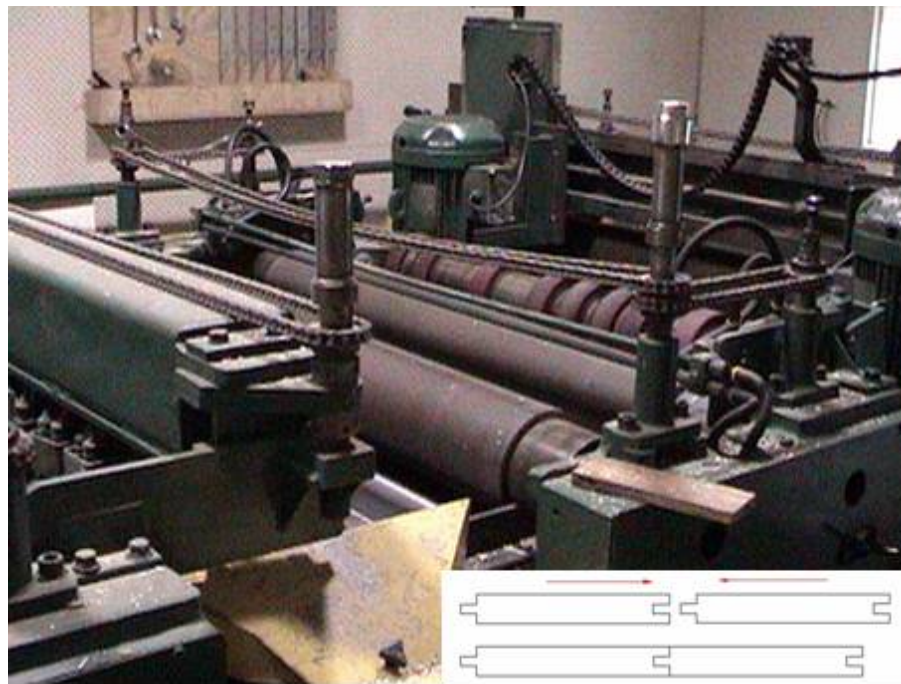


Figure 3.5 Double ended tenon-maker, machining the plywood webs

3.3.2 Selecting and testing the CIB components

The basic CIB is a combination of flanges and webs. Flanges are made of timber or LVL 45-mm deep and 90 mm wide. Beams were manufactured in two different lengths, 2.3 and 4.8 meters.

3.3.2.1 Selecting the timber flanges

Radiata pine timber was used for the flanges of beams. Suppliers mechanically graded this timber as MGP 10, which means that the average modulus of elasticity (E_{mean}) of these timbers was 10 GPa (kN/mm^2). However for this project, the modulus of elasticity of each timber flange was tested again in the SCION laboratory.

3.3.2.2 Matching the timber flanges

CIBs of different profile are comparable if individual components of each beam being compared possess similar material and mechanical properties. Of the three CIB components, web, infill material and flanges, timber flanges by nature possess the highest material variability (e.g. Timber Engineering step 1, 1995). As a result it was necessary to measure timber strengths and then to spread them (wood flanges of known stiffness) evenly among different designs before fabricating the beams. There is correlation between timber strength and some characteristics of the timber that can be measured non-destructively. Those characteristics are as follows:

1. Knots
2. Annual ring width
3. Density
4. Modulus of elasticity (MoE)
5. Combination of Knots and annual ring width
6. Combination of knots and density
7. Combination of knots and MoE

A number of research studies have been conducted to determine relationships between the engineering and material properties of timber. (Hoffmeyer ... (et al.) 1999, Johansson ... (et al.) 1992, Lackner ... (et al.) 1988.) All this research showed that the modulus of elasticity has highest correlation with bending strength, demonstrating that the coefficient of determination R^2 is in the range 0.73 to 0.51. At the present,

the modulus of elasticity (MoE) is recognized as the best individual predictor of strength in timber. (Johansson 2003) In New Zealand, matching and sorting procedures were carried out in two steps described below.

1. Matching the timber flanges

In this stage timber flanges, base on their MoE, were evenly distributed between various groups. Each group was used for fabrication of one type of CIB profile. The outcome was even distribution of MoE between various groups or profiles. Detailed descriptions of the procedure are given in the next section - (3.3.2.3).

2. Sorting and matching the beams

In this step fabricated beams of each group were divided into sets of three members and sorted in such a way that each set had flanges of similar MoE values. Section 3.4 describes the method.

These procedures allow both even distribution of MoE among the different profiles and within each set of the group. As explained in chapter 4, this method is used to evaluate the effect of web openings of different diameter within the profile and also to compare them with other profiles.

3.3.2.3 Testing and grouping the timber flanges

Three hundred sections of timber were visually examined for natural defects and 267 pieces of the timber were selected for use. Those timber sections were cut into 2.75 meter lengths and were used for manufacturing 96 CIBs with 2.3 meter final length. All the timber sections were numbered and tested using a four point bending test to evaluate their modulus of elasticity. Variation of the Young modulus was between 5 to 15 GPa. The test results were sorted by ascending modulus of elasticity and renumbered accordingly from 1 to 267: see Table A.1 in Appendix A. As a result the higher flange number (ID) reflects the higher flange MoE. Any pieces with module of elasticity lower than 7 GPa were rejected, which meant rejecting first any faulty flanges with flange ID in the range 1 to 40.

The remaining pieces were divided into nine matched groups, each group represented one profile. A group contained matched samples with MoE ranging from low to high, equally spread, as shown in Table A.2 in Appendix A. This was achieved by

spreading the 9 flanges with lowest acceptable ID among the nine groups and then the next 9 flanges with higher ID values were assigned to groups. In this way flanges with numbers 41 to 49 were spread among the nine different profiles accordingly followed by the number 50 to 58 and this was continued until the last row starting from 257 and ending at 265. Each cell in a table contains a pair of flange IDs, which represents top and bottom flanges of the relevant profile. As is shown in Table A.2 in Appendix A, each group was also colour-coded: see also Figure 3.6. This colour-coding system was used to identify each design during the machining process and manufacturing.

In the same fashion 56 pieces of timber were selected, including a spare, for the manufacture of 24 CIBs 5.4 meters long. These beams were also tested and sorted in a similar way to the short beams as previously described: see Tables A.3 and A.4 in Appendix A).



Figure 3.6 Colour-coded flanges after machining, ready for assembly

3.3.2.4 Selecting the LVL flanges

One hundred pieces of LVL each 2.75 meters long, 45 mm deep and 90 mm wide were selected to manufacture 48 CIBs with LVL flanges.

Material properties of LVL are more consistent than solid timber, which reduces the variation of MoE and therefore there was no reason to test all the pieces. As a result the modulus of elasticity was determined only for 20 pieces, which were chosen randomly from the stack and results appear in Table A.5 in Appendix A.

Length of the flanges

The length of the flanges was trimmed in three stages:

1. Length during the machining

All the flanges were cut to 2.75 and 5.4 meter lengths for the machining.

2. Length during the assembling

Timber and LVL were further trimmed to 2.45 and 5 meter lengths.

3. Final stage

After the manufacturing process was completed and polyurethane injected into the frame, the CIB beams were trimmed to the designed sizes which were 2.3 meter and 4.5 meter lengths.

Flanges were not sized to their final length in the first place, because during the machining process, or during, transferring some damage might occur to the end of the beams. Similarly, after injecting the polyurethane some of the foam overflowed from the open end of the beam. This extra length provided the required margin, and eventually this is trimmed to the required design size.

Expanding the project

After designing the new profiles, designs 9 and 16, it was decided to manufacture those sections along with the previous profiles. There was also a short fall in the manufacturing plan for fabricating long CIB beams with LVL flanges so I-beams were considered. Such was the interest shown by NZ SCION research in the CIB project, that additional funding was provided in order to expand the testing program, to incorporate LVL in the long CIBs. Having these long beams created the opportunity for carrying out the full-scale comparative bending test on them along with the previous designs.

Beams with timber flanges

- Profile 9 and 16, each one replicated three times over 2.3 m length
- Profile 9 and 16 each one replicated three times over 4.5 m length
- Profile 1 three beams over 4.5 m length

Beams with LVL flanges over 4.8 m length

- Profile 2, two beams
- Profile 4 and 11 , each one replicated twice
- Profile 8 , two beams

A total of 16 LVL flanges and 26 Timber-flanges over 4.8 meter length were selected and tested for MoE. The results of the MoE tests for six pieces of LVL flange are presented in Table A.6 in Appendix A. Those LVL pieces had been chosen randomly from 16 pieces. The results of the Young Modulus (E) for timber flanges are given in Table A.7 in Appendix A.

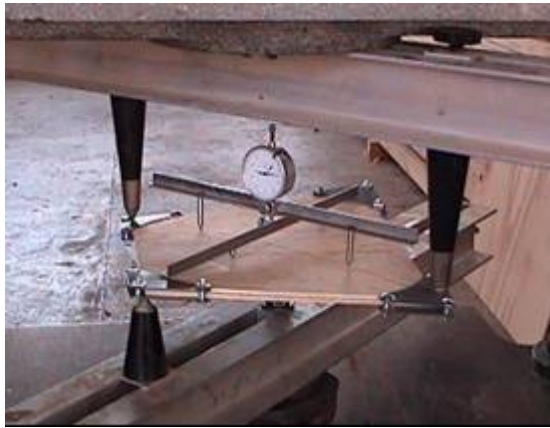
A similar method to that in the previous section was adopted to match the top and bottom timber flanges in such a way that each profile has a comparable modulus of elasticity: see Table A.8 in Appendix A.

3.3.2.5 Testing and preparing the webs

Three-ply structural plywood sheets grade DD, 9 mm thick, were used as a web material. Plywood sheets were manufactured to AS/NZS 2269 at the Origin Plywood Plant in New Zealand.

Testing the Plywood

Six specimens, which were randomly selected out of the 140 plywood sheets, were tested according to BS 4512 for modulus of rigidity, moisture content and density: see Figure 3.7(a). A summary of the results is given in Table A.9(a) in Appendix A. Modulus of elasticity (Figure 3.7(b)), bending strength with face grain parallel to the span and face grain perpendicular to the span were also determined for five samples and results are in Tables A.9(b) and A.9(c) in Appendix A.



a) Testing modulus of rigidity



b) Testing modulus of elasticity

Figure 3.7 Testing material properties of the 3ply-plywood

Preparing the webs

All the plywood sheets had an initial dimension of 1200×1200 mm. They were tongued and grooved by passing them through the double ended tenon-maker shown in Figure 3.5. The tongue and groove profile was created parallel to the face grain direction. Then Plywood webs were cut to 220, 240 and 290mm height across their face grain. The plywood webs, which were 220mm in height, were tapered on either edge by passing them through the planer-moulder to fit the groove machined in the flange.

Cutting across the face grain

The plywood used was 3-ply and 9-mm thick. Shear and bearing capacity of the ply veneer parallel to the grain is higher than perpendicular to the grain direction. By cutting across the face grain, two of the ply veneers are positioned such that the face grain is vertical toward the flange grain direction, while cutting along the face grain provides only one ply grain in desired direction.

3.3.2.6 Machining the flanges

The planer-moulder shown in Figure 3.4 was employed to machine three different flange designs, namely single grooved, double grooved and recessed as shown in Figure 3.8.

The planer-moulder used in this project could run up to six cutters simultaneously. The machine was adjusted in a way to create the profile and to remove a millimetre from both sides of the flanges. The main reason for machining the sides of the flange

is to produce a clean surface for laminating by removing any dust or dirt. Adhesives cannot bond well on the laminating area if the surface is covered by the dust or dirt and the outcome would be a weak glue line.

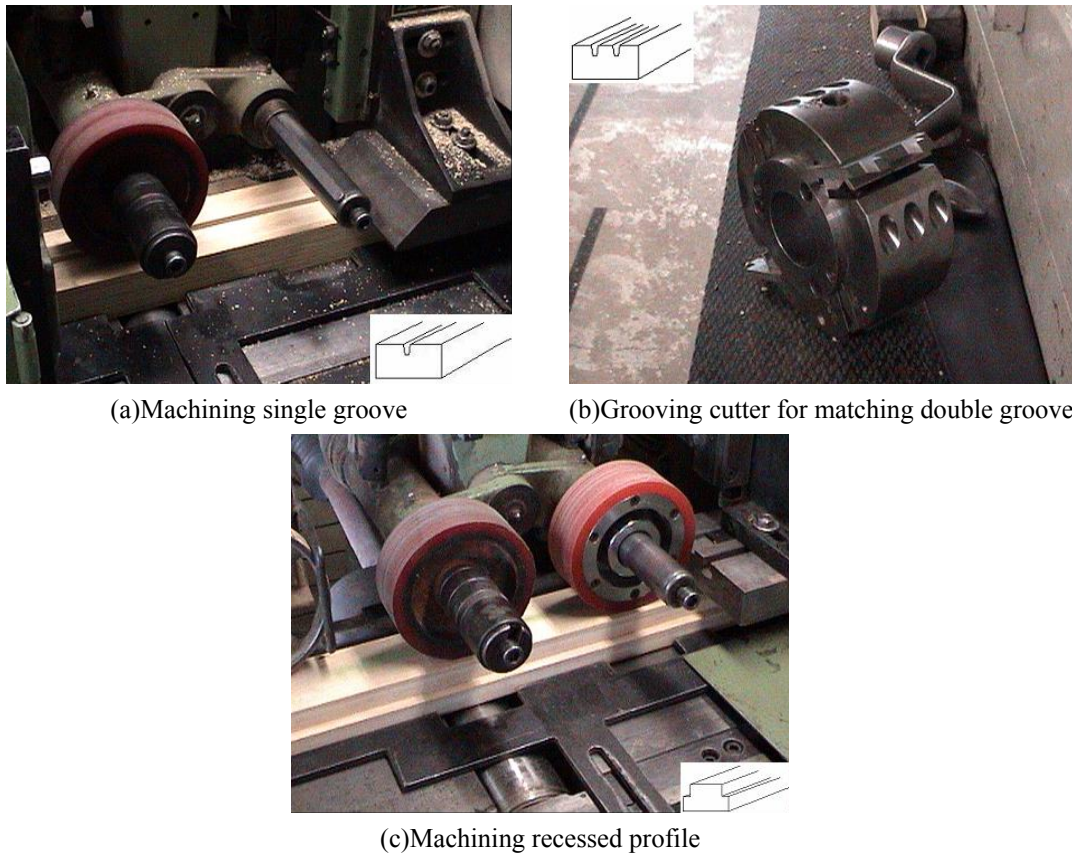


Figure 3.8 Machining different flange profiles

Each design required special cutter knives, shown in Figure 3.8(b), which were made in advance in NZ Waiariki Institute of Technology. The color-coded timber flanges and LVL flanges were divided into four groups and placed on the moulder in-feed table.

Four different groups were prepared for machining:

- Group 1: Profiles 6 and 13 colour coded orange
- Group 2: Profiles 3, 4, 10 and 11 colour coded red
- Group 3: Profiles 7, 8, 14 and 15 colour coded yellow, but profiles 1 and 2 also in this group were coded colourless
- Group 4: Profiles 5 and 12 colour coded blue

After completing each group, the process had to be stopped, in order to change the cutter-head for the next group. At the same time flanges were collected from the out-feed table and stacked again in four groups ready for transferring to the assembly building. A similar approach was used to machine the additional designs.

To achieve the right dimension for the timber profile it is important to have straight wood, of sufficient size, on the in-feed to machine the profile cleanly. If not, the machined profile can show “hit and miss”. This point is especially important when using already dried and dressed timber, which can have some variation along the width; for instance such timber can be a few millimetres thinner or thicker. The planer-moulder is set to a fixed size and when thinner timber passes through the machine an asymmetrical profile is created.

In the assembly building, all the CIB flanges were cut to 2450mm in length.

3.3.3 Assembling process

In general, an efficient assembly process can be achieved by two persons for the short 2.3 m beams, but four people are needed for the long 4.8 m beams. The author was able to do much of the machining and manufacturing with assistance as needed. In this way it was possible to have a direct control of the quality of the work and also to evaluate different profiles in terms of the cost and workmanship required in fabricating the various beams.

Assembling processes are summarized in the following steps:

- Preparing the glue
- Preparing the components
- Applying the glue
- Initial assembling
- Clamping the beam
- Releasing the clamp and transferring the beam to the curing place

Preparing the Glue

Adhesive was mixed with liquid hardener using a ratio of 100g adhesive to 33g liquid hardener.

3.3.3.1 Double I-Beams and LVL Double I-Beam

There follows a description of the assembly process for Double I-Beams and LVL Double I-Beams. This was the initial manufacture process for any of the beams and the assembly pattern described is repeated for other designs.

Glue was brushed within the flange slots and also brushed in the tapered area and tongue and groove surface of the plywood webs as shown in Figures 3.9(a), 3.9(b) and 3.9(c). The plywood webs were tapped into one slot and then into the second slot. Then the second flange was adjusted onto these two webs. In order to get the webs into the top flange, both flanges were tapped with a plastic hammer. First the webs were adjusted in the top and bottom flanges, then the connection between the tongue and groove joints was checked. If there was a gap, it was closed by tapping the webs from both ends. When the adjusting was completed the top flange was hit with a rubber hammer so that the flange was tight enough for transferring to the clamp: see Figure 3.9(d).



(a) Applying the glue to the grooving area



(b) Adjusting the webs within the grooved area



(c) Applying the glue to the webs



(d) Adjusting the top flange

Figure 3.9 Fabricating the Double I-beam

The beam was placed between two lengths of LVL, serving as packers, in the Taylor-clamp. These LVL packers help to distribute the clamp pressure evenly over the beam flanges: see Figure 3.10. Discussions with SCION Research staff led to the conclusion that a pressure of 60 Psi (41 kN/m²) would be adequate for obtaining a good bond between the webs and flanges.



Figure 3.10 Pneumatic press clamp (Taylor clamp)

A similar procedure was followed for assembling the long Double I-beam, but instead of a Taylor clamp a modified Glulam clamp was used as shown in Figure 3.11. Clamping in this way proved to be difficult and labour intensive. There is a possibility of web debonding when the beam is transferred to the clamp or when it is adjusted within a clamp.



Figure 3.11 Clamping system used for long I-beams and Double I-beams

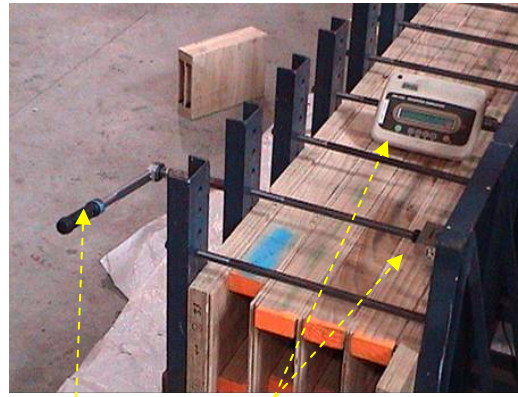
Unlike Box beams, Boxed I beams and Box Double I-beams, there is no need for the long double-I beam to remain in the clamp for number of hours. This is because of the self-clamping characteristics of tongue and groove profiles. Once the web is pressed in its groove then immediately the assembly can be removed from the clamp.

3.3.3.2 Box Beam

This design is the typical box beam although without a stiffener. Glue was applied on the flanges by a roll-spreader. Glue was also applied on the connection area of the plywood and brushed in the web's tongue and groove area. Then the web was placed on the flanges and fixed by a brad-nailer. The second web was placed next to the first web connected to each other by tongue and groove joints. The same procedure was repeated for the other side of the beam and then the assembled beam was transferred to the clamp as shown in Figures 3.12 and 3.13.



a) Box beam under the clamp



b) Torque wrench and load cell for controlling the clamp pressure

Figure 3.12. Laminated press for short Boxed profiles



(a) Fabrication of long span Boxed beam



(b) Using insulated covers and gas-fired heating for curing the beams

Figure 3.13 Modified Glulam press had been used for fabrication of the Boxed beams

3.3.3.3 Boxed I-Beams

Adhesive was prepared as explained previously. In this design the total mixing time, open assembly, close assembly and clamping time should not exceed 30 minutes when the temperature is 18° C or above. If the process takes longer then the glue will be too dry before clamping and the bond between web and flange will be poor. By measuring the required time for assembling the short 2.4 m beam and the long 4.8 m beam, it was established that it is possible to assemble 3 beams inside 30 minutes

provided two people work with the 2.4 meter beam and four persons work with the 4.8 meter beam.

Manufacturing the Boxed I-beam took place in two stages:

Stage 1

The middle web was glued in place. Adhesive was brushed within the slot of bottom and top flanges. Glue was also applied on the tapered part of the web and on the tongue and groove area of the plywood web. Plywood webs were adjusted in the bottom flange one by one and then the top flange grooving was fixed to the plywood web. The plywood tongue and groove joint was controlled and any gap between them, was adjusted by tapping the other end of the plywood webs. The upper flange was hit with a rubber hammer and then the beam was carried to the clamp. The clamping procedure is similar to that for profiles 3 and 4, but only 50 PSI pressure was applied.

Stage 2

Glue was prepared in the same fashion explained before, and then it was applied on one side of flanges and the webs by roll-spreader. After adjusting the plywood webs on one side the web is fixed in place using the brad-nailer and then the same procedure is repeated for the other side. The brad-nailer gun was used for holding the plywood webs in place before transferring to the lamination clamp as shown in Figures 3.12 and 3.13. Beams were placed between two packers of LVL 45mm deep, 300mm wide and 2400 mm long in order to even the pressure on the beams.

During each session four short beams were manufactured and then clamped for at least 7 hours. In order to reduce the curing time to 7 hours, a heating system was employed and the room temperature brought to 25-28°C. Six beams were manufactured in two sessions per day. The second session had up to 17 hours curing time so there was no need to increase the temperature.

A similar procedure was followed for fabricating the long Box beam, but in each session three beams were assembled and a modified Glulam press was used for clamping as shown in Figure 3.13.

3.3.3.4 Recessed Beams

Glue was brushed into the recessed area of the flanges. Glue was also applied on the web area, by roll-spreader. After webs were adjusted in their place the brad-nailer was used to hold the web against the flange. The same procedure was repeated for the other side of the beam. In this design before the final fixing by brad-nailer, a G-clamp was used to adjust the web in the recessed section, especially when the flange had some bending warp. In similar fashion to the assembly of the other design, the webs were joined together via their tongue and groove connections.

3.3.3.5 Boxed double I-beams

This profile is a combination of profiles 3 and 6. In the first stage the middle webs were adjusted in place as explained for profile 3 and then the side webs were glued in place.

Clamping pressure

First, all the 18 clamping bolts were closed by a pneumatic impact wrench and then tightened by a torque wrench. 60 N.m was the torque applied to the lamination clamp bolts. In order to have a better control on the clamping pressure, a load cell was used to check pressure, and it was attached within the middle clamp as shown in Figures 3.11 and 3.12. This load cell showed the actual load, which was carried by the clamp when the bolt was tightened by the torque wrench. This practical method made it possible to measure the exact value of torque for clamping. Through this method it was also possible to calculate K - the empirical constant for the threads.

Glue line pressure:

Chung 1964 indicates that the required pressure between glue lines should be 100 psi (70 kN/m²). Similarly BS EN 302-2 recommended that the pressure between glue lines should be $60 \pm 10 \text{KN} / \text{m}^2$.

3.3.4 I, Double I, Recess, Box, Box I and Box double I-beam

Fabrication of different profiles showed that I-beams and Double I-beams can be fabricated in one stage and immediately can be transferred to the storage room. Meanwhile Recess Box-beams, Box I-beams and Box double I-beams need to remain

under the clamp until the glue is cured. This curing time could be considered as a disadvantage for these profiles in comparison to I-beams and double I-beams. In a preliminary study carried out in NZ Scion, it was shown that staples could provide adequate pressure to substitute for the clamping procedure. In this trial after assembling the Box I-beam, webs were stapled every 10 cm with staples 38 mm deep and 10 mm wide. However, further study is required to identify the optimum distance between the staples and also a suitable size for the staples.

3.4 Sorting and numbering the beams after manufacturing

As explained earlier, the CIBs were assembled according to matched flange modulus of elasticity as shown in Tables A.2, A.4 and A.8 in Appendix A. After completing the manufacturing sessions, each beam was given an ID number. This number ranged from 199 to 346. The following section explains the numbering procedure.

3.4.1 Sorting and assigning the ID number to the timber flange beams

Fabricated beams with timber flanges can be compared to their own group and also to other profiles if they possess similar material properties together with identical dimensions. On the other hand, if material properties or dimensions differ then the accuracy of the results and judgments based on those results will be questionable. In order to achieve accuracy, the MoE of the flanges should be evenly distributed among different profiles or groups. This section explains how even distribution of the MoE within each profile was achieved and also how the Beam ID numbers were assigned. Once this was done it was possible not only to compare the different profiles, but also to compare the results within each profile.

There follows a description of the method which was employed to achieve the goal above.

Explaining the approach

A comparison of Tables 3.1(a) and 3.1(b) explains this statistical approach. The table is divided into two parts, to show initial matching and final matching. At the left side of the table there are four columns namely, set, sorting number, flange ID, top and bottom flange MoE. The first column shows the twelve beams were separated into

four sets and each set contained three members. The second column shows the sorting number from 1 to 11 which corresponded to the flange ID in column 3 and to the top and bottom flange MoE in column 4. Comparing column 4 of table 3.1(a) to that in 3.1(b) shows results of the even distribution of flange MoE among different profiles, which was explained earlier. At the right side of Table 3.1, under final matching, there are four columns namely, sorting no. in column 5 which corresponds to Flange ID in Column 6, Beam ID in Column 7 top and bottom flange MoE in Column 8. Comparing the average MoE given for each set in column 8 of table 3.1(a) shows the even distribution of MoE within the profile and comparing them to the same column in table 3.1(b) shows the even distribution among the profiles.

A similar approach was adopted for the rest of the profiles and is presented in Appendix A in Tables A.11(a to k) for short beams and Table A.12 for the long beams. Long beams were replicated only three times, which means each group has only one set consisting of three members. In this case initial matching and final matching remain the same.

Figure 3.14 summarizes the outcome of this method which is employed to all the profiles. The figure shows two graphs for each design, one demonstrates the distribution of E value for top and bottom flanges and the second graph presents the average E value of each group, which comprised four sets with three members.

From the information given in Appendix A, Tables A.11 (a to k), and A.12 it is possible to determine the following characteristics for each design:

- Recognize the profile base on their Beam ID
- Identify the flange MoE which is relevant to a particular flange ID

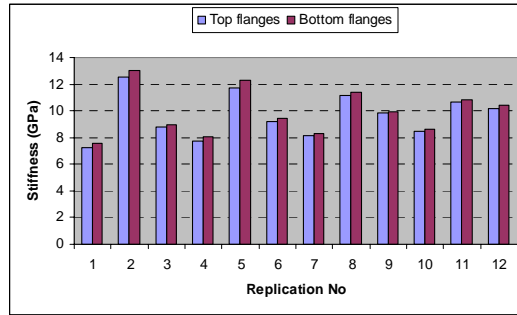
Table 3.1 Statistical method for sorting and numbering the beams

Table 3.1(a) Profile 1- I-beam

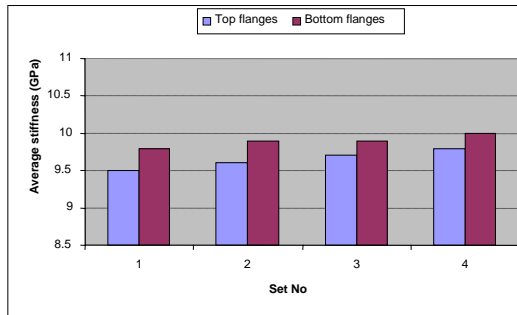
Set	Initial matching			Final matching			
	Profile (1)			Profile (1)-I-beam			
	Sorting. No	Top-Bottom Flanges ID	Top-Bottom MoE (kN/mm ²)	Sorting. No	Top-Bottom Flanges ID	BEAM ID	Top-Bottom MoE (kN/mm ²)
1	1	49-58	7.28-7.56	1	49-58	302	7.28-7.56
	2	67-76	7.76-8.03	12	247-256	303	12.54-13.03
	3	85-94	8.15-8.28	5	121-130	304	8.79-8.94
			AVE 7.84				AVE 9.69
2	4	103-112	8.45-8.59	2	67-76	305	7.76-8.03
	5	121-130	8.79-8.94	11	229-238	306	11.75-12.32
	6	139-148	9.21-9.46	6	139-148	307	9.21-9.46
			AVE 8.91				AVE 9.76
3	7	157-166	9.81-9.94	3	85-94	308	8.15-8.28
	8	175-184	10.19-10.42	10	211-220	309	11.12-11.37
	9	193-202	10.64-10.86	7	157-166	310	9.81-9.94
			AVE 10.31				AVE 9.78
4	10	211-220	11.12-11.37	4	103-112	311	8.45-8.59
	11	229-238	11.75-12.32	9	193-202	312	10.64-10.86
	12	247-256	12.54-13.03	8	175-184	313	10.19-10.42
			AVE 12.02				AVE 9.86

Table 3.1(b) Profile 6- Box-beam

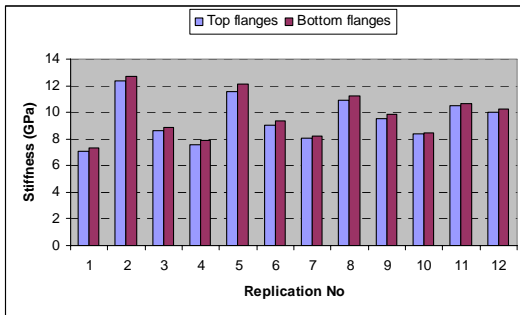
Set	Initial matching			Final matching			
	Profile 6			Profile (6)-Box beam			
	Sorting. No	Top-Bottom Flanges ID	Top-Bottom MoE (kN/mm ²)	Sorting. No	Top-Bottom Flanges ID	BEAM ID	Top-Bottom MoE (kN/mm ²)
1	1	41-50	7.02-7.32	1	41-50	200	7.02-7.32
	2	59-68	7.57-7.80	12	239-248	201	12.36-12.66
	3	77-86	8.06-8.16	5	113-122	202	8.59-8.84
			AVE 7.66				AVE 9.47
2	4	95-104	8.28-8.48	2	59-68	203	7.57-7.80
	5	113-122	8.59-8.84	11	221-230	204	11.40-11.88
	6	131-140	8.99-9.23	6	131-140	205	8.99-9.23
			AVE 8.74				AVE 9.48
3	7	149-158	9.47-9.82	3	77-86	206	8.06-8.16
	8	167-176	9.97-10.20	10	203-212	207	10.86-11.14
	9	185-194	10.46-10.65	7	149-158	208	9.47-9.82
			AVE 10.10				AVE 9.59
4	10	203-212	10.86-11.14	4	95-104	209	8.28-8.48
	11	221-230	11.40-11.88	9	185-194	210	10.46-10.65
	12	239-248	12.36-12.66	8	167-176	211	9.97-10.20
			AVE 11.72				AVE 9.67



I-beam-Distribution of MoE within top and bottom flanges



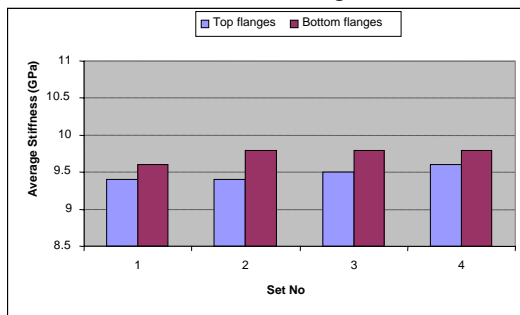
I-beam-Average MoE of four sets



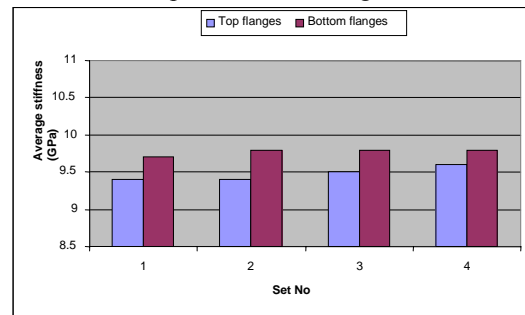
Double I-beam-Distribution of MoE within top and bottom flanges



Filled Double I-beam-Distribution of MoE within top and bottom flanges

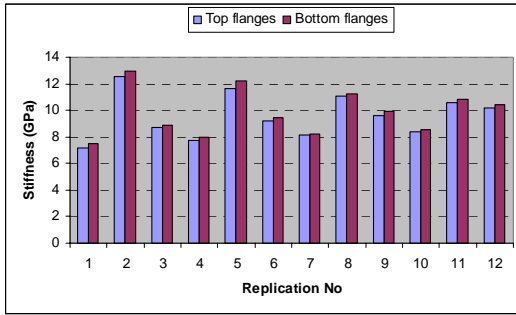


Double I-beam- Average MoE of four sets



Filled Double I-beam- Average MoE of four sets

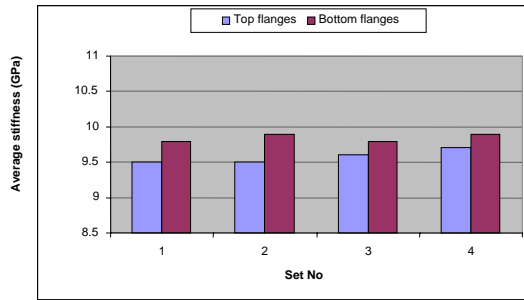
Figure 3.14 Distribution of MoE among different CIB profiles after final matching



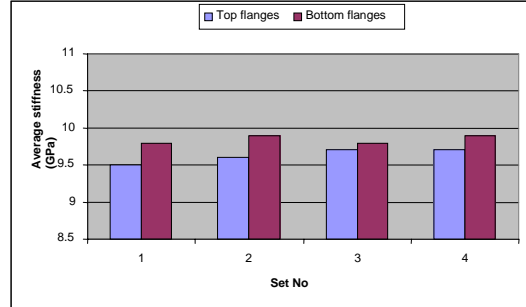
Recessed beam-Distribution of MoE within top and bottom flanges



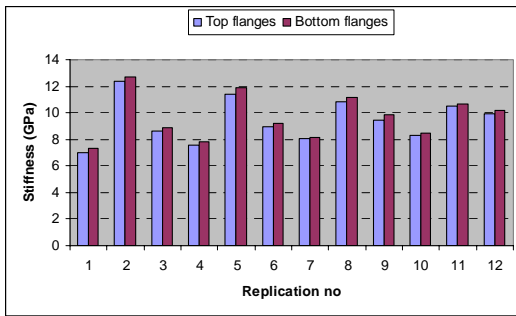
Filled Recessed beam-Distribution of MoE within top and bottom flanges



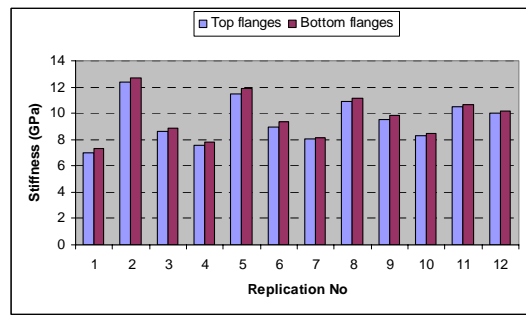
Recessed beam- Average MoE of four sets



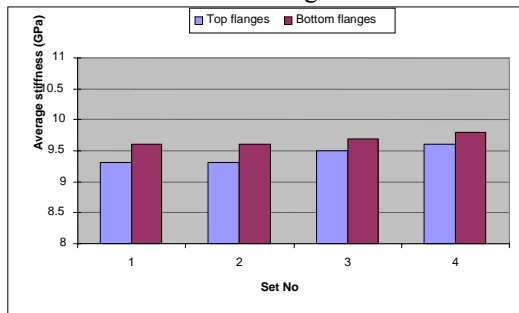
Filled Recessed beam- Average MoE of four sets



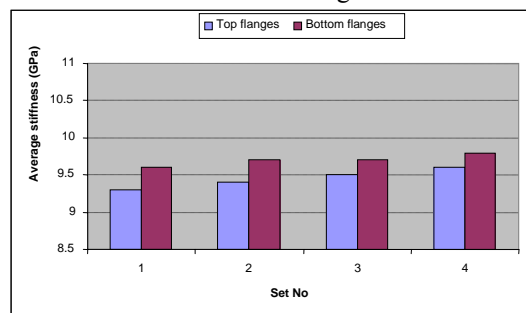
Box beam-Distribution of MoE within top and bottom flanges



Filled Box beam-Distribution of MoE within top and bottom flanges

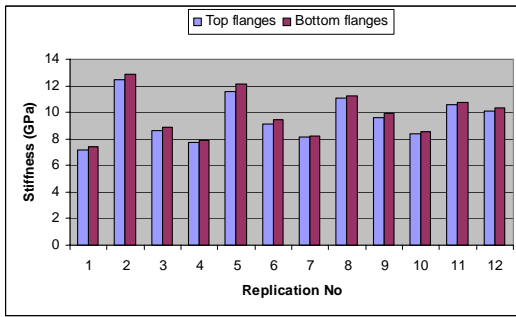


Box Beam- Average MoE of four sets



Filled Box Beam- Average MoE of four sets

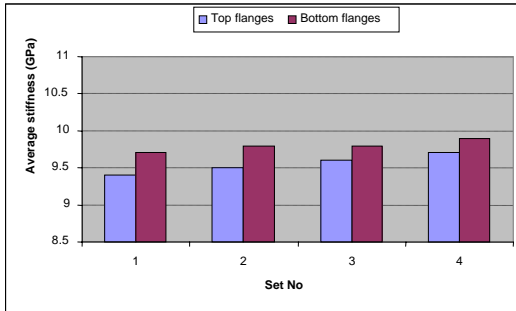
Figure 3.14 Continued



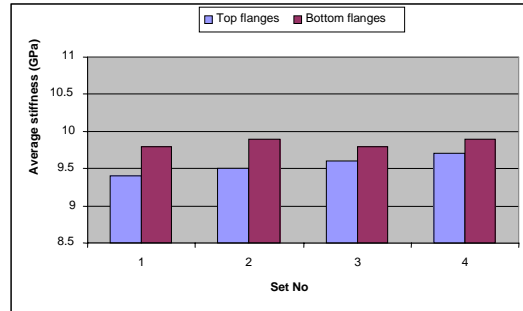
Boxed I-beam-Distribution of MoE within top and bottom flanges



Filled Boxed I-beam-Distribution of MoE within top and bottom flanges



Boxed I-beam- Average MoE of four sets



Filled Boxed I-beam- Average MoE of four sets

Figure 3.14 Continued

3.4.1.2 Assigning the ID number for the beams with LVL flanges

There was no need to apply the statistical method to obtain a balanced distribution of material properties among the various groups which were made with LVL flanges. This is because of the consistency of structural properties among the LVL products. However, ID numbers were assigned to these beams with LVL flanges to identify the various designs during the testing procedures.

ID numbers were tabulated in Appendix A, where Table A.13 concerns the short beams and Table A.14 concerns the long beams. These two tables along with Tables A.11 and A.12 can be used as the keys for identifying the profile base on their Beam ID. In these tables each design is given a name, as follows:

- | | |
|-----------------------------|---------------------------------------|
| 1. <i>I-beam</i> | 9. <i>Boxed Double I-beam</i> |
| 2. <i>LVL I-beam</i> | 10. <i>Filled Double I-beam</i> |
| 3. <i>Double I-beam</i> | 11. <i>Filled LVL Double I-beam</i> |
| 4. <i>LVL Double I-beam</i> | 12. <i>Filled Recessed beam</i> |
| 5. <i>Recessed beam</i> | 13. <i>Filled Box beam</i> |
| 6. <i>Box beam</i> | 14. <i>Filled Boxed I-beam</i> |
| 7. <i>Boxed I-beam</i> | 15. <i>Filled LVL Boxed I-beam</i> |
| 8. <i>LVL Boxed I-beam</i> | 16. <i>Filled Boxed double I-beam</i> |

3.5 MoE variation between the timber and LVL

Table 3.2 contains comparative values of MoE for LVL and NZ timber. $E_{0.05}$ and $E_{0.95}$ define the MoE of lower 5% and upper 5% of normal distribution graph. These two values are used in the equations 3.1 and 3.2 (Gulvanessian ... (et al.) 2002).

$$G_{k, \text{inf}} = \mu_G - 1.645 \sigma_G \quad (\text{Equation 3.1})$$

$$E_{0.05} = E_{\text{mean}} - 1.645 \text{ StDev}$$

$$G_{k, \text{sup}} = \mu_G + 1.645 \sigma_G \quad (\text{Equation 3.2})$$

$$E_{0.95} = E_{\text{mean}} + 1.645 \text{ StDev}$$

Table 3.2 Comparing the MoE of the LVL and NZ timber

NZ Material	No	E_{min}	E_{max}	E_{mean}	$E_{0.05}$	$E_{0.95}$	StDev
		(kN/mm ²)					
LVL	26	10.20	12.87	11.54	10.19	12.89	0.82
Timber	348	5.36	16.73	9.25	5.66	12.84	2.18

As Table 3.2 shows, the standard deviation for LVL samples was only 0.82 while that for timber reached 2.18. Also, the range between $E_{0.05}$ and $E_{0.95}$ for LVL is limited to 10.19 to 12.89 kN/mm², while it is 5.66 to 12.84 kN/mm² for timber. These test results show more evidence of material consistency in LVL.

3.6 Moisture content of the beams

The effect of the moisture content on mechanical properties of wood is well addressed in Bodge and Jayne 1982, Hoffmeyer 1995, Gaylord et al 1996 and Smith et al 2003.

Increasing the moisture content decreases the mechanical properties and vice versa. Hoffmayer states that one percent change in moisture content results 2% change in modulus of elasticity, 3% change in shear strength parallel to grain and 4% change in modulus of rupture parallel to grain.

After completion of the manufacturing, moisture content of the top and bottom flange of each beam was measured by using a capacitance-type moisture meter. The measurement was taken at 3 points, at both ends and at mid-length of the beams: results appear in Tables A.15 and A.16 in Appendix A. Top and bottom timber flanges had average moisture content of 12.09 and 12.03 % respectively, with standard deviations of 0.951 and 0.995 as shown in Table 3.3 and Figure 3.15. Top and bottom LVL flanges had average moisture content of 15.26 and 15.04 % respectively with standard deviations of 1.169 and 1.147 (Table 3.3 and Figure 3.16).

Table 3.3 Distribution of the moisture content after assembling the beam

Timber flanges							
Flanges	No	M_{min}	M_{max}	M_{mean}	$M_{0.05}$	$M_{0.95}$	StDev
		(%)	(%)	(%)	(%)	(%)	
Top	148	9.50	14.70	12.09	10.53	13.65	0.951
Bottom	148	8.70	14.30	12.03	10.39	13.67	0.995
LVL flanges							
Top	52	12.90	17.30	15.26	13.34	17.18	1.169
Bottom	52	12.50	17.30	15.04	13.15	16.93	1.147

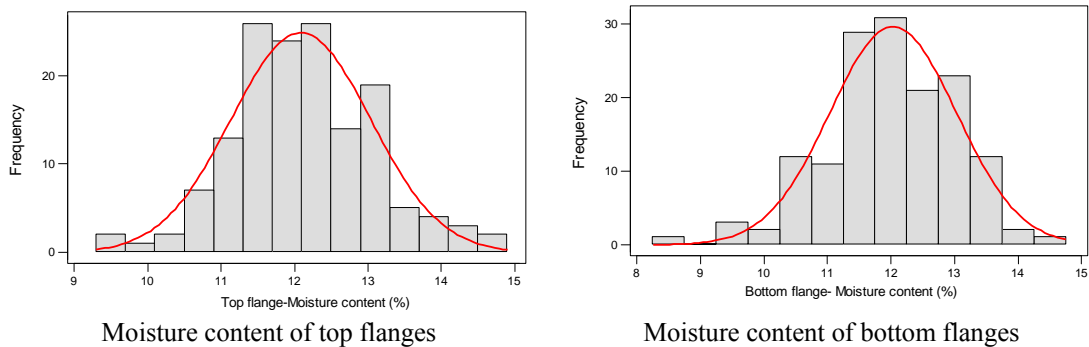


Figure 3.15 Distribution of the moisture content for top and bottom timber flanges

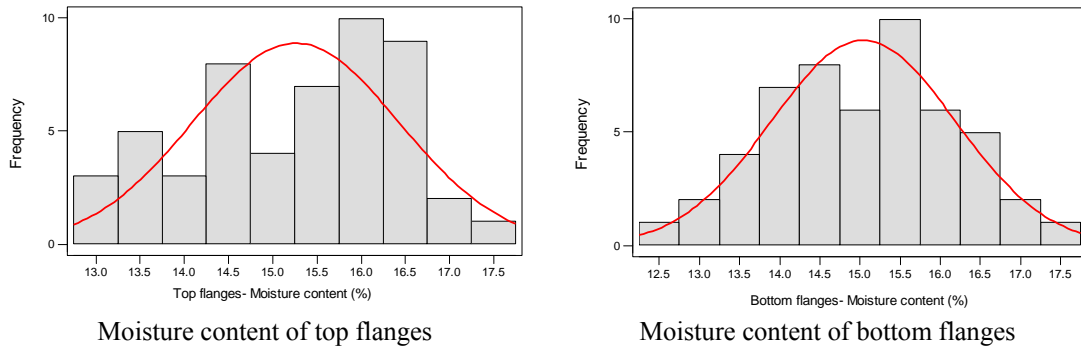


Figure 3.16 Distribution of the moisture content for top and bottom LVL flanges

Trimming the beams

All the short beams were trimmed to be 2.30 meters long and were marked for three and four point load testing. The short beams were marked so that they could provide a 2.10 m span for the three and four point bending test. Long beams were trimmed to be 4.80 meters long and also were marked for three and four point bending tests. As explained in chapter four, long beams were tested over three point bending at 4.50, 3.00, 2.10 and 1.45 m spans and four-point bending at a 4.35m span.

3.7 Using the injected polyurethane

In this project injected polyurethane was used as filling material instead of the conventional polystyrene sheets. The product has the commercial name ENDURATHANE 3225-100R. Two components are involved, namely Isocyanate and Polyol which can be mixed by a volume ratio of 100:100 or by a weight ratio of 108:100 and the cured foam has density of 32 kg/m^3 with compressive strength of 150 kN/m^2 (Endurathane product data 2000).

To inject the polyurethane one end of the beam has to be sealed, while the other end has a moveable cap. This Cap acted as a safety valve and it was forced open when the volume inside the beam was filled with foam. An opening of 3 mm diameter was made every 500 mm along the web. Foam was injected inside the beam through the first opening, and then through the second and so on until the beam was filled. Each injection required 100 seconds rise time before the next injection took place. After completion of the process beams were stored nearly a week before the start of tests.

That was six days longer than the 24 hours curing time, which was recommended by the manufacturer.

3.7.1 Advantages of injected polyurethane over polystyrene sheets

Compared to the polystyrene sheets which were used in the initial designs, injected polyurethane has the following advantages:

- It provided a better bonding on both webs and flanges
- It eliminated the need for gluing the polystyrene sheets to the webs and flanges
- It accelerated the manufacturing process

3.8 Weighing the beams

All the CIB beams were weighed, before and after being filled by injected polyurethane. The weight per meter length for each profile is shown in Tables A.17 and A.18 in Appendix A. Table A.17 concerns the beams made with timber flanges and Table A.18 concerns those made with LVL flanges. Weight per meter length is one of the characteristics that could be used for evaluation of the beam. Average weight per meter length (kg/m) for the different profiles both empty and filled are shown in Figures 3.17 and 3.18. At 4.9 kg/m, I-beams possess the lowest weight per meter length, while Boxed-double-I-beams exhibit the highest weight with an average value of 8.7 kg/m. Those profiles made of LVL flanges are significantly heavier than identical ones with timber flanges. For instance, LVL Double I-beams weighted for 6.4 kg/m, while this is reduced to 5.9 kg/m for timber flange Double I-beams. The greater density of the LVL could explain this, as described in section 3.8. The density of the foam was measured for different profiles, as is shown in Table 3.4 where density of the foam is in all cases higher than 32 kg/m^3 , which was the given value in the product data sheet. Comparing the foam density in different profiles shows an inverse relation with the distance between the webs, as distance reduces density increases. For instance, foam density for the 'narrow' Double I-beam and Box Double I-beam is 53.67 and 52.33 kg/m^3 respectively. Moreover, foam density is 36.32 and 35.22 kg/m^3 for 'broader' recessed and box beams respectively.

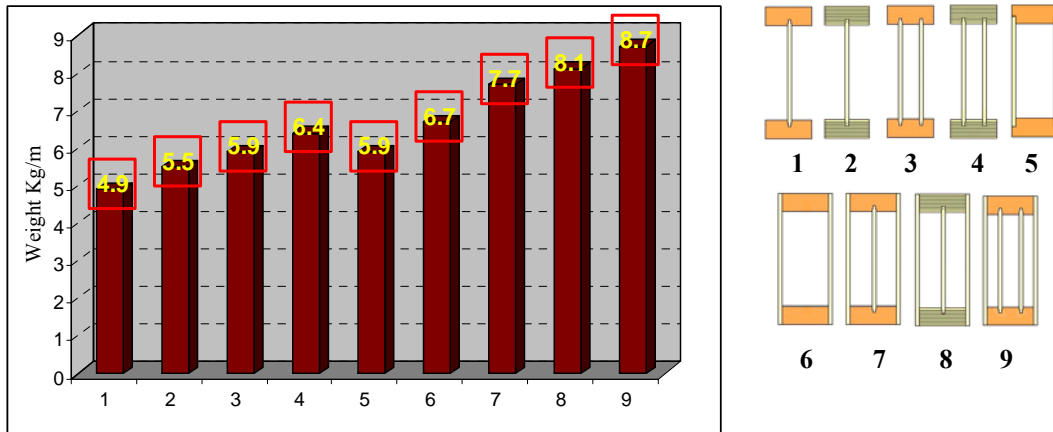


Figure 3.17 Average weight per meter length for the profiles without infill

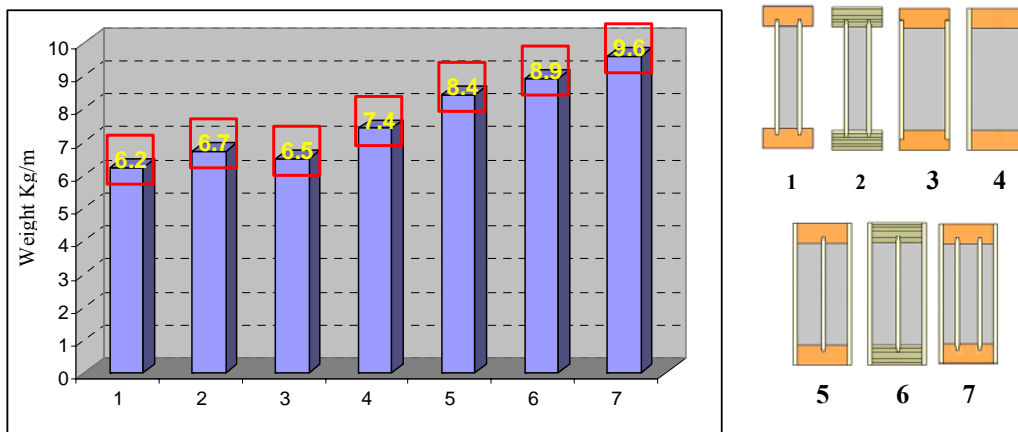


Figure 3.18 Average weight per meter length for the profiles with infill

Table 3.4. Foam density in different profiles

Beams	No	Without infill		With infill		Foam density	
		W/m	StDev	W/m	StDev	D	StDev
		kg/m		kg/m		kg/m ³	
Double I	15	6.00	0.31	6.24	0.31	53.67	3.53
Recessed	15	5.97	0.34	6.48	0.34	36.32	1.25
Box	15	6.74	0.34	7.36	0.39	35.22	1.52
Box I	15	7.74	0.37	8.41	0.30	42.00	2.68
Box double I	6	9.01	0.09	9.74	0.11	52.33	2.68

3.9 Measuring the density of the timber and LVL flanges

Density and moisture content of the timber and LVL flanges were measured by using the oven dried method according to BS 5268-2: 2002. The idea is to establish the relation between the density and E value of the flanges and also to monitor the moisture content of the flanges after testing procedures. A sample was taken from

each timber flange with approximate dimensions $100 \times 87 \times 40$ mm. Because LVL has such uniform density only 20 samples were taken from the LVL flanges. Density of the top and bottom flanges were measured before and after they were oven dried. The histogram and normal curve in figure 3.19 shows distribution of timber density before and after oven drying. A summary of the results for timber and LVL flanges is provided by Table 3.5. Those results show that oven dried samples of timber and LVL have average densities of 437.27 and 496.29 kg/m^3 respectively, while this is 492.72 kg/m^3 for timber and 556.00 kg/m^3 for LVL before drying. So it can be concluded that density of the LVL is 12% higher than the timber even if it is made from same species. This would explain why LVL flange profiles are heavier than their identical ones with timber flanges.

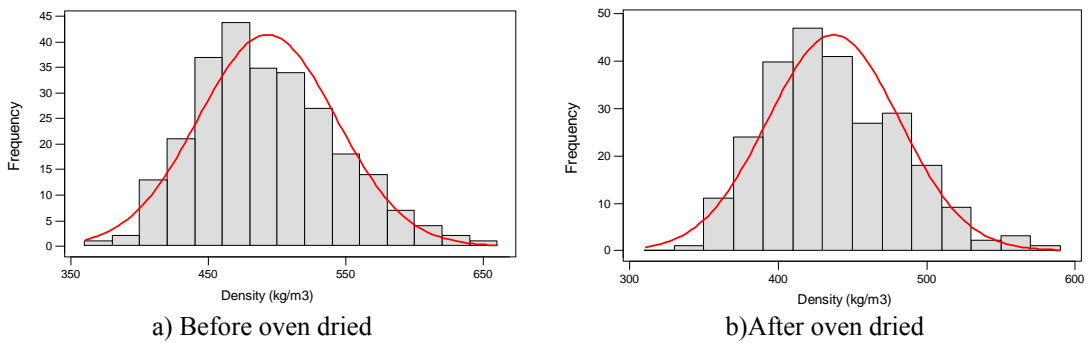


Figure 3.19 Density of the timber flanges before and after oven drying

Table 3.5 Density of the timber and LVL flanges before and after oven drying

Timber flanges							
Density	No	D_{min}	D_{max}	D_{mean}	D_{0.05}	D_{0.95}	StDev
		(kg/m^3)	(kg/m^3)	(kg/m^3)	(kg/m^3)	(kg/m^3)	
Before drying	260	373.50	645.31	492.72	410.32	575.12	50.09
After drying	253	332.67	574.42	437.27	364.46	510.08	44.26
LVL flanges							
Before drying	20	534.25	587.83	556.00	531.09	580.91	15.14
After drying	20	477.26	524.92	496.29	474.20	518.38	13.43

The correlation between density of the samples and their corresponding moduli of elasticity are shown in figure 3.20. The poor correlation between density and MoE is because those samples were not defect free specimens. As reported by Xu 2000 ,

Pellicane & Franco 1994, and Walker 1993 knottiness is recognised to have a negative effect in material properties of the timber. Furthermore the study done by Persson 2000, showed that there are other factors such as microfibrils that affect this relationship.

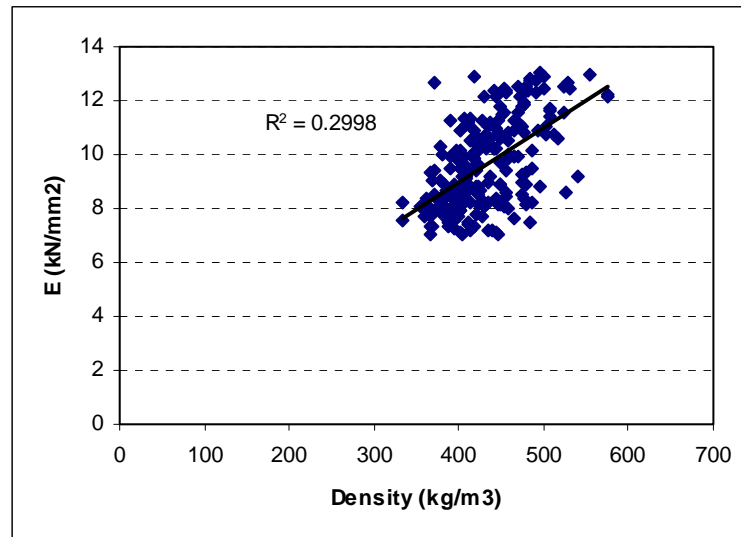


Figure 3.20. The correlation between modulus of elasticity and density

3.10 Manufacturing procedure: stage three

In this stage four different profiles namely, Double I-beam, Box beam, Box I-beam and I-beam were fabricated, but the I-beam samples were to act as reference samples. The testing procedures of the beam components and beam assemblies are similar to those described in stage 2; however, the following differences are identified.

3.10.1 Web and flange materials

In this stage OSB/3 (BS EN 12369-1:2001) was chosen as a web material and mechanically graded timbers, C16 and C24, with published moduli of elasticity respectively 8 and 11 kN/mm² were used as flange materials (BS EN 338 :2003).

3.10.2 Adhesive

Resorcinol-Phenol-Formaldehyde adhesive which is commercially named Aerodux 500 and liquid hardener 501 were used for bonding the webs to flanges (Aerodux 2005). The glue is a weight for weight mix of the resin and liquid hardener. This is because resin and liquid hardener have different densities and mixing them by volume results in uneven consumption of the components.

3.10.3 Testing and grouping the timber flanges according to their stiffness

All the timber lengths were numbered and their moduli of elasticity were determined using a four point bending test based on the recommendations of BS EN 408. Results are given in Tables A.18 and A.19 in Appendix A. A summary of the MoE tests are given in Table 3.6. These test results show that, variation of Young’s modulus is between 4.84 and 20.3 kN/mm² for C16, but between 7.06 and 18.33 kN/mm² for C24. Unexpectedly, it is realised that there is not much difference between C16 and C24 timber. Moreover, the mean and lower 0.05 MoE values of C16 and C24 were higher than those suggested in BS EN 308. Comparing C16 to C24 shows that performance of C16 is similar to C24: see Table 3.6. Histograms and normal distributions of E values for C16 and C24 timber are presented in figure 3.21.

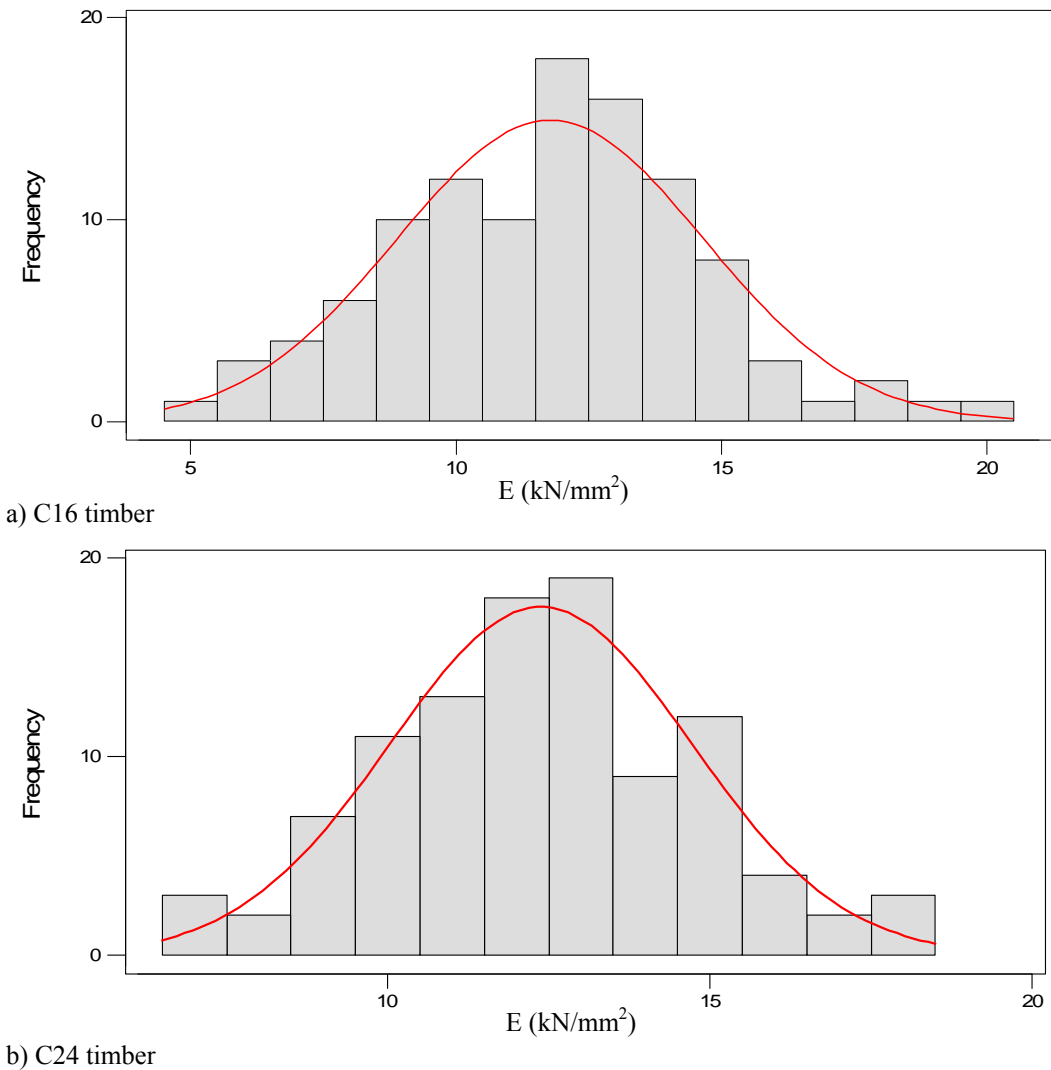


Figure 3.21 Distribution of MoE for C16 and C24 timber

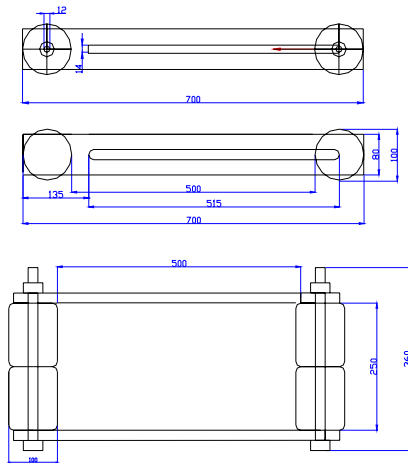
Table 3.6. Comparing the MoE of the C16 and C24 timber

Timber Flanges	No	E_{min}	E_{max}	E_{mean}	$E_{0.05}$	$E_{0.95}$	StDev
		(kN/mm ²)					
C16	108	4.84	20.30	11.77	7.02	16.52	2.888
C24	103	7.06	18.33	12.38	8.52	16.24	2.347
BS EN 338							
C16	---	---	---	8.00	5.40	---	---
C24	---	---	---	11.00	7.40	---	---

The timber was then visually examined for natural defects and divided into three groups namely, double groove, single groove and plain section. The straightest timber was chosen for double groove in order to minimise fabrication problems.

3.10.3 Fabrication of the beams

As was mentioned earlier, this fabrication procedure was similar to the one described in stage 2; however, in this stage a press was designed for assembling the I-beams and Double I-beams. The new roller press is shown in Figure 3.22 and it proved more efficient than the previous method, which is described in stage 2 for assembling the I-beams and Double I-beams.



a) Roller press dimensions



b) Passing the beam through Roller press



c) Over view of the roller press

Figure 3.22 Using roller press to assemble the Double and I-beam

3.11 Chapter summary and conclusions

This chapter has presented the manufacturing procedures for the beams in each of the three stages of work. Some key points taken from this chapter are:

- In stage one it was discovered that fabricating the beam with SIPs was difficult, as it need two different types of glue and it was not possible to taper the OSB faces.
- In stage two, manufacturing methods for different profiles are described. Manufacturing the different profiles showed that there is no need for mechanical fasteners, because proper bonding between web and flange is provided by using Resorcinol adhesive.
- The difficulty of clamping the long I and Double I beams with timber and LVL flanges was discovered.
- Testing the flange modulus of elasticity revealed lower values than were claimed by the NZ timber manufacturer.
- A statistical method was explained and was used to sort the timber flanges into profiles to which the Young Modulus could be evenly assigned. The outcome was that comparable beams were obtained within each group and also among different groups.
- Injected polyurethane is proved to be a suitable substitute for the polystyrene sheets, which had been used in stage one. Using injected polyurethane meant that beam frames could be assembled without any limitations imposed by SIPs and no glue was required to bond the polyurethane with webs and flanges.
- Measuring the foam density showed that it is always more than the level claimed in the manufacture data sheets (32 kg/m^3).

- Experimental work also showed that density of the infill material has an inverse relation with the distance between the webs. As the web distance decreases polyurethane density increases.
- A poor relationship was found between the modulus of elasticity and density, because other factors like knot area ratio and microfibril presence need to be considered in timber.
- In phase three, the Young modulus of the C16 and C24 timber flanges was tested and unexpectedly showed that C16 has an E_{mean} close to C24. Furthermore it was shown that E_{mean} and $E_{0.05}$ of C16 are significantly higher than that is suggested in BS EN 308.
- Roller clamps were designed for clamping the long I and Double I-beam and they proved to be an answer to the clamping difficulty faced in stage two.

Chapter 4: Testing procedures

This chapter describes the structural and durability testing procedures which were carried out on CIB beams in two stages.

- Stage one describes the testing procedures carried out in NZ SCION Research centre and is sub-divided by the nature of the tests:
 1. Structural tests
This section details the testing programme on CIBs, together with I-beams, Glulam and LVL beams. Several series of non-destructive and destructive tests were conducted to evaluate the structural properties of the beams.
 2. Durability tests
Durability tests were conducted to evaluate the structural performance of the beams before and after exposure to extreme weathering conditions.
- Stage two describes the complementary testing procedures, which were undertaken in the Structural Laboratory at Napier University. Only a brief explanation is provided in this section, because of the similarity of the testing in stage two and stage one.

Load testing

Methods of structural testing are improving rapidly. In metal structures, strains can be measured and associated to stresses, but this method is not applicable to the same extent to timber structures, due to the non-isotropic nature of timber and of timber products making it more difficult to test than more consistent materials such as steel or concrete. Nevertheless, it is possible to carry out meaningful load testing of timber or timber based structures. The purpose of static load testing is to determine the critical relation between loads and displacement. This in turn could define the capacity and safety of given structures. (Goldstein 1999, Schrieve 1980)

Non-destructive test measurements

There exist many viable non-destructive methods for evaluation of the mechanical properties of timber and timber products. Some of those now in use are listed below:

- Measurement of strain fields using laser-optical devices
- Recording changes induced by climate using an exposure test cabinet or a climate chamber
- Recording displacements, loads, strains, temperatures, using multi-channel measurement amplifiers
- Determining the dynamic modulus of elasticity by means of flexural vibrations
- Moisture content measurements using a Wood Moisture Meter

Destructive testing

In order to investigate the mechanical properties of timber and timber products, it is necessary to carry out destructive tests as well as non-destructive tests. In general conducting destructive tests is expensive and time consuming. If the number of test specimens destroyed is small, caution should be taken in interpreting the results, as they may not represent the whole range. Two destructive testing methods are listed below.

Determination and measurement of:

- Tensile, compression , bending, shear and torsion strengths
- Displacements and strains

4.1 Structural tests of CIBs

Test apparatus was setup to evaluate the stiffness and strength of the beams. Stiffness is proportional to Young's Modulus of Elasticity, which is proportional to the load/deflection value. The strength of the material controls its suitability for the intended purpose, so the performance of CIBs in bending, shear and bearing defines its potential applications.

This section describes the testing procedure for short and long manufactured-beams, together with Glulam and LVL beams. The term ,short beam, refers to beams with 2.10 m span; whereas long beam, refers to those that could have maximum span of 4.50 m. Manufactured-beams means those beams fabricated in NZ SCION or at the Napier University, Structural Laboratory.

4.1.1 General features of the beams

Manufactured beams have these characteristics:

1. Two cross-sectional sizes 290×88 mm and 290×106 mm,
2. Beams of each cross-section were made in both lengths of 2.4m and 4.8 m.
3. Timber flanges of 90 × 45mm were matched together according to their stiffness, but LVL flanges of 90 × 45mm had uniform properties, so they were not matched.
4. 9 mm three ply-plywood webs jointed with a tongue and groove profile into long lengths with face grain vertical to give good vertical load-bearing strength.
5. The connection between webs and flanges was provided by precision machined tapered glued joints or by laminated joints or by a combination of both.
6. All glued joints used formaldehyde adhesives for strength, durability and moisture resistance.

Full details were provided in chapter 3 on manufacturing the CIBs.

4.1.2 Describing the testing scheme- stage one

The experiments were intended to determine structural performance of the CIBs. Non-destructive tests preceded destructive tests. The non-destructive tests comprised: evaluation of the modulus of elasticity in bending, determination of apparent modulus of elasticity and determination of the shear modulus. Destructive tests comprised those to determine the maximum shear, maximum bending and maximum compression values for CIBs.

The study was then extended to investigate structural performance of those short beams, where a circular hole had been cut into their webs. The effects of four different hole diameters, 76, 102, 126 and 152mm or 3, 4, 5 and 6 inches, were investigated for most of the designs.

A testing procedure was also designed to investigate the maximum pulling resistance for the I-shaped sections with one or two webs.

Finally, a comparative study was undertaken between the manufactured-beams and existing engineered wood products. Solid sections of LVL and of Glulam beams were tested using the same procedure as for testing the CIBs and I-Beams. In order to have consistent results, each test was repeated at least 3 times, and in some cases they were replicated six times. The following pages describe the testing procedures in detail.

4.1.3 Testing the short beams

This section explains the five different testing procedures which were used to evaluate the structural properties of the short beams. Tests included:

1. Identifying stiffness of the beams using the three-point-bending test.
2. Finding the shear strength and stiffness of the beams using a four-point-bending test.
3. Investigating effects of hole-size on reduction of stiffness and shear capacity of the beams using three and four-point-bending tests.
4. Discovering maximum acceptable loading using compression / crushing tests.
5. Determining tensile strength of web to flange joints using a pulling test

Each of the above tests is described individually and the overall procedure for assessing the short beams is summarised as a flowchart in Figure 4.1, which illustrates the sequence of tests on the short beams.

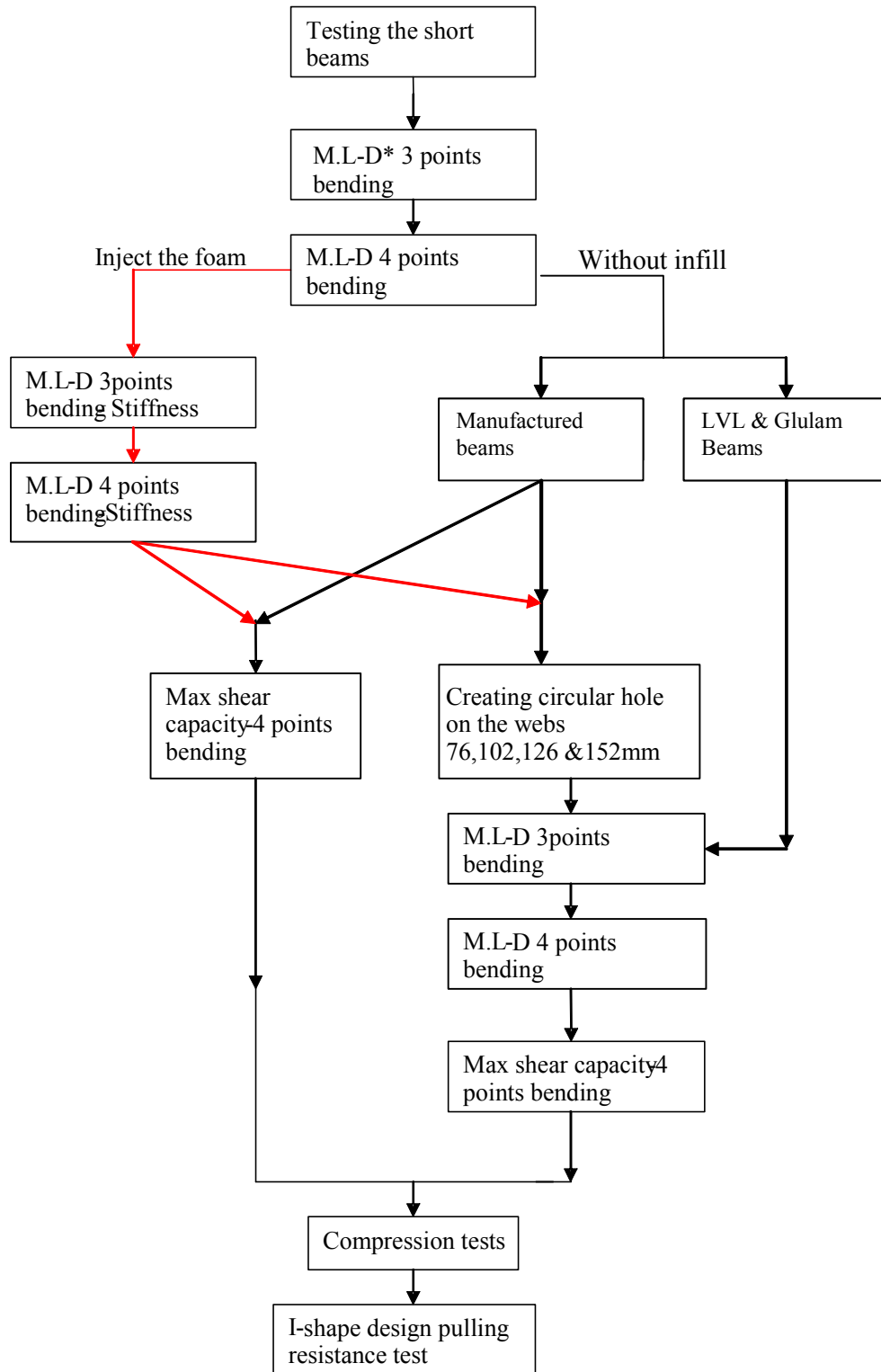


Figure 4.1 Testing procedures for evaluating the short span beams (2100 mm)

*M.L-D: Measuring load-deflection

4.1.1.1 Stiffness tests, three-point-bending

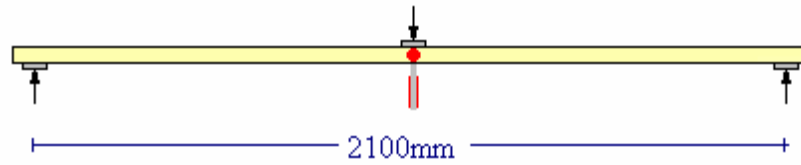
The short beams were simply supported at each end of a 2.10m span and loaded at the mid-point of the top flange as shown in Figure 4.2. Loads and deflections at mid-span were recorded continuously so that the apparent modulus of elasticity could be determined. The loading machine was adjusted to 0.05mm/s speed and beams were tested to no more than 25% of maximum loading capacity of the profile, to avoid structural damage to the specimen.

4.1.1.2 Shear strength and stiffness tests, four-point-bending

Beams to be tested, were simply supported at the ends of 2.10 m spans. The top flange was loaded at two points each of which was 600mm away from the nearest end support, so the distance between the load points was 900mm as shown in Figure 4.3. The beams were loaded to destruction at the chosen points. The 100mm bearing length was adequate to produce shear failure rather than bearing failure in the support area.

Loads and deflections were recorded continuously so that maximum shear capacity, apparent stiffness, bending plus shear, could all be determined over the given span. Manufactured beams were tested to maximum load. When the aim of the test was only evaluating the stiffness of the beam, as in the three point bending stiffness tests, beams were loaded to a fraction of maximum loading capacity so that they were not structurally damaged but load was sufficient to determine the young modulus. TR 002 and BS EN 408 were used as guidelines. The sequence of tests is summarised below:

- Testing the non-filled short beams to measure apparent modulus of elasticity, using three-point-bending and four-point-bending techniques.
- Testing the filled short beams to measure apparent modulus of elasticity using three-point-bending and four-point-bending before and after injecting the foam. The first reading gave a base figure and the second indicated change due to presence and effect of the foam.
- Measuring shear capacity of the filled and non-filled beams using the four-point-bending technique.



a) Measuring load deflection under three point bending

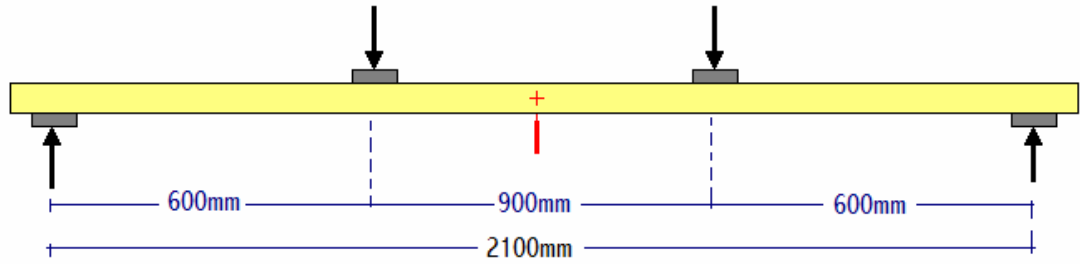


b) Testing filled LVL double I-beam under three point bending



c) Testing Boxed I-beam under three point bending

Figure 4.2 Non destructive testing procedure for short beams under three point bending



a) Measuring load deflection and shear capacity of short beam under four point bending



b) Filled LVL double I-beam under four-point-bending



c) Boxed Double I-beam under four-point-bending

Figure 4.3 Test arrangement for measuring load-deflection and shear strength under four-point-bending

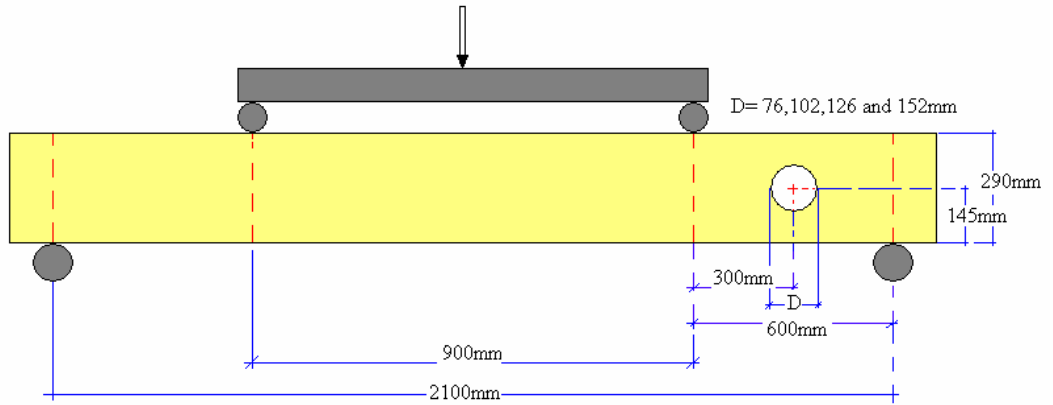
4.1.1.3 Testing the beams that contained web-openings

One hundred 290mm deep beams each containing a circular hole were loaded over their full span of 2.10m. Hole diameters chosen were 76mm (3 inches), 102mm (4

inches), 126mm (5 inches) and 152mm (6 inches). The hole was placed within the maximum shear region. The hole was cut through the webs of the beam and the centre of the circular hole was placed 300mm from the support and 145 mm from the top or bottom flanges. Beams were loaded to destruction and load/deflection measurements were made, so that the effect of the opening on beam stiffness and maximum shear capacity could be determined. Figures 4.4(a) and 4.4(b) show the arrangements for these tests, while figures 4.4(c) and 4.4(d) are post-failure illustrations of the filled Boxed I-beam and Double I-beam with 152 and 102 mm diameter holes respectively.

Testing procedures can be summarised as:

- Testing the short empty and filled beams to measure apparent modulus of elasticity using three-point-bending and four-point-bending both before and after making an opening through the webs.
- Measuring the maximum shear capacity of empty and filled beams using four-point-bending after making an opening through the webs



a) Test arrangement to evaluate the effect of a web opening on MoE and shear strength



b) Filled Box I-beam with web opening of 152 mm



c) Filled Box I-beam after failure



d) Double I-beam with web opening of 102 mm after failure

Figure 4.4 Test arrangement of the CIBs with a web opening

4.1.1.4 Compression / Bearing tests

Specimens for compression tests

After completion of the maximum shear tests, the sound (undamaged) part of each beam was separated from the broken part. Those elements were sized to a length of 1.40 meters to provide a 1.20m span for compression tests.

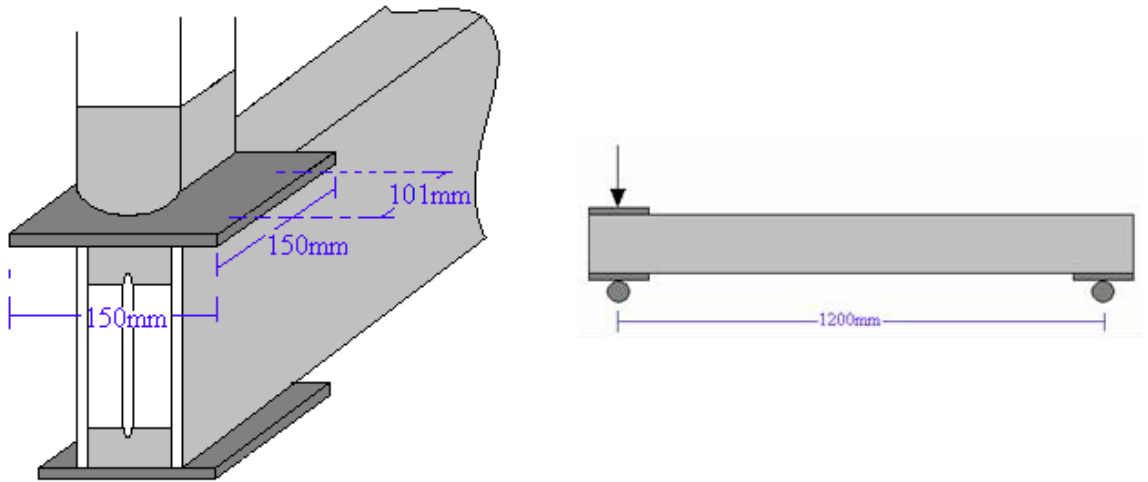
Description of the compression tests

These tests were carried out to determine the bearing capacity of the manufactured beams under concentrated load.

The beams were supported on two 150mm bearing plates at the ends of a 1.20m span. The top flange at one end of the beam was loaded to failure above the end support. The maximum load and the mode of failure were both recorded. Figures 4.5(a) shows the compression test arrangement and 4.5(b) shows the filled LVL double I-beam undergoing the bearing test. The movement rate of the loading head was set to 3mm per minute, which is much lower than 0.003 height of the beam mm/s, which is the value suggested in BS EN 408.

Summary:

- Testing the manufactured beams which had a timber or LVL flanges, with and without infill material



(a) Bearing test arrangement



(b) Filled Double I-beam under bearing test

Figure 4.5 Test apparatus for compression test

4.1.1.5 Pull out test

This test is specified by neither European nor British standards. For this purpose an in-house method was developed by the author and by Dr Bryan Walford to measure the maximum tensile strength of the flange to web joint.

4.1.1.5.1 Making the pull-out test apparatus

It is recognised that I-shaped designs, I-beams and Double I-beams, may be subjected to loads hanging on the edges of the bottom flange. Such loads could cause tensile failure within the component or element separation and that tendency had to be investigated.

The testing apparatus comprises two set of fingers, which fingers provide grips for holding the top and bottom flanges. The number of fingers can be either two or three, depending on the profile being tested. These fingers are connected to two U-shape frames which are in turn connected to a testing machine which moves the frames apart. The fingers and U-shaped frame are connected by steel bars which pass through circular holes made in each side of the fingers. These holes allow the steel bars to move easily through the fingers. The testing apparatus and two different test rigs are shown in figures 4.6(a) and 4.6(b).



(a) Testing the pulling resistance of an I-Beam



(b) Testing the pulling resistance of a Double I-Beam

Figure 4.6 Test rig for pulling test

4.1.1.5.2 Description of the pull-out test

One hundred millimetre lengths were cut from the undamaged ends of previously tested beams. The flanges were held within the fingers and pulled apart. The maximum load and mode of failure were recorded.

4.1.2 Testing the long beams

The aim of this testing procedure was to obtain the required data for calculating the modulus of elasticity in bending E_m , the apparent modulus of elasticity $E_{m,app}$, the shear modulus G and the maximum bending capacity of beams over 4.50 and 4.35 meter spans. The flowchart in Figure 4.7 shows the testing program which was developed to assess the structural properties of long, manufactured-beams.

Three-point-bending and four-point-bending tests were performed for the entire range of manufactured-beams. The results of these tests were then used to determine the apparent modulus of elasticity using both bending arrangements and to find the maximum bending capacity of the beams.

Two methods were used for measuring the shear modulus. In the first method, the shear modulus could be determined by calculating $E_{m,app}$ and E_m for each long beam, whereas in the second method, shear modulus could be determined by

calculating the apparent modulus of elasticity $E_{m,app}$ for each beam over four different spans.

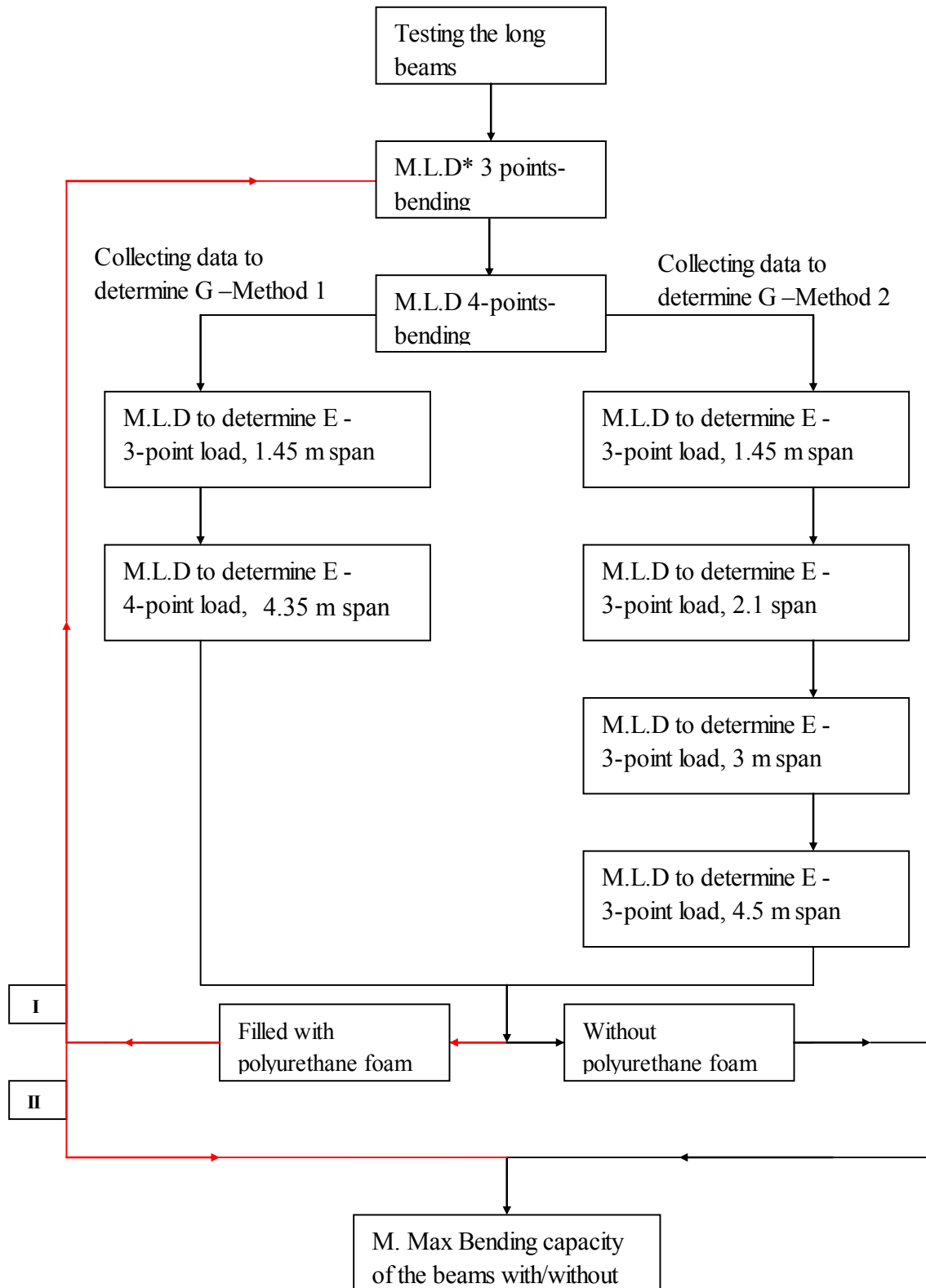


Figure 4.7 Shows the testing program which was developed to assess the long beams *M.L-D: Measuring load-deflection

4.1.2.1 Long span bending tests-three-point-bending

A simply supported beam was loaded at the centre point, causing bending over a span 4.50 m long. Load and deflection were continuously recorded, so that the apparent modulus of elasticity could be calculated: see Figures 4.8(a) and 4.8(b).

- Measuring apparent modulus of elasticity of each beam before and after it was filled with injected polyurethane using the three-point-bending method.

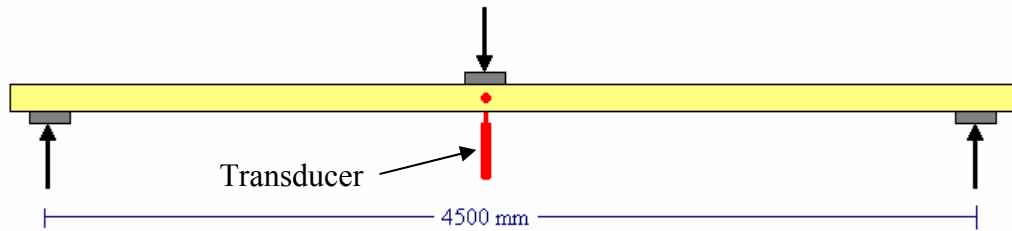


Figure 4.8 (a) Test arrangement to measure the load-deflection of the beam subjected to three-point-bending

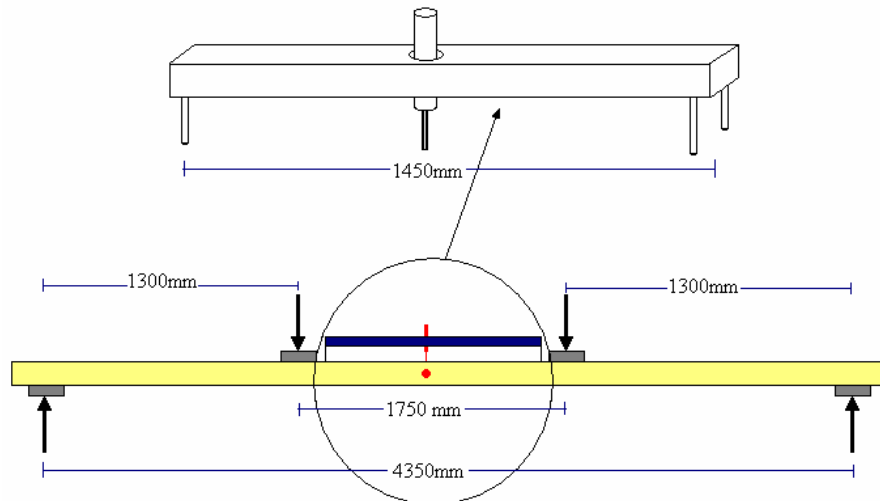


Figure 4.8 (b) Three points load test rig to measure load-deflection of filled boxed I-Beam over a 4.5m span

4.1.2.2 Determination of shear modulus - method one

Determination of modulus of elasticity in bending

Manufactured-beams 290mm deep were tested, simply supported at the ends giving a 4.35m span loaded by two loading heads. Each loading head was placed 1.30 m from the nearest support and 1.75 m from each other as shown in Figures 4.9(a) and 4.9(b). The aim was to measure the load deflection and from that to calculate the MoE under pure bending moment.



(a) Test arrangement to determine MoE in pure bending



(b) Measuring MoE in bending for double I-beam

Figure 4.9 Test arrangement and measurement of MoE in bending

Describing the apparatus and testing method

In order to measure relative deflection within pure bending area, a stand 1.45m long was made. That stand sat between two loading heads. A transducer was planted in the middle of the stand to measure the mid-span deflection relative to the legs of the stand. Figures 4.10(a) and 4.10(b) show the stand and the testing arrangement. Load-deflection results were recorded in order to determine the E_m .

- Measuring the load and deflection relative to supports and the stand legs for beams subjected to four-point-bending before injecting the polyurethane. This procedure was repeated after injecting the foam.

After completion of the preceding tests, the same beam was tested over a span of 1.45 meters with two end supports as shown in Figures 4.10(a) and 4.10(b). The beam was loaded at the centre point. Load and deflection relative to the supports was monitored continuously and the data was recorded to determine the $E_{m,app}$.

Summary:

- Measuring load-deflection relative to the supports for the beams subjected to three-point-bending before injecting the polyurethane. The procedure was repeated for the beams after foam was injected.

Shear modulus G , then can be calculated from the modulus of elasticity in bending E_m and the apparent modulus of elasticity $E_{m,app}$.

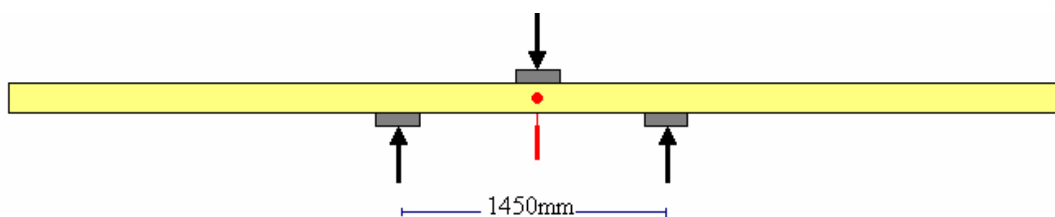


Figure 4.10(A) Test method to determine the apparent MoE over 1450mm span



Figure 4.10(B) LVL section subjected to three-point-bending over a 1450mm span

4.1.2.3 Determination of shear modulus - method two

In this method each beam was loaded at the middle point and was simply supported over spans measuring 4.50, 3.00, 2.10 and 1.45 meters, as shown in Figure 4.11. The load-deflection data was continuously recorded. Shear modulus G , could be determined by calculating the apparent modulus of elasticity of each beam for four different spans.

Summary:

- Measuring load-deflection relative to the support for beams subjected to three-point-bending over four different spans, before and after injecting the polyurethane.

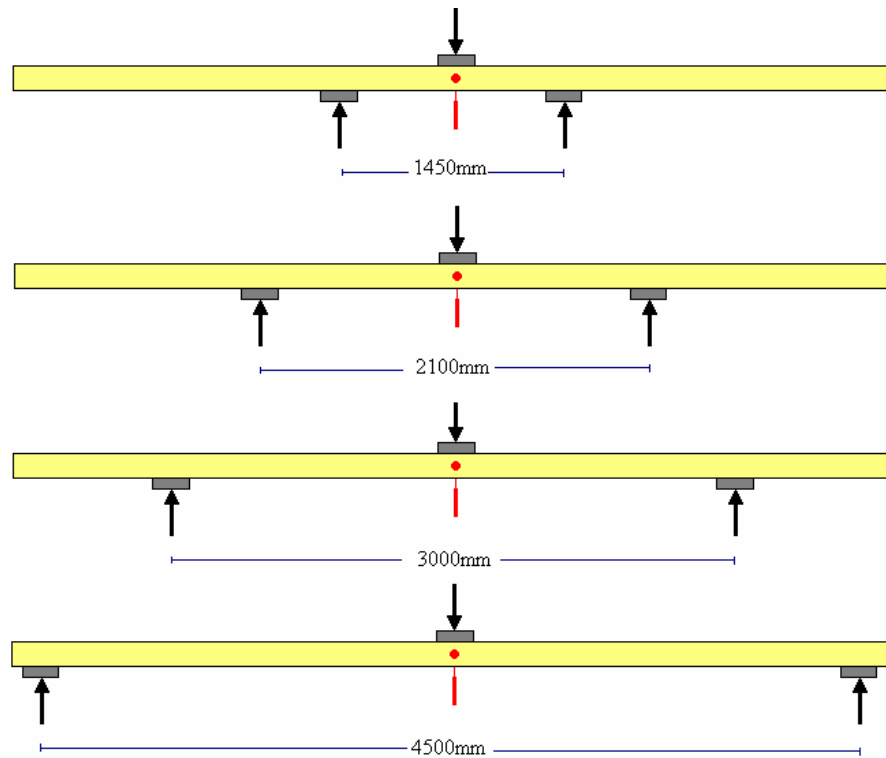


Figure 4.11 Test methods to measure E_{app} over 1.45, 2.10, 3.00 and 4.00 m spans

4.1.2.4 Long span bending tests, four-point-bending

Manufactured beams 290mm deep were tested to destruction each was simply supported at the ends of a 4.35m span and loaded with two loading heads, which were placed at 1.30 meters from the nearest support and 1.75 meters from each other. Loads and deflections were recorded continuously so that maximum bending moment and overall stiffness, bending plus shear, could be determined over the maximum span. The test arrangement is illustrated in figure 4.12.

- Measuring load-deflection relative to the supports for the beams subjected to four-point-bending without filling material. This procedure was later repeated for filled beams.
- Measuring maximum bending capacity of both empty and filled beams subjected to four point bending.

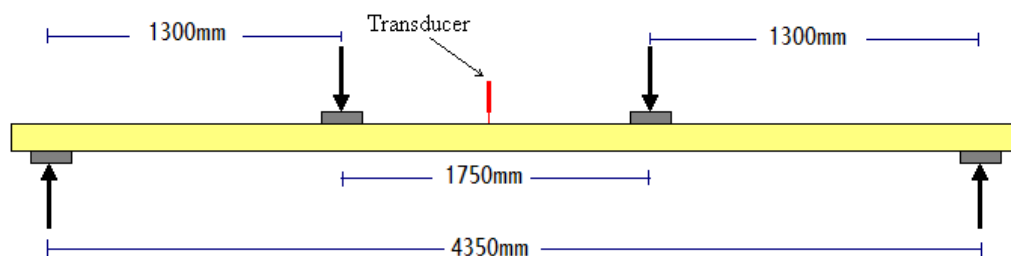


Figure 4.12 Test method to measure load-deflection relative to supports

4.2 Durability/Weathering tests

Tests were carried out to measure the effects of temperature variations and moisture on the mechanical properties of the CIBs in both empty and filled states. In general it is not possible to investigate the long-term effects by calculation, the procedures are entirely experimental. Tests undertaken in this research are described below.

The aim was to evaluate and demonstrate the effect of the polyurethane foam on durability of the beams. In this regard beams with and without infill material was exposed to severe weathering conditions and then the structural characteristics of the beams were assessed. The results from this comparative study were used to determine effect of the infill on long term durability of the beams. This study also assessed the performance of each component of the beams and of the adhesive.

4.2.1 Test specimens

Box beams were chosen for the durability tests. Beams were made of 9mm 3-ply plywood webs and 45×88mm timber flanges. All the 24 beams had the same height (290 mm) and width (106mm). Beams were 2.30m in length to provide a 2.10m span. Half of the beams were filled with injected polyurethane. More details about the manufacturing, numbering and matching process were given in chapter three.

4.2.2 Testing equipment

The following equipment was used for the durability testing procedure:

- Treatment tank
- Timber steaming room
- Kiln dryer
- Freezer
- Universal Testing Machine

- Displacement transducer
- Load cell

4.2.2.1 Treatment tank

The treatment tank is cylindrical, similar to the hull of a submarine, and like a submarine the tank is capable of withstanding high pressures, see Figure 4.13. This facility is normally used to force a mixture of water and preservative into the wood cells under high pressure. The amount of water, the temperature and the pressure could be monitored and adjusted constantly. This facility was used for stage one of the cycling procedure, which required immersion of the sample in water heated to 50° C.



(a)



(b)



(c)

Figure 4.13 Treatment tank used for durability test

(a) Treatment tank

(b) Floating the filled box beams in hot water (50 °C)

(c) Floating the empty box beams in hot water (50 °C)

4.2.2.2 Steaming treatment

This equipment is also normally used as part of a wood treatment process. In this procedure timber was exposed to the steam, which is produced by boiling water at 100 °C before starting the drying process. The steamer is also sometimes used after the drying process; for by exposing timber to high temperature and 100% humidity it is possible to restore the shape of distorted wood.

In this project, to create conditions of environmental stress, the steaming treatment was used in stages two and five as part of a cyclic procedure as shown in Figure 4.14.



Figure 4.14 Exposing the beams to steam and at 100 °C

4.2.2.3 Kiln drying

The kiln was a large oven, which is normally used for drying wet timber by circulating hot air around it. The timber dries by evaporation of the moisture from surface of the timber and by moisture moving to the surface from inside the timber. A kiln could control the temperature, the speed of air flow and sometimes the relative humidity was also controllable.

For research on the box beams the kiln was used to apply hot dry air at 100 °C in stages four and six of each cycle as shown in Figure 4.15. A plot of kiln temperature during several cycles is presented in Figure 4.16 where it is shown, that the temperature remained almost constant at 100 °C throughout.



Figure 4.15 Durability tests- Box beams inside the kiln

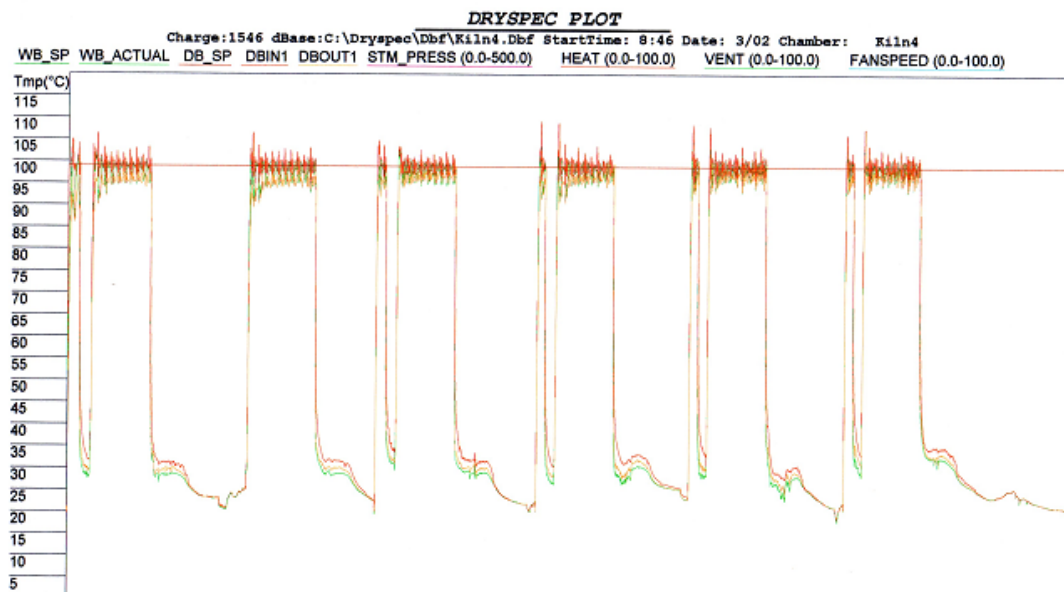


Figure 4.16 Kiln temperatures during the six cycles

4.2.2.4 Freezer

A large industrial freezer (2×2×3 m) was used for stage three of the cyclic test procedure. The freezer was capable of holding the cooling objects at the constant temperature of -20 °C.

4.2.3 Durability test procedures

Currently there is no unified method of measurement for assessing actual durability of most construction products; as a result assessment of the product is undertaken based on a combination of personal experience and published literature (Ratay 2005). Obviously there is no standard or testing procedure for evaluating durability of a CIB, as that is a new product. In order to create the durability tests, extreme weather conditions were identified, which may occur during the life time of the beam. In addition, ASTM C481-99 (1999) standard was used as a guide, because it provides testing methods for evaluating durability of a sandwich panel.

In the procedure developed at SCION, the test specimen was subjected to each of six different weathering conditions in succession and the cycle was repeated six times. The treatments applied to each beam are as follows:

1. Immersed in the treatment tank in hot water (50° C) for one hour
2. Transferred to steam room, where steamed for 3 hours at 100° C.
3. Stored in freezer at -20 ° C for 20 hours
4. Taken to kiln and heated for 3 hours at 100° C
5. Steamed for another 3 hours at 100° C
6. Completed one cycle by drying in the kiln at 100° C for 18 hours

Completion of each cycle took two days, and whole test was completed within 13 days. The time interval between the stages did not exceed thirty minutes. The cyclic procedure continued non-stop until all six cycles were completed. As shown in Table 4.1, 20 minutes was added to the required time of each stage. This additional time was to allow for the transference of the samples from one equipment to another.

The effect of load on deflection and the maximum shear strength of each beam were measured four times during each cycle, first before starting the cyclic procedure and then after completion of each two cycles. In all, six empty CIB and six foam filled CIBs were each assessed four times. The moisture content of the beams before and after the sixth cycle was also measured.

Table 4.1 Time table and sequence of Cycles 1 to 6

Cycle 1						
Date	02-Feb-04-04			03-Feb-04		
Time	2:00 p.m.	3:20 p.m.	6:40 p.m.	3:00pm	6:20 pm.	9:40 p.m.
Duration(h)	1	3	20	3	3	18
Condition	Hot water	Spraying steam	Cold air	Hot dry air	Spraying steam	Hot dry air
Cycle 2						
Date	04-Feb-04			05-Feb-04		
Time	4 p.m.	5:20 p.m.	8:40 p.m.	5:00p.m.	8:20 p.m.	11:40p.m
Duration(h)	1	3	20	3	3	18
Condition	Hot water	Spraying steam	Cold air	Hot dry air	Spraying steam	Hot dry air
Cycle 3						
Date	06-Feb-04			07-Feb-04		
Time	6 p.m.	7:20 p.m.	10:40 p.m.	7:00 p.m	10:20 p.m.	1:40 a.m.
Duration(h)	1	3	20	3	3	18
Condition	Hot water	Spraying steam	Cold air	Hot dry air	Spraying steam	Hot dry air
Cycle 4						
Date	08-Feb-04			09-Feb-04		
Time	8:00 a.m.	9:20 a.m.	12:40 p.m.	9:00p.m.	12:20 p.m.	3:40 a.m.
Duration(h)	1	3	20	3	3	18
Condition	Hot water	Spraying steam	Cold air	Hot dry air	Spraying steam	Hot dry air
Cycle 5						
Date	10-Feb-04			11-Feb-04		
Time	10:00p.m.	11:20 p.m.	2:40 a.m.	11:00p.m.	1:20a.m.	4:40 a.m.
Duration(h)	1	3	20	3	3	18
Condition	Hot water	Spraying steam	Cold air	Hot dry air	Spraying steam	Hot dry air
Cycle 6						
Date	12-Feb-04			13-Feb-04		
Time	12:00 p.m.	1:20 p.m.	4:40 p.m.	01:00 a.m.	4:20 a.m.	7:40 a.m.
Duration(h)	1	3	20	3	3	18
Condition	Hot water	Spraying steam	Cold air	Hot dry air	Spraying steam	Hot dry air

4.3 Describing the testing schemes, stage two

In this stage, I, Double I, Box and Box I, beams of 4.35m span were tested by three-point-bending and four-point-bending tests as shown in Figures 4.17 and 4.18. Compression tests were also carried out for beams of each profile. The testing procedures were similar to those explained in stage one. As explained in chapter three, the dimensions were identical to those in stage one. But the following differences should be noted:

1. In this stage, OSB/3 of 9mm thickness was used as a web material instead of plywood.
2. All the beams were tested over a 4.35m span, so no short-span beams were tested.
3. Lateral support was provided during the four-point-bending test.
4. A uniaxial testing machine, equipped with a hydraulic ram, was used instead of a screw-gear machine.

The results of stage two tests would be compared to those gained from stage one in order to assess the variation in performance of different materials.

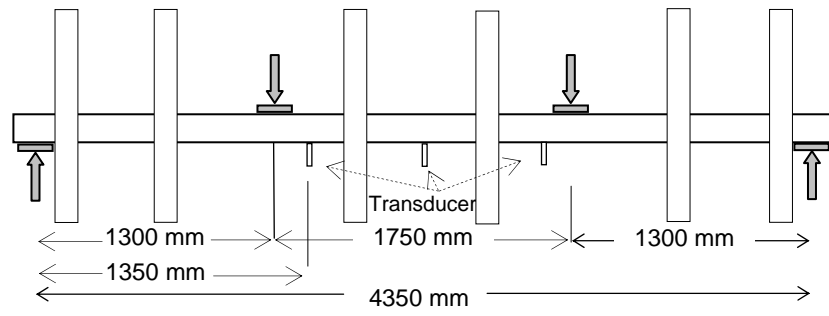


Figure 4.17 Test rig for long span beams undergoing four-point-bending

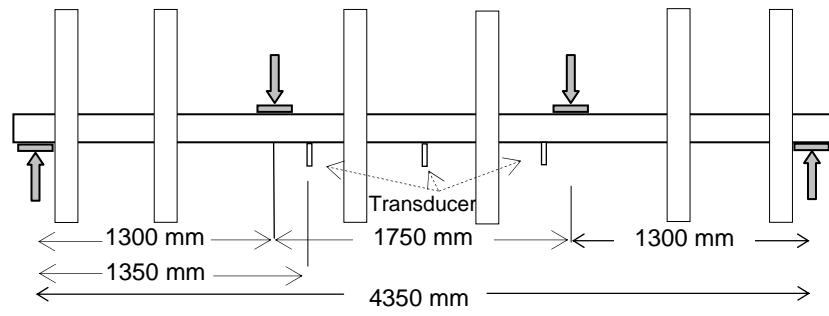


Figure 4.17 Test rig for long span beams undergoing four-point-bending

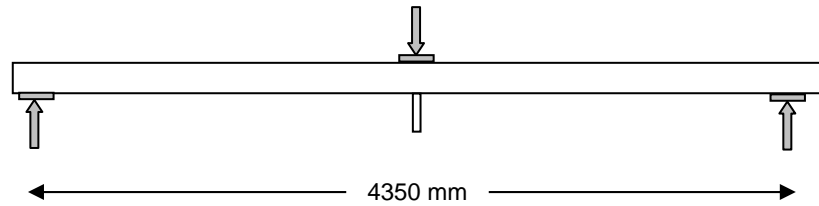


Figure 4.18 Test method for long span beams – Three-point-bending test

4.4 Full scale testing

Tests were conducted to validate the designs by using full-scale beams instead of scaled models. Even though a code of practice provides design procedures, they are not applicable for all types of structure (Ozelton and Baird 2002). In general, prototype testing is carried out to study performance and to determine load-deflection and strength behaviours. Carrying out full scale testing is the only way to examine a new product such as a CIB.

Full scale testing is expensive and time consuming, so care should be taken to plan the procedure properly and make sure that testing conditions represent the real conditions. In consequence, completion of stage one took seven months and stage two took a year to complete.

Full scale testing can be dangerous, so expert supervision is necessary. For instance, during the four-point-bending test a supporting plate shot out of its place by between 4 and 5 meters. In another instance the hydraulic ram was damaged because it could not cope with the deflection speed even though it was being operated at the (mm/s) rate well under 0.003 beam depth specified in BS 408.

Failure occurs fast and sometimes one failure quickly follows another, so video recording the test procedure was useful to review beam behaviour and to understand the actual mode of failure.

4.5 Methods of loading

The mechanical properties of a beam can be verified by using different test machines, but currently mechanical systems and hydraulic pistons such as those used in stages one and two are more common than other methods such as weights and levers.

The mechanical machine

In this method movement of a screw-gear causes displacement of a cross-head. This type of machine is suitable for maintaining a constant rate of displacement or strain (Bodig and Jayne 1993).

The hydraulic machine

In this method movement of the hydraulic piston causes displacement of the cross head (Blake 1985). Employing the hydraulic ram in the universal testing machine widens its capability for testing mechanical properties, for the testing machine can be operated at a constant rate of displacement or at constant rate of loading. In the literature sometimes the constant rate of displacement and the constant rate of loading are regarded as displacement control and force or load control respectively. These two methods of loading create different results beyond the linear limit of elasticity. A constant rate of displacement reduced loading beyond the linear limit. In contrast, a constant rate of loading increased displacement beyond the linear limit (Grandt 2003). In this study all the tests were conducted at a constant rate of displacement.

Strain gauge transducer

In both mechanical and hydraulic systems deformation can be measured by using mechanical, optical, or electrical systems. In this study a linear displacement sensor, called a strain gauge transducer, was employed for recording the deflection. Strain gauge transducers use a calibrated metal plate or beam that undergoes a small strain in one dimension. This mechanical deflection results in a small change in electrical resistance in the gauge wire. Kent and William (1999) state that electrical resistance of a strain gauge is remarkably stable when properly installed; however, improper installation of the gauge and its leads raises the transducer creep under load.

4.6 Summary and conclusion

This chapter described the testing procedures to determine the structural characteristics and long term durability of composite insulated beams (CIBs). Key points and discoveries are reviewed below:

- The difficulty of testing non-isotropic material was addressed and a brief discussion of non-destructive and destructive testing was provided.
- Testing procedures for evaluating the structural performance of the CIBs were explained in two stages.
- CIBs made from solid sections of LVL and of Glulam beams were evaluated in stage one.
- Descriptions were given of stiffness, shear, bending and bearing tests on the empty and filled CIBs together with ready made beams.
- A new pulling test was devised to measure the tensile resistance of I-beams and double I-beams exposed to a hanging load and a testing procedure was described.
- The lack of unified durability testing methods for evaluating the products was noted together with the lack of a procedure for testing the new CIBs.
- Testing procedures for evaluating the long term durability of the CIBs were developed and the testing process was described.
- Stage two of the testing programme was addressed briefly, because of the similarity between the two stages. Stage two comprised the complementary structural tests carried out in the Napier Laboratory. The only difference in the structural tests from stage one was that lateral support or restraint was provided during the four-point-bending tests. However, as explained in chapter three, OSB/3 was used as a web material and no short span beams were fabricated.
- Full-scale testing is expensive, time consuming and could be dangerous, so proper planning and expert supervision is required.
- Full-scale testing is necessary for measuring structural behaviour of the new structural elements.

- Failures in full-scale testing occur fast and sometimes one after the other, so recording the test provides an opportunity for reviewing the failure process and the chance to identify the exact mode of failure.
- Setting the uniaxial testing machine on constant rate of displacement or constant rate of loading creates different results unless testing is undertaken within the elastic limit of the test material. A constant rate of displacement was used in this study.

CHAPTER 5: INFLUENCE OF GEOMETRICAL PROFILES ON THE STRUCTURAL PERFORMANCE OF ENGINEERED COMPOSITE TIMBER BEAMS

5.1 Introduction

This chapter describes an investigation of the strength and deformation characteristics of lightweight timber composite beams manufactured with six different cross-sectional profiles, which are compared with the same characteristics of readily available laminated veneer lumber (LVL) and glued-laminated (Glulam) beams. The engineered profiles comprised solid timber or LVL flanges and three-ply plywood webs. The number of webs varied from one to four. All beams had an overall depth of 290 mm and were either 88 mm or 106 mm wide. A study was conducted to provide a comparison of the beam designs and to determine possible effects of cross-sectional configuration and connection details on the structural properties of the beams.

To enable a realistic analysis, twelve beams were replicated for each design. The individual components of the beams were tested prior to assembly to obtain the modulus of elasticity and shear modulus and were grouped to provide an even distribution of the material properties. The addition of extra webs to the I-beam profile significantly enhanced the bending and shear capacity of the beam while maintaining a high strength to weight ratio. The boxed I-beam proved to be the most efficient to manufacture and displayed superior structural performance compared with the rest of the profiles in terms of flexural stiffness, bending and shear capacity. The experimental results confirmed the significant contribution of shear deflection to the total deflection of I-beams, box beams and even solid section beams.

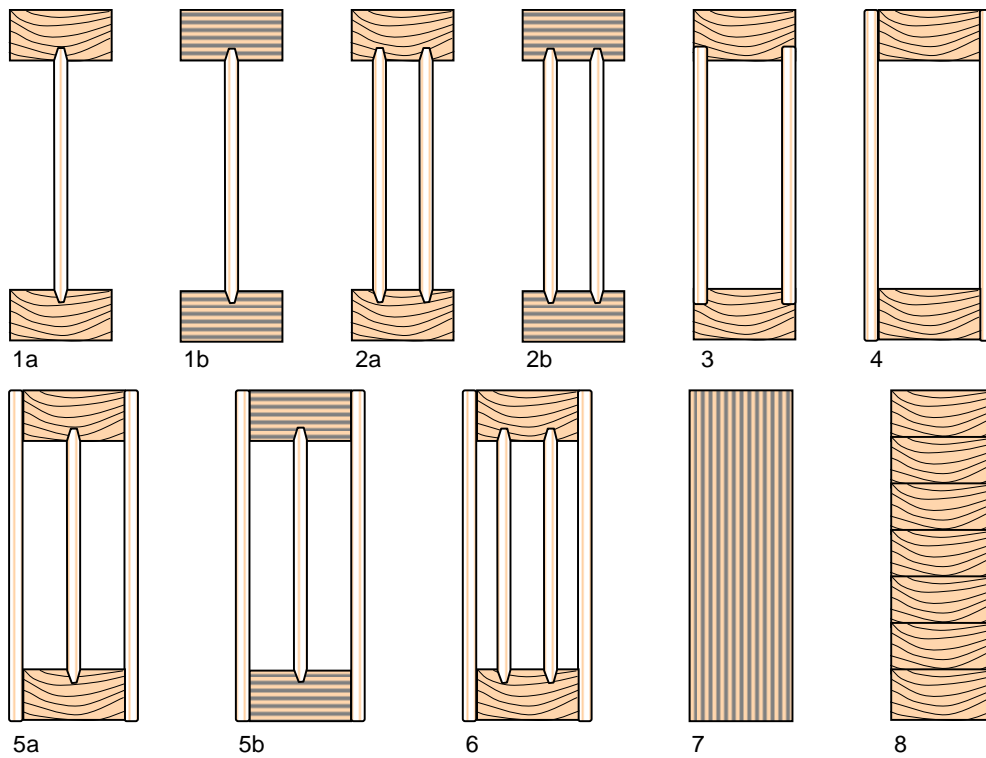
5.2 Background

Engineered timber structural members are products constructed from a combination of timber in its various forms, usually in small sections free from defects, or from wood based products using adhesives or other types of connections such as nails, screws or

staples. Such products are generally stronger, stiffer and more stable than solid sawn timber. The growing use of engineered timber structural components for timber-framed construction is increasing the need for more efficient geometrical properties, longer spans, reduced shrinkage, defect-free characteristics and economical solutions.

Beam members are predominantly subjected to bending, co-existing with shear, bearing and buckling. Besides having sufficient strength capabilities to resist these effects, it is important that the beams have adequate stiffness to avoid excessive deflection or local buckling of the cross-section. Traditionally, only the deflection component of a beam due to bending is considered, since the shear modulus for materials like steel is considerably higher as a percentage of the true elastic modulus than in timber. However, the shear deformation is a significant proportion of the overall deflection of a timber beam or an engineered timber beam. A number of factors, such as the geometrical configuration, the shear modulus of the web materials and the loading type and position, influence the shear deformation of a beam.

This chapter presents that part of a comprehensive study of the structural performance for a range of engineered composite timber beams concerning strength and deformation characteristics. The beams comprise six different cross-sectional profiles, bonded together by adhesives and comprising commercially available solid laminated veneer lumber (LVL) and glued-laminated timber beams, as shown in Figure 5.1. In order to provide a standard basis for comparison, no stiffeners or splice pieces were used. The influences of geometrical, cross-sectional, configurations on the shear characteristics of the engineered composite timber beams were investigated and their influence on the strength and stiffness properties of the beams were determined and compared.



Beams with timber flanges:

- (1a) I-beam; (2a) Double I-beam; (3) Recessed beam;
 (4) Box beam; (5a) Boxed I-beam; (6) Boxed double I-beam.

Beams with LVL flanges:

- (1b) I-beam; (2b) Double I-beam; (5b) Boxed double I-beam.

Solid section beams:

- (7) LVL beam; (8) Glulam beam.

Figure 5.1. Cross-sectional profiles of test beams

5.3 Manufacture of engineered beams

5.3.1 Geometric properties of the beams

In this study, nine types of composite beams with six different cross-sectional profiles were manufactured and two types of solid section, LVL and Glulam beams, were obtained from the market (Figure 5.1). All timber, plywood, LVL and Glulam products used in this study were produced from NZ Radiata pine.

The composite beams had solid timber or LVL flanges 88 mm wide and 45 mm deep and had overall dimensions of either 88 or 106 mm × 290 mm. Nine millimetre thick three-ply plywood of stress grade F11(AS/NZS 2269: 1994) was used for the webs of all composite beams. The solid timber flanges were cut from sections of New Zealand Radiata pine of grade F8 (NZS 3603:1993) and used in Profiles 1a, 2a, 3, 4, 5a and 6. The LVL sections were used for flanges of Profiles 1b, 2b and 5b. Each profile was produced in two lengths: 2.3 m (short beams) and 4.8 m (long beams) for effective spans of 2.1m and 4.35m, respectively. The short beams were replicated twelve times and the long beams three times. A structural adhesive for timber having a liquid hardener, a resorcinol formaldehyde from family of phenolic resin (ORICA, (2003)), was used for bonding the webs to the flanges. Ready-made LVL and Glulam beams were obtained from local manufacturers in New Zealand. Profiles 1a, 1b, 2a, 2b and 3 had overall dimensions of 88 × 290 mm and Profiles 4, 5a, 5b and 6 had overall dimensions of 106 × 290 mm. The solid LVL and Glulam beams were 88 × 290 mm.

Detailed information on manufacturing procedures is given in Chapter 4.

5.3.2 Material properties

Prior to manufacturing and cutting the sections to the desired sizes, a series of tests were carried out to determine the modulus of elasticity, shear modulus, density and moisture content of the timber, plywood and LVL. The modulus of elasticity of the timber and LVL flanges was measured in accordance with AS/NZS 4063 (1992) for both the short and long beams. Flanges were tested under four-point bending.

In order to make a realistic assessment and comparison of the performance of the beams with different geometrical configurations, it was necessary to group the components to provide an even distribution of the material properties and match them accordingly. This ensures each set of specimens comprised a range of components with similar material properties.

The modulus of elasticity of the timber varied from 5.4 to 16.7 kN/mm² with a mean value of 9.5 kN/mm², while more consistent results were obtained for LVL, ranging from 10.2 to 12.9 kN/mm² with a mean value of 11.5 kN/mm². The mean densities of the oven-dried timber, LVL and plywood were 437, 496 and 456 kg/m³, respectively (Table 5.1).

The whole programme lasted four months, from manufacturing to testing, during which the mean moisture content for LVL changed from 15.15% at manufacturing to an equilibrium value of 11.70 % during testing, whereas the moisture content of the timber sections remained little changed from 12.06% to 12.55%.

For plywood, six specimens were randomly selected out of 140 plywood sheets and tested for the modulus of elasticity, modulus of rigidity, moisture content and density. The full results are summarized in Table 5.1. The second moment of area and the section modulus of plywood were determined according to the recommendations of AS/NZS 2269 (1994). Using a transformed section method, to account for the difference in ply properties arising from the different grain directions, together with the test results from samples tested with face grain both parallel and perpendicular to the span, the modulus of elasticity for the plywood was found to be 11.13 kN/mm² and the equivalent thickness of three-ply plywood with face grain perpendicular to the beam span was 3.40 mm. The effective thickness contributed from the veneers perpendicular to the span is specified as only 3% of the thickness from the veneer parallel to the span but from the test results in a higher value of 0.067 was found, which is at least twice the value given in the NZ standard.

Table 5.1. Summary of material properties

Parameters	Unit	No of samples	Min	Mean	Max	Standard deviation
Modulus of elasticity for timber flanges (E)	(kN/mm ²)	348	5.36	9.25	16.73	2.18
Density of timber flanges before oven dried	(kg/m ³)	260	374	493	645	50
Density of timber flanges after oven dried	(kg/m ³)	253	333	437	574	44
Moisture content of timber flanges before test	(%)	296	8.70	12.06	14.70	0.97
Moisture content of timber flanges after test	(%)	251	5.21	12.55	14.33	1.40
Modulus of elasticity for LVL flanges (E)	(kN/mm ²)	26	10.20	11.54	12.87	0.82
Density of LVL flanges before oven dried	(kg/m ³)	20	534	556	588	15.14
Density of LVL flanges after oven dried	(kg/m ³)	20	477	496	525	13.43
Moisture content of LVL flanges before test	(%)	104	12.50	15.15	17.30	1.16
Moisture content of LVL flanges after test	(%)	20	10.60	11.70	12.96	0.92
Plywood shear modulus (G)	(kN/mm ²)	6	0.589	0.753	0.937	0.131
Density of Plywood webs before oven dried	(kg/m ³)	6	473	494	519	17
Density of Plywood webs after oven dried	(kg/m ³)	6	439	456	476	14
Moisture content of Plywood webs	(%)	6	7.71	8.24	9.02	0.57

5.3.3 Matching components for the beams

Unlike engineered products such as LVL and plywood, timber by nature possesses a high level of material variability. Previous research has shown that the highest level of correlation exists between the modulus of elasticity and the bending strength (Hoffmeyer ... et al. (1999), Johansson ... et al. (1992), Lackner and Foslie (1988)). Although mechanically graded timber MGP 10 with a known modulus elasticity of 10 kN/mm^2 was used, still the laboratory tests showed a broad variation from 5.4 to 16.7 kN/mm^2 (Table 5.1). As a result, it was decided to reject those boards with E values less than 7 kN/mm^2 and to evenly distribute and match the timber sections used as flanges according to the E values for different types of beams.

The timber sections were divided into eleven matched groups for the six short span profiles. The flanges of 12 beams were prepared from a group of 24 matched samples used in pairs so that E values spread equally from low to high. A similar procedure was adopted for the long span beams, each group comprising 6 matched samples used in pairs for the flanges of the 3 beams. This statistical arrangement made it possible to compare the results between the groups and within each group.

Since the variability among the tested LVL flanges was relatively insignificant in comparison with the timber ones, they were randomly distributed between the 3 different profiles. Further discussion on grouping and matching the beam components is provided in Chapter 3.

5.3.4 Plywood webs

The plywood sheets of $1200 \times 1200 \text{ mm}$ were passed through a double-ended tenoner for edge grooving. The tongue-groove profile parallel to the face grain direction of the plywood was used for joining sheets and creating webs for both short and long beams. The use of plywood oriented with the face grain perpendicular to the longitudinal axis of the beam was based on the fact that web crippling performance improves by increasing the number of plies perpendicular to the beam axis (Leichti ... et al. (1990)). During the

manufacturing process, glue line bonding was checked regularly by carrying out the chisel test in accordance with the recommendations of BS EN 391 (2001) for testing the Glulam glue line.

5.4 Testing procedure

All the short beams were first subjected to non-destructive three-point tests, as shown in Figure 5.2(a). Thereafter, the first set of 3 samples from each group was loaded to failure under four-point loading, as shown in Figure 5.2(b). For both tests, mid-span deflections relative to the supports were recorded.

Each long beam was first subjected to a series of three-point bending tests over spans of 1450, 2100, 3000 and 4500 mm, as shown in Figure 5.3 (a). This was followed by testing each beam under four-point bending during which the mid-span deflection relative to the supports was recorded, as shown in Figure 5.3(b). In all cases the maximum load applied did not exceed the proportional limit loads or cause any damage to the test beams. Subsequently, three beams from each group were tested to failure in four-point bending over a span of 4350 mm to determine the maximum bending strength of the beams. The load and the deflection relative to the supports were recorded. Typical short and long span beams under four-point bending are shown in Figure 5.4.

The procedure adopted for testing on both short and long beams was mainly based on the recommendations of BS EN 408 (1995) and EOTA (2000). Chapter 4 discussed the testing procedure in more detail.

5.5 Shear stress, shear factor and deflection equations

This section describes calculation of shear stress and shear factor for double I-beam as a typical example. Similar methods can be applied for I, recessed, box, boxed I, and boxed double I-beams. The deflection equations for the double I-beam under four and three point bending are then derived using the energy method and Castigliano's Theorem. These equations are then later used for determining the Young modulus and shear modulus of each profile.

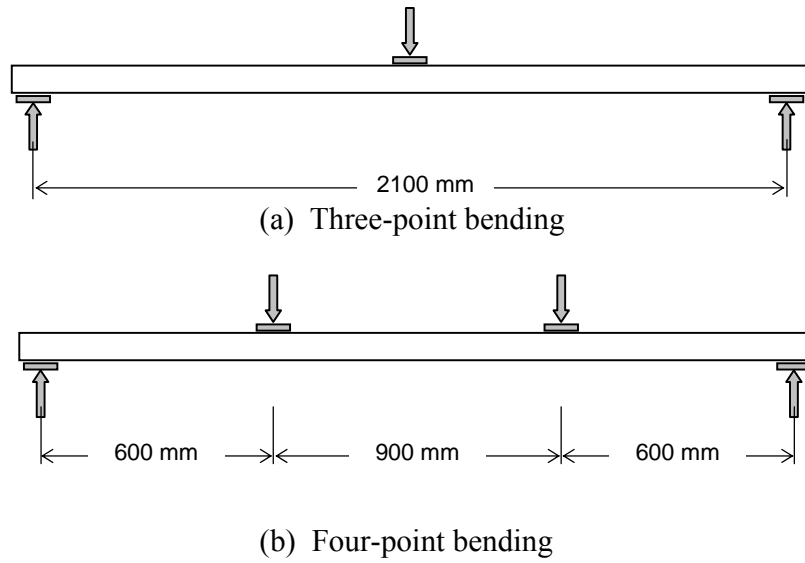


Figure 5.2 Test arrangement for short span beams

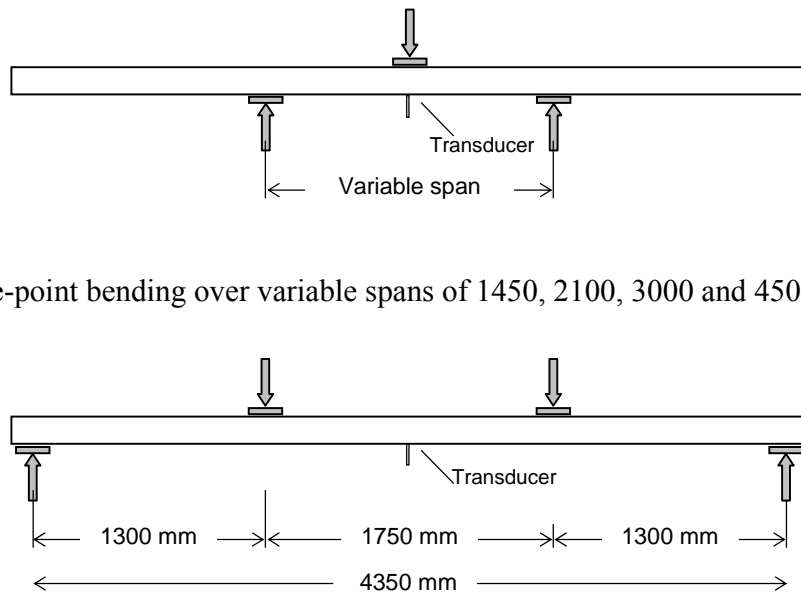


Figure 5.3 Test arrangement for long span beams



(a) A short span double I-beam



(b) A long span double I-beam

Figure 5.4 Typical beams tested over 2.1m and 4.35m span

5.5.1 Distribution of shear stress

Considering the flange and web portions separately, average distribution of shear stress, τ_{xy} , flange and web could be calculated as a function of y by using Equation 5.1, Jourawski's formula .

$$\tau_{xy} = \frac{V_y Q_z}{I_{zz} b} \quad \text{Equation 5.1}$$

Equation 5.2 and Figure 5.5 demonstrate the shear stress as a function of y for the upper flange region, where:

b is breadth of the flange, (mm)

$$b = 88 \text{ mm}$$

h is depth of the beam (mm)

$$h = 290 \text{ mm}$$

h_f is flange depth, (mm)

$$h_f = 45 \text{ mm}$$

h_w is clear distance between the flanges (mm)

$$h_w = 210 \text{ mm}$$

I_{zz} is second moment of area about the strong axis, (mm⁴)

$$I_{zz} = 1.25 \times 10^8 \text{ mm}^4$$

$$\tau_{xy} = \frac{V_y}{b I_{zz}} \underbrace{[b \times (0.5 h - y)]}_{\text{Area above } y} \times \underbrace{\left[y + \frac{(0.5 h) - y}{2} \right]}_{\text{Moment arm from centre of A to neutral axis}} \quad \text{Equation 5.2}$$

Q_z

$$\text{Hence } \tau_{xy} = \frac{V_y}{88 I_{zz}} [88 \times (0.5 \times 290 - y)] \times \left[y + \frac{0.5 \times 290 - y}{2} \right]$$

The shear stress of upper flange region as function of y is:

$$\tau_{xy} = \frac{V_y}{88 I_{zz}} (925100 - 44 y^2) \quad 100 \leq y \leq 145 \text{ mm}$$

Maximum shear stress in the flange, $\tau_{xy} = 4.41 \times 10^{-5} V_y$, occurs at $y = 100 \text{ mm}$ while increasing the y value creates decreasing flange shear stress and which reaches zero when $y = 145$ (Figure 5.6). Shear stress as a function of y for the upper region of the web can be calculated by using Equation 5.3, where:

b_w is overall breadth of the web, (mm):	$b_w = 2 \times 9 \text{ mm}$
E_{Timber} is young's modulus of the timber (N/mm^2):	9980 N/mm^2
E_{Plywood} is young's modulus of the plywood (N/mm^2):	11134 N/mm^2
n is Young's modulus ratio and $n = E_{\text{plywood}} / E_{\text{timber}}$:	$n = 1.1156$
$b_{w,Equ}$ is equivalent breadth of the web (mm):	$b_{w,Equ} = 20.08 \text{ mm}$

$$\tau_{xy} = \frac{V_y}{b_{w,Equ} I_{zz}} \left[\underbrace{(b \times h_f)(h/2 - h_f/2)}_{\substack{\text{Area of flange} \\ \text{Moment arm D of} \\ \text{flange centre about} \\ \text{neutral axis}}} + \underbrace{(h_w/2 - y)(b_{w,Equ})}_{\substack{\text{Area of web above y} \\ \text{Moment arm of} \\ \text{web area above y} \\ \text{about neutral axis}}} (y + 0.5(h_w/2 - y)) \right]$$

Qz Equation 5.3

Substituting the values in Equation 5.3 gives:

$$\tau_{xy} = \frac{V_y}{20.08 I_{zz}} \left[(88 \times 45) \left(\frac{290}{2} - \frac{45}{2} \right) + \left(\frac{200}{2} - y \right) (20.08) \left(y + \left(\frac{200}{2} - y \right) \right) \right]$$

So shear stress as a function of y for the web is:

$$\tau_{xy} = \frac{V_y}{20.08I_{zz}} (585500 - 10.04y^2) \quad 0 \leq y \leq 100\text{mm}$$

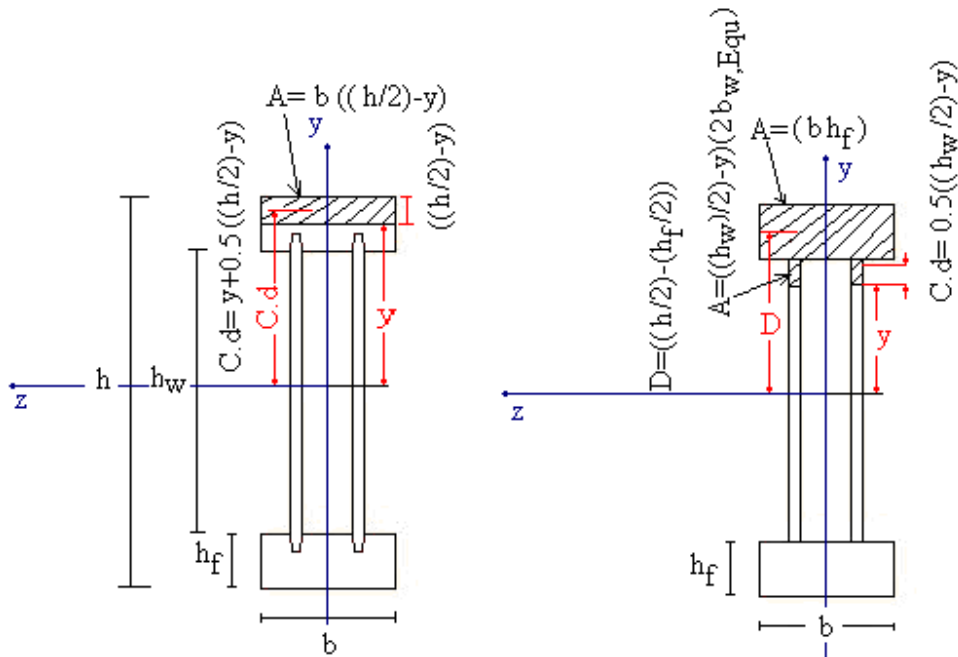


Figure 5.5 calculation of shear stress as a function of y for the flange and webs

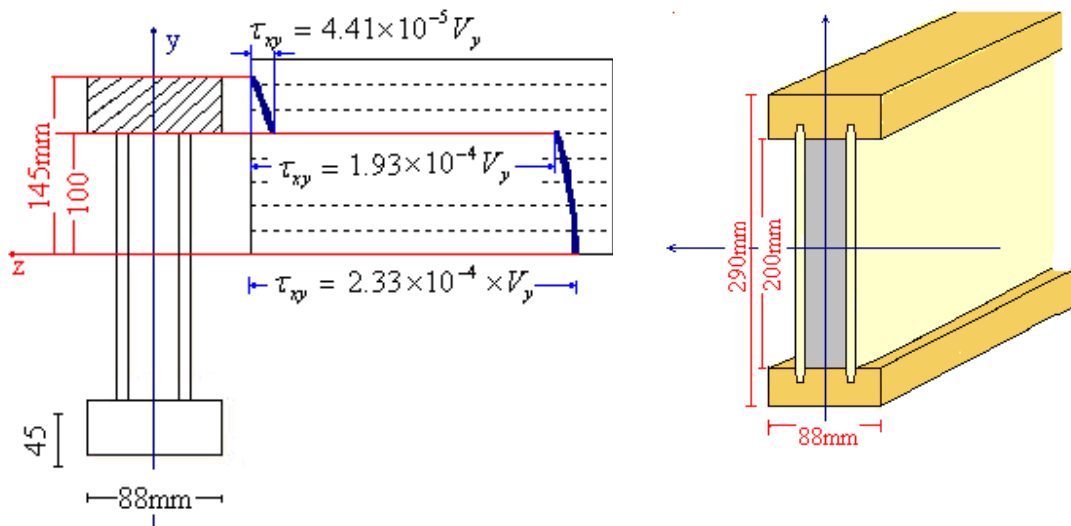


Figure 5.6 Distribution of shear stress in flange and web areas of a double I-beam

As shown in Figure 5.6, maximum shear stress in the webs, $\tau_{xy} = 2.33 \times 10^{-4} \times V_y$, occurs at the neutral axis of the beam cross section, $y = 0$. Value of the shear stress decreases upwards and minimum web shear stress occurs at $y = 100$ mm, which is $\tau_{xy} = 1.93 \times 10^{-4} \times V$.

Comparing the maximum shear stress of the web and flange for the double I-beam shows that the value of web shear stress is five times more than the flange shear stress.

5.5.2 Shear factor

CIBs can be considered as symmetrical prismatic beams of length L because external load is normal to the central axis. Energy stored in the beam can be measured by applying the stress energy method which is shown in Equation 5.4 (As used by Shames and Pitarresi, 1999):

$$U = \iiint \left[\frac{1}{2E} (\sigma_{xx}^2 + \sigma_{yy}^2 + \sigma_{zz}^2) - \frac{\nu}{E} (\sigma_{xx} \sigma_{yy} + \sigma_{yy} \sigma_{zz} + \sigma_{xx} \sigma_{zz}) + \frac{1}{2G} (\sigma_{xy}^2 + \sigma_{xz}^2 + \sigma_{yz}^2) \right] dV$$

Equation 5.4

If (X) is considered as the longitudinal axis of a CIB which is loaded in (Y) direction normal to longitudinal axis, then Equation 5.5 can be derived from Equation 5.4, since there is only one non-zero normal stress (σ_{xx}):

$$U^* = \iiint \left[\frac{1}{2E} (\sigma_{xx}^2) \right] dV$$

Equation 5.5

The bending stress of the beam is calculated by using the flexural formula $\sigma_{xx} = \frac{M_z y}{I_{zz}}$

then the flexural formula is substituted in Equation 5.5 to develop an expression for the normal stress, Equation 5.6 :

$$U = \iiint \frac{\sigma_{xx}^2}{2E} dv = \int_0^L \left[\int_A \frac{M_z^2 y^2}{2EI_{zz}} dA \right] dx = \int_0^L \left[\frac{M_z^2}{2EI_{zz}} \iint_A y^2 dA \right] dx \quad \text{Equation 5.6}$$

While $I_{zz} = \int_A y^2 dA$ then complementary strain energy in the xy plane can be obtained:

$$U = \int_0^L \left[\frac{M_y^2}{2EI_{zz}} \right] dx \quad \text{Equation 5.7}$$

Complementary shear strain energy could also be derived from the Equation 5.4 in similar fashion as explained previously:

$$U^* = \iiint_v \frac{\tau_{xy}^2}{2G} dv \quad \text{Equation 5.8}$$

Equation 5.8 can be simplified by using shear factor to derive Equation 5.9, α_y . The shear factor correlates the energy calculated using the actual shear stress distribution with that of a cross-section with the same area but with a constant distribution of shear stress. In this way the constant shear stress distribution is calculated from a rather simple equation.

$$U^* = \iiint_v \frac{\tau_{xy}^2}{2G} dv = \alpha_y \iiint_v \frac{\tau_{xy}^2}{2G} dv \quad \text{Equation 5.9}$$

If τ_{xy} in Equation 5.9 is substituted with the simple shear equation, $\tau_{xy} = \frac{V}{A}$, where A is the cross sectional area, then Equation 5.9 can be simplified to Equation 5.10 as:

$$U^* = \int_0^L \left[\iint_A \frac{V_y^2}{2GA^2} dA \right] dx = \alpha_y \int_0^L \frac{V_y^2}{2GA} dx \quad \text{Equation 5.10}$$

As a result the complementary strain energy due to bending induced shear for loading in the xy plane can be directly calculated from Equation 5.10. Similarly for loading in xz the plane strain energy can be calculated by using Equation 5.11 thus:

$$U^* = \alpha_z \int_0^L \frac{V_z^2}{2GA} dx \quad \text{Equation 5.11}$$

By substituting Equations 5.7 and 5.10 in Equation 5.4, the strain energy of the beam which is subjected to bending moment M and shearing force V can be expressed as Equation 5.12:

$$U = \int_0^L \frac{M^2}{2EI} + \alpha \int_0^L \frac{V^2}{2GA} dx \quad \text{Equation 5.12}$$

For the double I-beam the shear factor associated with shear strain energy can be calculated by using Equations 5.8 and 5.9. If τ_{xy} in Equation 5.8 and 5.9 are substituted by Equation 5.1 then Equations 5.8 and 5.9 can be rewritten as Equations 5.13 and 5.14:

$$U = \iiint_V \frac{1}{2G} \left[\frac{V_y Q_z}{I_{zz} b} \right]^2 dv \quad \text{Equation 5.13}$$

$$U = \alpha_y \iiint_V \frac{1}{2G} \left[\frac{V_y}{A} \right]^2 dv \quad \text{Equation 5.14}$$

Considering the difference between the first moment of the area for the flange and web portions then Equation 5.13 can be written as Equation 5.15:

$$U = \frac{1}{2G} \times \frac{V_y^2}{I_{zz}^2} \left\{ \iiint_v \frac{Q_{Flange}^2}{b^2} dv + \iiint_v \frac{Q_{Web}^2}{b_{w,Equ}^2} dv \right\} \quad \text{Equation 5.15}$$

Equation 5.14 can be further simplified as:

$$U = \alpha_y \frac{V_y^2}{A^2} \times \frac{1}{2G} \iiint_v dv \quad \text{then} \quad U = \alpha_y \frac{V_y^2}{A^2} \times \frac{1}{2G} \times AL$$

i.e.

$$U = \alpha_y \frac{V_y^2 L}{2AG} \quad \text{Equation 5.16}$$

Equations 5.15 and 5.16 are derived for calculating the strain energy due to shear, which can be written as Equation 5.17

$$U = \frac{1}{2G} \times \frac{V_y^2}{I_{zz}^2} \left\{ \iiint_v \frac{Q_{Flange}^2}{b^2} dv + \iiint_v \frac{Q_{Web}^2}{b_{w,Equ}^2} dv \right\} = \alpha_y \frac{V_y^2 L}{2AG} \quad \text{Equation 5.17}$$

Canceling terms from both sides of the Equation 5.17, and knowing that the beam is prismatic of length L and cross section area A then Equation 5.18 can be derived as:

$$\frac{1}{I_{zz}^2} \left\{ \int_0^L \left[\iint_{A_1} \frac{Q_{Flange}^2}{b^2} ds \right] dy + \int_0^L \left[\iint_{A_2} \frac{Q_{Web}^2}{b_{w,Equ}^2} ds \right] dy \right\} = \alpha_y \frac{L}{2A} \quad \text{Equation 5.18}$$

Integrating with respect to y on the left side of Equation 5.18 results in:

$$\frac{L}{I_{zz}^2} \left\{ \iint_{A_1} \frac{Q_{Flange}^2}{b^2} ds + \iint_{A_2} \frac{Q_{Web}^2}{b_{w,Equ}^2} ds \right\} = \frac{\alpha_y L}{2A} \quad \text{Equation 5.19}$$

From Equation 5.2 and 5.3, first moment of the area for flange and web are calculated as:

$$Q_{Flange} = 925100 - 44y^2 \quad 100 \leq y \leq 145mm \quad \text{Equation 5.20}$$

$$Q_{Web} = 585500 - 10.04 y^2 \quad 0 \leq y \leq 100mm \quad \text{Equation 5.21}$$

So the left side of Equation 5.19 can be substituted by the Equations 5.20 and 5.21. Integrating with respect to their areas determines their values as illustrated in Equations 5.22 and 5.23.

Area integration 1

$$\int_{-44}^{+44} \int_{+100}^{+145} \frac{(925100 - 44y^2)^2}{88^2} dy dz = 4.393 \times 10^{10} \quad \text{Equation 5.22}$$

Area integration 2

$$\int_{-10.04}^{+10.04} \int_0^{+100} \frac{(585500 - 10.04y^2)^2}{20.08^2} dy dz = 1.522 \times 10^{12} \quad \text{Equation 5.23}$$

$$A = (b \times h) - [(b - b_{w,Equ}) h_w] = 1.19 \times 10^4 \text{ mm}^2 \quad \text{Equation 5.24}$$

By substituting Equations 5.22, 5.23 and 5.24 in Equation 5.19 shear-factor for the double I-beam can be calculated.

Shear factor for timber flange double I-beam $\alpha_y = 2.38$ and complementary strain energy due to the shear stress in the beam resulting from a shear force V_y at the section can be calculated by using Equation 5.25.

$$U = 2.38 \times \int_0^L \frac{V_y^2 L}{2AG} \quad \text{Equation 5.25}$$

Roark ... et al.(2002) provides a simplified method for calculating the shear factor of I or box sections as shown in Equation 5.26, this is discussed in Section 5.5.1. Shear factor calculated in this way is close to the exact method explained previously. For instance shear factor for double I-beam can be calculated as follows when:

Distance from the neutral axis to the nearest surface, $D_1 = 100 \text{ mm}$

Distance from the neutral axis to the extreme fiber, $D_2 = 145 \text{ mm}$

The radius of gyration of section, $r = \sqrt{\frac{I}{A}} = 102.49 \text{ mm}$

$$\alpha = \left[1 + \frac{3(D_2^2 - D_1^2)D_1}{2D_2^3} \left(\frac{b}{b_{w,Equ}} - 1 \right) \right] \frac{4D_2^2}{10r^2} \quad \text{Equation 5.26}$$

thus $\alpha = 2.27$

5.5.3 Deformation of the beam

Castigliano's Theorem

Castigliano's second theorem states that in a linear elastic structure the partial derivative of strain energy with respect to the applied force is equal to the corresponding displacement at the point of application of the force that is in the direction of the force, which is expressed as Equation 5.27 (Ugural and Fenster 2003). In this way it is possible to write the stored energy in terms of individual forces like bending, shear and torsion. Furthermore it is possible to calculate displacement at any point by differentiating with respect to the involved forces.

$$\frac{\partial U}{\partial P_i} = \Delta \quad \text{Equation 5.27}$$

Equation 5.28 for calculating the beam displacement can be expressed by applying Castigliano's theorem in Equation 5.12

$$\Delta = \frac{1}{EI} \int_0^L M \frac{\partial M}{\partial P_i} dx + \frac{\alpha}{AG} \int_0^L V \frac{\partial V}{\partial P_i} dx \quad \text{Equation 5.28}$$

5.5.3.1 Derivation of the deflection equation for four point bending

By knowing the shear factor (α) from the previous section and applying the Castigliano theorem which is expressed in Equations 5.27 and 5.28, the equation for the deflection of the beam can be derived. To apply Castigliano's theorem, a hypothetical (dummy) point force R is introduced at centre of the beam (Figure 5.7). The dummy load is applied to mid-span because the equation for maximum deflection is concerned. A

similar procedure can be adopted for deriving the deflection expression at any point by placing the dummy load at the point of interest.

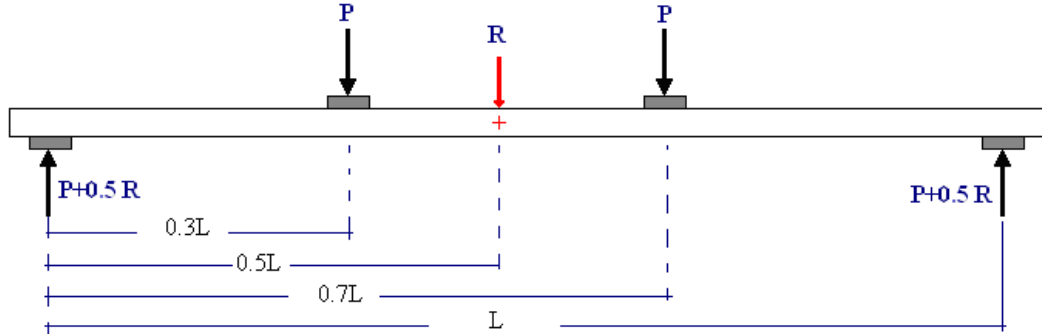


Figure 5.7 Actual loading (P) and dummy loading (R) on four point simply supported beam

For the applied force which is represented as P and R in Figure 5.7, the bending moment M and shearing force V are given as equilibrium in Equations 5.29 and 5.30:

$$M = \begin{cases} (P + 0.5R)x & 0 < x \leq 0.3L \\ 0.3LP + 0.5Rx & 0.3L < x \leq 0.5L \\ 0.3LP + 0.5LR - 0.5Rx & 0.5L < x \leq 0.7L \\ LP - Px + 0.5LR - 0.5Rx & 0.7L < x \leq L \end{cases} \quad \text{Equation 5.29}$$

$$V = \begin{cases} (P + 0.5R) & 0 < x \leq 0.3L \\ -0.5Rx & 0.3L < x \leq 0.5L \\ 0.5R & 0.5L < x \leq 0.7L \\ P + 0.5Rx & 0.7L < x \leq L \end{cases} \quad \text{Equation 5.30}$$

Deflection of the beam (Δ_1) resulting from the bending moment can be computed by using Equation 5.31. Equation 5.31 is derived by substituting the Equation 5.29 in the

first part of the Equation 5.28 which is $\left(\frac{1}{EI} \int_0^L M \frac{\partial M}{\partial P_i} dx \right)$.

$$\begin{aligned}
 \Delta_1 = & \frac{1}{EI} \left[\int_0^{0.3L} [(P + 0.5R)x] \left[\frac{d}{dQ} [(P + 0.5R)x] \right] dx + \right. \\
 & \frac{1}{EI} \left[\int_0^{0.3L} [(P + 0.5R)x] \left[\frac{d}{dR} [(P + 0.5R)x] \right] dx + \right. \\
 & \int_{0.3L}^{0.5L} (0.3LP + 0.5Rx) \left[\frac{d}{dR} (0.3LP + 0.5Rx) \right] dx + \\
 & \int_{0.5L}^{0.7L} (0.3LP - 0.5Rx + 0.5LR) \left[\frac{d}{dR} (0.3LP - 0.5Rx + 0.5LR) \right] dx + \\
 & \left. \int_{0.7L}^L (LP - Px + 0.5LR - 0.5Rx) \left[\frac{d}{dR} (LP - Px + 0.5LR - 0.5Rx) \right] dx \right]
 \end{aligned}
 \tag{Equation 5.31}$$

Knowing that the value of R is zero, then deflection of the beam caused by the bending moment can be calculated by Equation 5.32:

$$\Delta_1 = \frac{1}{EI} (3.3 \times 10^{-2} L^3 P)
 \tag{Equation 5.32}$$

In above calculation if the distance between the supports and the load head is considered as (a) instead of 0.3L, then Equation 5.32 for the deflection caused by bending moment can be written as Equation 5.33:

$$\Delta_1 = \frac{L^3}{6EI} \left[\frac{3a}{4L} - \left(\frac{a}{L} \right)^3 \right] P
 \tag{Equation 5.33}$$

Deflection of the beam (Δ_2) resulting from the shearing force can be calculated by solving the Equation 5.34, which is derived by substituting Equation 5.30 in the second part of the Equation 5.28 $\left(\frac{\alpha}{AG} \int_0^L V \frac{\partial V}{\partial P_i} dx \right)$

$$\Delta_2 = \frac{\alpha}{AG} \left[\left(\int_0^{0.3L} -(P + 0.5R) \left[\frac{d}{dR} [-(P + 0.5R)] \right] dx \right) + \int_{0.3L}^{0.5L} -0.5R \left[\frac{d}{dR} (-0.5R) \right] dx + \int_{0.5L}^{0.7L} (0.5R) \frac{d}{dR} (0.5R) dx + \int_{0.7L}^L \left[(P + 0.5R) \frac{d}{dR} (P + 0.5R) \right] dx \right]$$

Equation 5.34

As the value of R is equal to zero then deflection due to shear force can be calculated by using Equation 5.35 as:

$$\Delta_2 = \frac{\alpha}{AG} (0.3LP)$$

Equation 5.35

Overall deflection of the beam under four point bending can be calculated by using Equation 5.36. This overall deflection is equal to sum of the deflection caused by bending, Equation 5.33, and that caused by shear force, Equation 5.35.

$$\Delta_1 = \frac{L^3}{6EI} \left[\frac{3a}{4L} - \left(\frac{a}{L} \right)^3 \right] P + \frac{0.3\alpha}{AG} LP$$

Equation 5.36

5.5.3.2 Derivation of the deflection equation for three point bending

The equation for measuring the deflection of the beam under three-point bending can be derived by a similar method to that which has been described for four-point bending. In previous section it was necessary to introduce the dummy load at the point of interest in order to invoke Castigliano's theorem, but this time there is no need to apply the dummy load, as an actual point load (P) already exists at the mid-span (Figure 5.8).

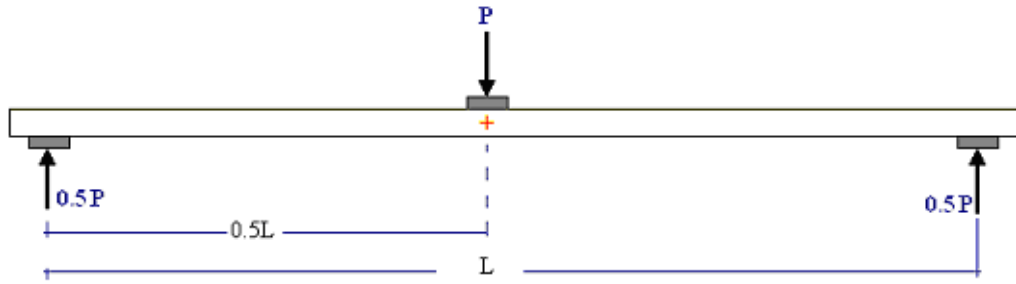


Figure 5.8 Actual loading (P) on three point simply supported beam

In Figure 5.8, the bending moment distribution is expressed by Equation 5.37, and shear force distribution is expressed by Equation 5.38:

$$M = \begin{cases} 0.5 P x & 0 < x \leq \frac{L}{2} \\ 0.5 (P L - P x) & \frac{L}{2} \leq x < L \end{cases} \quad \text{Equation 5.37}$$

$$V = \begin{cases} -0.5 P & 0 < x \leq \frac{L}{2} \\ 0.5 P & \frac{L}{2} \leq x < L \end{cases} \quad \text{Equation 5.38}$$

Deflection of the beam as a result of the bending moment (Δ_1) can be calculated by substituting the Equation 5.37 in Equation 5.28 as:

$$\Delta_1 = \frac{d}{dP} \left[\left(\frac{1}{2EI} \right) \left[\int_0^{0.5L} (0.5 P x)^2 dx + \int_{0.5L}^L 0.5^2 (P L - P x)^2 dx \right] \right] \quad \text{Equation 5.39}$$

Hence:

$$\Delta_1 = \frac{2.083 \times 10^{-2}}{EI} L^3 P \quad \text{Equation 5.40}$$

Deflection of the beam caused by the shear force (Δ_2) can be computed by substituting Equation 5.38 in Equation 5.28. Thus Equation 5.41 is derived as:

$$\Delta_2 = \frac{d}{dP} \left[\left(\frac{\alpha}{2GA} \right) \left[\int_0^{0.5L} (-0.5P)^2 dx + \int_{0.5L}^L (0.5P)^2 dx \right] \right] \quad \text{Equation 5.41}$$

so:

$$\Delta_2 = \frac{1}{4} \frac{\alpha}{GA} LP \quad \text{Equation 5.42}$$

Total deflection of the beam under three point loads can be calculated by employing Equation 5.43. This Equation is the sum of bending deflection from Equation 5.40 and shear deflection from Equation 5.42 thus:

$$\Delta = \frac{1}{48EI} L^3 P + \frac{\alpha}{4GA} LP \quad \text{Equation 5.43}$$

5.6 Discussion of Results

5.6.1 Determination of E and G

Figure 5.9 shows the apparent modulus of elasticity (E) versus the span length (L) for the different types of composite beams subjected to three-point bending. The apparent E values were obtained using the method given in BS EN 408 (1995) where the effect of the shear load is ignored and the P/Δ (load over deflection) value from the tests is used in the conventional formula (Equation 5.44):

$$E = \frac{L^3}{48I} \left(\frac{P}{\Delta} \right) \quad \text{Equation 5.44}$$

From the test results, it can be seen that as the span L increases, the effect of shear decreases and hence the apparent E values for the beams in bending approach the true values. Figure 5.9 also shows that shear not only affects the deformation characteristics of composite beams such as I or box beams but also affects solid sections like LVL and Glulam beams. LVL is seen to have a sharper slope than the Glulam. In other words, the

effect of the shear deflection is more pronounced in LVL. The arrangement of the LVL veneers may explain this result. Veneers of LVL are layered in such a way that the lower grade veneers are positioned in the inner core and higher grade ones on the outer face (Nelson, 1997).

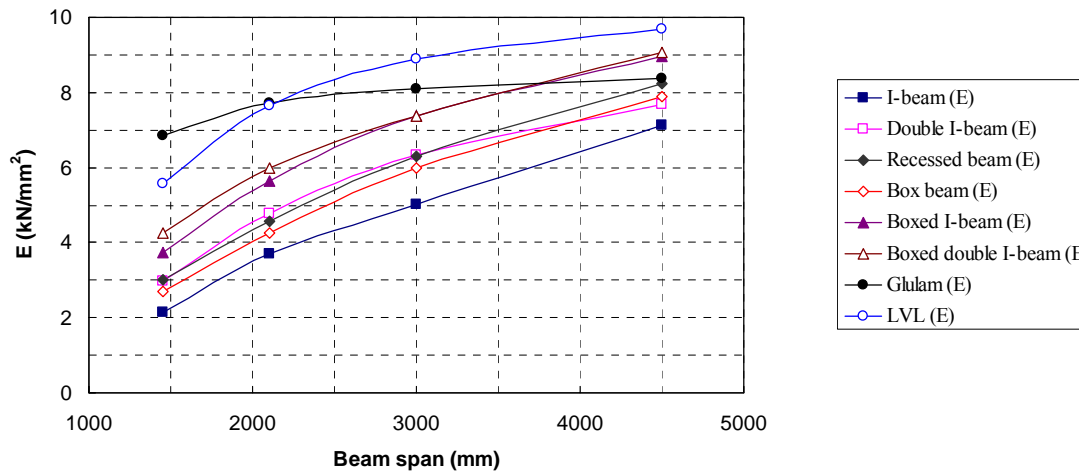


Figure 5.9 Modulus of elasticity vs span for three-point bending

In order to examine the effect of shear on the deflection of the beams, it was assumed that the modulus of elasticity (E) and shear modulus (G) remain constant during loading irrespective of loading method and span length. By considering each beam over two different spans or loading types, a pair of deformation equations can be derived, as explained in section 5.5, for determining the E and G values of the composite sections. A total of nine combinations were considered, as detailed in Table 5.2. The first 6 combinations included the results from three-point bending tests for spans L_1 and L_2 . For these combinations, E and G are found by solving the pair of equations shown as Equation 5.45, where the deflection per unit load is the sum of the bending and shear components:

$$\frac{\Delta_1}{P_1} = \frac{L_1^3}{48EI} + \frac{\alpha L_1}{4GA} \quad \text{and} \quad \frac{\Delta_2}{P_2} = \frac{L_2^3}{48EI} + \frac{\alpha L_2}{4GA} \quad \text{Equation 5.45}$$

where Δ_1/P_1 and Δ_2/P_2 are the corresponding mid-span deflections per unit applied load, L_1 and L_2 are two different spans of the beam under three-point bending, I is the second moment of area, and α is the shear factor.

Table 5.2. Testing combinations for calculating E and G

Different testing combinations				
No	Testing arrangements	Span (mm)	Testing arrangements	Span (mm)
1	3-point bending	1450	3-point bending	2100
2		1450		3000
3		1450		4500
4		3000		4500
5		2100		3000
6		2100		4500
7	3-point bending	1450	4-point bending	4350
8		2100		4350
9		3000		4350

For the remaining three combinations in Table 5.2, three-point bending with span of L_1 and four-point bending with span of L_2 were adopted and E and G are determined by solving the pair of formulae in Equation 5.46:

$$\frac{\Delta_1}{P_1} = \frac{L_1^3}{48EI} + \frac{\alpha L_1}{4GA} \quad \text{and} \quad \frac{\Delta_2}{P_2} = \frac{L_2^3}{6EI} \left[\frac{3a}{4L_2} - \left(\frac{a}{L_2} \right)^3 \right] + \frac{\alpha a}{GA} \quad \text{Equation 5.46}$$

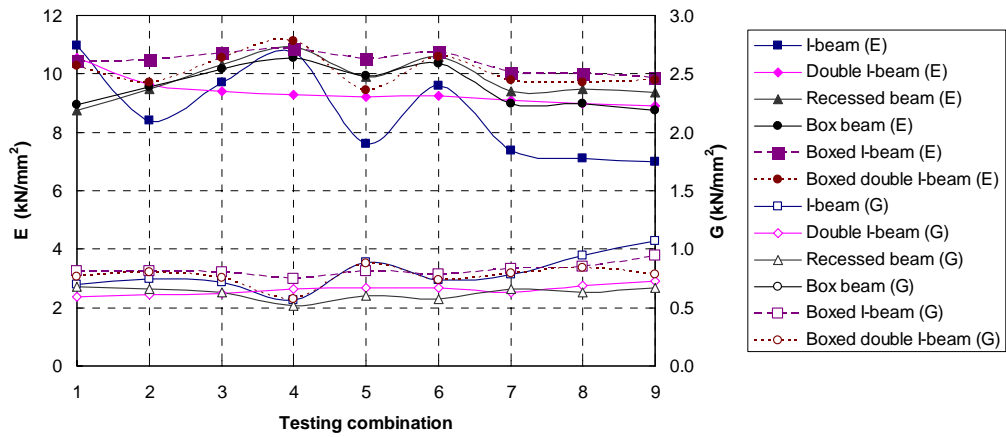
where a is the distance between the supports and the load head in the four-point loaded beams. Shear factors, α , can be calculated by using either the exact or an approximate method as explained in section 5.5; however Roark's formula (Roark, 2003) was found to be very accurate when compared with an exact method based on strain energy principles. The values of shear factors for all cross-sections are summarized in Table 5.3. The values of the

cross-sectional area A and second moment of area I calculated using the transformed-section method are also listed in Table 5.3.

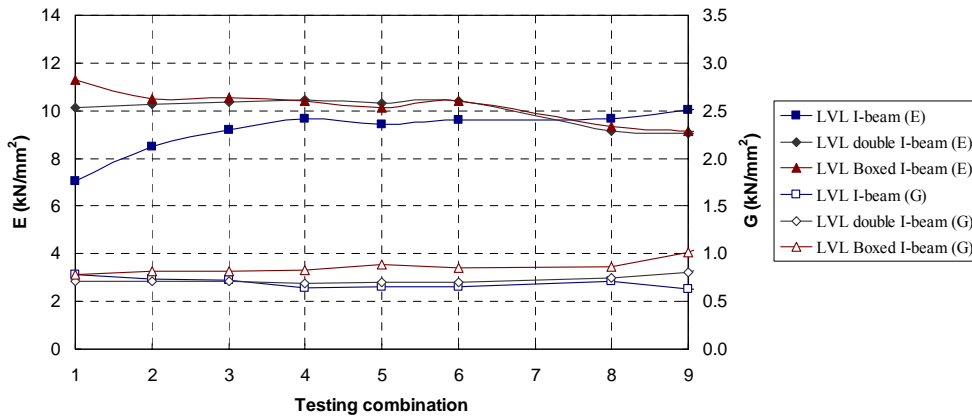
Table 5.3. Shear factor, sectional area and second moment of area of the beams

	α (Roark's formula)	α (exact calculation)	A (10^4 mm^2)	I (10^8 mm^4)
I-beam	3.59	3.64	0.99	1.23
Double I-beam	2.27	2.38	1.19	1.25
Recessed beam	2.34	2.45	1.17	1.25
Box beam	2.82	3.32	1.40	1.36
Boxed I-beam	2.32	2.77	1.56	1.38
Boxed double I-beam	2.04	2.49	1.76	1.40
LVL I-beam	3.99	4.02	0.96	1.22
LVL Double I-beam	2.49	2.58	1.13	1.25
LVL Boxed I-beam	2.43	2.83	1.46	1.36
Glulam beam	---	1.2	2.23	1.03
LVL beam	---	1.2	2.79	2.12

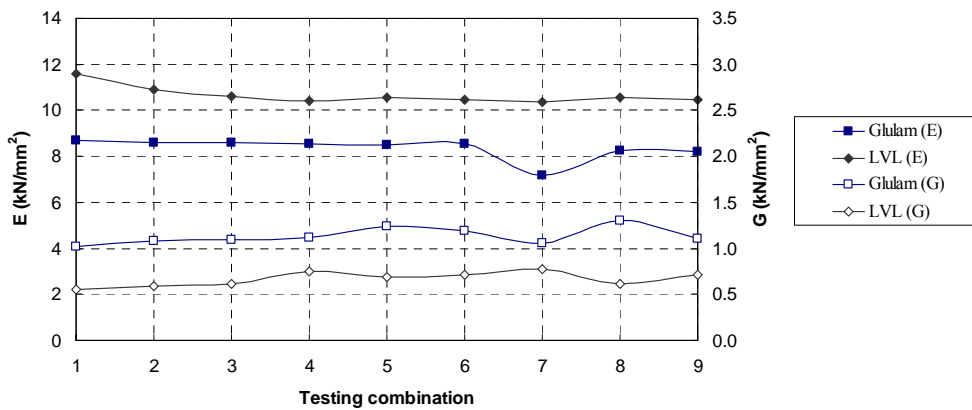
The E and G values of the long beams with timber and LVL flanges, obtained from 9 different combinations, are given in Figures 5.10(a) and 5.10(b) while for the solid LVL and Glulam beams E and G values are shown in Figure 5.10(c). In Table 5.4, the E values of timber flanges prior to manufacture are compared with the E values of the composite beams. The reduction in E values in comparison with the E values of the corresponding timber flanges ranged from 0% for the box beams, boxed I-beams and boxed double I-beams to 6%, 7% and 14% for double I-beams, recessed beams and I-beams, respectively. This may be due to the rigidity of the beam. The results in Table 5.4 show that as the rigidity of the beams increases, the reduction of the elastic modulus decreases. In other words, the rigidity of the beam affects bending test results.



(a) Manufactured beams with timber flanges



(b) Manufactured beams with LVL flanges



(c) Glulam and LVL beams- Ready made sections

Figure 5.10 E and G values for different combinations

Table 5.4. Comparison of elastic modulus for the timber flanges and the fabricated beams

Profile	Mean value of E		Timber flange vs fabricated beam reduction
	Timber flanges (kN/mm ²)	Fabricated beam (kN/mm ²)	
I-Beam	10.16	8.72	14
Double I-beam	9.98	9.37	6
Recessed beam	10.55	9.80	7
Box beam	9.50	9.58	NS
Boxed I-beam	10.20	10.41	NS
Boxed double I-beam	10.10	10.11	NS

*NS: Not significant

5.6.2 Failure modes and ultimate strength

In general, the failure of the short beams, with the exception of the boxed double I-beam, started in the plywood webs. This was followed by failure of the bottom flange, which often occurred at the loading point as shown in Figure 5.11. Unlike the rest of the beams, flexural failure of the timber flange in the boxed double I-beam caused the beam failure. Maximum load-deflection curves for the various profiles, which were tested under four-point bending over a 2100 mm span are given in Figure 5.12.

Experimental tests show that additional webs would increase the loading capacity of beams significantly though this is not proportionate to the number of webs. This can be explained by the material variability and uneven distribution of the load between the webs. Thus the webs would not fail simultaneously and this in turn results in uneven distribution of the load. In the case of boxed I-beams, finite element analysis shows in addition that the middle web sustains a larger proportion of the load than the side webs from the beginning. Chapter 6 discusses that issue in more detail.



a) LVL I-beam



b) Box beam



c) Recessed beam



d) Boxed I-beam

Figure 5.11 Failure modes for various beams under four-point bending over 2.1 m span

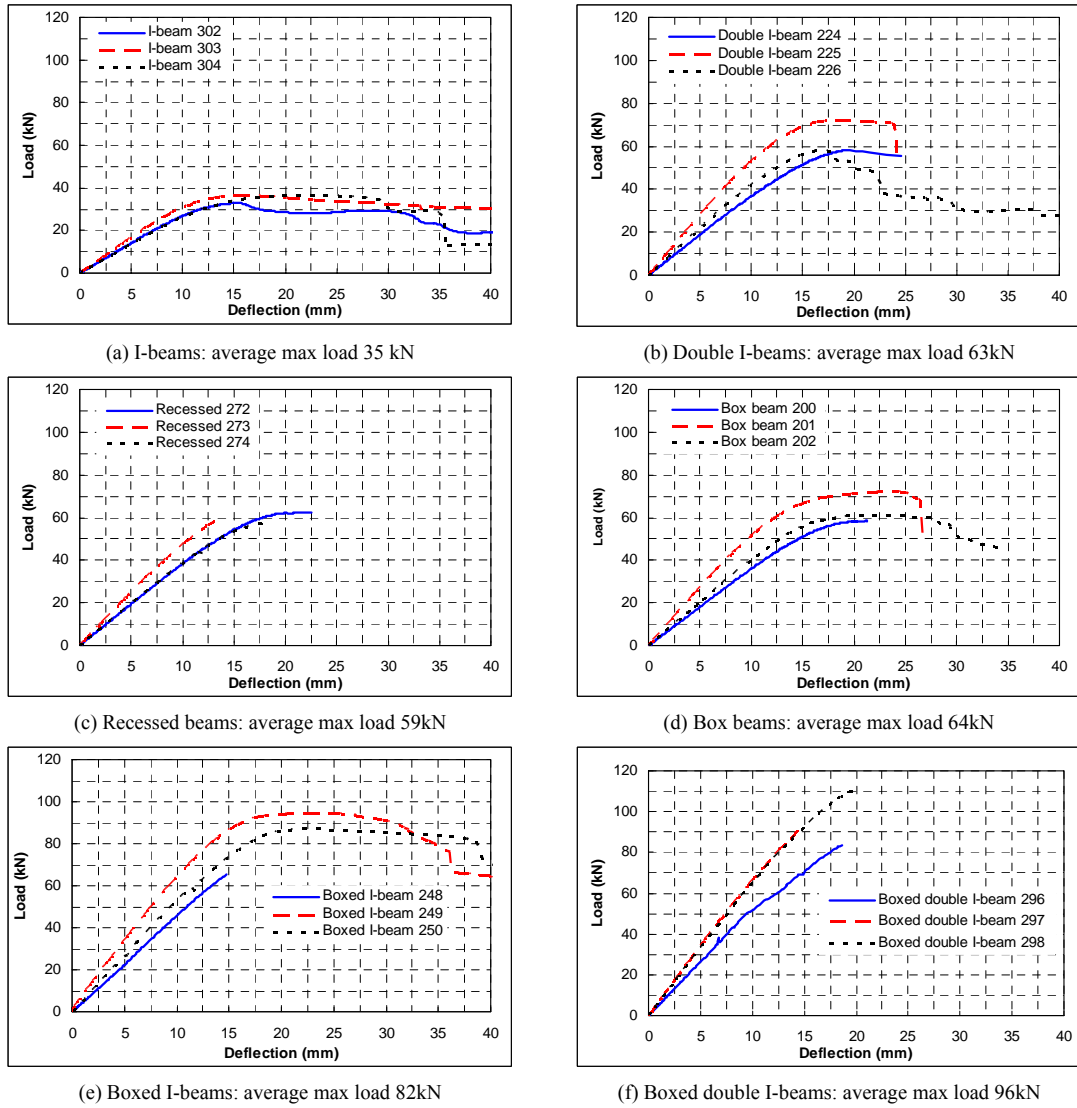
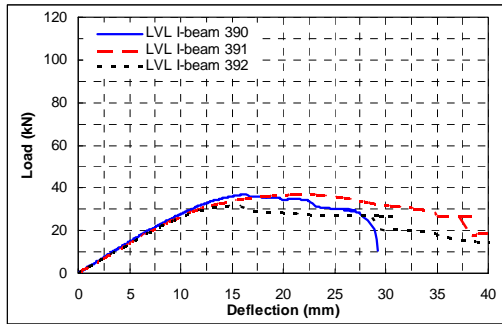
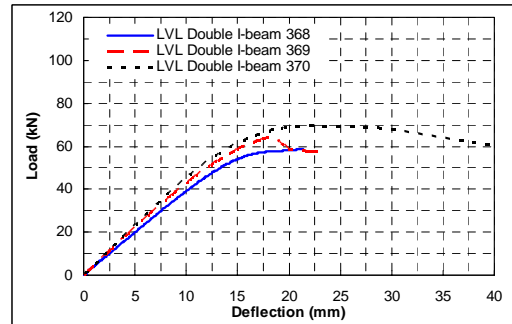


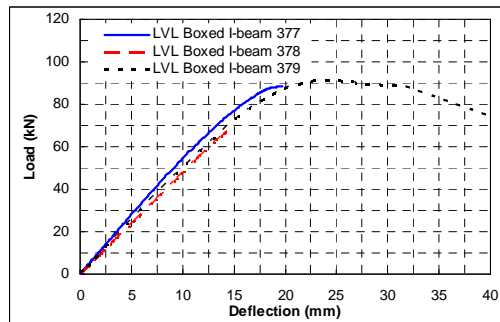
Figure 5.12 Load-deflection relationships for short beams of varied profiles under four-point bending



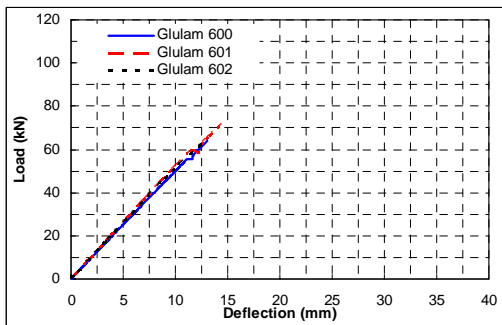
(g) LVL I-beams: average max load 35kN



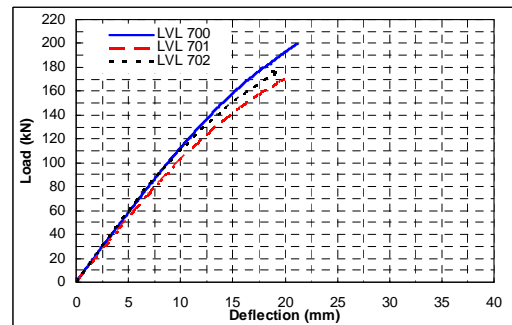
h)LVL Double I-beams: average max load 67kN



(i) LVL Boxed I-beams: average max load 91kN



(j) Glulam: average max load 67kN



(k) LVL: average max load 183kN

Figure 5.12 (Continued) Load-deflection relationships for short beams of varied profiles under four-point bending

Flexural failure was the dominant cause of collapse in the long beams including the double I-beams, recessed beams, box beams, boxed I-beams, boxed double I-beams and LVL boxed I-beams while in the I-beam, LVL I-beams and LVL double I-beams, the beams collapsed due to web failure. It is observed that the short span and long span I-beams and LVL I-beams, after reaching the maximum capacity, exhibited considerable ductility as crushing of the ply-web continued. Figure 5.13 shows the maximum load deflection curves for the various profiles tested under four-point bending over a 4350mm span.

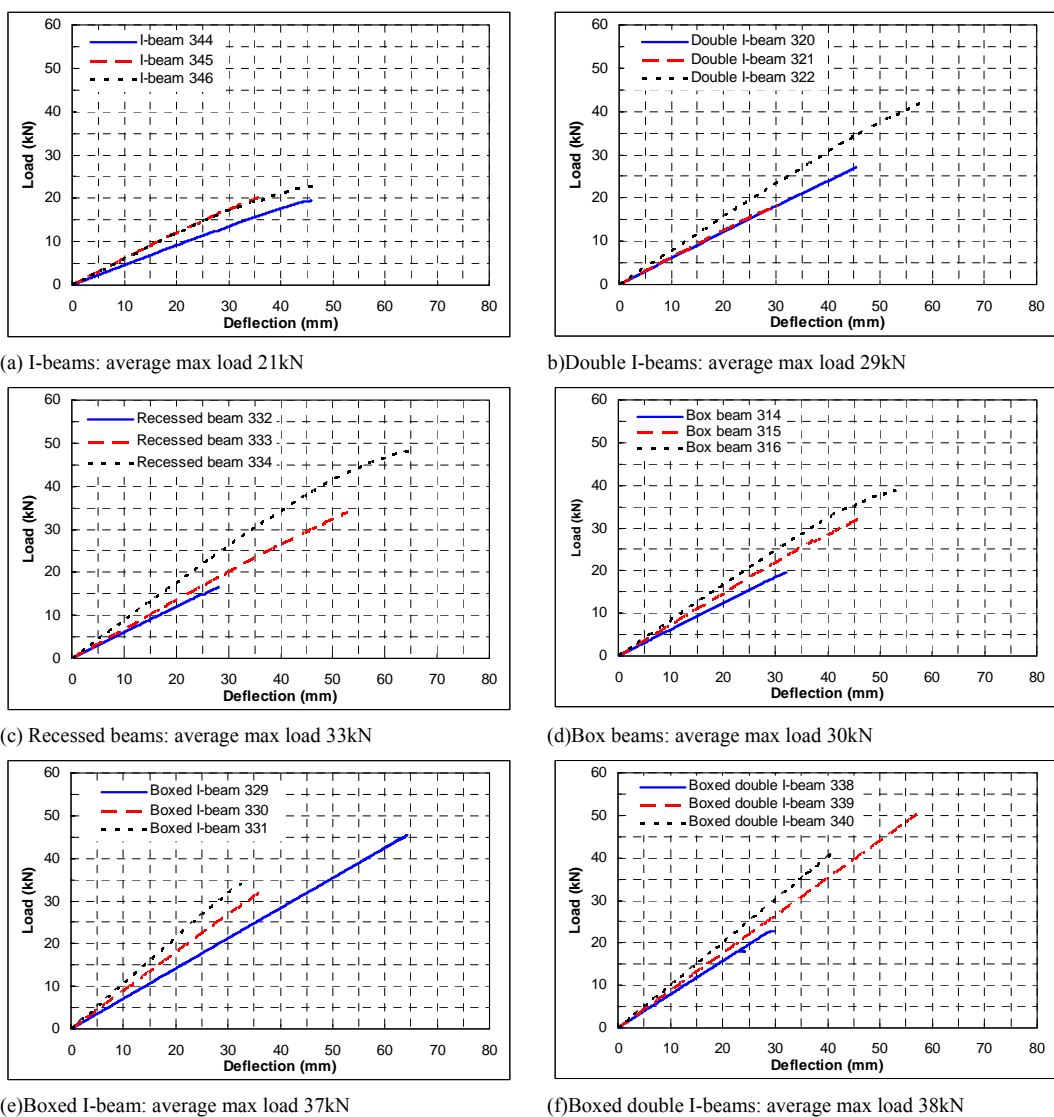
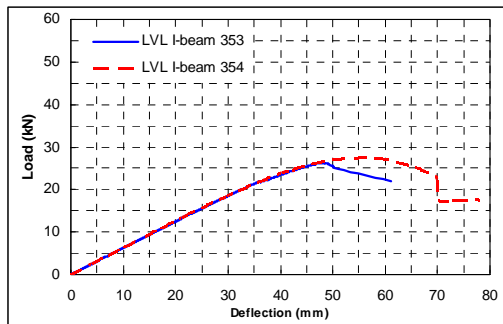
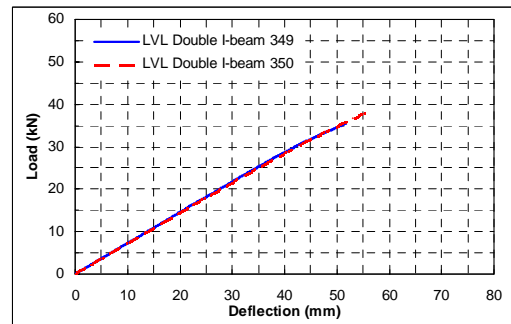


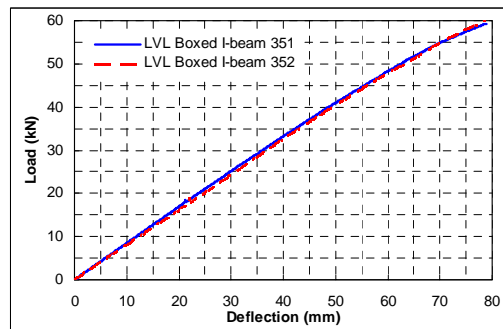
Figure 5.13 Load-deflection curves for long span beams of varied profiles under four-point bending



(g) LVL I-beams, average max load 27kN



(h) LVL Double I-beams: Average max load 39kN



(i) LVL Boxed I-beam: average max load 60kN

Figure 5.13 (Continued) Load-deflection curves for long span beams of varied profiles under four-point bending.

The test results for short and long beams for each profile are presented in Tables 5.5 and 5.6. All results in these tables are based on the four-point bending tests except for one column, which gives the slope of the P- Δ curve for the three-point bending tests. Using the I-beam as a reference, the use of additional webs to create a double I-beam, recessed beam or box beam increased the loading capacity of the short span beams by up to 83% and of the long span beams by up to 57% while the unit weight of the beams increased only by 20% for the double I-beam and recessed beam and 37% for the box beam. Similarly, adding additional webs in the LVL flanged beams increased the loading capacity by 99% and 44% for the short and long beams, respectively, while the unit weight of the beams increased by only 16%.

Table 5.5 Mechanical properties of short span beams

Beam span 2.1 m	Beam Weight	Slope of $P-\Delta$ curves		Max load	Mid span deflection	M_{\max}	σ_m	τ	τ_{panel}	τ_{rolling}
		3-P bending	4-P bending	Mean	At max load			Flange	Web	Web
Profile	(kg/m)	(kN/mm)	(kN/mm)	(kN)	(mm)	(kNm)	(N/mm ²)	(N/mm ²)	(N/mm ²)	(N/mm ²)
I-Beam	4.9	2.128	2.953	35	18	10.62	12.47	0.79	6.16	4.94
Double I-Beam	5.9	3.082	4.573	63	18	18.85	21.56	1.37	5.85	4.35
Recessed beam	5.9	2.898	4.271	59	18	17.77	20.34	1.29	5.58	4.05
Box beam	6.7	3.150	4.367	64	22	19.22	19.87	1.26	6.63	2.32
Boxed I-beam	7.7	3.715	5.512	82	20	24.72	25.01	1.58	6.09	2.36
Boxed double I-beam	8.7	4.541	6.729	102	17	28.66	29.14	1.85	6.30	1.91
LVL I-beam	5.5	2.029	2.817	35	18	10.56	12.52	0.79	8.86	3.32
LVL double I-beam	6.4	3.223	4.395	67	22	20.00	23.29	1.48	8.91	3.09
LVL Boxed I-beam	8.1	4.125	5.150	91	25	27.25	29.16	1.85	9.23	1.82
Glulam beam^I	10.6	3.676		67	13	19.96	22.87	2.27		
LVL beam^{II}	15.3	7.626	11.659	183	19	54.93	39.11	5.03		

I: Glulam beams with dimensions of 94 × 235 mm;

II: LVL beams with dimensions of 90 × 302 mm.

Table 5.6. Mechanical properties of long span beams

Beam span 4.35 m	Slope of $P-\Delta$ curves		Max load	Mid span deflection	EI	M_{max}	σ_m	τ	τ_{panel}	$\tau_{rolling}$
	3-P bending	4-P bending	Ave	at max load				Flange	Web	Web
Profile	(kN/mm)	(kN/mm)	(kN)	(mm)	(10^{12} Nmm ²)	(kNm)	(N/mm ²)	(N/mm ²)	(N/mm ²)	(N/mm ²)
I-Beam	0.460	0.582	21	43	1.070	13.13	15.52	0.45	4.46	2.19
Double I-Beam	0.507	0.673	29	44	1.174	18.87	21.85	0.64	3.38	1.57
Recessed beam	0.542	0.721	33	49	1.225	21.37	24.80	0.73	4.02	1.68
Box beam	0.566	0.731	30	44	1.307	19.65	20.89	0.61	3.71	0.87
Boxed I-beam	0.651	0.892	37	44	1.433	24.14	25.42	0.74	3.39	0.79
Boxed double I-beam	0.671	0.891	38	41	1.420	24.83	25.64	0.75	2.72	0.69
LVL I-beam	0.427	0.628	27	52	1.134	17.45	20.68	0.60	6.76	2.53
LVL double I-beam	0.546	0.719	39	60	1.229	25.64	29.86	0.87	5.27	1.83
LVL Boxed I-beam	0.625	0.825	60	78	1.365	38.88	41.60	1.22	6.08	1.20
Glulam beam	0.445	0.603	42	-----	0.85	27.59	39.62	1.45		
LVL beam	1.058	1.499	100	-----	2.16	67.67	47.29	2.85		

Comparison of two-web types including recessed beams, double I-beams and box beams with a three-web type such as boxed I-beams under similar loading conditions shows that the additional webs increased the loading capacity by 28% for the short beams and 16% for the long beams, while the unit weight of the beams increased by 30% for the recessed beams and double I-beams but only 15% for the box beams. Similarly, the loading capacity for the short and long LVL flanged beams was enhanced by 35% and 53%, respectively, while the unit weight of the beams increased only by 27%. Comparison of the results of the boxed I-beam with the boxed double I-beam shows no significant improvement in bending capacity, as this was restricted by the flange strength.

The structural performance of the short beams with LVL flanges was reasonably close to that of timber flanged beams as shown in Table 5.5 and Figure 5.12, whereas their performances in long beams were significantly improved as recorded in Table 5.6 and Figure 5.13. Enhancement in the structural performance of the LVL flanged beams is due to neutralizing the natural timber defects by dispersing them randomly during the manufacturing process and this effect is more pronounced as the span is increased. A comparison of the load-deformation characteristics shows a similar performance in stiffness for the beams with timber and LVL flanges up to service load levels, while at higher load levels timber flanged beams often experienced a loss in strength and stiffness due to natural defects within the timber. However, this problem could be resolved by proof loading the timber flanges before fabricating the beams.

5.6.3 Prediction of the failure mode

Maximum bending and shear stresses occurred in the beam flanges and webs, respectively, and these are shown together with the corresponding bending and panel shear strengths in Tables 5.5 and 5.6 respectively. The characteristic values of shear strength for panel shear and rolling shear on plywood are given as 4.7 and 1.9 N/mm², while the characteristic values of bending strength are given as 25.4 and 38 N/mm² for timber and LVL flanges, respectively (NZS 3603:1993).

The panel shear stresses in the short beams exceed the panel shear strength in all cases. The rolling shear stresses also exceed the corresponding strength for all cases

except the boxed double I-beams and LVL boxed I-beams. The bending stress exceeds the bending strength only in the boxed double I-beams. For all the beams except the boxed double I-beams, the actual failure was due to shear. It can be seen from the stress calculations that the combined panel shear and rolling shear caused the beam to fail. In the case of the boxed double I-beams, both the flexural and shear strengths are exceeded. According to the stress calculations, at a load level of 71 kN, the shear stress in the boxed double I-beam web is equal to the maximum strength of plywood at 4.7 N/mm^2 , while the bending stress in timber flanges is 22 N/mm^2 , which is lower than its ultimate strength of 25 N/mm^2 . Therefore, the beam is expected to fail in shear. However, the actual mode of failure in this case is in flexure. The flexural stresses are close enough to the strength, which casts some doubt as to which mode of failure to predict for this beam. In the case of the LVL boxed I-beam, the panel shear stress exceeds the characteristic strength thus causing the failure.

Examination of the stress and strength results for the long span beams given in Table 5.6 shows that except for the I-beam, all the timber flanges failed in flexural bending, which is consistent with the failure mode observed in the laboratory. The stress results indicate that a combination of panel shear and rolling shear caused the failure in the I-beams and LVL I-beams, while failure in LVL double I-beams that initiated in plywood webs was due to panel shear. However, flexural failure in LVL flanges caused the failure in LVL boxed I-beams. This failure cannot be predicted since according to the calculations given in Table 5.6, when the load reaches 46 kN, the plywood web stress is at the ultimate strength of 4.7 N/mm^2 while the stress in the LVL flange reaches 33 N/mm^2 , which is lower than its ultimate strength of 38 N/mm^2 . As a result, panel shear should cause the failure, whereas flexural failure was observed during the testing. This case is similar to the short span boxed double I-beam described above.

Because the rolling shear stress is directly affected by the gluing area for both short and long beams, increasing the grooving depth of I-beams, double I-beams, LVL I-beams and LVL double I-beams can enhance the rolling shear strength to enhance the overall structural performance of the beams. This will be particularly effective for long span I-beams because rolling shear is the dominant factor controlling their

strength. At the present there is no research information available on effect of the grooving depth. Manufacturers adopt different grooving depths perhaps because of their experience or their own experimental tests. For instance, New Zealand manufacturers use 10 mm grooving depth, while UK manufacturer apply 12 mm grooving depth for fabricating I-beams.

5.7 Chapter summary and conclusions

This chapter has described and discussed results of experimental procedures for evaluating the geometrical variability on structural performance of the empty, CIB beams, LVL and Glulam beams. Furthermore an analytical procedure based on the energy method and Castigliano's theorem was developed for calculating the shear stress, shear factor and deflation of the various beams with different cross-sections. The following conclusions can be drawn from the results of these analytical and experimental studies:

- Experimental results show that shear has a significant effect on the total deflection of the beams and this extends to the solid sections like LVL as well.
- The modulus of elasticity and shear modulus can be calculated by solving the pair of deflection/load equations, using results from a combination of two different tests. However, in order to achieve reliable results, it is necessary to use a number of different combinations.
- The mean value of the elastic modulus calculated for the fabricated beams is lower than those measured for their flanges.
- The bending capacity of lightweight beams made with LVL flanges is more consistent than that for similar beams made with timber flanges as natural defects are dispersed harmlessly.
- Creating the double I-beams or boxed I-beams by simply employing additional webs significantly enhanced the bending capacity of the beams as well as their shear capacity while at the same time preserving the high strength to weight ratio.
- Boxed I-beams with plywood webs and timber or LVL flanges are found to be the optimum design among the fabricated beams in terms of structural performance and ease of manufacturing.

- It is shown that in most cases, it is possible to predict the failure mode by comparing the theoretical stresses with the characteristic values of the components.

CHAPTER 6: INVESTIGATING THE STRUCTURAL PERFORMANCE OF MULTI-WEB I-BEAMS

6.1 Introduction

This chapter compares the structural performance of nine different light composite timber beams including I-beams. Beams were made with 9mm plywood webs, which were glued to timber/LVL flanges. Finished beams had 'I' or rectangular cross sections with a height of 290mm and width of 88 or 106mm depending on their cross-sections. The differences between the profiles lie in the methods of connection and in the number of webs.

Extensive laboratory testing was carried out to determine the effect of circular web-openings on the load/deflection and the shear capacity of the different profiles. This was followed by determination of the maximum bearing capacity of each design. The tension resistance of the flange to web connection in single and double I-beams was also evaluated by using the new testing method which was introduced in chapter 4.

Increasing the diameter of the circular hole was found to lead to a significant reduction in the maximum loading capacity of the beams, but it had less effect on load/deflection performance. Additional webs were found to significantly enhance the structural performance of the I-beam. In terms of pulling resistance, experimental results show that tensile stress perpendicular to the grain direction of the flange is a controlling factor for evaluating the resistance of the beam under hanging loads.

6.2. Background

In recent years, several studies have been undertaken to enhance the structural performance of I-beams by using fibre reinforced polymers (FRP) (Dagher ... et al., 1999 and Tingley, 1999). Even though these studies show a significant increase in strength properties of FRP reinforced I-beams, the high costs involved limited their use to research.

In chapter 5 and in Bahadori-Jahromi ... et al., (2006) it was shown the improvement in the bending and shear properties of I-beams can be obtained by adding additional webs and using a different web-flange connection. This chapter investigates three further aspects of the research, namely:

- (i) the effect of the circular web-openings on the load carrying capacity of the beams,
- (ii) the bearing capacity of each section type and
- (iii) the pulling resistance of I-section beams.

Shear and bearing tests were conducted on 290mm deep composite beams for nine different profiles (Figure 6.1). Twelve replicas of each profile were made. The twelve members of each group were divided to four sets in such a way that the average flange modulus of elasticity (MoE) of each set was similar to the average MoE of the other sets within its own group and all other groups. As a result all the beams were fabricated with materials which had similar properties. This equal distribution of material properties made it possible to make realistic comparisons among the different profiles. Chapters 3 and 4 discussed fabricating and matching the components of the different profiles in more detail.

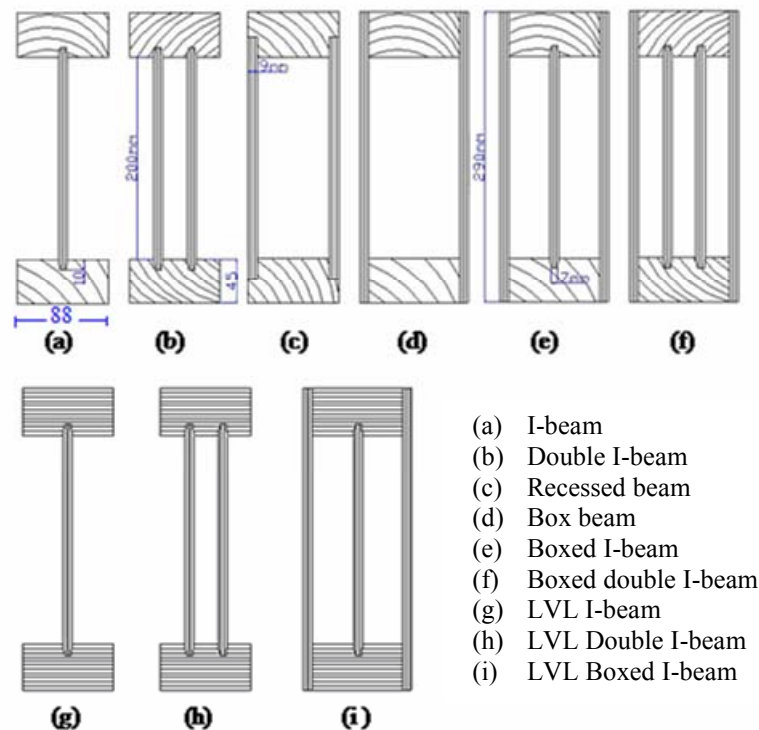


Figure 6.1 Cross section of the beams, made with timber/ LVL flanges and plywood webs

6.3. Description of the light composite beams

The light composite beams referred to were plywood webbed beams with mechanically stress-graded timber or LVL flanges. The beams could be used as a repetitive member such as a flooring system and also as a non-repetitive member such as a main beam.

Their general features were:

- Two sizes 290×88 mm and 290×106 mm, with overall length 2.3 m.
- Flanges were either mechanically stress graded Radiata pine timber or LVL, they were 88×45 mm, with average modulus elasticity of 9.45 and 11.54 kN/mm², respectively.
- All webs were made of 9mm thick three ply plywood, which was stress graded as F11 (AS/NZS 2269: 1994) and jointed with a tongue and groove profile into long lengths with face grain vertical.
- Top and bottom flanges were connected through one, two, three or four plywood webs.
- Three methods were used to connect the web(s) to flanges as follows: tongue and groove connection for I-beams, and double I-beams; recess connection for recessed beams; and a combination of laminated and tongue and groove connection for box I-beams and box double I-beams. All shown in Figure 6.1.
- All the glue joints used SYLVIC R15, with liquid hardener SYLVIC L5, which is resorcinol formaldehyde from the family of phenolic resin (ORICA adhesives and resins 2004).

6.4. Testing procedure

6.4.1 Effect of the circular web-opening

The 290mm deep beams were loaded in four point bending over their full spans of 2.1m with different diameter circular holes cut in the webs (Figure 6.2). The effects of hole sizes of 76mm (3 inches), 102mm (4 inches) and 152mm (6 inches) diameter were studied. Beams without web openings were also tested for comparison purposes. Each circular hole was cut in the webs between the loading head and the nearest support where the maximum shear force occurs (Figures 6.2 and 6.3). The

centre of the circular hole was placed at 300 mm from the support and 145 mm from the top and bottom flanges. Beams were loaded to destruction and load/deflection measurements were made so that the effect of the holes on the beam stiffness and maximum shear capacity could be determined.

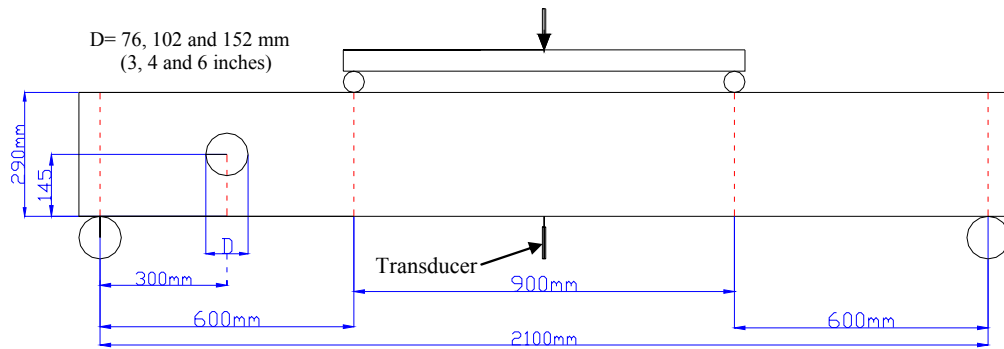


Figure 6.2. Test arrangement for measuring maximum loading capacity of the beams

Testing was carried out in two stages as follows:

- Testing the beams by using the four point bending test before and after making the hole on the webs to measure their stiffness characteristics by plotting the load/deflection slopes. In all cases, the maximum load applied did not exceed the proportional limit loads or cause any damage to the test beams.
- Measuring the maximum shear capacity of the beams subjected to four point bending after making the opening in the webs.

For both tests, mid-span deflections relative to the supports were recorded. The procedure adopted for testing of the beams was broadly based on the recommendations of BS EN 408 (1995).



a) Web opening 152mm diameter



b) Web opening 76 mm diameter

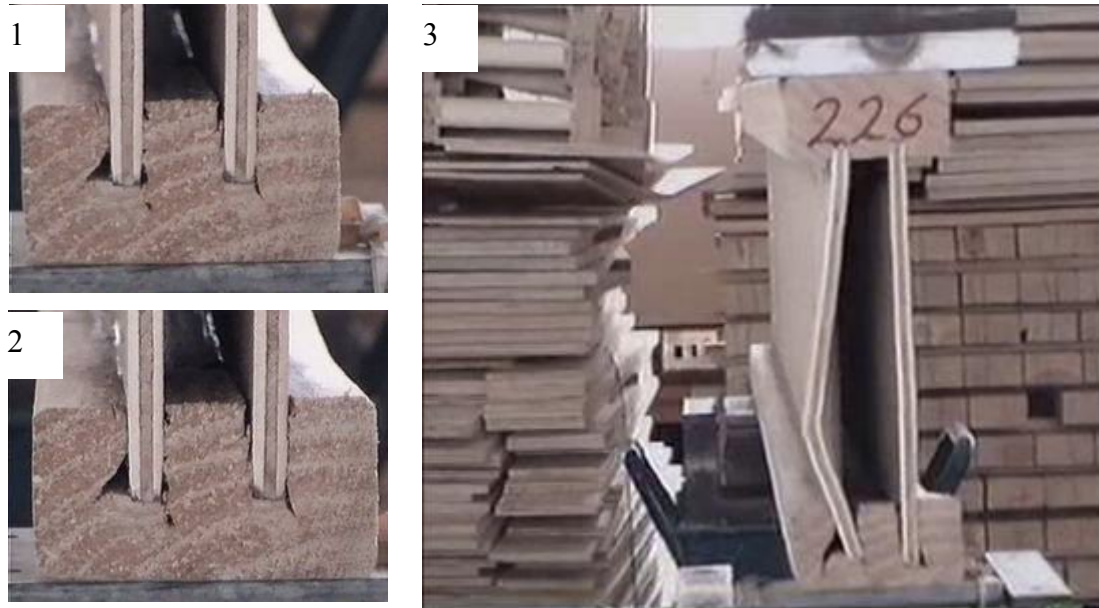
Figure 6.3 Four points bending tests, boxed I-Beam and double I-beam with web opening

6.4.2 Bearing capacity tests

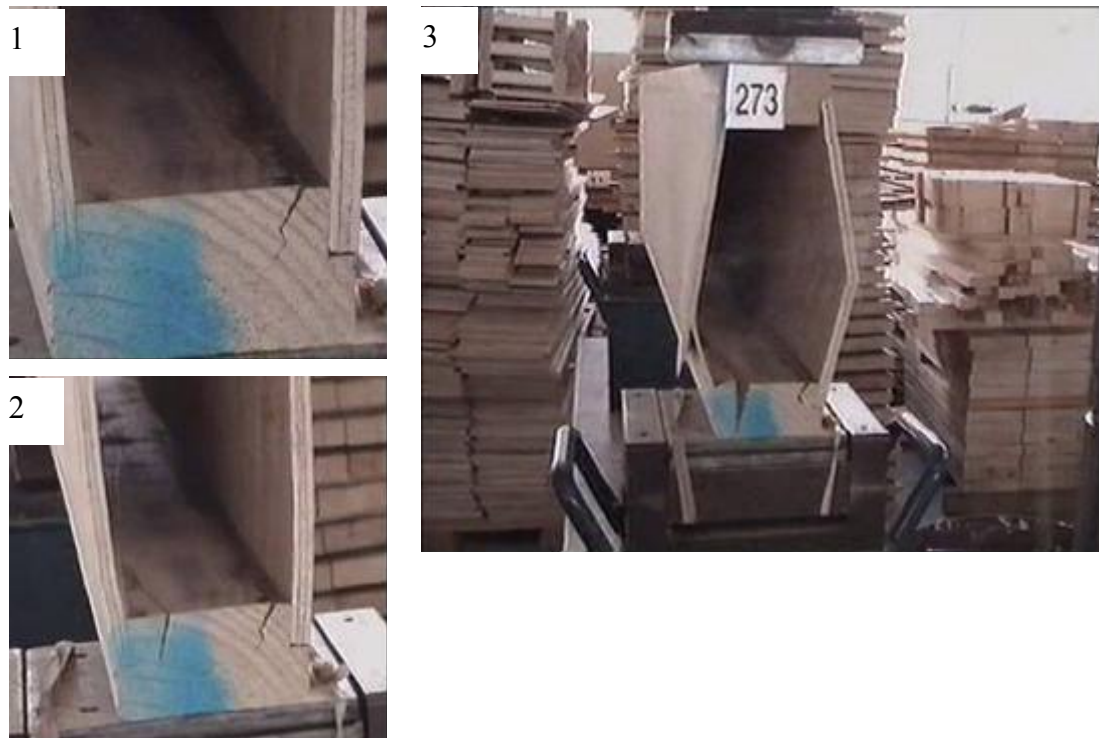
These tests were carried out to determine the bearing capacity of the manufactured beams under concentrated load in accordance with EOTA Technical Report 002 (2000). Test specimens, 1.2 metres long, were cut from undamaged sections of the beams previously tested for stiffness and shear strength. The beams were simply supported on 150mm long bearing plates. The top flange of the beam was loaded to failure above one of the end supports. The maximum load and the mode of failure were recorded. The test arrangement is shown in Figure 6.4, while Figure 6.5 shows the double I-beam and recessed beam after failing under compression load.



Figure 6.4. Test arrangement for measuring maximum bearing capacity of the beams



a) Double I-beam



b) Recessed beam

Figure 6.5. Failure of the double I-beam (top) and recessed beam (bottom) under compression load

6.4.3 Pulling test

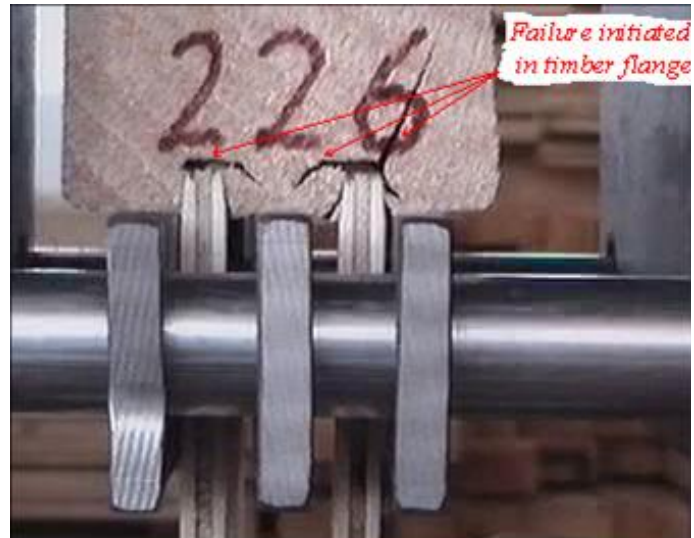
It is recognised that I-Shape designs may be exposed during service to loads hanging on the edges of the bottom flange. This type of loading could cause a different mode of failure, in addition to those of bending, shear and compression.

The testing arrangement used was developed jointly by Ali Bahadori and Bryan Walford in the New Zealand Forest Research Institute. The testing apparatus consists of two set of fingers. These fingers constitute the grips for holding the top and bottom flanges. Depending on which beam design is tested, the number of fingers can be either two or three. These fingers themselves are connected to two U-shape frames, which are in turn connected to the testing machine. Connection between the fingers and U-Shape frame is provided via steel bars, which pass through the circular holes made in each side of the fingers. These holes are made in such a way that a steel bar can be moved easily with the fingers. The testing apparatus and two different testing arrangements are shown in Figures 6.6a to 6.6d.

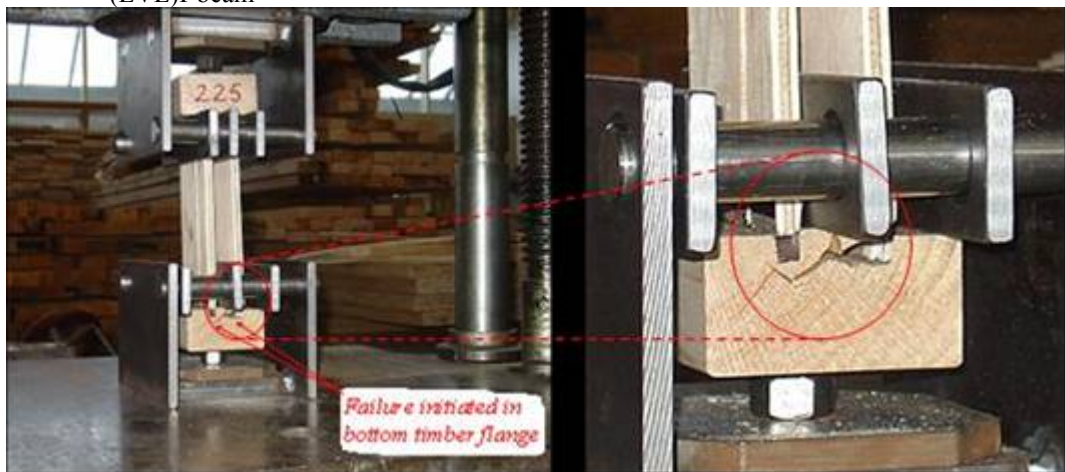
Testing was carried out on beam specimens, 100mm in length, which were cut from the undamaged ends of previously tested beams. The flanges were held within the fingers and pulled apart. The maximum load before failure was recorded. For each design, nine specimens were tested at a loading rate of 5mm per minute.



a) Testing apparatus used to measure pulling resistance of (LVL)I-beam



b) Failure in Double I- beam during pulling test



c) Testing arrangement for measuring the pulling resistance of Double I-beam

d) Failure in Double I-beam, magnified from the left photo

Figure 6.6 Testing apparatus for tension pulling test

6.5 Finite element modelling

CIB beams were modelled using finite element (FE) analysis software ‘LUSAS’, in order to determine the stress distribution and predict the failure mode together with areas of high stress concentration.

6.5.1 Anisotropic nature of wood

Wood by its nature is a highly anisotropic material. This is due to the elongated shapes of wood cells and the oriented structure of the cell walls. Furthermore anisotropic behaviour is caused by differential development of the cell sizes during

growth seasons and partially from a chosen direction of particular cell types (Timber Engineering Step 1, 1995).

A completely anisotropic material has 21 independent elastic constants and will have no plane of symmetry for the material properties. However wood can be described as an orthotropic material, because it has unique and independent mechanical properties along its three perpendicular axes: longitudinal (L), radial (R) and tangential (T). An *orthotropic* material has nine elastic constants when modelling a 3D continuum and has two orthogonal planes of symmetry.

The engineering constants which must be provided are as follows:

E_L, E_T, E_R = Young's moduli in L, T and R directions respectively
 ν_{ij} = Poisson's ratio for transverse strain in the j-direction when stressed in the i-direction, that is, $\nu_{ij} = -\varepsilon_j/\varepsilon_i$

G_{RT}, G_{LT}, G_{LR} = shear moduli in the R-T, L-T and L-R planes, respectively.

These material parameters are used to form the **Compliance Matrix**, $[S_{ij}]$, which relates strain to stress, as following:

$$[\varepsilon] = [S_{ij}] [\sigma] \quad \text{Equation 6.1}$$

Matrix of elastic coefficients for orthotropic material:

$$S_{ij} = \begin{bmatrix} \frac{1}{E_L} & \frac{-\nu_{RL}}{E_R} & \frac{-\nu_{TL}}{E_T} & 0 & 0 & 0 \\ \frac{-\nu_{LR}}{E_L} & \frac{1}{E_R} & \frac{-\nu_{TR}}{E_T} & 0 & 0 & 0 \\ \frac{-\nu_{LT}}{E_L} & \frac{-\nu_{RT}}{E_R} & \frac{1}{E_T} & 0 & 0 & 0 \\ 0 & 0 & 0 & \frac{1}{G_{RT}} & 0 & 0 \\ 0 & 0 & 0 & 0 & \frac{1}{G_{LT}} & 0 \\ 0 & 0 & 0 & 0 & 0 & \frac{1}{G_{LR}} \end{bmatrix} \quad \text{Equation 6.2}$$

In above matrix, Equation 6.2, there are nine independent constants because:

$S_{ij} = S_{ji}$ (the matrix is symmetric) and therefore:

$$\begin{aligned}v_{LR}/E_L &= v_{RL}/E_R \\v_{LT}/E_L &= v_{TL}/E_T \\v_{RT}/E_R &= v_{TR}/E_T\end{aligned}\tag{Equation 6.3}$$

Equation 6.3 is derived by using the concept of strain energy (Bodig and Jayne, 1993).

6.5.2 Modelling the bearing and pulling test

Linear elastic analysis was considered for bearing and pulling tests. Flanges and webs are defined as orthotropic material. The following assumptions are considered:

1. Orthotropic and Geometric axes of the composite are coincident
2. Average values of material properties along the Tangential and Radial axes are considered within the T-R plane thus:

$$E_T = E_R = (E_T + E_R)/2\tag{Equation 6.4}$$

For instance Sitka Spruce young moduli are 425.7 and 772.2 N/mm² along the tangential and radial axes as shown in Table 6.1, so the average value of 598.95 N/mm² is used.

3. Orthotropic angle is 90°

6.5.2.1 Explaining the assumptions

Figure 6.7 is used to explain the logic for the first assumption. The first assumption considers that the Geometric and Orthotropic axes are coincident, which might not be the case in reality. Defining the exact axes of Orthotropy requires the measurement of two angles known as grain angle and ring angle for each individual flange. Measuring these angles is time consuming and then introducing the local coordinate for each flange is required. Considering such a procedure would be impractical, since it is not possible to measure these angles for the commercial beams.

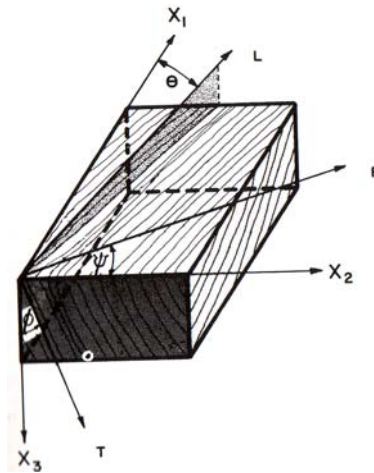


Figure 6.7 Grain angle θ and Ring angle ϕ

The second assumption considers the timber to have planar isotropy. As it is shown in figure 6.8, timber is extracted from different areas of the log and this directly affects the direction of the Tangential and Radial axes.

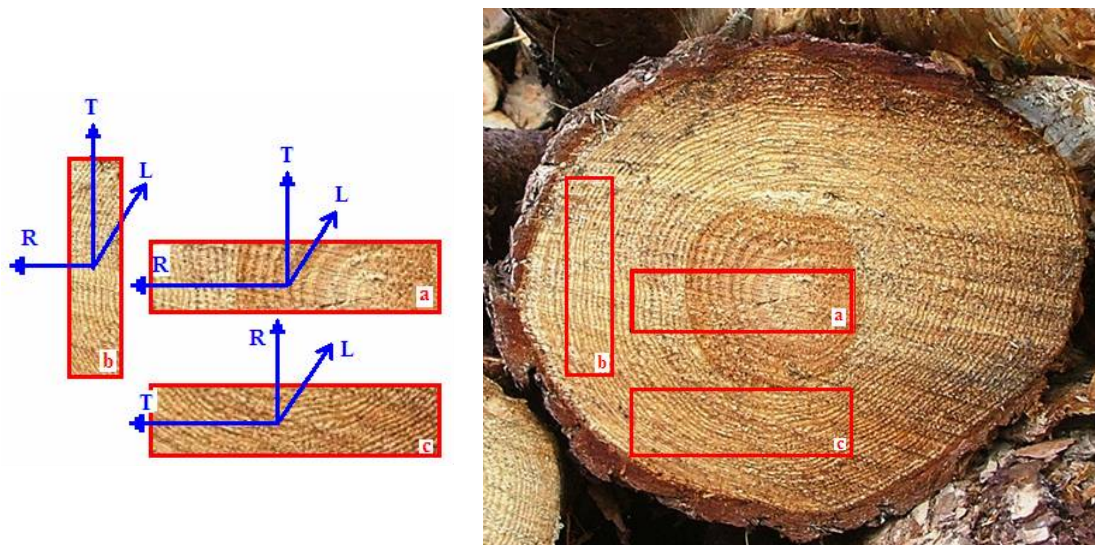


Figure 6.8 Timber is cut from different areas of the log

6.5.2.2 Computational modelling

Currently there is no information available about mechanical properties of the NZ Radiata pine in the Radial and Tangential axes. However, in the Wood Handbook (1999) there are complete mechanical properties of a few species including Douglas-fir, Sitka Spruce and Engelmann Spruce. It was decided to use the elastic and Poisson ratio of Sitka Spruce, since both species come under the softwood category and also they have similar elastic moduli along the longitudinal axes and similar shear moduli in the Longitudinal-Radial planes. The material properties of Sitka

Spruce, which was used for the FE analysis, are given in table 6.1. The Poisson ratio (μ) is denoted as LR, LT, RT, TR, RL and TL. The first letter of subscript refers to the direction of applied stress and the second letter to the direction of lateral deformation. For instance μ_{LT} is the Poisson ratio for tangential deformation caused by stress along the longitudinal axis.

Table 6.1 Elastic parameters and Poisson ratio for Sitka Spruce at 12% moisture content

Specie	E_L (N/mm ²)	E_T/E_L	E_R/E_L	G_{LR}/E_L	G_{LT}/E_L	G_{RT}/E_L
Sitka Spruce	9900	0.043	0.078	0.064	0.061	0.003
	μ_{LR}	μ_{LT}	μ_{RT}	μ_{TR}	μ_{RL}	μ_{TL}
	0.372	0.467	0.435	0.245	0.04	0.025

Based on the ratio given in Table 6.1 and Young modulus along the longitudinal axes (E_L) the elastic ratio and shear modulus values along the three axes can be determined. The value of E_L is determined by using the four point bending test. Table 6.2 shows the value that has been used for finite element analysis in this study.

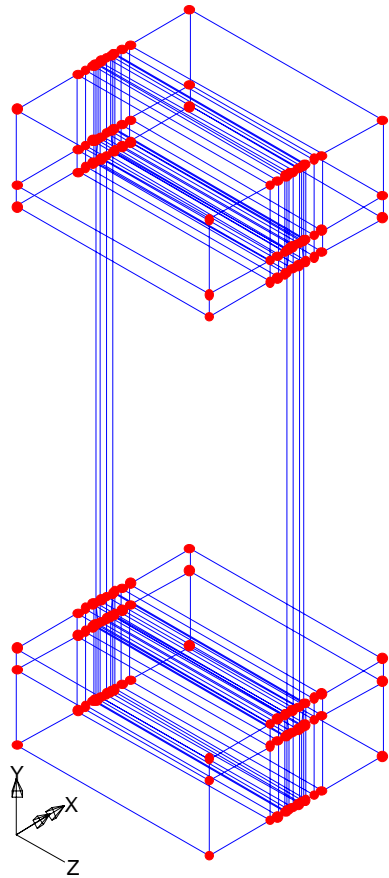
Table 6.2 Mechanical properties of the beam components for FE analysis

<u>Timber flanges</u>	<u>LVL flanges</u>
$E_L = 9490$ (N/mm ²) $\rho = 493$ (kg/m ³) $\mu_{RT} = \mu_{yx} = 0.435$ $\mu_{TR} = \mu_{xy} = 0.245$ Ave $\mu = 0.34$ $E_T = E_x = 408.07$ (N/mm ²) $E_R = E_y = 740.22$ (N/mm ²) $E_L = E_z = 9490$ (N/mm ²) $G_{RT} = G_{xy} = 28.47$ (N/mm ²)	$E_L = 11450$ (N/mm ²) $\rho = 556$ (kg/m ³) $\mu_{RT} = \mu_{yx} = 0.435$ $\mu_{TR} = \mu_{xy} = 0.245$ Ave $\mu = 0.34$ $E_T = E_x = 478.76$ (N/mm ²) $E_R = E_y = 868.45$ (N/mm ²) $E_L = E_z = 11540$ (N/mm ²) $G_{RT} = G_{xy} = 33.40$ (N/mm ²)
<u>Plywood middle veneer</u>	<u>Plywood side veneers</u>
$\rho = 494$ (kg/m ³) $\mu_{RT} = \mu_{yx} = 0.435$ $\mu_{TR} = \mu_{xy} = 0.245$ Ave $\mu = 0.34$ $E_T = E_x = 478.76$ (N/mm ²)	$\rho = 494$ (kg/m ³) $\mu_{RL} = \mu_{yz} = 0.04$ $\mu_{LR} = \mu_{zy} = 0.372$ Ave $\mu = 0.206$ $E_R = E_x = 868.45$ (N/mm ²)

$E_R = E_y = 868.45 \quad (\text{N/mm}^2)$	$E_L = E_y = 11134 \quad (\text{N/mm}^2)$
$E_L = E_z = 11134 \quad (\text{N/mm}^2)$	$E_T = E_z = 478.762 \quad (\text{N/mm}^2)$
$G_{RT} = G_{yx} = 33.40 \quad (\text{N/mm}^2)$	$G_{LR} = G_{zy} = 712.58 \quad (\text{N/mm}^2)$

6.5.3 Results of the finite element analysis

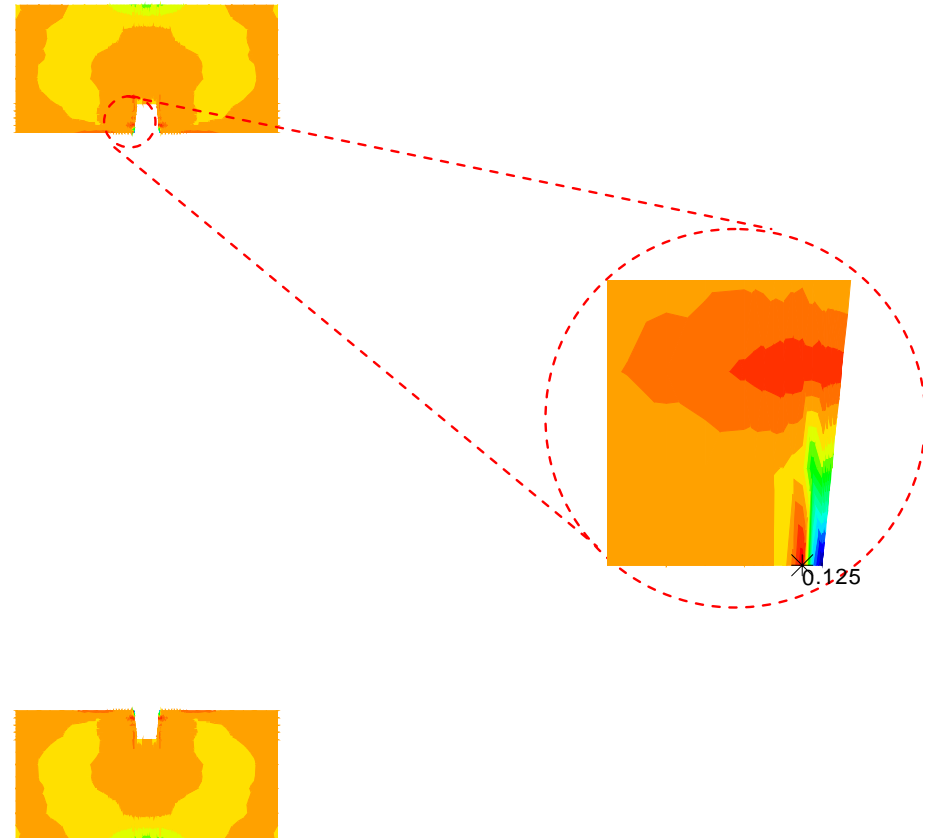
Linear finite element analysis was carried out for different profiles being subjected to bearing and pulling loads. As described earlier, flanges and web(s) are defined as orthotropic material. For instance, the result of compression stress and the area of stress concentration in the flanges of I-beams, double I-beams and box I-beams exposed to a unit load of 1 kN are shown in Figure 6.9. Complete results of finite-element analysis appear in the discussion section where they are summarised in Tables 6.5 and 6.7.



LOAD CASE = 1
 Loadcase 1
 RESULTS FILE = 1
 STRESS
 CONTOURS OF SMax

Dark Blue	-0.401175
Blue	-0.367743
Light Blue	-0.334312
Cyan	-0.300881
Greenish Cyan	-0.26745
Green	-0.234019
Light Green	-0.200587
Yellow-Green	-0.167156
Yellow	-0.133725
Light Yellow	-0.100294
Orange	-0.0668624
Light Orange	-0.0334312
Yellow-Orange	0
Orange	0.0334312
Red-Orange	0.0668624
Red	0.100294

Max 0.1251 at Node 1822
 Min -0.4098 at Node 355



a) I-beam

Figure 6.9 Distribution of the maximum principal stress on timber flange under compression

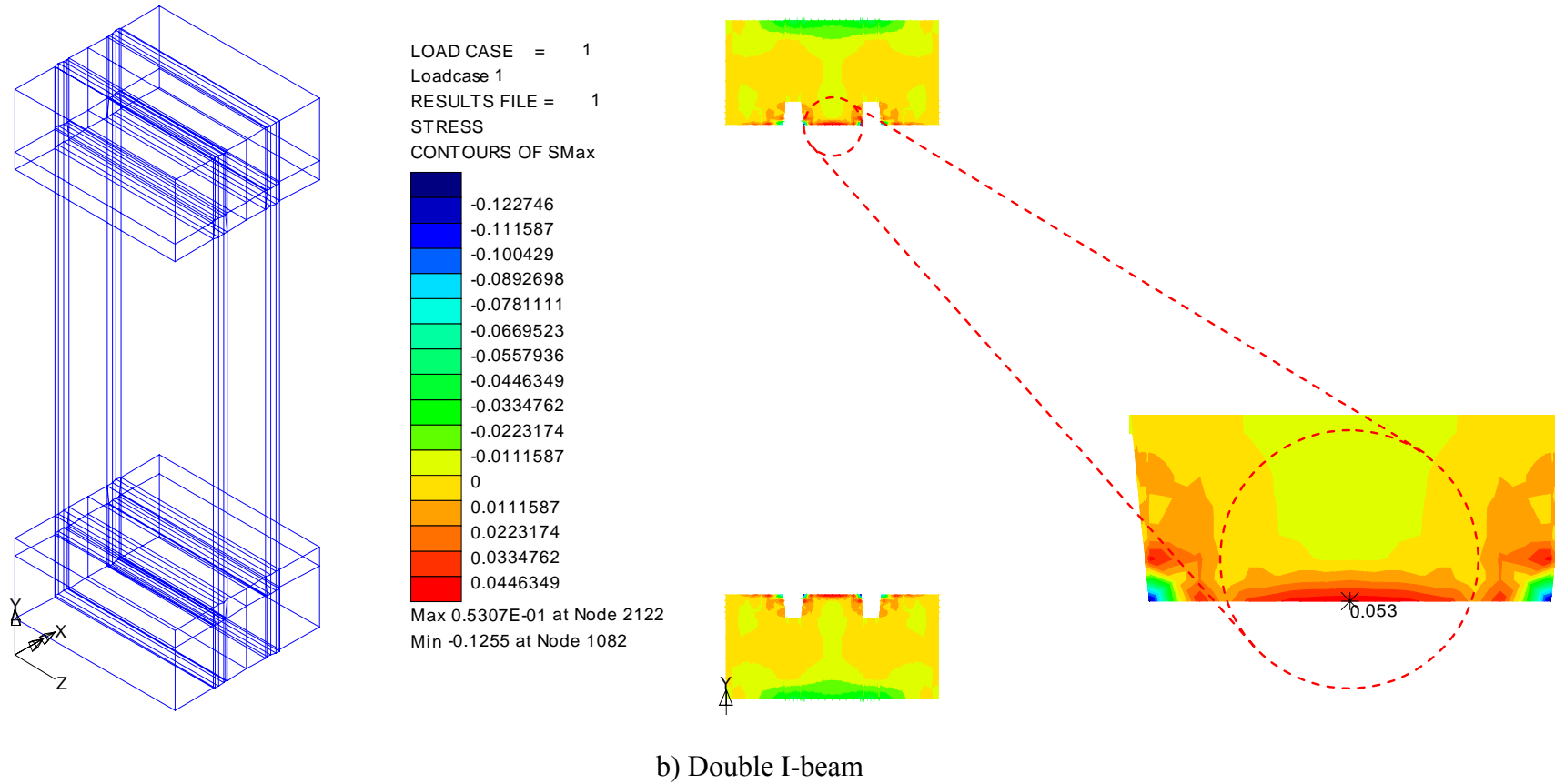
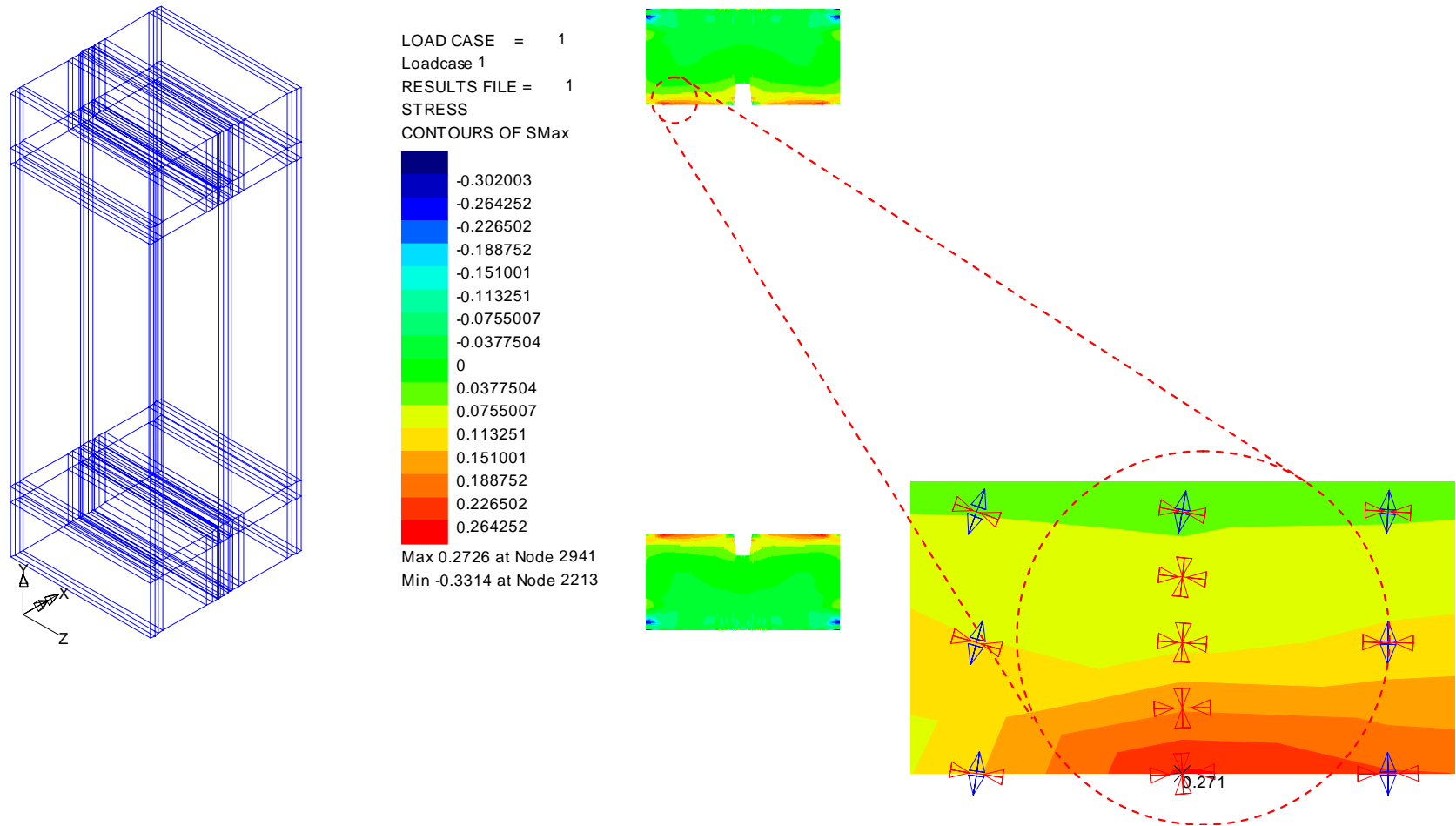


Figure 6.9 Distribution of the maximum principal stress on timber flange under compression (Cont.)



c) Box I-beam

Figure 6.9 Distribution of the maximum principal stress on timber flange under compression (Cont.)

6.6 Buckling of the plywood web

6.6.1 Plywood web subjected to compression load

When cross section of the beams including (LVL) I-beam, (LVL) Double I-beam, Recess beam, Box beam, (LVL) Box I-beam and Box Double I-beam are subjected to compression load, their plywood web(s) act as a column and naturally it is susceptible to buckling (Figure 6.10).

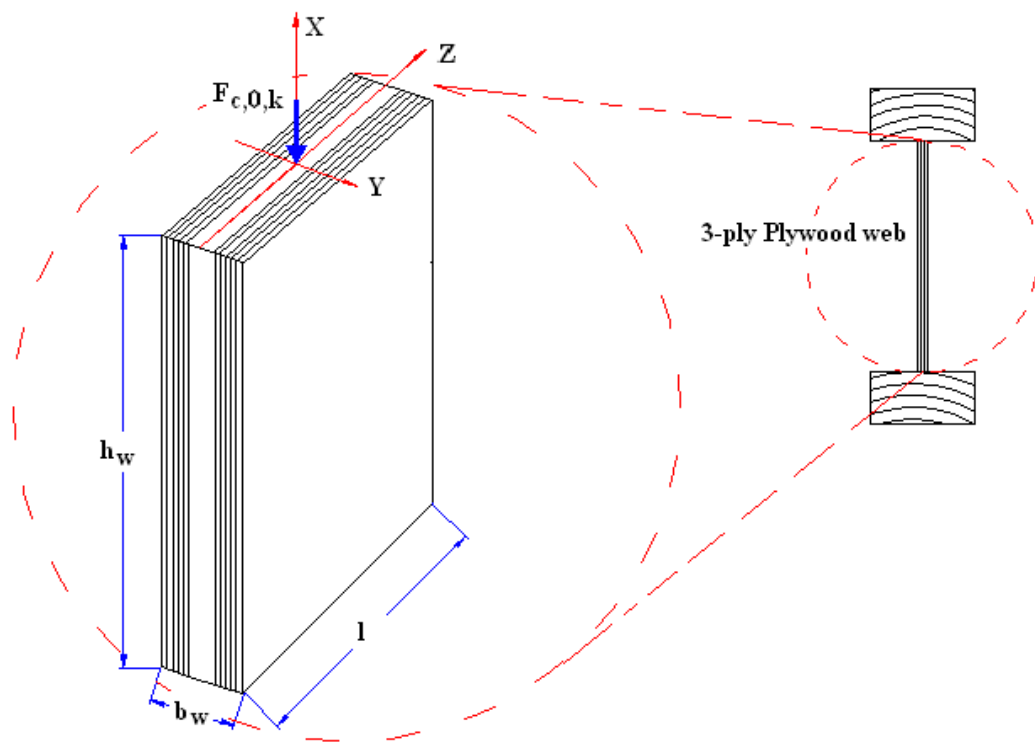


Figure 6.10 Plywood web under compression load

The maximum compression capacity of plywood web before buckling is initiated can be calculated using the recommendations of Eurocode 5 (BS EN 1995-1-1:2004) for stability of a column, where complete calculation procedures are given for a timber flange I-beam. A similar approach is adopted to identify the buckling limit of the other profiles. Complete results are presented in the discussion part, section 6.7.

6.6.2 Geometric properties

The geometrical properties of the I-beam were similar to those of the one explained in section 6.3 and figure 6.1, except that the plywood height is varied from 150mm to 500mm using 25mm steps. The plywood web height was varied in order to

investigate effect of web height on the buckling load limit. Calculation results for various plywood heights are presented at 50mm steps instead of actual 25mm steps to summarise the results. Parameters are defined below:

- Height of the plywood web, h_w : $h_w = 150, 175 \dots 500$ mm
- Breadth of the plywood web, b_w : $b_w = (2 \times 3 + 0.067) = 6.201$ mm
- Breadth of the plywood, b_w , is the transformed section, and 0.067 is the effective contribution of the middle veneer (Bahadori-Jahromi ... et al., 2005)
- Depth of plywood web, bearing length, l : $l = 150$ mm
- Modulus of elasticity, E_{Plywood} : $E_{\text{mean, Ply}} = 11000$ N/mm²
- Characteristic compressive strength, $f_{c, 0}$: $f_{c, 0} = 21.6$ N/mm²

6.6.3 Slenderness

The radii of gyration about y and z, i_y (mm) and i_z (mm) can be calculated by using Equation 6.5.

$$i_y = \sqrt{\frac{I_y}{A}} \quad \text{and} \quad i_z = \sqrt{\frac{I_z}{A}} \quad \text{Equation 6.5}$$

In Equation 6.5:

I_y and I_z are the second moments of area about strong (major) y and weak (minor) x axes: $I_y = 1.74 \times 10^6$ mm⁴ and $I_z = 2.98 \times 10^6$ mm⁴

A is the cross-sectional area of plywood: $A = 930.15$ mm²

Thus the radii of gyration are:

$$i_y = 43.30 \text{ mm} \quad \text{and} \quad i_z = 1.79 \text{ mm}$$

Effective height of the plywood is considered as: $h_{w,ef} = 0.7 h_w$, because the Plywood web is fully restrained between the flanges, so the effective plywood height can be calculated as:

h_w	(mm)	150	200	250	300	350	400	450	500
$h_{w,ef}$	(mm)	105	140	175	210	245	280	315	350

The slenderness ratios corresponding to bending about axes y and z, λ_y and λ_z can be determined from equation 6.6.

$$\lambda_y = \frac{h_{w,ef}}{i_y} \text{ and } \lambda_z = \frac{h_{w,ef}}{i_z} \quad \text{Equation 6.6}$$

Hence slenderness ratios for plywood webs with different height about y and z axes are:

h_w	(mm)	150	200	250	300	350	400	450	500
$h_{w,ef}$	(mm)	105	140	175	210	245	280	315	350
λ_y		2.43	3.23	4.04	4.85	5.66	6.47	7.28	8.08
λ_z		58.66	78.21	97.7	117.31	136.87	156.42	175.97	195.52

The relative slenderness ratios corresponding to bending about axes y and z, $\lambda_{rel,y}$ and $\lambda_{rel,z}$ can be determined from Equation 6.7.

$$\lambda_{rel,y} = \left(\frac{\lambda_y}{\pi} \right) \sqrt{\frac{f_{c,0,d}}{E_{mean,Ply}}} \text{ and } \lambda_{rel,z} = \left(\frac{\lambda_z}{\pi} \right) \sqrt{\frac{f_{c,0,d}}{E_{mean,Ply}}} \quad \text{Equation 6.7}$$

Results for the relative slenderness ratios about axes y and z are given below:

h_w (mm)	150	200	250	300	350	400	450	500
λ_y	2.43	3.23	4.04	4.85	5.66	6.47	7.28	8.08
$\lambda_{rel,y}$	0.034	0.046	0.057	0.068	0.080	0.091	0.103	0.114
λ_z	58.66	78.21	97.76	117.31	136.87	156.42	175.97	195.52
$\lambda_{rel,z}$	0.827	1.103	1.379	1.655	1.931	2.206	2.482	2.758

6.6.4 Compressive instability factors

The instability factors of a plywood web about axes y and z, k_y and k_z can be calculated from Equation 6.8 where $B_c = 0.1$ is the straightness factor of plywood.

$$K_y = 0.5 [1 + B_c (\lambda_{rel,y} - 0.3) + \lambda_{rel,y}^2] \quad \text{Equation 6.8}$$

$$K_z = 0.5 [1 + B_c (\lambda_{rel,z} - 0.3) + \lambda_{rel,z}^2]$$

Values of instability factors along y and x axes in plywood webs of varying height are derived from equation 6.8 and summarised below.

h_w (mm)	150	200	250	300	350	400	450	500
$\lambda_{rel,y}$	0.034	0.046	0.057	0.068	0.080	0.091	0.103	0.114
k_y	0.487	0.488	0.489	0.491	0.492	0.494	0.495	0.497
$\lambda_{rel,z}$	0.827	1.103	1.379	1.655	1.931	2.206	2.482	2.758
k_z	0.869	1.149	1.505	1.937	2.445	3.029	3.690	4.426

The compressive instability factors of a plywood web about axes y and z, k_{cy} and k_{cz} can be calculated from Equation 6.9.

$$K_{c,y} = \frac{1}{K_y + \sqrt{K_y^2 - \lambda_{rel,y}^2}} \quad \text{and} \quad K_{c,z} = \frac{1}{K_z + \sqrt{K_z^2 - \lambda_{rel,z}^2}} \quad \text{Equation 6.9}$$

Results of the compressive instability factors derived from Equation 6.9 are given below.

h_w (mm)	150	200	250	300	350	400	450	500
k_y	0.487	0.488	0.489	0.491	0.492	0.494	0.495	0.497
k_{cy}	1.027	1.026	1.025	1.024	1.023	1.022	1.020	1.019
k_z	0.869	1.149	1.505	1.937	2.445	3.029	3.690	4.426
k_{cz}	0.882	0.681	0.475	0.340	0.253	0.196	0.156	0.127

6.6.5 Assessment of the lateral compressive buckling of the plywood web

Clause 6.3.2(4) in Eurocode 5 (EC5) requires that for $\lambda_{rel,y} > 0.3$ or and $\lambda_{rel,z} > 0.3$, Equation 6.10 should be satisfied.

$$\frac{\sigma_{c,0}}{k_{c,y} f_{c,0}} + \frac{\sigma_{m,y}}{f_{m,y}} + k_m \frac{\sigma_{m,z}}{f_{m,z}} \leq 1$$

$$\frac{\sigma_{c,0}}{k_{c,z} f_{c,0}} + \frac{\sigma_{m,y}}{f_{m,y}} + k_m \frac{\sigma_{m,z}}{f_{m,z}} \leq 1$$

Equation 6.10

But if the section is under pure compression without any bending moment, then equations are simplified to Equation 6.11

$$\frac{\sigma_{c,0}}{k_{c,y} f_{c,0}} \leq 1 \quad \text{and} \quad \frac{\sigma_{c,0}}{k_{c,z} f_{c,0}} \leq 1$$

Equation 6.11

Equation 6.11 can be written as: $\sigma_{c,0} = k_{c,y} f_{c,0}$ knowing that $\sigma_{c,0} = \frac{F}{A}$ so the buckling load of the plywood, along the strong and weak axes, can be determined from equation 6.12.

$$F = k_{c,y} \sigma_{c,0} A \quad \text{and} \quad F = k_{c,z} \sigma_{c,0} A \quad \text{Equation 6.12}$$

Buckling load limits were calculated for I-beams with different web heights using equation 6.12 and results are shown below.

h_w	(mm)	150	200	250	300	350	400	450	500
k_{cy}		1.027	1.026	1.025	1.024	1.023	1.022	1.020	1.019
σ_{c,0}	(N/mm ²)	22.19	22.17	22.14	22.12	22.09	22.07	22.04	22.02
k_{cz}		0.882	0.681	0.475	0.340	0.253	0.196	0.156	0.127
σ_{c,0}	(N/mm ²)	19.06	14.71	10.25	7.34	5.48	4.23	3.37	2.74
F	(kN)	17.73	13.68	9.54	6.83	5.09	3.94	3.13	2.55

There is a non-linear inverse relationship between web height and buckling load limit. For instance, a single plywood web with dimension of $l \times h_w \times b_w = 150 \times 150 \times 9\text{mm}$ when fully restrained can carry an axial load of up to 17.73 kN, but when the plywood web height increases to 500mm the buckling load limit is reduced to 2.55 kN. A similar method was used to calculate the buckling load limit of the different profiles and is discussed in section 6.7.2.

6.7 Discussion of the results

6.7.1 Effect of the web opening

Strength

The average results of the load/deflection measurements for the beams before and after making the web openings are summarised in Table 6.3 and Figure 6.11. These results show that increasing the diameter of the web opening leads to a significant reduction in the maximum load capacity of the beams, but its effect on load/deflection behaviour is not significant.

From the results of tests carried out on beams with no web openings shown in Table 6.3, it is found that the additional web in the double I-beam and recessed beam increases the maximum load capacity of the beams by 78% and by 67%, respectively, compared to the single web I-beam. The two additional webs in the box I-beam enhance the load capacity of the beam by 130% compared to the single web I-beam. Similar patterns were repeated with the LVL double I-beam and LVL box I-beam when they were compared to the results for the single web LVL I-beam.

For a web opening of 76mm, there is no reduction in the load capacity of the I-beam and box I-beam. A reduction in capacity of approximately 10% was found for all other beams tested. When the hole diameter is increased to 102mm, the load capacity of the I-beam is reduced by 6% while double I-beam performance remains unchanged. The 20% reduction in the load capacity of the recess beam and box I-beam is more significant.

Finally, when the maximum hole size of 152mm is considered, strength decreased further. The strength reduction results in Table 6.3 show that the maximum reduction of load capacity was limited to 25% and 24% for the recessed beam and LVL box I-beam while the reduction of strength in the I-beam, double I-beam and box I-beam is limited to less than 20%.

Table 6.3 Bending test results for beams with web openings

Profile	Web opening 0 mm			Web opening 76 mm			Web opening 102 mm			Web opening 156 mm		
	Max P	Δ at Max load	Strength reduction	Max P	Δ at Max load	Strength reduction	Max P	Δ at Max load	Strength reduction	Max P	Δ at Max load	Strength reduction
	(kN)	(mm)	(%)	(kN)	(mm)	(%)	(kN)	(mm)	(%)	(kN)	(mm)	(%)
I-beam	35.4	18	0	35.8	18	0.0	33.4	18	6	28.8	17	19
Double I-beam	62.8	18	0	56.8	17	10	56.9	16	9	50.7	16	19
Recess beam	59.2	20	0	54.7	18	8.0	48.4	14	18	44.1	14	25
Box I-beam	82.4	20	0	81.4	20	0.0	65.6	17	20	67.4	17	18
LVL I-beam	35.2	19	0	32.0	18	9.0	----	----	----	32.0	17	9
LVL Double I-beam	66.7	23	0	----	----	----	----	----	----	----	----	----
LVL Box I-beam	90.8	26	0	----	----	----	----	----	----	69.2	15	24

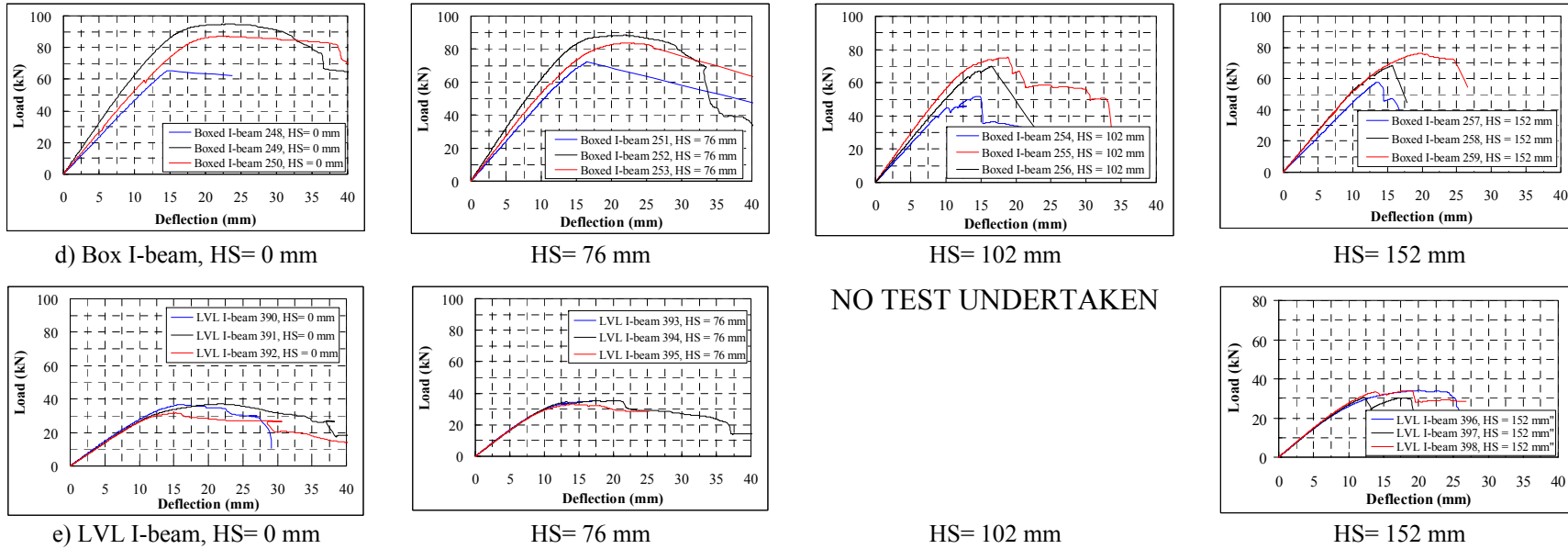


Figure 6.11 Load deflection graphs for different circular web openings



a)I-beam- 152mm



b)Recessed beam- 152mm



c)Double I-beam- 102 mm

Figure 6.12 Beams with circular web opening before and after failure



d)Box I-beam 76mm



e)LVL I-beam 76mm

Figure 6.12 Beams with circular web opening before and after failure (Cont.)

Stiffness

As discussed in Chapter 4, stiffness is proportional to Young's Modulus of Elasticity, which itself is proportional to the load/deflection value. In other words the value of load over deflection indicates stiffness of the beam. Table 6.4 shows the summary of the load/deflection results for I-beams, double I-beams and boxed I-beams with web openings 0mm, 76mm, 102mm and 152mm in diameter. The value of the load over deflection is presented as K , where the following nomenclature applies:

NF: No foam or without infill material

H 0:

H 76: Hole or opening diameter and the following number indicates the

H 102: diameter of the circular opening

H 152:

For instance $K_{NF,H 102}$, indicates value of the load over deflection for a beam without infill and web opening of 102 mm.

For each profile three values are shown as follows:

- 1 $K_{NF,H 0}$: Load/deflection value before creating the web opening
- 2 $K_{NF,H 76}$: Value of the load/deflection after creating the web opening of 76, 102 and 152 mm
- 3 $K_{NF,H 102}$: Load deflection ratio
- $K_{NF,H 152}$
- $K_{NF,H 76}/K_{NF,H 0}$
- $K_{NF,H 102}/K_{NF,H 0}$
- $K_{NF,H 152}/K_{NF,H 0}$

The average load deflection ratio for web opening of 152 mm, $K_{NF,H 152}/K_{NF,H 0}$, in table 6.4 shows 10% to 11% reduction of stiffness for the I-beams, double I-beams and boxed I-beams. Web openings of 76mm and 102 mm have negligible effect on the stiffness of the double I and boxed I-beams, but holes of those sizes cause average reductions of 6% and 10% in stiffness for I-beams. Test results for the LVL I-beams show 14% reduction of stiffness for the web opening of 76mm and 20% for the web opening of 152mm. These outcomes are important as in most cases stiffness is the governing design parameter rather than strength. For instance, if a beam is to be used in a flooring system, serviceability governs the design, but is directly affected by the stiffness and Young modulus of the section. Chapters 7 and 8 discuss this issue in detail.

Table 6.4 Effect of a circular web opening in load/deflection of short span beams

	I-beams					
I-Beam	ID:305	ID:306	ID:307	AVE	SD	C_v
$K_{NF,H 0}$ (kN/mm)	2.306	3.560	3.209	3.02	0.65	21.39
$K_{NF,H 76}$ (kN/mm)	2.158	3.253	3.071	2.83	0.59	20.74
$K_{NF,H 76}/K_{NF,H 0}$	0.94	0.91	0.96	0.94	0.02	2.33
I-Beam	ID:308	ID:309	ID:310	AVE	SD	C_v
$K_{NF,H 0}$ (kN/mm)	2.986	3.242	3.137	3.12	0.13	4.12
$K_{NF,H 102}$ (kN/mm)	2.488	3.004	2.906	2.80	0.27	9.80
$K_{NF,H 102}/K_{NF,H 0}$	0.83	0.93	0.93	0.90	0.05	6.03
I-Beam	ID:311	ID:312	ID:313	AVE	SD	C_v
$K_{NF,H 0}$ (kN/mm)	3.137	2.469	3.156	2.92	0.39	13.39
$K_{NF,H 152}$ (kN/mm)	2.751	2.427	2.649	2.61	0.17	6.35
$K_{NF,H 152}/K_{NF,H 0}$	0.88	0.98	0.84	0.90	0.07	8.26
	Double I-beam					
Double I-Beam	ID:227	ID:228	ID:229	AVE	SD	C_v
$K_{NF,H 0}$ (kN/mm)	3.480	5.070	3.925	4.16	0.82	19.73
$K_{NF,H 76}$ (kN/mm)	3.706	4.816	3.957	4.16	0.58	14.00
$K_{NF,H 76}/K_{NF,H 0}$	1.06	0.95	1.01	1.01	0.06	5.70
Double I-Beam	ID:230	ID:231	ID:232	AVE	SD	C_v
$K_{NF,H 0}$ (kN/mm)	3.400	4.704	4.387	4.16	0.68	16.33
$K_{NF,H 102}$ (kN/mm)	3.460	4.461	4.319	4.08	0.54	13.27
$K_{NF,H 102}/K_{NF,H 0}$	1.02	0.95	0.98	0.98	0.03	3.52
Double I-Beam	ID:233	ID:234	ID:235	AVE	SD	C_v
$K_{NF,H 0}$ (kN/mm)	3.446	4.592	4.609	4.22	0.67	15.81
$K_{NF,H 152}$ (kN/mm)	3.488	3.859	3.734	3.69	0.19	5.11
$K_{NF,H 152}/K_{NF,H 0}$	1.01	0.84	0.81	0.89	0.11	12.28
	Box I-beam					
Boxed I-Beam	ID:251	ID:252	ID:253	AVE	SD	C_v
$K_{NF,H 0}$ (kN/mm)	4.736	6.112	5.184	5.34	0.70	13.13
$K_{NF,H 76}$ (kN/mm)	4.591	5.873	5.410	5.29	0.65	12.27
$K_{NF,H 76}/K_{NF,H 0}$	0.97	0.96	1.04	0.99	0.05	4.59
Boxed I-Beam	ID:254	ID:255	ID:256	AVE	SD	C_v
$K_{NF,H 0}$ (kN/mm)	4.185	5.721	5.298	5.07	0.79	15.65
$K_{NF,H 102}$ (kN/mm)	4.424	5.615	5.121	5.05	0.60	11.84
$K_{NF,H 102}/K_{NF,H 0}$	1.06	0.98	0.97	1.00	0.05	4.85
Boxed I-Beam	ID:257	ID:258	ID:259	AVE	SD	C_v
$K_{NF,H 0}$ (kN/mm)	4.804	5.259	5.788	5.28	0.49	9.32
$K_{NF,H 152}$ (kN/mm)	4.220	4.752	5.117	4.70	0.45	9.61
$K_{NF,H 152}/K_{NF,H 0}$	0.88	0.90	0.88	0.89	0.01	1.49

The effect of opening size on the stiffness of each beam design can be seen by examining the slope of the load/deflection curves in Figure 6.11. Failure in the majority of cases occurred at the weakest point of shear area where the web opening was located as shown in Figure 6.12. However, in the timber/LVL flange box I-beam with 76 mm hole size, some of the failures occurred in the clear area. This is because the weakening effect of the 76mm opening is not as severe as for 102 mm or 152 mm web opening, therefore variability of the web material could compensate for this reduction of strength. In other words the uncut area of the web may be weaker than the area with the 76 mm web opening.

6.7.2 Bearing capacity of the beams

Results of the bearing capacity tests are given in Table 6.5. The maximum load for each design is given in column 1. The additional webs in the double I-beams, box beams, box I-beams and box double I-beams were found to improve on the maximum bearing capacity of the timber flange I-beam by 91%, 23%, 107% and 189%, respectively. Similarly, additional webs in the LVL double I-beams and LVL box I-beams raised the maximum bearing capacity of the LVL flange I-beams by 73% and 135% respectively. Exceptionally, the additional web in the recessed beam has a minor effect by enhancing the maximum bearing capacity of the beam just 6%. The double I-beams exhibited best performance in comparison with other profiles. This could be due to the groove providing a superior web to flange connection in comparison to recess or laminated connections.

Table 6.5 Average bearing capacity and flange tensile and shear stresses per unit load

Profiles	Max load	Numerical flange stress per unit load		Numerical stress-strength ratio per unit load	
		$\sigma_{t,max}$	$\tau_{s,max}$	$\frac{\sigma_{t,max}}{f_{90,t}}$	$\frac{\tau_{s,max}}{f_v}$
	(kN)	(N/mm ²)	(N/mm ²)		
I-beam	25.91	0.13	0.47	0.052	0.051
Double I-beam	49.35	0.05	0.20	0.020	0.022
Recessed beam	27.57	0.13	0.16	0.052	0.017
Box beam	31.86	0.15	0.34	0.060	0.037
Box I-beam	53.61	0.27	0.52	0.108	0.056
Box double I-beam	74.84	0.10	0.21	0.040	0.023
LVL I-beam	26.44	0.11	0.40	0.044	0.043
LVL Double I-beam	45.80	0.07	0.18	0.028	0.019
LVL Box I-beam	62.23	0.31	0.48	0.124	0.052

$\sigma_{t,max}$: Maximum principal stress (Tension)

$\tau_{s,max}$: Maximum shear stress

6.7.3 Failure modes

Failure in the I-beams and double I-beams was initiated by buckling of the web followed by cracking of the flange, whereas in the recessed beams, box beams, LVL and timber I-beams and box double I-beams, flange cracking was observed first followed by web buckling. Flange cracking in the LVL or timber I-beams and LVL or timber double I-beams was initiated around the groove area, whereas in the case of the box beams, recess beams, LVL or timber box I-beams and box Double I-beams cracking started in the flange area close to the side webs, as seen in Figure 6.5.

In order to develop a better understanding of this behavior, a finite element model of the bearing capacity test was developed using the LUSAS software package (2005), as shown in Figure 6.9. The flange maximum tensile and shear stresses predicted by the model for a unit load are presented in Table 6.5. Jain (2004) reported stress limits for NZ Radiata pine of 2.49 N/mm^2 for tension perpendicular to the grain ($f_{90,t}$) and 9.27 N/mm^2 for shear (f_v). These values were used to calculate, the flange stress-strength ratios in Table 6.5.

A buckling analysis of the plywood webs was carried out for the different cross-sections using a procedure similar to that described in section 6.6. The analysis is conducted in accordance with the recommendation of Eurocode 5, Clause 6.3 for stability of the members. The results of this analysis along with the corresponding flange tensile and shear stress/strength ratios are given in Table 6.6. Based on these results, it can be concluded that failure in the timber or LVL I-beams and timber and LVL double I-beams is initiated with web buckling, since at the buckling load limit the value of the tensile and shear ratios remain lower than 1. In contrast, the tensile ratio exceeds its limit in the recessed beams, box beams, timber or LVL Box I-beams and box double I-beams when they are exposed to the buckling load limit. So it can be predicted that, in those profiles, failure is initiated with flange tension cracking. The finite element model correctly identifies the point at which the tension cracking failure initiates. The location of the maximum flange principal stress is found to occur at the groove in the top flange in the I-beam model and at a point on the top flange near the outer edge in the box I-beam model as shown in Figure 6.9.

Table 6.6 Buckling limit load and corresponding tensile and shear ratios

Profile	Failure load	Buckling limit to EC5	Flange <u>tensile</u> ratio at buckling load	<i>Flange <u>shear</u> ratio at buckling load</i>
	(kN)	(kN)		
I-beam	25.91	13.68	0.71	0.69
Double I-beam	49.35	27.36	0.55	0.59
Recess beam	27.57	27.36	1.43	0.47
Box beam	31.86	27.36	1.65	1.00
Box I-beam	53.61	36.86	4.00	2.07
Box double I-beam	74.84	50.36	2.02	1.14
LVL I-beam	56.44	13.68	0.60	0.59
LVL double I-beam	45.80	27.36	0.77	0.53
LVL box I-beam	62.23	37.26	4.64	1.93

It should be noted that since the sequence of failures depends on the buckling load, the sequence will change if the height of the beam is increased or reduced. Figure 6.13 shows the variation of the buckling load limit for the I-beams, double I-beams and box I-beams when the web height is varied from 150 to 500mm. Plywood web height is the clear distance between top and bottom flanges.

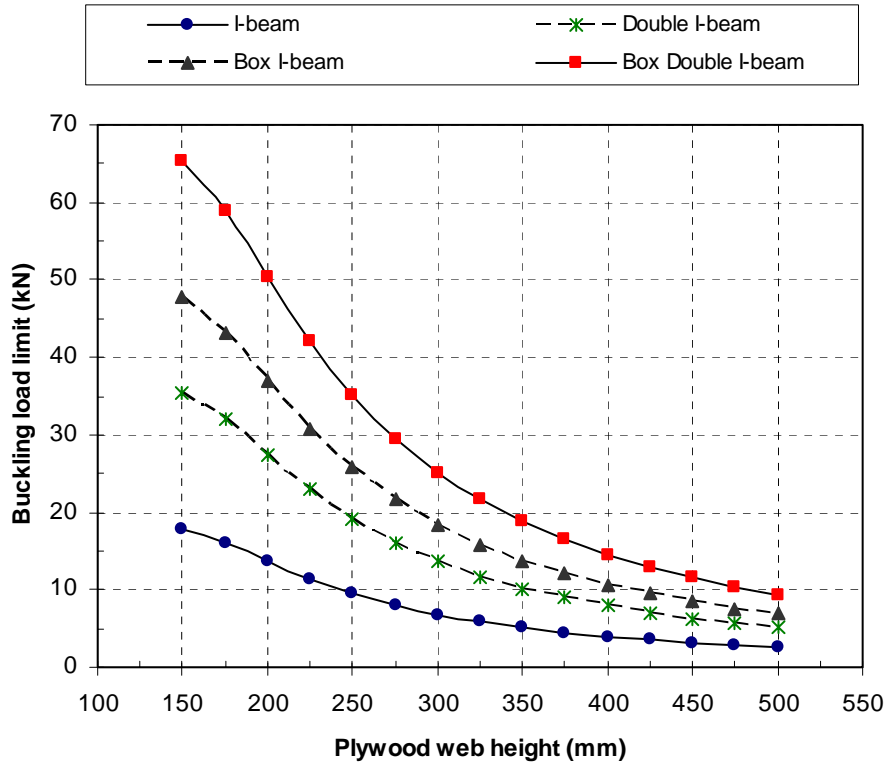


Figure 6.13 Buckling load limit corresponding to plywood web height

The experimental and analytical procedures show that combination of web buckling due to vertical compressive load and flange cracking due to local tension caused the bearing failure of the different cross sections. Therefore provision of infill material could increase the bearing capacity of the section, improve the buckling resistance of the webs and improve distribution of tensile stress in the flange. Further discussion on the effects of infill material on structural performance of the composite beams is presented in chapter 9.

6.7.4 Pulling resistance

The pulling resistance measurements of the timber/LVL flange I and double I-beams, obtained from experimental tests, are given in Table 6.7. The experimental results

show that the strength of a section is directly proportional to the number of webs in that section.

The results of these tests show that the structural glue provides perfect bonding between the webs and flanges. Failure occurred either in the top or bottom flanges but not in glue line as shown in Figure 6.6. In order to determine the factor controlling failure, hanging loads of 1kN were applied to the finite element model shown in Figure 6.9. The resulting maximum tensile and shear stresses in the flange and web of each beam are reported in Table 6.7. Comparing the stress-strength ratio of the LVL or timber I-beam and double I-beam in Table 6.7 shows that pulling resistance of the beams depends on tensile strength perpendicular to the grain of the flange.

Table 6.7 Maximum pulling resistance and flange and web stresses

Profile	Ave sample length	Max pulling resistance	Numerical flange stress per unit load		Numerical flange stress-strength ratio per unit load		Numerical web stress per unit load		Numerical web stress-strength ratio per unit load	
			$\sigma_{t,max}$	$\tau_{s,max}$	$\frac{\sigma_{t,max}}{f_{90,t}}$	$\frac{\tau_{t,max}}{f_v}$	$\sigma_{t,max}$	$\tau_{s,max}$	$\frac{\sigma_{t,max}}{f_{0,t}}$	$\frac{\tau_{t,max}}{f_v}$
	(mm)	(kN)	(N/mm ²)	(N/mm ²)			(N/mm ²)	(N/mm ²)		
I-beam	101.2	6.5	4.71	2.22	1.89	0.24	1.88	0.98	0.05	0.11
Double I-beam	100.8	13.9	2.19	1.06	0.88	0.11	1.07	0.54	0.03	0.06
LVL I-beam	100.3	6.7	4.34	1.99	1.74	0.22	1.93	0.99	0.05	0.11
LVL Double I-beam	100.5	13.3	1.99	0.99	0.80	0.11	1.10	0.56	0.03	0.06

$\sigma_{t,max}$: Maximum principal stress (Tension)

$\tau_{s,max}$: Maximum shear stress

6.8 Summary and conclusions

The effect of circular web openings of different diameters on stiffness and strength of the nine different beam profiles have been discussed and compared. The bearing capacity of each profile and pulling resistance of the LVL/ timber I and double I-beams has been investigated. A finite element model has been used to simulate and predict bearing and pulling failures. In addition, an analytical procedure based on Eurocode 5 was developed to predict the buckling load limit of a beam profile exposed to compressive load.

This study shows that the diameter of the circular hole has a major effect on the reduction of the maximum loading capacity of the beams, whereas its effect on load/deflection of the beams is less pronounced.

The effect of the web opening on reduction of stiffness is more severe for I-beams or LVL I-beams than for double I or boxed I-beams. For instance, web openings of 76mm and 102mm have negligible effect on the stiffness reduction of the double, and boxed I-beams, but it caused 6% and 10% stiffness reduction in I-beams.

Additional webs significantly enhance the structural performance of the I-beams. For instance, it is shown that shear loading capacity of double I-beams and box I-beams with 152mm web openings is 52% and 101% higher than for the I-beam without a web opening.

The poor performance of the recessed beam under compressive load highlights the importance of the web-flange connection method.

The compressive stress test results proved that failure is caused by a combination of web buckling and flange cracking, where the sequence of failure is governed by the cross-section of the profile and the height of the beam.

For pulling resistance, experimental results show that tension stress perpendicular to the grain direction of the flange is a controlling factor for evaluating the resistance of the beam under hanging loads

CHAPTER 7: DEVELOPMENT OF THE PARAMETRIC MODEL TO ASSESS THE PERFORMANCE OF THE CIB BASED ON EUROCODES

7.1 Introduction

This chapter provides a description of the analytical model which was developed for assessment of the CIB beams used in timber flooring systems. The permissible span for a double I-beam was evaluated using the model. In addition, it is explained that this model can be used to predict the maximum permissible span of any CIB profile together with its governing design criteria. These analytical procedures were used for the parametric study which is presented in chapter 8. Finally, it is shown that increasing the beam/joist stiffness is the most straightforward way to avoid or reduce excess timber floor vibration.

As all the calculations are based on Eurocodes, so the chapter begins with a brief discussion of several Eurocodes and leads on to the reasons for developing and adopting the Eurocodes. Moreover, the current and future status of Eurocodes in the UK is assessed to demonstrate their relevance.

7.2 Eurocodes

Eurocodes are the European standards for designing both buildings and civil engineering structures. These codes of practice are prepared to establish a set of common technical rules for design work and replace differing rules in the various member states of EU. This is part of the European Union's effort to remove the technical obstacles to trade, because Eurocodes facilitate the functioning of a single market for products and engineering services. Eurocodes relevant to civil engineering comprise 10 main codes, and except for EN 1990, each comes in a number of parts.

EN 1990: Basis of structural design is the key document to the Eurocode standards for it explains the principles and requirements for safety, serviceability and durability of structures.

EN 1991: Actions on structures, second only to EN 1990 in importance, provides comprehensive information on all actions (loads) that should normally be considered and calculated in the design of building or civil engineering work. It has four parts. The first considers self and imposed loads together with actions due to fire, snow, wind, heat, construction activities and accidents. The other three parts deal with traffic loads on bridges, actions by cranes or machinery and actions on silos or tanks.

EN1995 provides the design rules for building and civil engineering works in timber. Eurocode EN1995 should be always used in conjunction with Eurocodes EN 1990 and 1991.

Eurocodes are produced and published by CEN, the Standards body for Europe. The members are the National Standards Bodies (NSBs) for instance British Standard Institute (BSI), in the UK.

7.2.1 National title page, foreword and Annex

A National title page, a National Foreword together with a National Annex, could be added to the document prepared by CEN. The National Annex is an essential document because it enables local use of the Eurocode. For instance, the National Annex provides country specific data like a snow or wind map or values where a symbol only is given in the Eurocode. In Britain, the BSI is responsible for preparing and publishing the National Annex.

7.2.2 Status of Eurocodes in UK

The British Standards Institute (BSI) states that currently Eurocodes have the same status as BSI codes and within a few years they will replace the British documents. Furthermore, completion of the all the Eurocodes is scheduled for 2006. (BSI 2005)

7.2.3 EN1995 Eurocode 5: Design of timber structures

EN1995 Eurocode 5 consists of three parts: common rules for buildings, structural fire design rules and bridge construction rules. Eurocode 5 employs limit state theory whereas the current BSI timber codes use the permissible stress concept (BSI 2005).

Permissible stress design

In permissible stress design, also known as modular ratio or elastic design, the stress level is always limited to the elastic zone. It is possible to calculate the stress for a material by using the linear relation of stress-strain; however, there are two major problems in this method. First, in most cases the design will be conservative. Second, as quality of the materials is increased and the safety margins are reduced, the assumption that stress is directly proportional to strain becomes unjustifiable (Arya 2002).

Limit state design

This theory originally came from the former Soviet Union in the 1930s and developed in Europe in the 1960s. Most of the modern codes are based on this philosophy. According to the limit state philosophy, structural design should fulfil two criteria. Ultimate limit state design concerns safety for users and structure, so bending, shear or bearing failure characteristics are specified. Serviceability limit state design concerns the functioning of the structure, in terms of comfort for the users and appearance of the construction, so acceptable deflection or vibration characteristics are specified (BS EN 1990, 2002).

7.3 Design model based on Eurocode 5

This section explains the design model which was developed to assess a timber floor constructed with CIB joists. In this model, a double I-beam (Figure 7.1) is chosen as the representative CIB profile, but this model can also be adapted to evaluate box and box I-beams together with I-beams and solid timber joists.

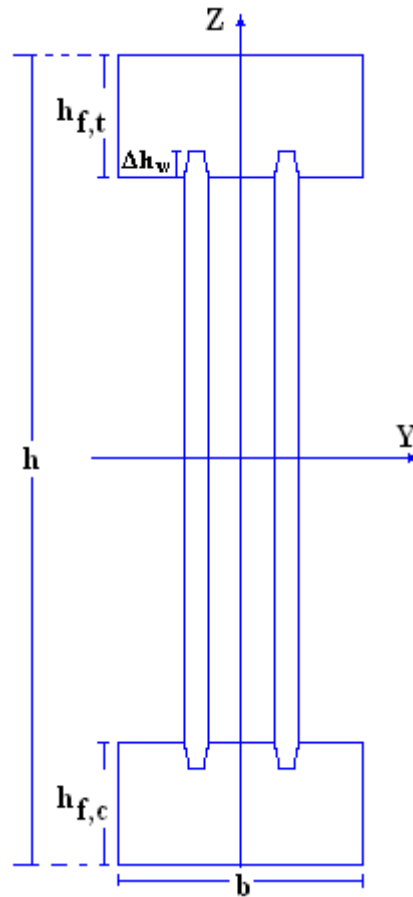


Figure 7.1 Cross section of the model design, double I-beam

7.3.1 Geometric properties

The geometric properties of the flooring system with double I-beam joists were specified as follows:

Floor span, L (mm):	$L = 5600$ mm
Floor breadth, B (mm):	$B = 5600$ mm
Breadth of the flange b (mm):	$b = 90$ mm
Depth of the joist h (mm):	$h = 300$ mm
Spacing of the joists s (mm):	$s = 400$ mm
Breadth of the webs b_w (mm):	$b_w = 18$ mm
Compressive or tensile flange depth $h_{f,c}$ or $h_{f,t}$ (mm):	$h_{f,c} / h_{f,t} = 45$ mm
Clear distance between flanges h_w (mm):	h_w (mm) = 210 mm
Glued embedded length of the web into the flanges	$\Delta h_w = 12$ mm

Δh_w (mm):

Mean characteristic elastic modulus of timber, parallel to the grain, $E_{0,mean,timber}$ (N/mm²): $E_{0,mean,timber} = 8000$ (N/mm²)

Mean characteristic elastic modulus of OSB web, $E_{m,0,mean,OSB}$ (N/mm²): $E_{m,0,mean,OSB} = 4930$ (N/mm²)

Young's modulus ratio (OSB to timber)
 $n = E_{m,0,mean,OSB} / E_{0,mean,timber}$ $n = 0.616$

Equivalent breadth of the web, b_{wEqu} (mm): $b_{wEqu} = 11.01$ (mm)

Thickness of P5 particleboard t (mm): $t = 22$ mm

Mean characteristic elastic modulus of P5 particleboard, $E_{0,mean,P5}$ N/mm² $E_{0,mean,P5} = 3500$ (N/mm²)

Bearing length l (mm): $l = 100$ (mm)

7.3.2 Basic variables

In this design procedure, C refers to the clause in Eurocode 5. For instance C 2.2.2 refers to the Clause 2.2.2 in Eurocode 5 (EC5).

Design limit states:	Ultimate limit	C 2.2.2
	Serviceability	C 2.2.3
Flange strength class:	C16	BS EN 338
Load duration class:	Permanent	C2.3.1.2(2)
	Medium-term	C2.3.1.2(2)
Service class	2	C2.3.1.3(3)

Characteristic values of permanent and variable actions: g_k and q_k in (kN/m²)

Density of the timber ρ_{timber} (kg/m³): 370 kg/m³

Density of the OSB ρ_{OSB} (kg/m³): 550 kg/m³

Cross area of the timber flanges, A_{Flange} (mm²): $A_{timber} = 8100$ mm²

Cross area of the OSB webs, A_{osb} (mm²): $A_{OSB} = 3780$ mm²

Weight per meter length for Double I-beam, 5.076 kg/m

$$W_{\text{Double I-beam}} = \frac{(A_{OSB} \times \rho_{OSB} + A_{timber} \times \rho_{timber})}{10^6}$$

Weight per area for Double I-beam $m_{joist} = 12.69$ kg/m²

$$m_{\text{joist}} = W_{\text{Double I-beam}} / (s / 1000)$$

Permanent action of Double I-beam,

$$g_{m,\text{joist}} = 0.124 \text{ kN/m}^2$$

$$g_{m\text{joist}} = m_{\text{joist}} (9.81 / 1000)$$

Weight per area for floor (BS 5268-7.1: 1989)

$$m_{\text{imposed}} = 50 \text{ kg/m}^2$$

Permanent action $g_{k1} = 50 \times (9.81 / 1000)$

$$g_{k1} = 0.49 \text{ kN/m}^2$$

Total permanent action $g_k = g_{k1} + g_{m\text{joist}}$

$$g_k = 0.614 \text{ kN/m}^2$$

Variable action, q_k (Table 6.2 in Eurocode 1-1-1)

$$q_k = 1.5 \text{ kN/m}^2$$

Cross sectional area of the floor joist, $A = bh - [(b - b_w)h_w] = 11880 \text{ mm}^2$

Equivalent cross sectional area of Double I-beam,

$$A_{\text{Equ}} = bh - (b - b_{w,\text{Equ}})h_w = 10412.1 \text{ mm}^2$$

Second moment of area about the strong axis, I_y (mm^4)

$$I_y = \left[\frac{(bh^3)}{12} \right] - \left[\frac{[(b - b_{w,\text{Equ}})h_w^3]}{12} \right] = 141539467.5 \text{ mm}^4$$

Second moment of area about the weak axis, I_z (mm^4)

$$I_z = \left[b^3 \frac{h_{fc}}{6} \right] + \left[(0.5b_{w,\text{Equ}})^3 \frac{h_w}{6} \right] + b_{w,\text{Equ}} \times h_w (11 + 0.25b_{w,\text{Equ}})^2 = 5910629.4 \text{ mm}^4$$

Section modulus about strong axis, W_y (mm^3)

$$W_y = \frac{I_y}{0.5h} = 943596.45 \text{ mm}^3$$

Section modulus about the weak axis, W_z (mm^3)

$$W_z = \frac{I_z}{0.5h} = 131347.32 \text{ mm}^3$$

Torsional constant

The torsional constant, I_{tor} (mm^4) was calculated using the ‘soap bubble’ analogy, also known as Prandtl’s membrane analogy, in conjunction with the LUSAS finite element package (Figure 7.2). The calculation was achieved by creating an imaginary mesh on the beam surface using triangular elements and employing the LUSAS solver. The ‘soap bubble’ analogy is for sections made from a single material, but the composite beam cross-section is made from two or more materials, so a transformed section

method had to be used before modeling the section. The value of the torsional constant for this cross-section was ascertained to be: $I_{tor} = 3.80 \times 10^6 \text{ (mm}^4\text{)}$.

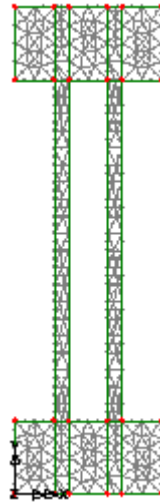


Figure 7.2 Double I-beam cross section modeled by LUSAS software to obtain the torsional constant, I_{tor}

7.3.3 Characteristic properties

7.3.3.1 Characteristic material properties of timber

All characteristic properties of the timber, except the 5% characteristic shear modulus ($G_{0.05}$), are obtained from Table 1 in BS EN 338. The equation given in Annex A of BS EN 338 was used to calculate the value of $G_{0.05}$

Characteristic bending strength $f_{m,k}$ (N/mm ²)	$f_{m,k} = 16 \text{ N/mm}^2$
Characteristic tensile strength, parallel to the grain $f_{t,0,k}$ (N/mm ²)	$f_{t,0,k} = 10 \text{ N/mm}^2$
Characteristic tensile strength, perpendicular to the grain $f_{t,90,k}$ (N/mm ²)	$f_{t,90,k} = 0.5 \text{ N/mm}^2$
Characteristic compressive strength, parallel to the grain $f_{c,0,k}$ (N/mm ²)	$f_{c,0,k} = 17 \text{ N/mm}^2$
Characteristic compressive strength, perpendicular to the grain $f_{c,90,k}$ (N/mm ²)	$f_{c,90,k} = 2.2 \text{ N/mm}^2$
Characteristic shear strength $f_{v,k}$ (N/mm ²)	$f_{v,k} = 1.8 \text{ N/mm}^2$
Mean value of elastic modulus, parallel to the grain,	$E_{0,mean} = 8000 \text{ N/mm}^2$

$E_{0,\text{mean}}$ (N/mm ²)	
Fifth percentile value of modulus of elasticity parallel to the grain, $E_{0.05}$ (N/mm ²)	$E_{0.05} = 5400 \text{ N/mm}^2$
Mean value of shear modulus G_{mean} (N/mm ²)	$G_{\text{mean}} = 500 \text{ N/mm}^2$
Fifth percentile value of shear modulus $G_{0.05}$ (N/mm ²)	$G_{0.05} = 337.5 \text{ N/mm}^2$
Characteristic density of C16 timber joist ρ_k (kg/m ³)	$\rho_k = 310 \text{ kg/m}^3$
Mean density of C16 timber joist ρ_{mean} (kg/m ³)	$\rho_{\text{mean}} = 370 \text{ kg/m}^3$

7.3.3.2 Characteristic material properties of OSB

Characteristic material properties of OSB/3 are obtained from Table 2 in BS EN 12369-1(2001).

Characteristic bending strength $f_{m,k,\text{OSB}}$ (N/mm ²)	$f_{m,0,k,\text{OSB}} = 18 \text{ N/mm}^2$
Characteristic tensile strength, parallel to the grain $f_{t,0,k,\text{OSB}}$ (N/mm ²)	$f_{t,0,k,\text{OSB}} = 9.9 \text{ N/mm}^2$
Characteristic compressive strength, parallel to the grain $f_{c,0,k,\text{OSB}}$ (N/mm ²)	$f_{c,0,k,\text{OSB}} = 15.9 \text{ N/mm}^2$
Characteristic compressive strength, perpendicular to the grain $f_{c,90,k,\text{OSB}}$ (N/mm ²)	$f_{c,90,k,\text{OSB}} = 12.9 \text{ N/mm}^2$
Characteristic panel shear strength $f_{v,\text{panel},k,\text{OSB}}$ (N/mm ²)	$f_{v,\text{panel},k,\text{OSB}} = 6.8 \text{ N/mm}^2$
Mean Characteristic Panel shear modulus $G_{v,\text{Panel},\text{mean},\text{OSB}}$ (N/mm ²)	$G_{v,\text{panel},\text{mean},\text{OSB}} = 1080 \text{ N/mm}^2$
Characteristic Planar Shear $f_{r,\text{planar},k}$ (N/mm ²)	$f_{r,\text{planar},k} = 1.0 \text{ N/mm}^2$
Mean Characteristic Planar Shear modulus $G_{r,\text{planar},\text{mean},\text{OSB}}$	$G_{r,\text{planar},\text{mean},\text{OSB}} = 50 \text{ N/mm}^2$
Characteristic density of OSB $\rho_{k,\text{OSB}}$ (kg/m ³)	$\rho_{k,\text{OSB}} = 550 \text{ kg/m}^3$
Mean bending modulus of OSB $E_{m,0,\text{mean},\text{OSB}}$ (N/mm ²)	$E_{m,0,\text{mean},\text{OSB}} = 4930 \text{ N/mm}^2$

7.3.4 Design material properties

7.3.4.1 Design material properties of timber

The design value of a strength property, X_d is calculated as:

$$X_d = k_{\text{mod}} X_k / \gamma_m \quad \text{Equation 7.1}$$

Where X_k is the characteristic value of the strength property

k_{mod} is modification factor for duration of load and moisture content

$k_{\text{mod}} = 0.8$ (Table 3.1 Eurocode 5)

γ_m is partial factor for material properties for ultimate limit states

$\gamma_m = 1.3$ (table 2.3 Eurocode 5)

Depth factor

Clause 3.2(2) of Eurocode 5 introduces the depth factor k_h for rectangular solid timber section with characteristic density of $\rho_k < 700 \text{ kg/m}^3$, when the depth in bending or width in tension is less than 150 mm. For such a case the characteristic values for $f_{m,k}$ and $f_{t,0,k}$ are increased by the depth factor k_h (Equation 7.2). That was done for the double I-beam, and also for the rest of the profiles during assessment of the bending and tensile stress affecting the flanges.

$$k_h = \min \left\{ \begin{array}{l} \left(\frac{150}{h} \right)^{0.2} \\ 1.3 \end{array} \right. \quad \text{Equation 7.2}$$

h is the depth for bending members or width for tension members, in mm.

Design bending strength for timber, $f_{m,d}$:

$$f_{m,k} = (f_{m,k} k_h) \quad k_h = \frac{(150)^{0.2}}{45} = 1.272 \quad \text{where } h_{f,c} / h_{f,t} = 45 \text{ mm}$$

Thus, the design values of the timber bending strengths can be determined as follows

$$f_{m,k} = 20.35 \text{ N/mm}^2 \quad f_{m,d} = \frac{k_{\text{mod}} f_{m,k}}{\gamma_m} = 12.52 \text{ N/mm}^2$$

Design tensile strength parallel to the grain, $f_{t,0,d}$:

$$f_{t,0,k} = (f_{t,0,k} k_h) \quad k_h = \left(\frac{150}{90}\right)^{0.2} = 1.108 \text{ where } b = 90 \text{ mm}$$

Therefore, the design value of the timber tensile strength parallel to the grain can be determined as follow:

$$f_{t,0,k} = 11.08 \text{ N/mm}^2 \quad f_{t,0,d} = \frac{k_{\text{mod}} f_{t,0,k}}{\gamma_m} = 6.82 \text{ N/mm}^2$$

Design tensile strength perpendicular to the grain, $f_{t,90,d}$:

$$f_{t,90,d} = \frac{(k_{\text{mod}} f_{t,90,k})}{\gamma_m} = 0.31 \text{ N/mm}^2$$

Design compressive strength parallel to the grain, $f_{c,0,d}$:

$$f_{c,0,d} = \frac{(k_{\text{mod}} f_{c,0,k})}{\gamma_m} = 10.46 \text{ N/mm}^2$$

Design compressive strength perpendicular to the grain, $f_{c,90,d}$:

$$f_{c,90,d} = \frac{(k_{\text{mod}} f_{c,90,k})}{\gamma_m} = 1.35 \text{ N/mm}^2$$

Design shear strength, $f_{v,d}$:

$$f_{v,d} = \frac{(k_{\text{mod}} f_{v,k})}{\gamma_m} = 1.12 \text{ N/mm}^2$$

7.3.4.2 Design material properties of OSB

From Equation 7.1, the design value for a strength property, X_d is calculated:

$$X_d = \frac{k_{\text{mod}} X_k}{\gamma_m}$$

Where $k_{\text{mod}} = 0.55$ (Table 3.1 Eurocode 5)

$\gamma_m = 1.2$ (Table 2.3 Eurocode 5)

Thus, the design values of the OSB strengths can be determined as follows:

Design bending strength for OSB, $f_{m,d,OSB}$:

$$f_{m,d,OSB} = \frac{k_{mod} f_{m,k,OSB}}{\gamma_m} = 8.25 N / mm^2$$

Design tensile strength parallel to the grain, $f_{t,0,d,OSB}$:

$$f_{t,0,d,OSB} = \frac{k_{mod} f_{t,0,k,OSB}}{\gamma_m} = 4.54 N / mm^2$$

Design compressive strength parallel to the grain, $f_{c,0,d,OSB}$:

$$f_{c,0,d,OSB} = \frac{(k_{mod} f_{c,0,k,OSB})}{\gamma_m} = 7.29 N / mm^2$$

Design compressive strength perpendicular to the grain, $f_{c,90,d,OSB}$:

$$f_{c,90,d,OSB} = \frac{(k_{mod} f_{c,90,k,OSB})}{\gamma_m} = 5.91 N / mm^2$$

Design panel shear strength, $f_{v,panel,d,OSB}$:

$$f_{v,panel,d,OSB} = \frac{(k_{mod} f_{v,panel,k,OSB})}{\gamma_m} = 3.12 N / mm^2$$

Design planar shear strength, $f_{r,planar,d,OSB}$:

$$f_{r,planar,d,OSB} = \frac{(k_{mod} f_{v,planar,k,OSB})}{\gamma_m} = 0.46 N / mm^2$$

7.3.5 Characteristic loads and deformations**Characteristic loads**

Characteristic value of linearly distributed permanent action of the floor, G_k (kN/m):

$$G_k = g_k \frac{s}{1000} = 0.246 kN / m$$

Characteristic value of linearly distributed variable action of the floor, Q_k (kN/m):

$$Q_k = q_k \frac{s}{1000} = 0.600 kN / m$$

Maximum characteristic bending moment due to the permanent action, $M_{g,k,max}$ (kN/m):

$$M_{g,k,max} = G_k \frac{L^2}{8 \times 10^6} = 0.96 kNm$$

Maximum characteristic bending moment due to the variable action, $M_{q,k,max}$ (kN/m):

$$M_{q,k,max} = Q_k \frac{L^2}{8 \times 10^6} = 2.35 kNm$$

Maximum characteristic shear force due to the permanent load, $V_{g,k,max}$ (kN)

$$V_{g,k,max} = G_k \left(\frac{L}{2} \right) \left(\frac{1}{1000} \right) = 0.69 kN$$

Maximum characteristic shear force due to the variable load, $V_{q,k,max}$ (kN)

$$V_{q,k,max} = Q_k \left(\frac{L}{2} \right) \left(\frac{1}{1000} \right) = 1.68 kN$$

$$F_{c,90,q,k} = V_{q,k,max} = 1.68 kN$$

Characteristic bearing force due to the permanent load, $F_{c,90,g,k}$ (kN):

$$F_{c,90,g,k} = V_{g,k,max} = 0.69 kN$$

Maximum characteristic shear force due to the variable load, $F_{c,90,q,k}$ (kN):

$$F_{c,90,q,k} = V_{q,k,max} = 1.68 kN$$

Characteristic deformations

Maximum characteristic deflection, $w_{g,k,max}$ (mm), due to the permanent load is calculated from equation 7.3.

$$w_{g,k,max} = \left[\frac{(M_{g,k,max} L^2)}{(9.6 E_{0,mean} I_y)} + \frac{(\phi M_{g,k,max})}{(G_{mean} A_{Equ})} \right] 10^6 = 3.36 mm \quad \text{Equation 7.3}$$

In Equation 7.3, ϕ is the shear factor. Chapter 5 section 5.5.2 describes two methods for calculating the shear factor, exact method and approximate method. Moreover, it is shown that result of the approximate method from Roark's formula is close to the

exact method, so Roark's formula (Equation 7.4) is adopted to calculate the shear factor in this design procedure and also in the parametric study in Chapter 8.

$$\phi = \left[1 + \left[\frac{1.5 \left[h^2 - (h - 2h_{fc})^2 \right] (h - 2h_{fc})}{h^3} \right] \left[\left(\frac{b}{b_{w,Equ}} \right) - 1 \right] \right] \left(\frac{h^2}{10r_y^2} \right) \quad \text{Equation 7.4}$$

For the radius of gyration of the section, $r_y = 116.6$ mm shear factor $\phi = 3.204$

Substituting the values in equation 7.3, maximum characteristic deflection is defined as:

$$w_{g,k,max} = 3.36 \text{ mm}$$

In a similar way, maximum characteristic deflection due to the variable load, $w_{q,k,max}$, is calculated from Equation 7.5.

$$w_{q,k,max} = \left[\frac{(M_{q,k,max} L^2)}{(9.6E_{0,mean} I_y)} + \frac{(\phi M_{q,k,max})}{(G_{mean} A_{Equ})} \right] 10^6 = 8.23 \text{ mm} \quad \text{Equation 7.5}$$

Hence $w_{q,k,max} = 8.23$ mm

7.3.6 Design loads and stresses

Eurocode 0 (EN 1990:2002) requires that the design value of effect of combined actions, E_d , for persistent or transient design situations (fundamental combinations) should be calculated from:

$$\sum_{j \geq 1} \gamma_{G,j} G_{k,j} + \gamma_P P + \gamma_{Q,1} Q_{k,1} + \sum_{i > 1} \gamma_{Q,i} \psi_{0,i} Q_{k,i} \quad \text{Equation 7.6}$$

Where

$G_{k,j}$ Is the characteristic value of the permanent action j,

$Q_{k,i}$ Is the characteristic value of the variable action j,

P Is a prestressing action

$\gamma_{G,j}$ Is the partial factor the permanent action

γ_P Is partial factor for prestressing actions

$\gamma_{Q,i}$ Is the partial factor the variable action

$\psi_{0,i}$ is the factor for combination value of the variable action

Here $i = j = 1$, therefore equation 7.6 is simplified as:

$$\gamma_G G_k + \gamma_Q Q_k \quad \text{Equation 7.7}$$

Partial factors are given in table A 1.2(B) in EC0 (EN 1990: 2002)

$$\gamma_G = 1.35 \quad \gamma_Q = 1.5$$

Thus the design loads and stresses can be determined as follows:

Design bending moment about the strong axis y, $M_{y,d}$:

$$M_{y,d} = \gamma_G M_{g,k,\max} + \gamma_Q M_{q,k,\max} \quad \text{Equation 7.8}$$

Therefore $M_{y,d} = 4.82 \text{ kN.m}$

Design shear force, V_d :

$$V_d = \gamma_G V_{g,k,\max} + \gamma_Q V_{q,k,\max} = 3.45 \text{ kN} \quad \text{Equation 7.9}$$

Hence $V_d = 3.45 \text{ kN}$

Design bearing force, $F_{c,90,d}$:

$$F_{c,90,d} = \gamma_G F_{c,90,g,k} + \gamma_Q F_{c,90,q,k} \quad \text{Equation 7.10}$$

Hence $F_{c,90,d} = 3.45 \text{ kN}$

Design stresses can be calculated by substituting the design loads in the following equations.

Design bending stress about the strong axis y, $\sigma_{m,y,d}$:

$$\sigma_{m,y,d} = \frac{M_{y,d} 10^6}{W_y} \quad \text{Equation 7.11}$$

Therefore $\sigma_{m,y,d} = 5.11 \text{ N/mm}^2$

Design bending compressive stress about the strong axis y on the extreme fibres of timber flanges $\sigma_{f,c,t,\max,d}$ (N/mm^2) :

$$\sigma_{f,c,d} = \frac{M_{y,d} h_{f,c,n} 10^6}{I_y} \quad \text{Equation 7.12}$$

Where $h_{f,c,n}$ is the distance from the geometric centre of the compressive flange to the neutral axis

$$h_{f,c,n} = 0.5 h - 0.5 h_{f,c} \quad \text{Equation 7.13}$$

Therefore $h_{f,c,n} = 127.5$ mm

Replacing the values in equation 7.12 result:

$$\sigma_{f,c,max,d} = 4.34 \text{ N/mm}^2$$

Design bending induced tensile stress on the timber flange $\sigma_{f,t,d}$ (N/mm²):

$$\sigma_{f,t,d} = \frac{M_{y,d} h_{f,t,n} 10^6}{I_y} \quad \text{Equation 7.14}$$

Where $h_{f,t,n}$ is the distance from the geometric centre of the tensile flange to the neutral axis

$$h_{f,t,n} = 0.5h - 0.5h_{f,t} \quad \text{Equation 7.15}$$

Therefore $h_{f,t,n} = 127.5$ mm

Substituting the values in equation 7.14 gives:

$$\sigma_{f,t,d} = 4.34 \text{ N/mm}^2$$

Design bending induced compressive stress is equal to design bending induced tensile stress since $h_{f,c,n} = h_{f,t,n} = 127.5$ mm

Design bending compression and tension stress on the OSB web $\sigma_{w,c,d}$ and $\sigma_{w,t,d}$ (N/mm²):

As in the previous situation, the design bending compression of the web is equal to the design bending tension stress of the web, therefore the result becomes $\sigma_{w,c/t,d}$.

$$\sigma_{w,c/t,d} = \frac{n M_{y,d} h_{w,max} 10^6}{I_y} \quad \text{Equation 7.16}$$

Where $h_{w,max}$ in Equation 7.16 is the distance from the outermost fibres of the OSB web to the neutral axis.

$$h_{w,max} = 0.5h_w + \Delta h_w \quad \text{Equation 7.17}$$

Hence $h_{w,max} = 117$ mm

Substituting the values in Equation 7.16 yields: $\sigma_{w,c/t,d} = 2.45 \text{ N/mm}^2$

Design planar (rolling) shear stress on the OSB web $\tau_{mean,d}$ (N/mm²)

Design planar shear stress on the OSB web can be calculated from equation 7.18

$$\tau_{mean,d} = \frac{10^3 n V_d Q}{4 I_y \Delta h_w} \quad \text{Equation 7.18}$$

In Equation 7.18 Q is the first moment of area about the neutral axis and is calculated from equation 7.19.

$$Q = b h_{f,c} \left(\frac{h}{2} - \frac{h_{f,c}}{2} \right) + \left(b_{w,Equ} \frac{b_w}{2} \right) \frac{b_w}{4} \quad \text{Equation 7.19}$$

Hence $Q = 5.775 \times 10^5 \text{ (mm}^3\text{)}$

Replacing the values in equation 7.18, design rolling shear stress is obtained as:

$$\tau_{mean,d} = 0.181 \text{ (N/mm}^2\text{)}$$

Design bearing stress of the flange, $\sigma_{c,90,d}$:

$$\sigma_{c,90,d} = \frac{10^3 F_{c,90,d}}{b l} \quad \text{Equation 7.20}$$

Hence $\sigma_{c,90,d} = 0.382 \text{ N/mm}^2$

Design compressive stress of the web

$$\sigma_{c,90,d,web} = \frac{10^3 F_{c,90,d}}{b_w l} \quad \text{Equation 7.21}$$

Therefore $\sigma_{c,90,d,web} = 1.917 \text{ N/mm}^2$

7.3.7 Ultimate limit state design (ULS)

Ten different criteria based on Eurocode 5 are here defined and are later used to evaluate the permissible span of the model joist in ultimate limit state (ULS) design:

1. Axial compression and tension in the timber flanges due to bending ($B_{c/t,f}$)
2. Compression in the extreme fibres of the timber flanges due to bending ($C_{b,f}$)
3. Tension in the extreme fibres of the timber flanges due to bending ($T_{b,f}$)
4. Compression in the extreme fibres of the OSB web due to bending ($C_{b,w}$)
5. Tension in the extreme fibres of the OSB web due to bending ($T_{b,w}$)
6. Panel shear in the OSB web (S_p)
7. Planar (rolling) shear in the OSB web (S_R)
8. Lateral stability when subjected to bending (LS_b)

9. Compression perpendicular to the timber grain (bearing) (C_{\perp})
10. Compression parallel to the OSB panel length (C_{\parallel})

Axial compression and tension in the timber flanges due to bending ($B_{c/t,f}$)

$$\sigma_{m,y,d} \leq f_{m,y,d} \quad \text{or} \quad \frac{\sigma_{m,y,d}}{f_{m,y,d}} \leq 1 \quad \text{Equation 22}$$

Then $\frac{\sigma_{m,y,d}}{f_{m,y,d}} = 0.408$ so the condition ≤ 1 is satisfied.

Compression in the extreme fibre of the timber flanges due to bending ($C_{b,f}$)

$$\sigma_{f,c,d} \leq k_c f_{c,0,d} \quad \text{or} \quad \frac{\sigma_{f,c,d}}{k_c f_{c,0,d}} \leq 1 \quad \text{Equation 23}$$

where:

$k_c = 1$ if lateral stability is assessed so:

Therefore $\frac{\sigma_{f,c,d}}{f_{c,0,d}} = 0.415$ satisfy the condition.

Tension in the extreme fibre of the timber flanges due to bending ($T_{b,t}$)

$$\sigma_{f,t,d} \leq f_{t,0,d} \quad \text{or} \quad \frac{\sigma_{f,t,d}}{f_{t,0,d}} \leq 1 \quad \text{Equation 24}$$

Hence $\frac{\sigma_{f,t,d}}{f_{t,0,d}} = 0.554$ meets the condition requirement.

Compression in the extreme fibre of the OSB web due to bending ($C_{b,w}$)

$$\sigma_{w,c,d} \leq f_{c,0,d,OSB} \quad \text{or} \quad \frac{\sigma_{w,c,d}}{f_{c,0,d,OSB}} \leq 1 \quad \text{Equation 25}$$

Thus $\frac{\sigma_{w,c,d}}{f_{c,0,d,OSB}} = 0.340$ satisfy the condition.

Tension in the extreme fibre of the OSB web due to bending ($T_{b,w}$)

$$\sigma_{w,t,d} \leq f_{t,0,d,OSB} \quad \text{or} \quad \frac{\sigma_{w,t,d}}{f_{t,0,d,OSB}} \leq 1 \quad \text{Equation 26}$$

Hence $\frac{\sigma_{w,t,d}}{f_{t,0,d,OSB}} = 0.540$ meet the condition requirement.

Panel shear in the OSB web (S_p)

$$F_{v,w,Ed} \leq k_{Panel\ Shear} \cdot f_{v,0,d} \quad \text{or} \quad \frac{F_{v,w,Ed}}{k_{Panel\ Shear}} \leq 1 \quad \text{Equation 27}$$

Where $k_{Panel\ Shear}$ is calculated from equation 7.22

$$k_{Panel\ Shear} = \begin{cases} b_w h_w \left[1 + \frac{0.5(h_{ft} + f_{fc})}{h_w} \right] & \text{if } h_w \leq 35b_w \\ 35b_w^2 \left[1 + \frac{0.5(h_{ft} + h_{fc})}{h_w} \right] & \text{if } 35b_w \leq h_w \leq 70b_w \end{cases} \quad \text{Equation 7.28}$$

Therefore $k_{panel\ shear} = 2.295 \times 10^3 \text{ mm}^2$

Design panel shear force is the same as V_d

$$F_{v,w,Ed} = V_d = 3.45 \text{ kN}$$

So the ratio of design shear force to design panel shear resistance becomes:

$$\frac{F_{v,w,Ed} \times 10^3}{k \cdot f_{v,panel,OSB}} = 0.54 \text{ and therefore this condition } \leq 1 \text{ is satisfied.}$$

Planar (rolling) shear in the OSB web (S_R)

$$\tau_{mean,d} \leq \begin{cases} f_{v,90,d} & \text{if } h_f \leq 4b_{ef} \\ f_{v,90,d} \left(\frac{4b_{ef}}{h_f} \right)^{0.8} & \text{if } h_f \geq 4b_{ef} \end{cases} \quad \text{Equation 7.29}$$

In Equation 7.29, b_{ef} is the effective thickness of the web, which is equal to the thickness of the single web for a box beam and to a half thickness of the web for an I-beam (Eurocode 5, 2004). The effective thickness, b_{ef} , for a double I-beam is held to be the thickness of one single web $b_{ef} = 9 \text{ mm}$ and h_f is the height of the glue line, which is for I-beams and double I-beams $h_f = \Delta h_w$ whereas it is $h_f = h_{fc}$ or h_{ft} for box I-beam.

In Equation 7.29, because $h_f \geq 4b_{ef}$ then rolling shear, $\tau_{mean,d}$, has to satisfy the lower equation as:

$$\tau_{mean,d} \leq f_{v,90,d} \left(\frac{4b_{ef}}{h_f} \right)^{0.8} \quad \text{if } h_f \geq 4b_{ef} \quad \text{Equation 7.30}$$

Substituting the values in equation 7.30 results:

$$0.181 \leq 0.385 (N/mm^2) \quad \text{for } 45 \geq 4 \times 9$$

Lateral stability when beams are subjected to bending (LS_b)

The design bending stress should satisfy the Equation 7.31.

$$\sigma_{m,y,d} \leq k_{crit} f_{m,d} \quad \text{or} \quad \frac{\sigma_{m,y,d}}{k_{crit} f_{m,d}} \leq 1 \quad \text{Equation 7.31}$$

In equation 7.31, k_{crit} is the lateral factor, which can be considered as $k_{crit} = 1$ where lateral stability is present. When lateral stability is present the result for this criterion is similar to that for the first criterion for axial compression and tension in the timber flanges due to bending. Therefore:

$$\frac{\sigma_{m,y,d}}{f_{m,y,d}} = 0.408 \quad \text{meets the condition.}$$

If lateral stability is not provided then the lateral factor, k_{crit} , has to be considered. The lateral factor then reduces bending strength thus enabling lateral buckling to occur. Lateral factor, k_{crit} , can be calculated from equation 7.32.

$$k_{crit} = \begin{cases} 1 & \text{for } \lambda_{rel,m} \leq 0.75 \\ 1.56 - 0.75 \lambda_{rel,m} & \text{for } 0.75 < \lambda_{rel,m} \leq 1.4 \\ 1 / \lambda_{rel,m}^2 & \text{for } \lambda_{rel,m} > 1.4 \end{cases} \quad \text{Equation 7.32}$$

In Equation 7.32, $\lambda_{rel,m}$ is the relative slenderness ratio corresponding to bending, which can be calculated from equation 7.33.

$$\lambda_{rel,m} = \sqrt{\frac{f_{m,k}}{\sigma_{m,crit}}} \quad \text{Equation 7.33}$$

In equation 7.33, $\sigma_{m,crit}$ is the critical bending stress which can be obtained from equation 7.34.

$$\sigma_{m,crit} = \frac{\pi \sqrt{E_{0.05} I_z G_{0.05} I_{tor}}}{L_{ef} W_y} \quad \text{Equation 7.34}$$

In equation 7.34, L_{ef} is the effective length of the beam. Eurocode 5 provided a value for effective length according to the supporting condition and load configuration. Effective length for a simply supported beam under uniform distributed load is equal to $L_{eff}=0.9 L$ (mm)

Effective length has to be increased by twice the beam's depth, $2 h$, when load is applied at the compression edge of the beam.

$$L_{eff}=0.9 L + 2 h \quad \text{Equation 7.35}$$

Therefore the effective length of the beam is, $L_{ef}= 5640\text{mm}$

Critical bending stress is calculated by substituting the values in equation 7.34 as:

$$\sigma_{m,crit}= 3.816 \text{ (N/mm}^2\text{)}$$

The relative slenderness value is obtained by substituting the characteristic bending strength and critical bending stress in equation 7.33 thus:

$$\lambda_{rel,m}= 2.31$$

Lateral buckling factor, k_{crit} , is defined, by substituting the $\lambda_{rel,m}$ in equation 7.32 so

$$K_{crit}= 0.187$$

When the values above are placed in equation 7.31, the result shows that a double I-beam 5600mm long does not satisfy the lateral stability criteria without lateral restraint.

$$\sigma_{m,y,d} \leq k_{crit} f_{m,d} \text{ or } 5.11 \geq 0.187 \times 12.52$$

Compression perpendicular to the timber grain (bearing) (C_{\perp})

This criteria has to satisfy equation 7.36

$$\sigma_{c,90,d} \leq k_c \cdot f_{c,90,d} \quad \text{or} \quad \sigma_{c,90,d} / k_c \cdot f_{c,90,d} \leq 1 \quad \text{Equation 7.36}$$

Where $k_{c,90}$ is a factor which consider the load configuration, the possibility of splitting and the degree of compressive deformation $k_{c,90}=1$ as defined in Eurocode 5.

Replacing the values in equation 7.36 shows that the criterion for evaluating the compression perpendicular to the timber grain, C_{\perp} , is satisfied.

$$\sigma_{c,90,d} / k_c \cdot f_{c,90,d} = 0.283 N / mm^2 \leq 1$$

Compression parallel to the OSB panel length (C_{\parallel})

$$\sigma_{c,0,d,web} \leq f_{c,0,d,web} \quad or \quad \sigma_{c,0,d,OSB} / f_{c,0,d,OSB} \leq 1 \quad \text{Equation 7.37}$$

Then $\sigma_{c,0,d,OSB} / f_{c,0,d,OSB} = 0.263 \leq 1$ So this condition is satisfied.

7.3.8 Serviceability limit state design (SLS)

According to Sven Ohlsson, one of the main contributors to the vibration section in Eurocode 5 (Ohlsson 1982 and 1988), two criteria are defined under serviceability limit state design, which are static deflection and vibration (Table 7.1). A vibration criterion has three sub-criteria, fundamental frequency (f), deflection under unit point load (a) and unit impulse velocity response (v). The current UK National Annex suggests two options for evaluating the vibration criteria. Both options are considered in this analytical procedure.

Table 7.1 Serviceability limit state criteria

<u>Deflection</u>	{	1. Static deflection (Δ)	} Option A
<u>Vibration</u>		2. Natural frequency (f_1)	
	3. Deflection under unit point load (a)		
	4. Unit impulse velocity response (v)		
	5. Natural frequency (f_1')	} Option B	
	6. Deflection under unit point load (a')		
7. Unit impulse velocity response (v')			

The following pages describe the evaluation procedure for the double I-beam of 5600 mm span under serviceability conditions.

7.3.8.1 Static deflection (Design deformation)

In UK National Annex to EN 1995-1-1 the requirement for the net final deflection of the timber floor, $w_{net,fin}$, with a plastered or plasterboard ceiling, including creep deflection, is expressed as follows:

$$w_{net,fin} \leq L / 250 \tag{Equation 7.38}$$

In order to obtain the net final deflection, $w_{net,fin}$, the combination of deflections (Figure 7.3) caused by permanent and variable actions has to be determined.

$$w_{net,fin} = w_{inst} + w_{creep} - w_c \tag{Equation 7.39}$$

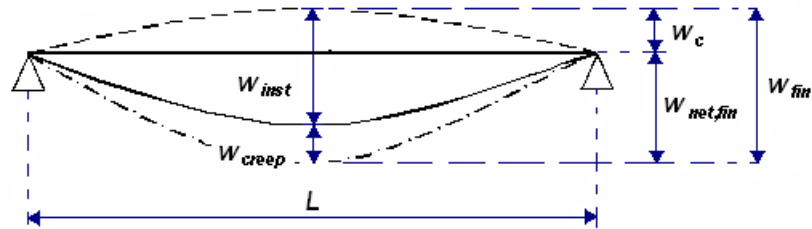


Figure 7.3 Components of the deflection (Reproduced from Eurocode 5)

Symbols in Equation 7.39 and figure 7.3 are defined as:

- w_c (mm): is the pre-camber
- w_{inst} (mm): is the instantaneous deflection
- w_{creep} (mm): is the creep deflection
- w_{fin} (mm): is the final deflection
- $w_{net,fin}$ (mm): is the net final deflection

The combination of the actions under serviceability criteria is defined in Eurocode 0 (EN 1990:2002) as follows:

$$\sum_{j \geq 1} G_{k,j} + P + Q_{k,1} + \sum_{i > 1} \psi_{0,i} Q_{k,i} \tag{Equation 7.40}$$

Where in Equation 7.33,

- $G_{k,j}$: Characteristic value of permanent action j
- P: Relevant representative value of a pre-stressing action
- $Q_{k,1}$: Characteristic value of the leading variable action 1

Ψ_0 : Factor for combination value of a variable action

$Q_{k,i}$: Characteristic value of the accompanying variable action i

Equation 7.40 can be simplified to equation 7.41 as $i=j=1$ and $P = 0$

$$G_k + Q_k \quad \text{Equation 7.41}$$

Now components of deflection under permanent and variable action can be determined.

Component of deflection under permanent action

Instantaneous deflection, due to the permanent action, $w_{g,inst}$:

$$w_{g,inst} = w_{g,k,max} \quad \text{Equation 7.42}$$

Value of the $w_{g,k,max}$ is obtained from equation 7.3 therefore $w_{g,inst} = 3.36$ mm

Final deflection due to the permanent action $w_{g,fin}$ can be calculated from equation 7.43.

$$w_{g,fin} = w_{g,inst} + w_{g,creep} = w_{g,inst} (1 + k_{def}) \quad \text{Equation 7.43}$$

In equation 7.43 k_{def} is the deformation factor. Deformation factor for solid timber of service class 2 is $K_{def} = 0.8$ (Table 3.2 in Eurocode 5). Hence

$$w_{g,fin} = 6.05 \text{ mm}$$

Instantaneous deflection due to the variable action $w_{q,inst}$:

$$w_{q,inst} = w_{q,k,max} \quad \text{Equation 7.44}$$

Value of the $w_{q,k,max}$ is calculated from equation 7.5 hence $w_{q,inst} = 8.23$ mm

Final deflection due to the variable action, $w_{q,fin}$ (mm):

$$w_{q,fin} = w_{q,inst} + w_{q,creep} = w_{q,inst} (1 + \Psi_2 k_{def}) \quad \text{Equation 7.45}$$

In Equation 7.45, the factor for quasi-permanent value of a variable action is defined as Ψ_2 . Value of Ψ_2 factor is 0.3 for imposed loads on domestic and residential buildings (Eurocode 0, Table A.1.1). Therefore $w_{q,fin} = 10.19$ mm

The final deflection due to combined permanent and variable actions, w_{fin} , can be calculated as follows:

$$w_{fin} = w_{g,fin} + w_{q,fin} \quad \text{Equation 7.46}$$

Thus $w_{fin} = 16.26$ mm

The net final deflection $w_{net,fin}$ can be calculated as:

$$w_{net,fin} = w_{fin} + w_c \quad \text{Equation 7.47}$$

In Equation 7.47, it is assumed that pre-camber deformation, w_c , to be zero then

$$w_{net,fin} = 16.26$$

Substituting the values on equation 7.38 confirm that a double I-beam of 5600mm span would satisfy the static deflection criteria.

$$16.26 < 22.4\text{mm}$$

7.3.8.2 Vibration-Option A

Fundamental frequency, f_1

Fundamental frequency of the floor, f_1 , should exceed than 8 Hz ($f_1 > 8$).

Clause 7.3.3(4) of Eurocode 5 states that for a rectangular floor with overall dimensions of $L \times B$, simply supported along all four edges and with timber joists having a span of L metres, the fundamental frequency, f_1 , can be estimated as:

$$f_1 = \frac{\pi}{2L^2} \sqrt{\frac{(EI)_L}{m}} \quad \text{Equation 7.48}$$

In equation 7.48 $(EI)_L$ is the equivalent plate bending stiffness of the floor about an axis perpendicular to the beam direction (y-axis in this case) in Nm^2/m :

$$(EI)_L = E_{0,mean} I_y / s \quad \text{Equation 7.49}$$

Therefore $(EI)_L = 2.832 \times 10^6 \text{ Nm}^2/\text{m}$

Small m represents the mass of the timber floor per unit area in kg/m^2

$$m = m_{imposed} + m_{joist} \quad \text{Equation 7.50}$$

In this case $m = 63.69 \text{ kg}/\text{m}^2$

Inserting the values above in equation 7.48 gives $f_i = 10.56$ Hz and as $f_i > 8$ Hz that means the requirement for fundamental frequency of the floor is satisfied.

Deflection under unit point load

The deflection of a timber floor under unit point load should satisfy the following equation:

$$a = w / F \leq a_d \quad \text{Equation 7.51}$$

Where -

a is the deflection of the timber floor under unit point load in mm/kN

w is the maximum instantaneous vertical deflection caused by a vertical concentrated static force F at any point on the floor,

F is unit point load and $F = 1$ kN

a_d is the design value of the deflection of the timber floor under unit point load in mm/kN

Deflection of the timber floor under unit point load, a , can be calculated from Equation 7.52 which is given in the UK National Annex to Eurocode 5.

$$a = \frac{k_{dist} 1000 L^3 k_{shear}}{48 k_{comp} EI_{joist}} \quad \text{Equation 7.52}$$

Where -

k_{dist} is the factor to account for proportion of point load distributed to adjacent joists by floor decking, and can be calculated as:

$$k_{dist} = \max \{0.42 - 0.09 \ln [14 (EI)_B / s^4], 0.35\} \quad \text{Equation 7.53}$$

In Equation 7.53, $(EI)_B$ is the equivalent plate bending stiffness (board stiffness) of the floor about an axis parallel to the beam direction (y-axis in this case) in Nmm^2/m .

$$(EI)_B = E_{0,mean,P5} \times 1000 t^3 / 12 \quad \text{Equation 7.54}$$

Therefore $(EI)_B = 3.106 \times 10^9 \text{ N mm}^2/\text{m}$

Inserting that value in Equation 7.53 yields the result: $k_{dist} = 0.372$

k_{shear} is the amplification factor to account for shear deflection: $k_{\text{shear}} = 1.15$

k_{comp} is the factor to account for composite action between joists and floor decking, where the floor decking is nailed or screwed to joists $k_{\text{comp}} = 1.1$

EI_{joist} is the flexural rigidity of the floor joist about an axis perpendicular to the beam direction (y-axis in this case) in N mm^2 can be calculated as:

$$EI_{\text{joist}} = E_{0,\text{mean}} I_y \text{ hence } EI_{\text{joist}} = 1.133 \times 10^4 \text{ N.mm}^2$$

The deflection of the timber floor under unit point load is determined by inserting the values above in Equation 7.52 giving: $a = 1.257 \text{ mm/kN}$

The design value of the deflection of the timber floor under unit point load, a_d , can be determined based on Clause 2.6(a) in UK National Annex to Eurocode 5 as:

$$a_d = \begin{cases} 1.75 \text{ mm/kN} & \text{For spans} \leq 4500 \text{ mm} \\ 64500 / L^{1.25} \text{ mm/kN} & \text{For spans} > 4500 \text{ mm} \end{cases} \quad \text{Equation 7.55}$$

Therefore $a_d = 1.331$

Substituting values for 'a' and 'a_d' in Equation 7.51 shows that this criterion is satisfied as $1.257 < 1.331$.

Unit impulse velocity response

From Clause 7.3.3 in Eurocode 5, for residential floors with a fundamental frequency greater than 8 Hz ($f_1 > 8 \text{ Hz}$), the following equation should be satisfied:

$$v \leq v_d = b_f^{(f_1 \zeta^{-1})} \quad \text{Equation 7.56}$$

Where -

v is the unit impulse velocity response in m/ N s^2 , i.e. the maximum initial value of the vertical floor vibration velocity in m/s caused by a unit impulse (1 Ns)

v_d is the design limit for unit impulse velocity

b_f is a parameter for assessing v

ζ is the modal damping ratio and it is considered $\zeta = 0.01$ (1%)

The value of v can be determined from:

$$v = \frac{4(0.4 + 0.6 n_{40})}{m B L + 200} (m / Ns^2) \quad \text{Equation 7.57}$$

n_{40} is the number of first-order modes with natural frequencies up to 40 Hz; its value can be obtained from equation 7.58.

$$n_{40} = \left\{ \left[\left(\frac{40}{f_1} \right)^2 - 1 \right] \left(\frac{B}{L} \right)^4 \frac{(EI)_L}{(EI)_B} \right\}^{0.25} \quad \text{Equation 7.58}$$

In this equation unit of $(EI)_B$ has to change to $N \text{ m}^2/\text{m}$ to match the unit of $(EI)_L$ therefore $(EI)_B = 3.106 \times 10^3 \text{ Nm}^2/\text{m}$, then $n_{40} = 10.50$

The value of unit impulse velocity response, v , is determined by inserting the values for n_{40} , m , B and L in Equation 7.57 which yields: $v = 0.012 \text{ m} / Ns^2$

The value of b_f can be determined from Fig 7.2 in Eurocode 5 or equation 7.59.

$$b_f = \begin{cases} 150 - (30(a - 0.5) / 0.5) & \text{if } 0.5 \leq a \leq 1 \\ 120 - (40(a - 1)) & \text{if } 1 \leq a \leq 2 \\ 80 - (30(a - 2) / 2) & \text{if } 2 \leq a \leq 2 \end{cases} \quad \text{Equation 7.59}$$

For $a = 1.257 \text{ mm/kN}$ (Equation 7.43), $b_f = 109.09$

The design value of the unit impulse velocity, v_d , in right side of the equation 7.56 is determined by substituting the values for b_f , ζ and f to yield:

$$v_d = 0.015 \text{ m}/Ns^2$$

Hence $v < v_d$ ($0.012 < 0.015$) and so the requirement for the unit impulse velocity response of the floor is satisfied.

7.3.8.3 Vibration-Option B

As mentioned earlier, the procedure for option B is exactly similar to that used for option A. The difference between these two options lay in the given equations for, fundamental frequency and deflection under unit point load. There follows the design

procedure for evaluating the vibration criteria according to option B of UK National Annex (UK National Annex 2004).

Fundamental frequency, f_1'

$$f_1' = \frac{3\pi}{4L^2} \sqrt{\frac{(EI)'_L}{m}} \quad \text{Equation 7.60}$$

Where $(EI)'_L = 1.2(EI)_L$, therefore $f_1' = 17.356 \text{ Hz}$ which is well above the 8 Hz design limit.

Deflection under unit point load, a'

$$a' = \frac{F_{ser,point} \alpha L}{(EI)_{bay}} \left[\frac{L^2}{48} + \frac{2h^2}{5} \right] \left(\frac{s}{600} \right) \quad \text{Equation 7.61}$$

Where -

$F_{ser,point}$ is the concentrated point load ($F_{ser,point} = 1000 \text{ N}$)

α is the load distribution factor ($\alpha = 0.5$)

$(EI)_{bay}$ is the stiffness of one bay of the floor ($(EI)_{bay} = 106 (EI)_L$ s/1000 in Nmm^2)

Hence $a' = 0.947 \text{ mm/kN}$

The design value of the deflection of the timber floor under unit point load, a_d , is similar to option A and it is determined from equation 7.46 as: $a_d = 1.331 \text{ mm/kN}$.

The deflection under unit point load thus satisfies the condition ($a' \leq a_d$) because $0.947 < 1.331$.

Unit impulse velocity response

Equation 7.57 for unit impulse velocity remains the same; however, values of n_{40} and b_f are calculated by using f_1' , $(EI)'_L$ and a' in the equations 7.58 and 7.59 respectively. So by calculation $n_{40} = 8.288$ and $b_f = 123.206$.

Replacing those values in equation 7.48 gives the result $v' = 9.781 \times 10^{-3} \text{ m/Ns}^2$

The limiting value or design value of unit impulse velocity, v_d , is calculated from equation 7.56, which is similar to unit impulse velocity, but values for f_1' and the new

b_f are used. Thus by calculation $v'_d = 0.019 \text{ m/Ns}^2$ so unit impulse velocity satisfies the condition ($v' \leq v'_d$) because it is well below the design limit ($9.871 \times 10^{-3} < 0.019$).

Comparing the values of the vibration criteria calculated with both options, shows that the option B result is less conservative than that derived from option A. Chapter 8 discusses the implications in more detail.

7.3.9 Outcome of the design procedures

The above calculations show that the permissible span of a 5600 mm double I-beam with the described properties would satisfy the ULS and SLS criteria for timber floor design, as long as lateral restraints are provided.

7.4 Maximum permissible span

The design procedure which is described in section 7.2 can be repeated to obtain the maximum span under each ULS and SLS criterion. The procedure is demonstrated in the flowchart Figure 7.4 overleaf.

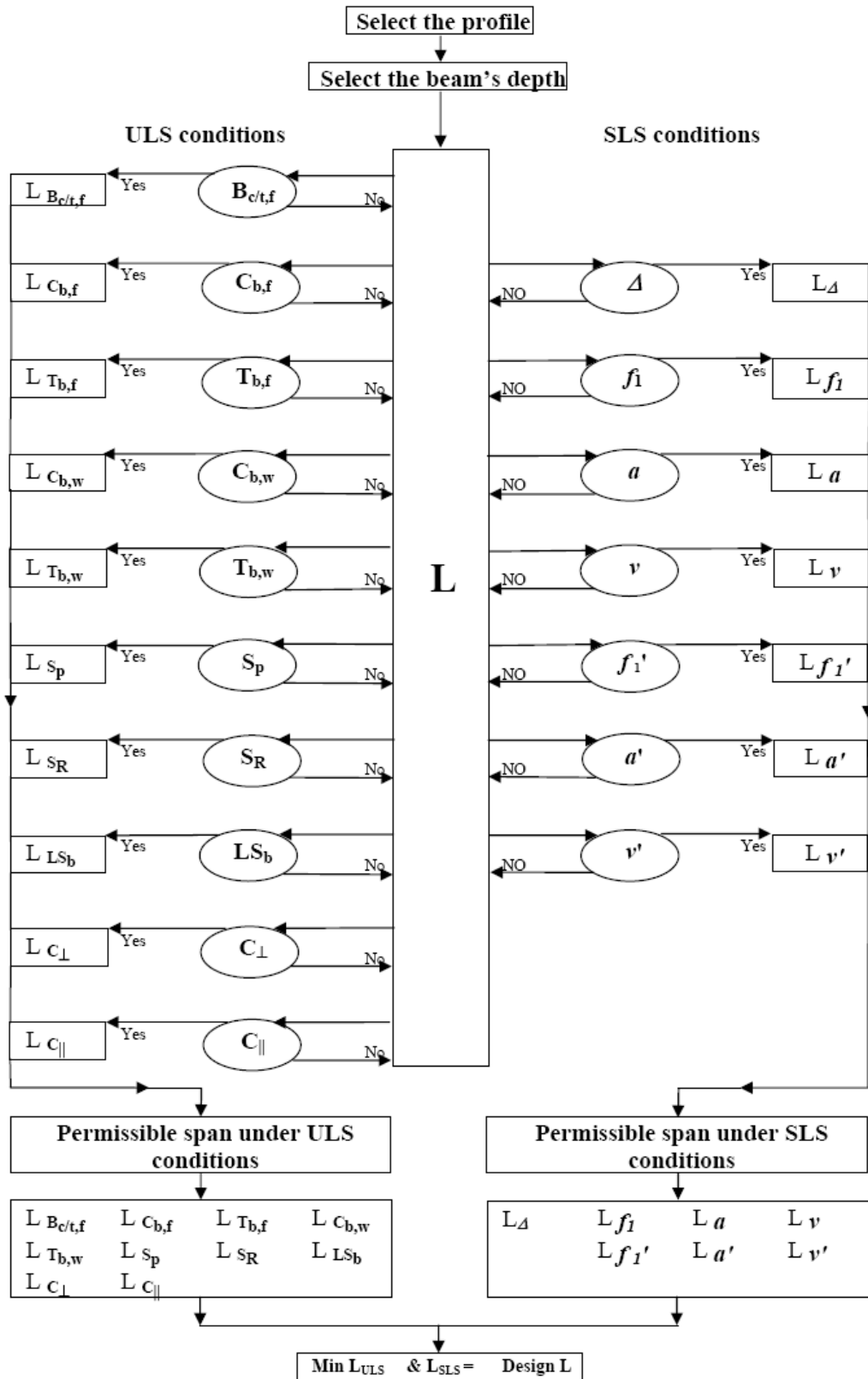


Figure 7.4 Procedure for identifying the maximum permissible span of the profile

For this method, a random span is selected and evaluated against the first condition, $B_{c/t,f}$. If the selected span satisfies the condition then its value is increased and again evaluated against the condition. This process is continued till the maximum span length, which satisfies the condition, is identified and that span length, ' $L_{B_{c/t,f}}$ ' is recorded. This process is repeated for all of the conditions and the maximum span length under each is recorded. The lowest value among the recorded spans is the maximum permissible span of the profile and its corresponding condition is considered to be the governing design condition. For instance, the maximum span under each condition was calculated for the previous double I-beam section (Table 7.2). The lowest span length or permissible span of the section was found to be 5.65m. This value corresponds to the deflection under unit point load 'a' from option A. Mean while adopting option B results in the permissible span increasing to 6.05m, which is associated with deflection under unit point load 'a' as in option A.

Table 7.2 - Permissible span for Double I-beam of 300mm depth with OSB web and C16 timber flange

a) Under ULS conditions

$b \times h$	$B_{c/t,f}$	$C_{b,f}$	$T_{b,f}$	$C_{b,w}$	$T_{b,w}$	S_p	S_R	LS_b	C_{\perp}	C_{\parallel}
(mm)	(m)	(m)	(m)	(m)	(m)	(m)	(m)	(m)	(m)	(m)
90 × 300	8.80	8.75	7.55	9.80	7.70	34.80	11.80	8.80	19.75	21.25

b) Under SLS conditions

$b \times h$	Deflection	Vibration					
		Option A			Option B		
	Δ	f_1	a	v	f_1'	a'	v'
(mm)	(m)	(m)	(m)	(m)	(m)	(m)	(m)
90 × 300	6.30	6.40	5.65	6.40	8.20	6.05	8.20

The procedure above is the base model for the parametric study, which is conducted in chapter eight, where effects of geometrical and material variability on structural performance of timber flooring systems are studied. The four different profiles examined are I-beam, double I-beam, box beam and box I-beam.

7.5 Reduction of inconvenient floor vibration

The other main difference between BS 5268 and Eurocode 5 is that the latter contains vibration criteria for evaluating the serviceability of a floor. Traditionally engineers are familiar with the horizontal swaying of tall buildings, which is caused by winds or earthquakes, but the concept of vibration has only recently been applied to serviceability in the context of evaluating vertical floor movements. As discussed earlier, Eurocode 5 defines three conditions in order to avoid excessive vibration as:

- Fundamental frequency (Equation 7.48)
- Deflection under unit point load (Equations 7.52 and 7.55)
- Unit impulse velocity response (Equations 7.56 and 7.57)

From the design perspective, increasing the stiffness is the most controllable and straightforward measure for avoiding excessive vibration. This can be observed from the equations for evaluating the vibration of flooring systems given in this chapter. As an example, the previously described model for the double I-beam was evaluated again with C24 timber flanges used instead of C16. The results of vibration criteria for both conditions are given in Table 7.3.

Table 7.3 Comparison between the vibration criteria of C16 and C24 Double I-beams

		$E_{0,mean}$	f	a	a_d	v	v_d
		(N/mm ²)	(Hz)	(mm/kN)	(mm/kN)	(m/Ns ²)	(m/Ns ²)
Double I-beam	C16	8000	10.56	1.257	1.331	0.0122	0.0151
	C24	11000	12.19	0.930	1.331	0.0119	0.0146

Employing the C24 timber flange instead of C16 in a double I-beam of 300mm depth and 5600mm span results in:

- 15% increase in fundamental frequency
- 26% decrease in deflection under unit point load
- 2% decrease in unit impulse velocity.

The effect of E on unit impulse velocity, v , is not significant in this example because the value of v is influenced by n_{40} and m (Equation 7.57). In this case their effect is not significant as shown in Table 7.4.

Table 7.4 Effect of m and n_{40} on value of v and v_d

		m	n₄₀	v	v_d
		(Kg/m ²)		(m/Ns ²)	(m/Ns ²)
Double I-beam	C16	63.69	10.50	0.0122	0.0151
	C24	64.70	10.48	0.0119	0.0146

From Table 7.4 and preceding calculation it can be concluded that increasing the stiffness, E , creates a positive effect by reducing the vibration of a light timber floor. This improvement is caused by the high stiffness to weight ratio characteristic of the timber.

7.6 Summary and conclusions

This chapter describes the analytical procedures, which were used for a parametric study detailed in chapter eight. A descriptive discussion on Eurocodes was provided, because all the designs and calculations presented are based on Eurocodes. There followed a description of the model example, which was developed for assessing the timber floor constructed with double I-beams of 300 mm depth and 5600 mm span. The model example evaluated the double I-beam by introducing various conditions under ULS and SLS design methods. The following key points can be concluded from this chapter:

- Eurocodes were developed to ensure uniform construction practice for all members of the EU as part of the effort to resolve the obstacles to trade between member states.
- There are ten main Eurocodes for construction, but the first two, Eurocode 0 and Eurocode 1, are the key documents used in conjunction with all others.
- At present Eurocodes have equal status with British Standards but in a few years they will completely replace those standards.
- Eurocode 5 is the code of practice for timber design. The major difference between Eurocode 5 and BS 5268 lies in the adopted design philosophy.
- Eurocode 5 introduced vibration criteria for designing timber floors and that is an important additional measure not present in BS 5268.
- The described design model can predict the maximum permissible span and can also identify the governing design criteria for the various beam profiles.
- In designing light timber floors, one of the most convenient options to avoid excessive vibration is to increase the stiffness of the beam/ joists. As increasing stiffness has enables floors to meet the Eurocode vibration criteria.

CHAPTER 8: PARAMETRIC EVALUATION OF MULTI-WEBBED COMPOSITE JOISTS BASED ON EUROCODE 5

8.1 Introduction

Beams are primary structural members which are commonly used in flooring systems. The introduction of engineered beams offers long span, low cost and light weight joists in comparison to traditional solid timber sections. However, the vibration criteria in the design codes may significantly reduce the permissible span of the joists for domestic construction.

This chapter investigates the influence of geometric and material variability on permissible spans of multi-webbed composite joists. The aim was achieved by conducting comparative parametric studies on a series of timber flooring systems built with multi-webbed composite engineered joists, in this case CIBs, together with studies on other floor systems made with traditional solid timber joists. Chapter 7 described the model on which the parametric study is based. That model was devised using the recommendations of BS EN 1995-1-1(2004) and the recent UK National Annex to EN1995-1-1, (2004).

The requirements under both ultimate limit states and serviceability limit states have been calculated. In UK National Annex to BS EN 1995-1-1 (EC5) two options, A and B, are provided for vibrational performance design of timber floors and those methods have also been compared and assessed. Methods A and B both differ in the equations given for measuring the natural frequency and the deflection under unit point load.

Geometric variability involved using I, double I, box and box I, beam/joist profiles. The variations between the profiles were web-flange connection details and the number of webs, which varied from one to three depending on the profile. Material variability was provided by building OSB and plywood webs, which were considered in conjunction with flanges of C16 and C24 timber. This study shows that serviceability would in general govern design requirements in UK timber flooring systems. Out of four different sub-criteria defined under the serviceability conditions,

the deflection under unit point load is the governing condition in most cases. It was found that the correct choice of materials and beam profile can enhance the permissible span by up to 34%. When lateral restraint is not provided, lateral stability becomes the controlling criterion as beam depth increases. An inverse relationship has been found between the permissible span and the beam depth for an I-beam profile, whereas for the double I-beams a constant permissible span was observed for varied beam depths. For the box and boxed I-beams, the permissible span will increase in proportion to beam depth. This study also shows that the effect of lateral stability on solid timber joists is less pronounced than for engineered beams.

8.2. Parametric study

A series of parametric studies were carried out on timber flooring systems built from solid timber joists and on others built from multi-webbed engineered joists, including I, double-I, box and box I beams, see Figure 8.1. Particleboard was used as decking for both floors. The joist depth was varied from 75 to 225mm at steps of 25mm for the solid joists and from 150 to 500mm at steps of 50 mm for the engineered joists. The solid joists were 50mm wide, while the engineered joists were made of the timber flanges 90mm wide and 45mm deep, together with 9mm three-ply plywood or OSB web(s). Details of the engineered joists are shown in Figure 8.1.

Two timber grades, C16 and C24, were studied for use as the solid joists and the flanges of the engineered joists. Joist spacing of $s = 400$ and 600mm were considered.

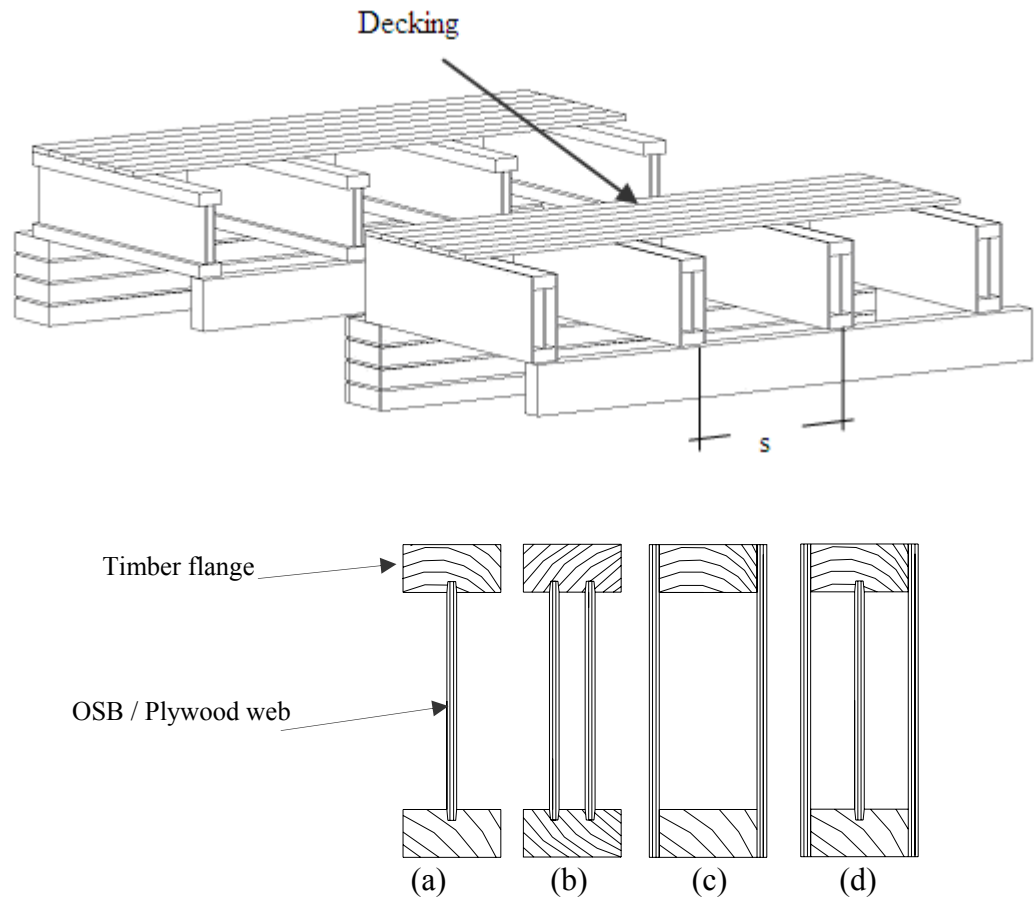


Figure 8.1 Engineered joists used in flooring systems: (a) I-beam, (b) Double I-beam, (c) Box beam, (d) Box I-beam.

The design calculations for the parametric study were based on the recommendations of BS EN 1995-1-1 for solid timber joists and glued thin-webbed beams, together with the latest UK National Annex. Each analysis covered both the ultimate limit states (ULS) and serviceability limit states (SLS) criteria.

8.2.1 Ultimate limit states design (ULS)

The ultimate limit states are associated with collapse and other similar forms of structural failure and concern the safety of people and the structure. These states include loss of equilibrium, failure due to rupture, fatigue or excessive deformation, instability, mechanism transformation and sudden system change for the structure or its parts.

The following ten ULS criteria were considered for the engineered joists (I, double I, box and box I, beams):

1. Axial compression and tension in the timber flanges due to bending ($\mathbf{B}_{c/t,f}$)
2. Compression in the extreme fibres of the timber flanges due to bending ($\mathbf{C}_{b,f}$)
3. Tension in the extreme fibres of the timber flanges due to bending ($\mathbf{T}_{b,f}$)
4. Compression in the extreme fibres of the plywood/ OSB web due to bending ($\mathbf{C}_{b,w}$)
5. Tension in the extreme fibres of the plywood/ OSB web due to bending ($\mathbf{T}_{b,w}$)
6. Panel shear in the plywood/ OSB web (\mathbf{S}_p)
7. Planar (rolling) shear in the plywood/ OSB web (\mathbf{S}_R)
8. Lateral stability subjected to bending (\mathbf{LS}_b)
9. Compression perpendicular to the timber grain (bearing) (\mathbf{C}_\perp)
10. Compression parallel to the plywood face grain or OSB panel length (\mathbf{C}_\parallel)

The following four ULS criteria were used for the solid timber joists:

1. Bending (\mathbf{B})
2. Shear (\mathbf{S})
3. Compression perpendicular to the grain (bearing) (\mathbf{C}_\perp)
4. Lateral stability of the timber joists subjected to bending (\mathbf{LS}_b)

When the study was designed to evaluate each SLS and ULS criterion, then the joists were subsequently regarded as in a condition matching a criterion above and each was specified by the criterion number. For example, results from rolling shear tests are described as for beams in condition 7.

8.2.2 Serviceability limit state design (SLS)

The serviceability limit states are associated with conditions of normal use and concern the functioning of the structure or structural members, comfort of people and appearance of the construction work.

Deflection and *vibration* are the SLS criteria used for assessing the permissible span. Each optional method includes four sub-categories of movement as shown overleaf:

<u>Deflection</u>	{	1. Static deflection (Δ)	}	Option A
<u>Vibration</u>		2. Natural frequency (f_1)		
	3. Deflection under unit point load (a)	Option B		
	4. Unit impulse velocity response (v)			
	5. Natural frequency (f_1')			
6. Deflection under unit point load (a')				
7. Unit impulse velocity response (v')				

8.2.3 Loading

Dead or permanent load (G), excluding the floor joists, was assumed to be 0.50 kN/m^2 for the intermediate floors, which were also assumed to have 60 minute fire resistance (TRADA, 1994). Imposed or live load (Q) was considered to be below 1.5 kN/m^2 for normal construction (Pye and Harrison 2003).

8.2.4 Assumptions

The following assumptions were made in the analysis:

1. No allowances were made in the calculation for partition loads.
2. Compressive flanges were restrained by the floor decking and torsional rotation was considered to be prevented at the supports.
3. Bearing length was kept at 100mm in all cases.
4. Weight of the joist for each profile was added to the permanent load.
5. Grooving depth of 10mm was assumed for double I and box I beams, but was increased to 12mm for I beams in order to enhance their gluing areas.

8.2.5 Characteristic values of the material properties

The characteristic values of the material properties used for solid timber and engineered products are based on the published codes of practice. The characteristic values of C16 and C24 solid section timber and timber flanges, New Zealand F11 plywood and OSB/3 webs, and P5 particleboards for floor decking were taken from (BS EN 338:2003), (NZS 3603:1993) and (EN 12369-1:2001) respectively.

8.3 Lateral buckling factor

Lateral buckling factor (k_{crit}) is the factor that is defined in EC5 to evaluate lateral stability of the beam. It is considered as $k_{\text{crit}}=1$ when lateral restraints are provided. But in absence of lateral restraints this value should be obtained from equation 6.34

in EC5. In order to obtain this factor, the torsion constant should be calculated for each profile. EC5 defines the torsion constant as the torsional moment of inertia (I_{tor}). This value is calculated by using Prandtl's membrane, or soap bubble analogy (Ugural ... et.al, 2003) in conjunction with LUSAS software (LUSAS, 2005). More details on calculating the I_{tor} are given in chapter 7.

8.4. Discussion of the results

Sample sets of calculated permissible spans for C16 box I-beams with plywood webs and for solid timber joists at 400mm spacing are listed in Tables 8.1 and 8.2 respectively, while the complete data sets for all the profiles are illustrated in Figures 8.2 to 8.6. The permissible spans of the various engineered joists for the ULS criteria correspond to conditions 1 to 10, and are given in Table 8.1 and Figures 8.2 to 8.5, while figures for the SLS criteria correspond to conditions 11 to 17. Similarly, the permissible spans of the solid timber joists are given in Table 8.2 and Figure 8.6, where the ULS criteria correspond to conditions 1 to 4 and the SLS criteria correspond to conditions 5 to 11.

It can be observed from Table 8.1 that panel shear (S_p), compression parallel to the grain ($C_{||}$) and compression perpendicular to the grain (C_{\perp}) are not critical. The results for lateral stability (LS_b) are the same as those under condition 1, since k_{crit} is taken as unity. Similarly, shear and compression are not critical for the solid timber joists as shown in Table 8.2.

Table 8.1 Permissible spans of box I-beams with C16 timber flanges and plywood webs ($s = 400$ mm, $G = 0.5$ kN/m² and $Q = 1.5$ kN/m²)

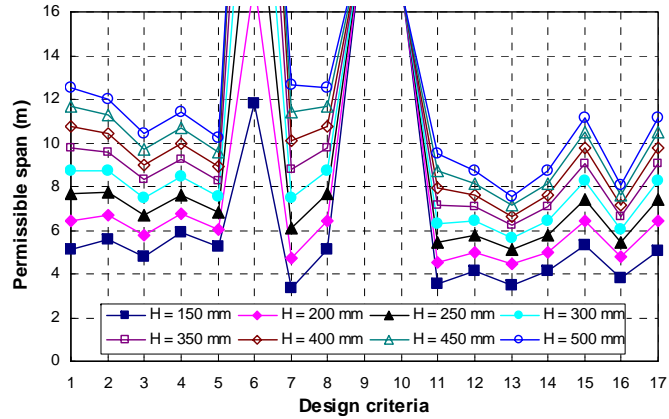
(a) Ultimate limit states (ULS)

Condition	1	2	3	4	5	6	7	8	9	10
$B_f \times H$	$B_{c/t,f}$	$C_{b,f}$	$T_{b,f}$	$C_{b,w}$	$T_{b,w}$	S_P	S_R	LS_b	C_{\perp}	C_{\parallel}
(mm)	(m)	(m)	(m)	(m)	(m)	(m)	(m)	(m)	(m)	(m)
90 × 150	5.70	6.25	5.40	4.80	4.30	11.65	14.95	5.70	19.65	51.00
90 × 200	7.30	7.60	6.55	6.15	5.50	17.05	20.60	7.30	19.50	50.65
90 × 250	8.75	8.85	7.65	7.40	6.60	22.40	26.10	8.75	19.40	50.30
90 × 300	10.15	10.05	8.70	8.55	7.65	27.70	31.40	10.15	19.25	49.95
90 × 350	11.40	11.20	9.65	9.65	8.60	32.90	36.55	11.40	19.10	49.55
90 × 400	12.65	12.30	10.60	10.70	9.55	38.00	41.50	12.65	19.00	49.25
90 × 450	13.85	13.35	11.55	11.70	10.45	37.70	46.30	13.85	18.85	48.90
90 × 500	15.00	14.40	12.45	12.65	11.35	36.95	51.00	15.00	18.70	48.55

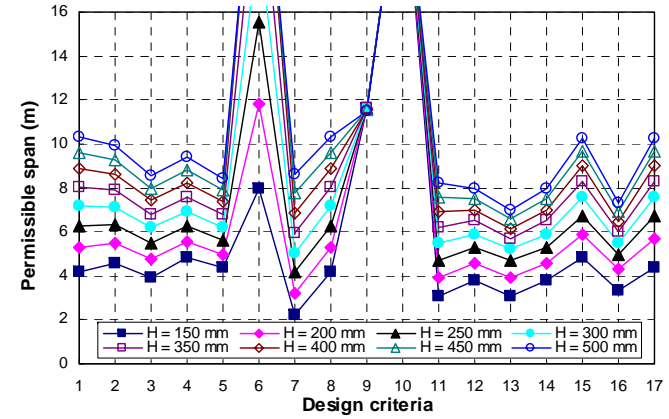
* B_f : Breadth of the flange, H: Depth of the joist

(b) Serviceability limit states (SLS)

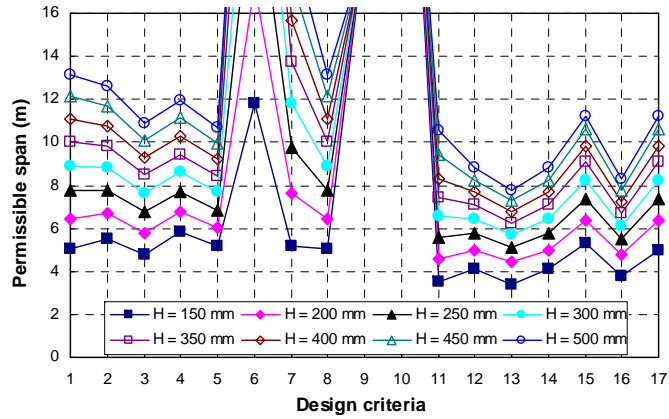
Criteria	Deflection	Vibration								
		Option A			Option B			Improvement for B		
Condition	11	12	13	14	15	16	17	15 vs. 12	16 vs. 13	17 vs. 14
$B_f \times H$	Δ	f_1	a	v	f_1'	a'	v'			
(mm)	(m)	(m)	(m)	(m)	(m)	(m)	(m)	(%)	(%)	(%)
90 × 150	3.90	4.35	3.75	4.35	5.55	4.15	5.50	29	7	19
90 × 200	5.05	5.25	4.75	5.25	6.75	5.10	6.75	28	6	28
90 × 250	6.10	6.05	5.45	6.05	7.75	5.85	7.75	29	5	29
90 × 300	7.15	6.80	6.10	6.80	8.70	6.55	8.70	28	5	28
90 × 350	8.15	7.45	6.70	7.45	9.55	7.20	9.55	28	5	28
90 × 400	9.10	8.10	7.25	8.10	10.40	7.80	10.33	29	4	29
90 × 450	10.05	8.70	7.80	8.70	11.15	8.35	11.15	29	4	29
90 × 500	11.00	9.25	8.35	9.25	11.85	8.90	11.85	28	5	28



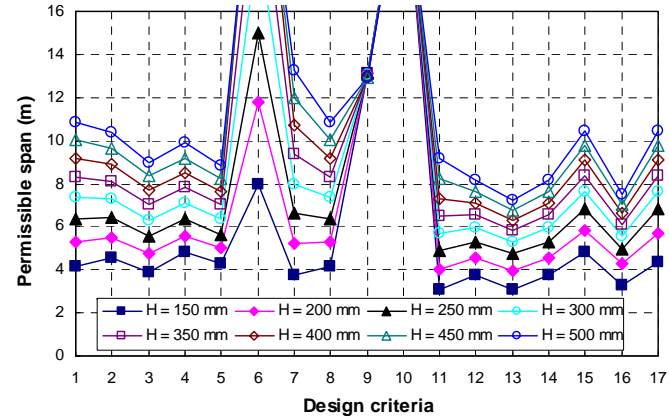
a) I-beams at $s = 400$ mm



b) I-beams at $s = 600$ mm

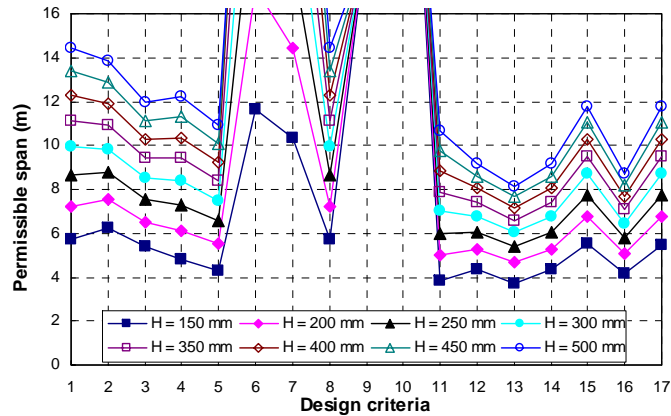


c) Double I-beams at $s = 400$ mm

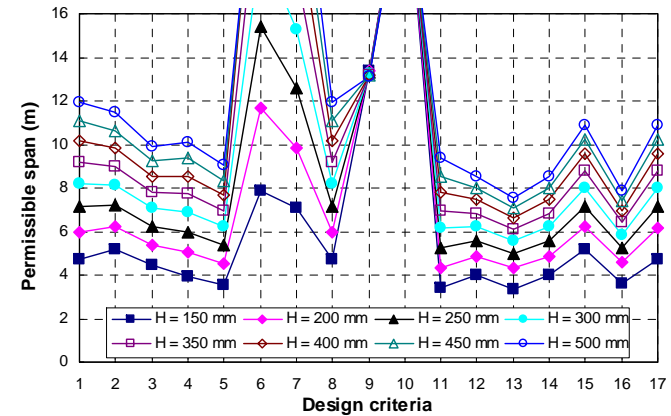


d) Double I-beams at $s = 600$ mm

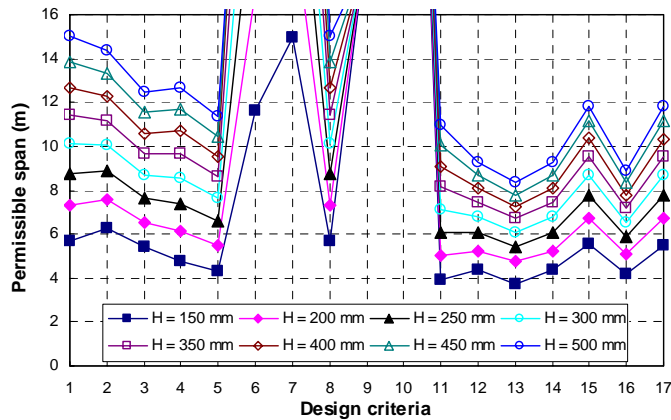
Figure 8.2 Permissible spans for engineered joists with C16 flanges and Plywood webs, based on different design criteria



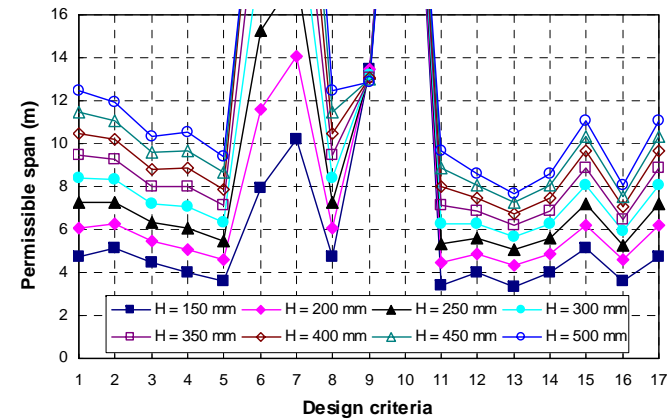
e) Box beams at $s = 400$ mm



f) Box beams at $s = 600$ mm

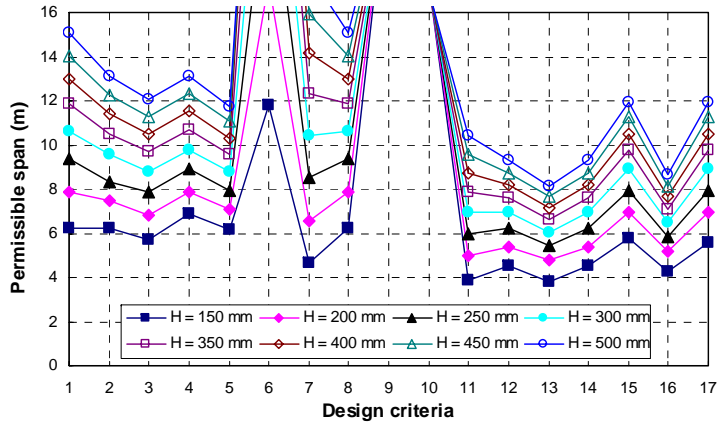


g) Box I-beams at $s = 400$ mm

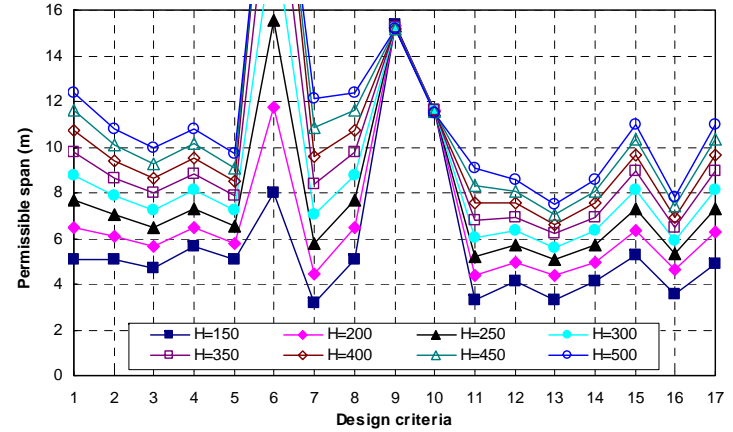


h) Box I-beams at $s = 600$ mm

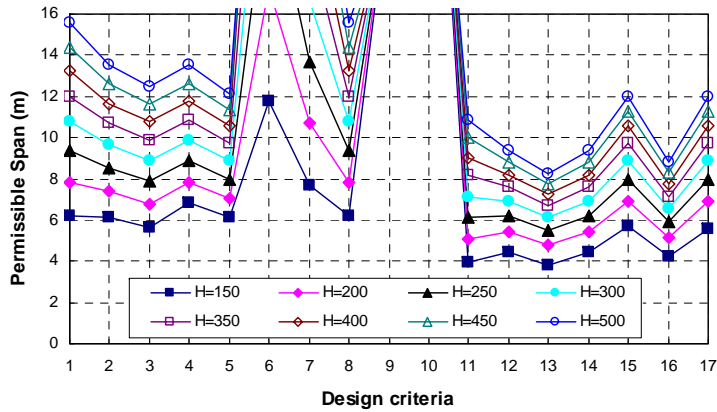
Figure 8.2 Permissible spans for engineered joists with C16 flanges and Plywood webs, based on different design criteria (cont.)



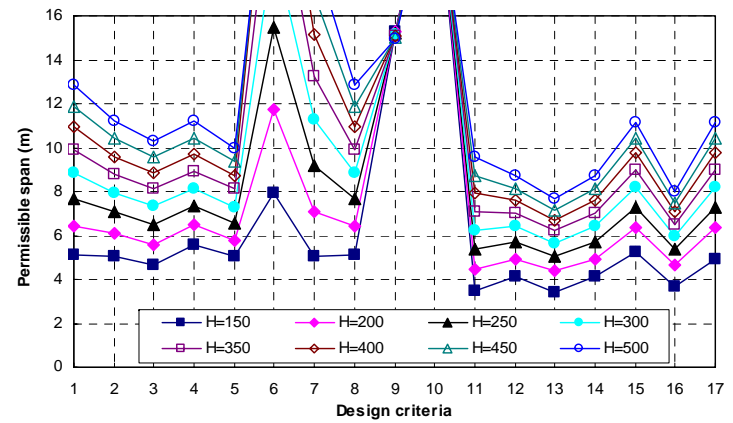
a) I-beams at $s = 400$ mm



b) I-beams at $s = 600$ mm

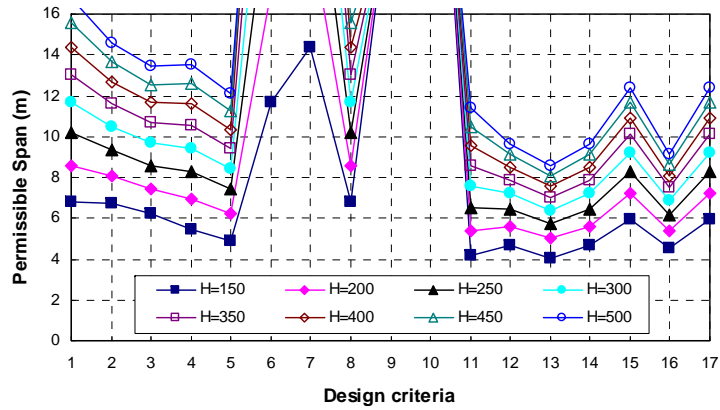


c) Double I-beams at $s = 400$ mm

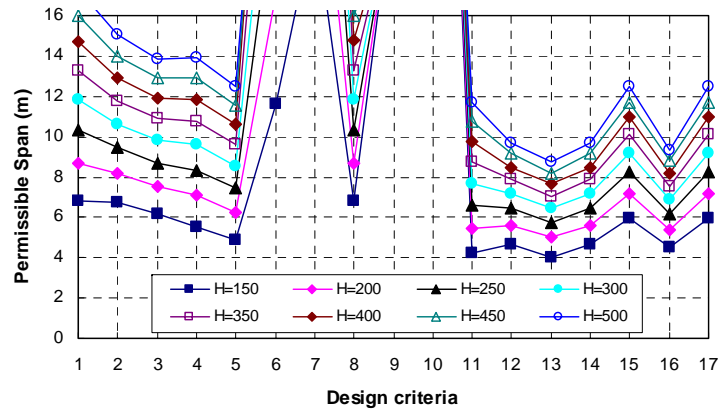


d) Double I-beams at $s = 600$ mm

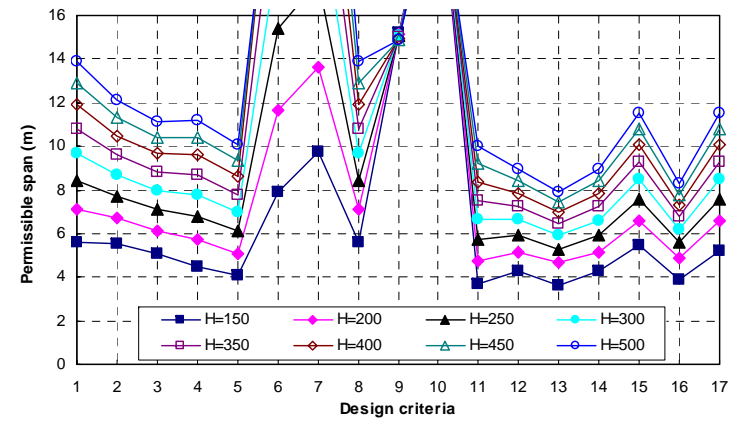
Figure 8.3 Permissible spans for engineered joists with C24 flanges and Plywood webs, based on different design criteria



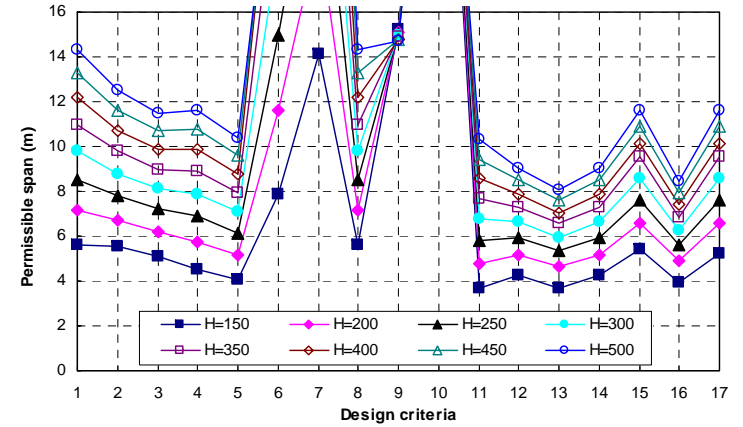
e) Box beams at $s = 400$ mm



g) Box I-beams at $s = 400$ mm

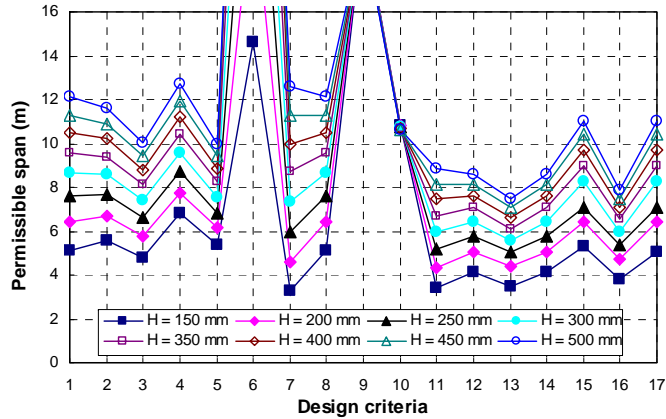


f) Box beams at $s = 600$ mm

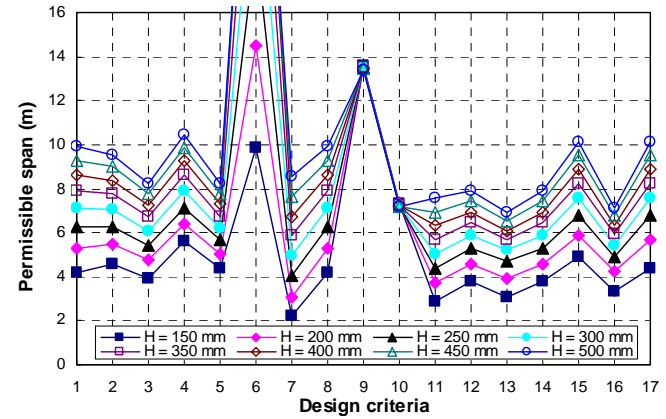


h) Box I-beams at $s = 600$ mm

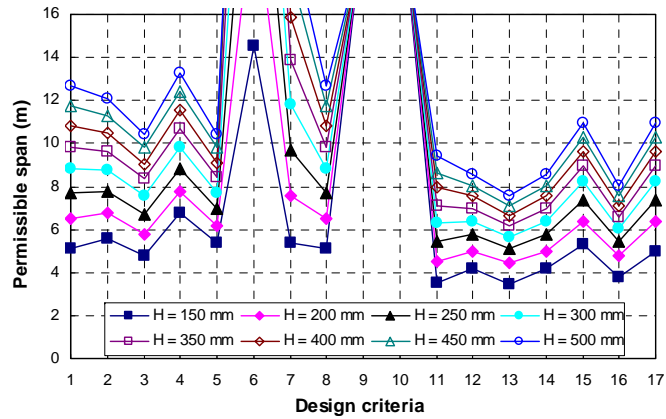
Figure 8.3 Permissible spans for engineered joists with C24 flanges and Plywood webs, based on different design criteria (cont.)



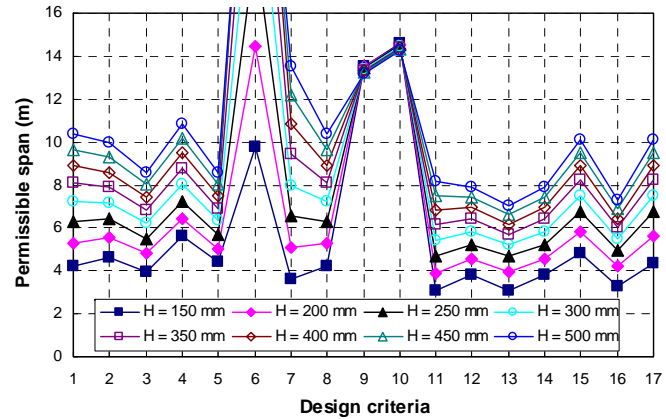
a) I-beams at $s = 400$ mm



b) I-beams at $s = 600$ mm

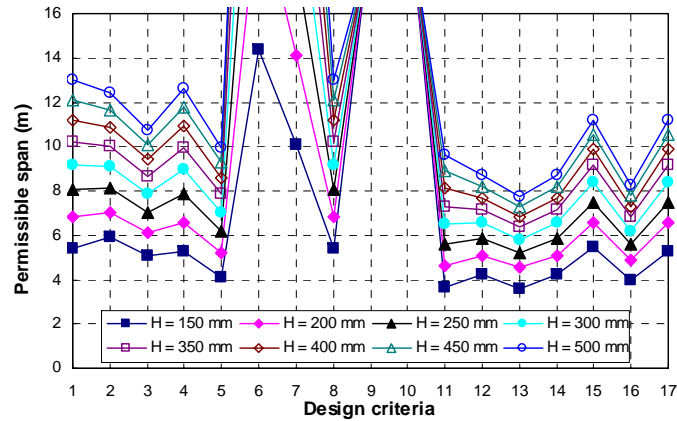


c) Double I-beams at $s = 400$ mm

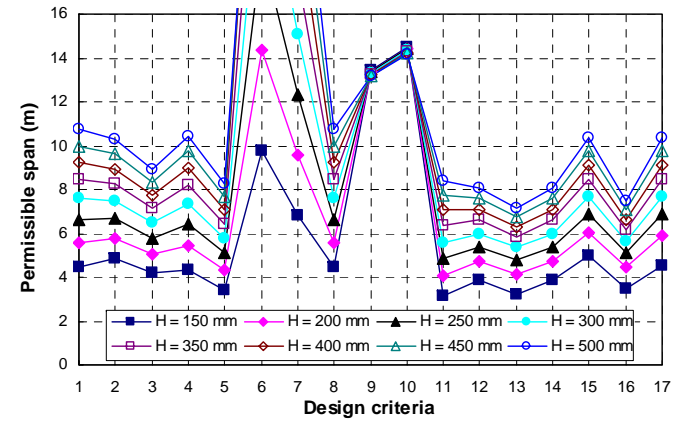


d) Double I-beams at $s = 600$ mm

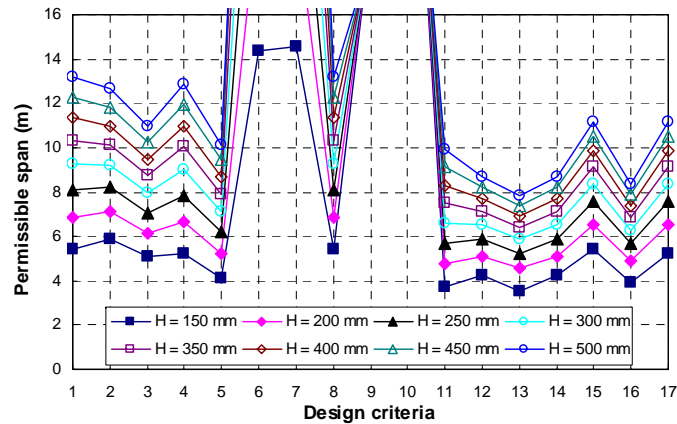
Figure 8.4 Permissible spans for engineered joists with C16 flanges and OSB webs, based on different design criteria



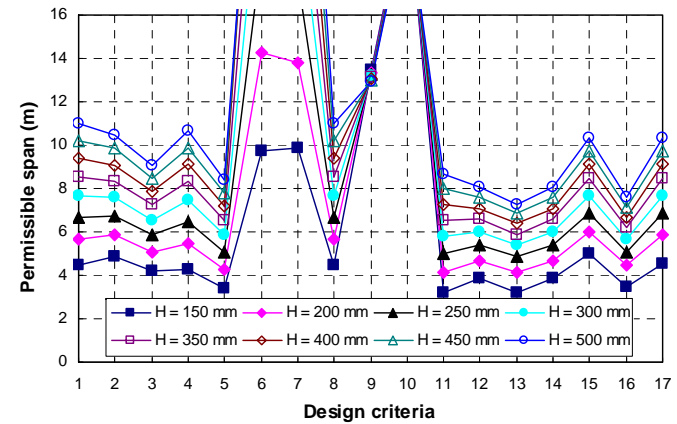
e) Box beams at $s = 400$ mm



f) Box beams at $s = 600$ mm

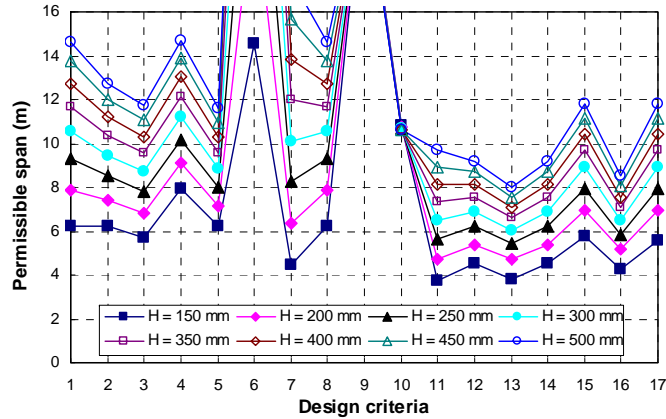


g) Box I-beams at $s = 400$ mm

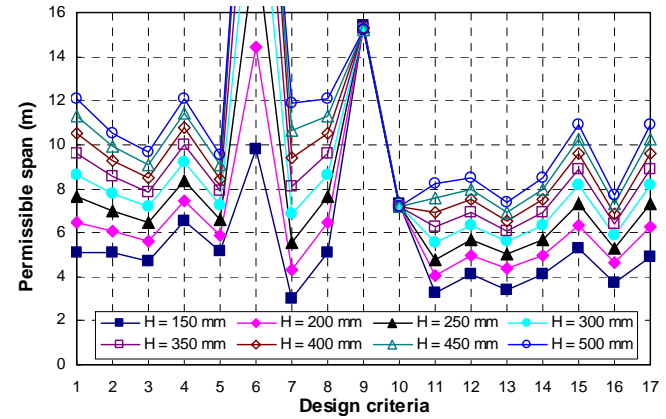


h) Box I-beams at $s = 600$ mm

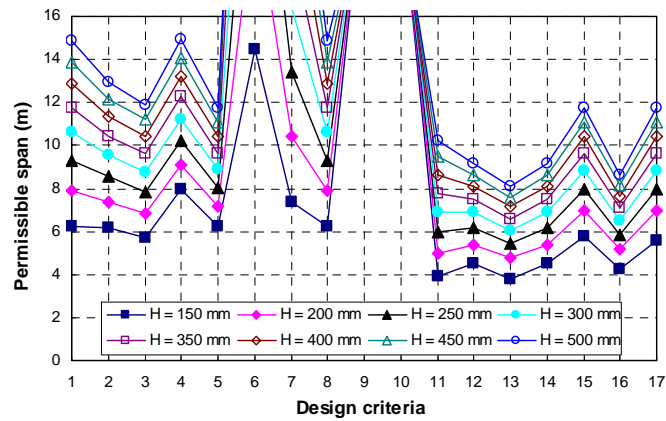
Figure 8.4 Permissible spans for engineered joists with C16 flanges and OSB webs, based on different design criteria (cont.)



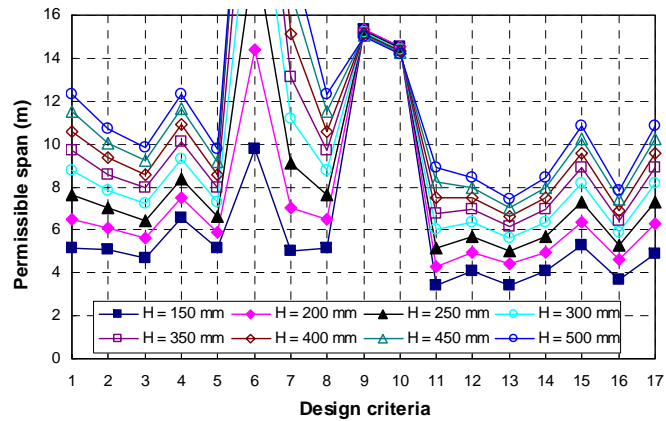
a) I-beams at $s = 400$ mm



b) I-beams at $s = 600$ mm

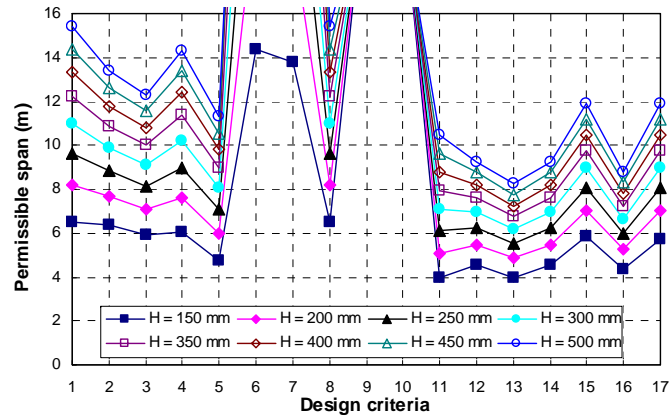


c) Double I-beams at $s = 400$ mm

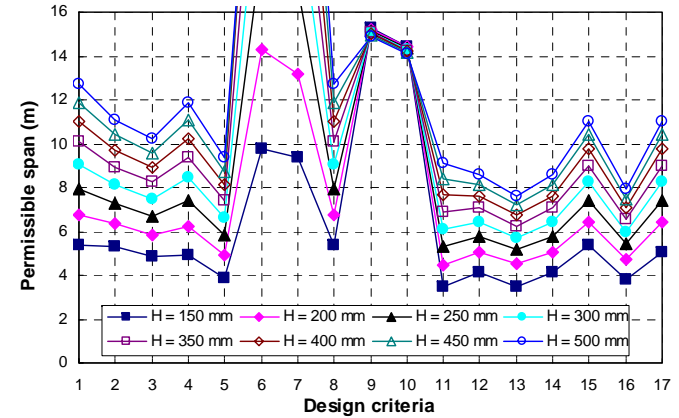


d) Double I-beams at $s = 600$ mm

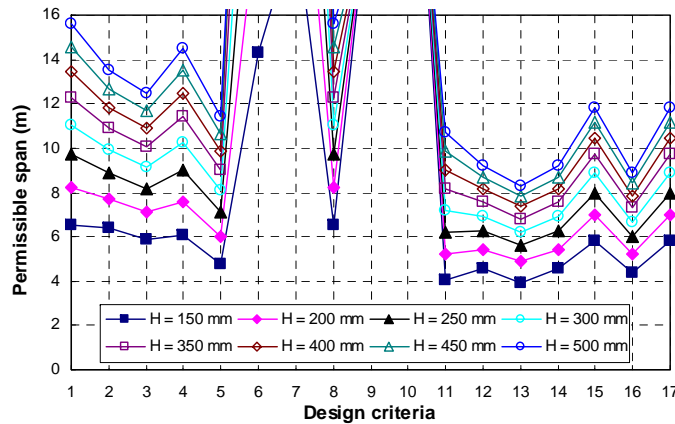
Figure 8.5 Permissible spans for engineered joists with C24 flanges and OSB webs, based on different design criteria



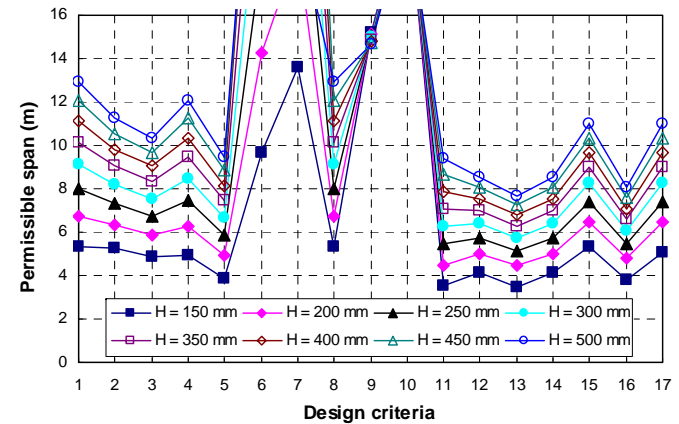
e) Box beams at $s = 400$ mm



f) Box beams at $s = 600$ mm



g) Box I-beams at $s = 400$ mm



h) Box I-beams at $s = 600$ mm

Figure 8.5 Permissible spans for engineered joists with C24 flanges and OSB webs, based on different design criteria (cont.)

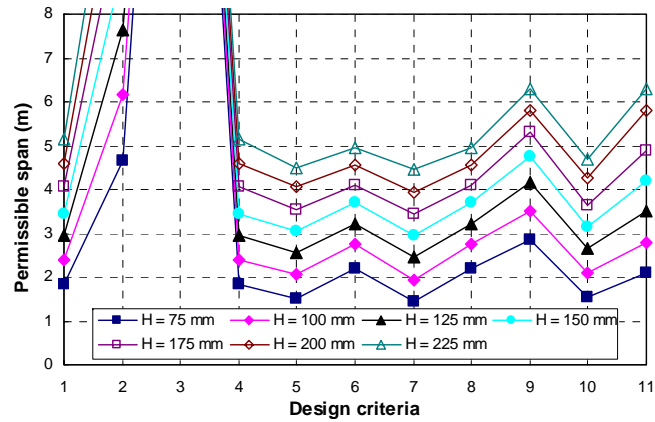
Table 8.2 Permissible spans of C16 solid timber joists ($s = 400$ mm, $G = 0.5$ kN/m² and $Q = 1.5$ kN/m²)

(a) Ultimate limit states (ULS)

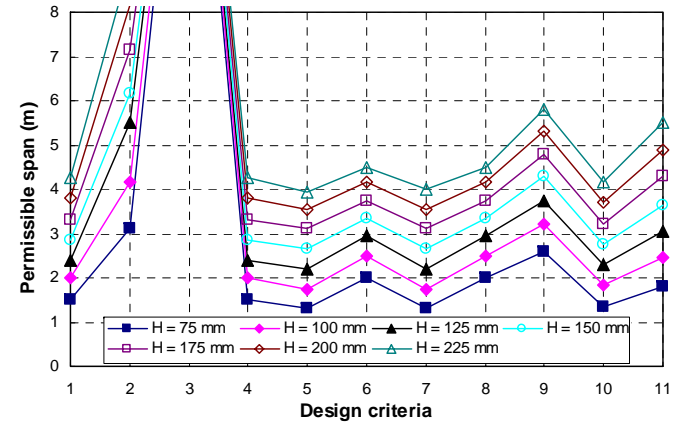
Condition	1	2	3	4
$B_f \times H$	B	S	C_{\perp}	LS_b
(mm)	(m)	(m)	(m)	(m)
50 × 75	1.85	4.65	23.95	1.85
50 × 100	2.40	6.15	24.25	2.40
50 × 125	2.95	7.65	24.55	2.95
50 × 150	3.45	9.10	24.85	3.45
50 × 175	4.05	10.55	25.10	4.05
50 × 200	4.60	12.00	25.40	4.60
50 × 225	5.15	13.40	25.70	5.15
75 × 200	5.55	17.55	37.15	5.55
75 × 225	6.25	19.55	37.45	6.25

(b) Serviceability limit states (SLS)

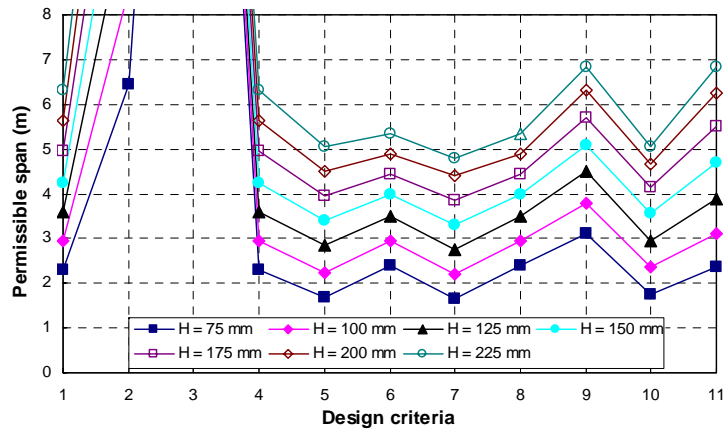
Criteria	Deflection	Vibration								
		Option A			Option B			Improvement for B		
Condition	5	6	7	8	9	10	11	9 vs. 6	10 vs. 7	11 vs. 8
$B_f \times H$	Δ	f_1	a	v	f_1'	a'	v'	%	%	%
(mm)	(m)	(m)	(m)	(m)	(m)	(m)	(m)			
50 × 75	1.50	2.20	1.45	2.20	2.85	1.55	2.10	30	7	-5
50 × 100	2.05	2.75	1.95	2.75	3.50	2.10	2.80	27	8	2
50 × 125	2.55	3.20	2.45	3.20	4.15	2.65	3.50	30	8	9
50 × 150	3.05	3.70	2.95	3.70	4.75	3.15	4.20	28	7	14
50 × 175	3.55	4.10	3.45	4.10	5.30	3.65	4.90	29	6	20
50 × 200	4.05	4.55	3.95	4.55	5.80	4.25	5.80	27	8	27
50 × 225	4.50	4.95	4.45	4.95	6.30	4.70	6.30	27	6	27
75 × 200	4.55	4.95	4.50	4.95	6.30	4.75	6.30	27	6	27
75 × 225	5.15	5.35	4.90	5.35	6.85	5.15	6.85	28	5	28



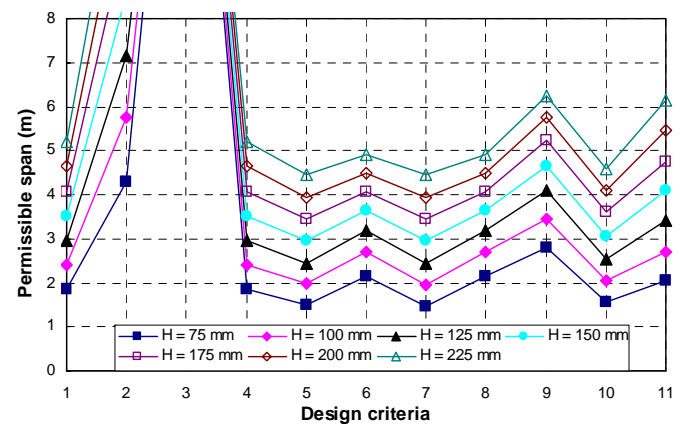
a) C16 solid timber joists at $s = 400$ mm



b) C16 solid timber joists at $s = 600$ mm



c) C24 solid timber joists at $s = 400$ mm



d) C24 solid timber joists at $s = 600$ mm

Figure 8.6 Permissible spans for solid timber joists based on different design criteria

Under serviceability conditions, except for the shallow engineered joists where $H = 150$ and 200mm , the permissible spans based on the unit impulse velocity criterion are very close to those based on the natural frequency criterion for Option B. This is because in a given equation for calculating the velocity v , if the natural frequency is below 8Hz then the equation will be violated. In other words, a natural frequency of 8Hz is regarded as the lower limit for unit impulse velocity response. As shown in Figures 8.2 to 8.6, however, the permissible spans for beam heights of 150 and 200mm , based on the unit impulse velocity criterion condition 17, are slightly lower than those based on the natural frequency criterion condition 15.

8.4.1 Controlling criteria under the ULS conditions

For the I-beams with C16 timber flanges, rolling shear, condition 7, is the controlling criterion when the grooving depth is 10mm . This can be improved by increasing the grooving depth to increase the glued area and enhance the rolling shear capacity. Increasing the grooving depth of the I-beam from 10 to 12mm shifts the controlling criterion to condition 5 for the deep I-beams with Plywood webs. For the deep OSB webbed I-beams, however, the controlling criteria shift to conditions 3 and 10. Even though increasing the grooving depth could enhance the rolling shear resistance, it may not be practical to increase the depth as this may lead to splitting or knifing of the timber flange caused by punching shear and would create difficulties for fabrication.

For the double I-beams with C16/C24 timber flanges and Plywood/OSB webs, condition 5 gradually supersedes condition 3 as the controlling criterion with the increase of the beam depth. Rolling shear is no longer the controlling criterion for these beams, since the grooved area is doubled compared to that in I-beams.

Condition 5, tension in the web induced by bending, is critical for the box beams and the box I-beams due to the depth and formation of their external webs compared to those of the double I-beams.

For the C16 and C24 solid timber long-span joists, bending is often the critical criterion under the ULS conditions and shear is unlikely to be the decisive factor as the first moment of area is significantly higher than those of engineered joists.

8.4.2 Critical criteria under the SLS conditions

Static deflection and vibration categories were investigated under SLS conditions. In general for both engineered and solid timber beams, deflection under the unit point load was found to be the controlling criterion. The exception was for I-beams with OSB webs, when the controlling criterion changed from static deflection to deflection under unit point load as the beam depth increased. Permissible spans for the solid timber joists calculated using EC5, were found to be close to the values recommended by BS 5268-2 (2002) or NHBS (2000). For instance, the permissible span for C24 calculated to EC5 option A results in a 2.4% shorter span in comparison to a result calculated using BS5268-2. In contrast, use of EC5 option B leads to a 1.17% longer permissible span than that calculated using BS5268-2.

The design permissible spans which satisfy both the ULS and SLS requirements are listed in Table 8.3, where the controlling criteria for each case are shown in brackets.

For the I-beams with C16 timber flanges, the permissible spans are controlled by rolling shear for depths up to 300mm at the spacing of 600mm, and by the unit point load deflection for depths of over 300mm.

The permissible spans of C16 solid timber joists for the 400mm spacing are governed by the unit point deflection, whereas the static deflection becomes the governing factor for spans of 600mm. The deflection under unit point load remains the controlling criterion for the C24 solid timber joists at both 400 and 600mm spacing.

8.4.3 Comparison of options A and B regarding the permissible span

In comparison to option A, the equations in Option B give higher values for the natural frequency f_1 and the design limit of unit impulse velocity, v_d , and they also decrease the values for deflection under unit point load, a , and the unit impulse velocity response v . This in turn leads to an increase of the permissible span by 28% based on the natural frequency and unit impulse velocity criteria and by 4-7% based on the deflection under unit point load.

Tables 8.3(a) to 8.3(d) show that when Option B is used to calculate the permissible spans of engineered joists, they increase by up to 7% for a 400mm joist spacing and

by 4% for a joist spacing of 600mm in most cases, but for I-beams there is little or no gain.

Table 8.3 Design permissible spans for different profiles

a) Engineered joists with plywood webs and C16 timber flanges for $s = 400$ and 600 mm

$s = 400$ mm												
C16	Option A				Option B				Option B vs. Option A			
Profile	I-beam	Double I-beam	Box beam	Box I-beam	I-beam	Double I-beam	Box beam	Box I-beam	I-beam	Double I-beam	Box beam	Box I-beam
$B_f \times H$												
(mm)	(m)	(m)	(m)	(m)	(m)	(m)	(m)	(m)	(%)	(%)	(%)	(%)
90×150	3.35(S_R)	3.40(<i>a</i>)	3.70(<i>a</i>)	3.75(<i>a</i>)	3.35(S_R)	3.55(Δ)	3.85(Δ)	3.90(Δ)	0	4	4	4
90×200	4.45(<i>a</i>)	4.45(<i>a</i>)	4.70(<i>a</i>)	4.75(<i>a</i>)	4.50(Δ)	4.60(Δ)	5.00(Δ)	5.05(Δ)	1	3	6	6
90×250	5.10(<i>a</i>)	5.10(<i>a</i>)	5.40(<i>a</i>)	5.45(<i>a</i>)	5.45(<i>a'</i>)	5.50(<i>a'</i>)	5.80(<i>a'</i>)	5.85(<i>a'</i>)	7	8	7	7
90×300	5.65(<i>a</i>)	5.70(<i>a</i>)	6.05(<i>a</i>)	6.10(<i>a</i>)	6.05(<i>a'</i>)	6.10(<i>a'</i>)	6.45(<i>a'</i>)	6.55(<i>a'</i>)	7	8	7	7
90×350	6.20(<i>a</i>)	6.25(<i>a</i>)	6.60(<i>a</i>)	6.70(<i>a</i>)	6.60(<i>a'</i>)	6.70(<i>a'</i>)	7.10(<i>a'</i>)	7.20(<i>a'</i>)	6	7	8	7
90×400	6.65(<i>a</i>)	6.80(<i>a</i>)	7.15(<i>a</i>)	7.25(<i>a</i>)	7.15(<i>a'</i>)	7.25(<i>a'</i>)	7.65(<i>a'</i>)	7.80(<i>a'</i>)	8	7	7	8
90×450	7.15(<i>a</i>)	7.30(<i>a</i>)	7.65(<i>a</i>)	7.80(<i>a</i>)	7.60(<i>a'</i>)	7.80(<i>a'</i>)	8.20(<i>a'</i>)	8.35(<i>a'</i>)	6	7	7	7
90×500	7.55(<i>a</i>)	7.80(<i>a</i>)	8.15(<i>a</i>)	8.35(<i>a</i>)	8.05(<i>a'</i>)	8.30(<i>a'</i>)	8.70(<i>a'</i>)	8.90(<i>a'</i>)	7	6	7	7
								Ave	5	6	7	7

Table 8.3 a) cont.

s = 600 mm													
90×150	2.25(S_R)	3.05(<i>a</i>)	3.35(<i>a</i>)	3.35(<i>a</i>)	2.25(S_R)	3.10(Δ)	3.40(Δ)	3.40(Δ)	0	2	1	1	
90×200	3.20(S_R)	3.95(<i>a</i>)	4.30(<i>a</i>)	4.35(<i>a</i>)	3.20(S_R)	4.05(Δ)	4.35(Δ)	4.45(Δ)	0	3	1	2	
90×250	4.15(S_R)	4.75(<i>a</i>)	5.00(<i>a</i>)	5.05(<i>a</i>)	4.15(S_R)	4.90(Δ)	5.25(<i>a'</i>)	5.30(<i>a'</i>)	0	3	5	5	
90×300	5.05(S_R)	5.30(<i>a</i>)	5.60(<i>a</i>)	5.65(<i>a</i>)	5.05(S_R)	5.55(<i>a'</i>)	5.85(<i>a'</i>)	5.95(<i>a'</i>)	0	5	4	5	
90×350	5.70(<i>a</i>)	5.80(<i>a</i>)	6.10(<i>a</i>)	6.20(<i>a</i>)	5.95(S_R)	6.10(<i>a'</i>)	6.40(<i>a'</i>)	6.50(<i>a'</i>)	4	5	5	5	
90×400	6.15(<i>a</i>)	6.30(<i>a</i>)	6.60(<i>a</i>)	6.75(<i>a</i>)	6.45(<i>a'</i>)	6.60(<i>a'</i>)	6.95(<i>a'</i>)	7.05(<i>a'</i>)	5	5	5	4	
90×450	6.60(<i>a</i>)	6.75(<i>a</i>)	7.10(<i>a</i>)	7.25(<i>a</i>)	6.90(<i>a'</i>)	7.05(<i>a'</i>)	7.40(<i>a'</i>)	7.55(<i>a'</i>)	5	4	4	4	
90×500	7.00(<i>a</i>)	7.20(<i>a</i>)	7.55(<i>a</i>)	7.70(<i>a</i>)	7.30(<i>a'</i>)	7.50(<i>a'</i>)	7.90(<i>a'</i>)	8.05(<i>a'</i>)	4	4	5	5	
									Ave	2	4	4	4

Table 8.3 Design permissible spans for different profiles (cont.)

b) Engineered joists with plywood webs and C24 timber flanges for $s = 400$ mm and 600 mm

$s = 400$ mm												
C24	Option A				Option B				Option B vs. Option A			
Profile	I-beam	Double I-beam	Box beam	Box I-beam	I-beam	Double I-beam	Box beam	Box I-beam	I-beam	Double I-beam	Box beam	Box I-beam
$B_f \times H$												
(mm)	(m)	(m)	(m)	(m)	(m)	(m)	(m)	(m)	(%)	(%)	(%)	(%)
90×150	3.80(<i>a</i>)	3.80(<i>a</i>)	4.05(<i>a</i>)	4.05(<i>a</i>)	3.90(Δ)	3.95(Δ)	4.20(Δ)	4.25(Δ)	3	4	4	5
90×200	4.80(<i>a</i>)	4.80(<i>a</i>)	5.00(<i>a</i>)	5.00(<i>a</i>)	5.00(Δ)	5.10(Δ)	5.40(Δ)	5.40(<i>a'</i>)	4	6	8	8
90×250	5.45(<i>a</i>)	5.50(<i>a</i>)	5.75(<i>a</i>)	5.75(<i>a</i>)	5.85(<i>a'</i>)	5.90(<i>a'</i>)	6.15(<i>a'</i>)	6.20(<i>a'</i>)	7	7	7	8
90×300	6.05(<i>a</i>)	6.10(<i>a</i>)	6.40(<i>a</i>)	6.45(<i>a</i>)	6.50(<i>a'</i>)	6.55(<i>a'</i>)	6.85(<i>a'</i>)	6.90(<i>a'</i>)	7	7	7	7
90×350	6.65(<i>a</i>)	6.70(<i>a</i>)	7.00(<i>a</i>)	7.05(<i>a</i>)	7.10(<i>a'</i>)	7.15(<i>a'</i>)	7.50(<i>a'</i>)	7.55(<i>a'</i>)	7	7	7	7
90×400	7.15(<i>a</i>)	7.25(<i>a</i>)	7.55(<i>a</i>)	7.65(<i>a</i>)	7.65(<i>a'</i>)	7.75(<i>a'</i>)	8.05(<i>a'</i>)	8.20(<i>a'</i>)	7	7	7	7
90×450	7.65(<i>a</i>)	7.75(<i>a</i>)	8.05(<i>a</i>)	8.20(<i>a</i>)	8.15(<i>a'</i>)	8.30(<i>a'</i>)	8.65(<i>a'</i>)	8.80(<i>a'</i>)	7	7	7	7
90×500	8.10(<i>a</i>)	8.25(<i>a</i>)	8.55(<i>a</i>)	8.75(<i>a</i>)	8.65(<i>a'</i>)	8.80(<i>a'</i>)	9.15(<i>a'</i>)	9.35(<i>a'</i>)	7	7	7	7
								Ave	6	7	7	7

Table 8.3 b) cont.

$s = 600 \text{ mm}$													
90×150	3.15(S_R)	3.40(a)	3.65(a)	3.65(a)	3.15(S_R)	3.45(Δ)	3.70(Δ)	3.70(Δ)	0	1	1	1	
90×200	4.35(Δ)	4.40(a)	4.65(a)	4.65(a)	4.35(Δ)	4.45(Δ)	4.75(Δ)	4.80(Δ)	0	1	2	3	
90×250	5.05(a)	5.05(a)	5.30(a)	5.35(a)	5.20(Δ)	5.35(a')	5.60(a')	5.60(a')	3	6	6	5	
90×300	5.60(a)	5.65(a)	5.90(a)	5.95(a)	5.90(a')	5.95(a')	6.20(a')	6.25(a')	5	5	5	5	
90×350	6.20(a)	6.20(a)	6.45(a)	6.55(a)	6.45(a')	6.50(a')	6.80(a')	6.85(a')	4	5	5	5	
90×400	6.60(a)	6.70(a)	6.95(a)	7.05(a)	6.95(a')	7.10(a')	7.30(a')	7.45(a')	5	6	5	6	
90×450	7.05(a)	7.15(a)	7.45(a)	7.60(a)	7.40(a')	7.50(a')	7.80(a')	7.95(a')	5	5	5	5	
90×500	7.50(a)	7.65(a)	7.90(a)	8.05(a)	7.80(a')	8.00(a')	8.30(a')	8.45(a')	4	5	5	5	
									Ave	3	4	4	4

Table 8.3 Design permissible spans for different profiles (cont.)

c) Engineered joists with OSB webs and C16 timber flanges for $s = 400$ mm and 600 mm

$s = 400$ mm												
C16	Option A				Option B				Option B vs. Option A			
Profile	I-beam	Double I-beam	Box beam	Box I-beam	I-beam	Double I-beam	Box beam	Box I-beam	I-beam	Double I-beam	Box beam	Box I-beam
$B_f \times H$												
(mm)	(m)	(m)	(m)	(m)	(m)	(m)	(m)	(m)	(%)	(%)	(%)	(%)
90×150	3.25(S_R)	3.45(<i>a</i>)	3.55(<i>a</i>)	3.55(<i>a</i>)	3.25(S_R)	3.55(Δ)	3.65(Δ)	3.70(Δ)	0	3	3	4
90×200	4.30(Δ)	4.45(<i>a</i>)	4.55(<i>a</i>)	4.60(<i>a</i>)	4.30(Δ)	4.50(Δ)	4.65(Δ)	4.75(Δ)	0	1	2	3
90×250	5.05(<i>a</i>)	5.10(<i>a</i>)	5.20(<i>a</i>)	5.25(<i>a</i>)	5.15(Δ)	5.45(Δ)	5.60(Δ)	5.65(<i>a'</i>)	2	7	8	8
90×300	5.60(<i>a</i>)	5.65(<i>a</i>)	5.80(<i>a</i>)	5.85(<i>a</i>)	5.95(Δ)	6.05(<i>a'</i>)	6.20(<i>a'</i>)	6.25(<i>a'</i>)	6	7	7	7
90×350	6.10(<i>a</i>)	6.20(<i>a</i>)	6.35(<i>a</i>)	6.40(<i>a</i>)	6.55(<i>a'</i>)	6.60(<i>a'</i>)	6.80(<i>a'</i>)	6.85(<i>a'</i>)	7	6	7	7
90×400	6.60(<i>a</i>)	6.65(<i>a</i>)	6.85(<i>a</i>)	6.90(<i>a</i>)	7.05(<i>a'</i>)	7.10(<i>a'</i>)	7.30(<i>a'</i>)	7.41(<i>a'</i>)	7	7	7	7
90×450	7.10(<i>a</i>)	7.10(<i>a</i>)	7.30(<i>a</i>)	7.40(<i>a</i>)	7.50(<i>a'</i>)	7.60(<i>a'</i>)	7.80(<i>a'</i>)	7.90(<i>a'</i>)	6	7	7	7
90×500	7.45(<i>a</i>)	7.55(<i>a</i>)	7.75(<i>a</i>)	7.85(<i>a</i>)	7.90(<i>a'</i>)	8.05(<i>a'</i>)	8.25(<i>a'</i>)	8.35(<i>a'</i>)	6	7	6	6
								Ave	4	6	6	6

Table 8.3 c) cont.

s = 600 mm													
90×150	2.20(S_R)	3.05(Δ)	3.15(Δ)	3.20(Δ)	2.20(S_R)	3.05(Δ)	3.15(Δ)	3.20(Δ)	0	0	0	0	
90×200	3.10(S_R)	3.90(Δ)	4.05(Δ)	4.15(Δ)	3.10(S_R)	3.90(Δ)	4.05(Δ)	4.15(Δ)	0	0	0	0	
90×250	4.05(S_R)	4.70(Δ)	4.80(a)	4.85(a)	4.05(S_R)	4.70(Δ)	4.85(Δ)	5.00(Δ)	0	0	1	3	
90×300	4.95(S_R)	5.25(a)	5.35(a)	5.40(a)	4.95(S_R)	5.45(Δ)	5.60(Δ)	5.65(a')	0	4	5	5	
90×350	5.65(a)	5.70(a)	5.85(a)	5.90(a)	5.70(Δ)	6.00(a')	6.15(a')	6.20(a')	1	5	5	5	
90×400	6.10(a)	6.15(a)	6.30(a)	6.40(a)	6.35(Δ)	6.45(a')	6.60(a')	6.70(a')	4	5	5	5	
90×450	6.50(a)	6.60(a)	6.75(a)	6.85(a)	6.80(a')	6.90(a')	7.05(a')	7.15(a')	5	5	4	4	
90×500	6.90(a)	7.00(a)	7.15(a)	7.25(a)	7.15(a')	7.30(a')	7.45(a')	7.60(a')	4	4	4	5	
									Ave	2	3	3	3

Table 8.3 Design permissible spans for different profiles (cont.)

d) Engineered joists with OSB webs and C24 timber flanges for $s = 400$ mm and 600 mm

$s = 400$ mm												
C24	Option A				Option B				Option B vs. Option A			
Profile	I-beam	Double I-beam	Box beam	Box I-beam	I-beam	Double I-beam	Box beam	Box I-beam	I-beam	Double I-beam	Box beam	Box I-beam
$B_f \times H$												
(mm)	(m)	(m)	(m)	(m)	(m)	(m)	(m)	(m)	(%)	(%)	(%)	(%)
90×150	3.75(Δ)	3.80(a)	3.95(a)	3.95(a)	3.75(Δ)	3.90(Δ)	4.00(Δ)	4.05(Δ)	0	3	1	3
90×200	4.75(Δ)	4.80(a)	4.90(a)	4.90(a)	4.75(Δ)	5.00(Δ)	5.10(Δ)	5.20(Δ)	0	4	4	6
90×250	5.45(a)	5.45(a)	5.55(a)	5.60(a)	5.65(Δ)	5.85(a')	6.00(a')	6.00(a')	4	7	8	7
90×300	6.05(a)	6.05(a)	6.20(a)	6.20(a)	6.50(Δ)	6.50(a')	6.65(a')	6.65(a')	7	7	7	7
90×350	6.60(a)	6.60(a)	6.75(a)	6.80(a)	7.05(a')	7.10(a')	7.25(a')	7.30(a')	7	8	7	7
90×400	7.10(a)	7.15(a)	7.25(a)	7.35(a)	7.55(a')	7.65(a')	7.80(a')	7.85(a')	6	7	8	7
90×450	7.55(a)	7.60(a)	7.75(a)	7.85(a)	8.05(a')	8.15(a')	8.30(a')	8.40(a')	7	7	7	7
90×500	8.00(a)	8.10(a)	8.25(a)	8.30(a)	8.50(a')	8.60(a')	8.80(a')	8.90(a')	6	6	7	7
								Ave	4	6	6	6

Table 8.3 d) cont.

s = 600 mm													
90×150	3.00(S_R)	3.40(Δ)	3.45(Δ)	3.50(a)	3.00(S_R)	3.40(Δ)	3.45(Δ)	3.55(a')	0	0	0	1	
90×200	4.05(Δ)	4.30(Δ)	4.45(Δ)	4.50(a)	4.05(Δ)	4.30(Δ)	4.45(Δ)	4.50(a')	0	0	0	0	
90×250	4.80(Δ)	5.05(a)	5.15(a)	5.15(a)	4.80(Δ)	5.15(Δ)	5.30(Δ)	5.45(a')	0	2	3	6	
90×300	5.55(Δ)	5.60(a)	5.70(a)	5.75(a)	5.55(Δ)	5.90(a')	6.00(a')	6.05(a')	0	5	5	5	
90×350	6.10(a)	6.15(a)	6.25(a)	6.30(a)	6.25(Δ)	6.45(a')	6.55(a')	6.60(a')	2	5	5	5	
90×400	6.55(a)	6.60(a)	6.75(a)	6.80(a)	6.85(a')	6.90(a')	7.05(a')	7.10(a')	5	5	4	4	
90×450	6.95(a)	7.05(a)	7.20(a)	7.25(a)	7.20(C_∥)	7.40(a')	7.50(a')	7.60(a')	4	5	4	5	
90×500	7.20(a)	7.45(a)	7.60(a)	7.70(a)	7.20(C_∥)	7.80(a')	7.95(a')	8.05(a')	0	5	5	5	
									Ave	1	3	3	4

Table 8.3 Design permissible spans for different profiles (cont.)

e) C16 solid timber joists for $s = 400$ and 600 mm

C16	s = 400 mm			s = 600 mm		
B_f × H	Option A	Option B	Option B vs. Option A	Option A	Option B	Option B vs. Option A
(mm)	(m)	(m)	(%)	(m)	(m)	(%)
50×75	1.45(a)	1.50(Δ)	3	1.30(Δ)	1.30(Δ)	0
50×100	1.95(a)	2.05(Δ)	5	1.75(Δ)	1.75(Δ)	0
50×125	2.45(a)	2.55(Δ)	4	2.20(Δ)	2.20(Δ)	0
50×150	2.95(a)	3.05(Δ)	3	2.65(Δ)	2.65(Δ)	0
50×175	3.45(a)	3.55(Δ)	3	3.10(Δ)	3.10(Δ)	0
50×200	3.95(a)	4.05(Δ)	3	3.55(Δ)	3.55(Δ)	0
50×225	4.45(a)	4.50(Δ)	1	3.95(Δ)	3.95(Δ)	0
Ave			3	Ave		0

f) C24 solid timber joists for $s = 400$ and 600 mm

C24	s = 400 mm			s = 600 mm		
B_f × H	Option A	Option B	Option B vs. Option A	Option A	Option B	Option B vs. Option A
(mm)	(m)	(m)	(%)	(m)	(m)	(%)
50×75	1.65(a)	1.70(Δ)	3	1.45(a)	1.50(Δ)	3
50×100	2.20(a)	2.25(Δ)	2	1.95(a)	2.00(Δ)	3
50×125	2.75(a)	2.85(Δ)	4	2.45(a)	2.45(Δ)	0
50×150	3.30(a)	3.40(Δ)	3	2.95(a)	2.95(Δ)	0
50×175	3.85(a)	3.95(Δ)	3	3.45(a)	3.45(Δ)	0
50×200	4.40(a)	4.50(Δ)	2	3.95(a)	3.95(Δ)	0
50×225	4.80(a)	5.05(Δ)	5	4.45(a)	4.45(Δ)	0
Ave			3	Ave		1

8.4.4. Influence of material variation

The influence of material variation on the permissible span is shown in Table 8.4 where OSB webs and C16 timber flanges are used as the reference materials.

In general, the influence of flange material on the permissible span of the floor joists is greater than that of the web material. Using plywood as web material enhances the permissible span by 5% for the box I-beams made of C16 timber flanges for joist spacings of 400 or 600mm. Using C24 timber for flanges increases the permissible span by 6 to 8% for the multi-webbed beams and by up to 17% for the I-beams. As shown in Tables 8.3(a) and 8.3(c), the permissible span for shallow C16 I-beams at the spacing of 600mm is much lower than that of the double I-beams, since it is governed by rolling shear. Using the C24 timber flanges shifts the governing criteria from ULS to SLS and consequently increases the permissible span significantly. In other words, when the rolling shear is not critical, the use of C24 timber flanges and plywood webs could enhance the permissible span by 7%: see Table 8.4.

8.4.5. Effect of geometric variation

Table 8.5 shows the influence of geometric variations on the permissible span in comparison with the I-beam. A box I-beam configuration with plywood webs and C16 timber flanges results in a 9% increase in the permissible span for beam spacing of 400mm and this rises to 20% when the spacing is increased to 600mm; this is because rolling shear limits the permissible span of the I-beams.

When a C24 box I-beam containing plywood webs is compared with a C16 I-beam containing an OSB web, the box I-beam performs 17% or 29% better for joist spacings of 400 and 600mm respectively. Thus, the combined effect of material and geometrical variability results in up to 29% increase in the permissible span of beams with the same depth. Moreover, if EC5 option B is adopted, then the calculated overall enhancements can reach 25% for a spacing of 400mm and 34% for a spacing of 600 mm.

Table 8.4 Enhancement of permissible span due to material variations

Profiles	s = 400 mm				s = 600 mm			
	Ply vs OSB		C24 vs C16		Ply vs OSB		C24 vs C16	
	C16 flange	C24 flange	OSB web	Plywood web	C16 flange	C24 flange	OSB web	Plywood web
	(%)	(%)	(%)	(%)	(%)	(%)	(%)	(%)
I-beam	2	1	9	7	2	3	16	17
Double I-beam	1	1	8	8	2	1	8	8
Box beam	4	3	7	6	5	4	8	6
Box I-beam	5	4	7	6	5	4	7	6

Table 8.5 Enhancement of permissible span due to geometric variations

	s = 400 mm			s = 600 mm		
	Double I vs I-beam	Box vs I-beam	Box I vs I-beam	Double I vs I-beam	Box vs I-beam	Box I vs I-beam
	(%)	(%)	(%)	(%)	(%)	(%)
C16 flange + OSB web	2	5	5	11	14	16
C16 flange + Plywood web	2	7	9	11	18	20
C24 flange + OSB web	1	3	3	4	6	7
C24 flange + Plywood web	1	5	6	2	7	8

8.4.6. Lateral stability and geometric configurations

In the above calculations, it was assumed that lateral displacement of the compressive edge is prevented throughout its length and torsional rotation is also prevented at its supports. When those conditions are not satisfied, EC5 introduces a factor k_{crit} which takes into account the reduced bending strength due to lateral buckling.

Figures 8.7(a) and 8.7(b) show the relationship between the lateral buckling factor and the beam depth for the various composite beams with spacings of 400 and 600 mm when lateral stability becomes a governing criterion. It is obvious that the lateral buckling factor k_{crit} decreases with the increase in the beam depth for all the geometric configurations. For a given beam depth, there are no significant differences in the values of k_{crit} between the I and the double I-beams and between the box and the box I-beams, which means that an additional web does not greatly influence k_{crit} . However, there is a marked difference between the I-sections (I-beams and double I-beams) and box sections (box-beams and box I-beams), demonstrating that the box sections effectively increase the value of k_{crit} so as to enhance the lateral stability resistance. This is because of the direct relation of k_{crit} to the width of the beams. The magnitude of the difference is about 0.07 for both $s = 400$ and 600mm. In theory, k_{crit} should not be influenced by the joist spacing for a given beam profile and depth; however, the comparison of Figures 8.7(a) and 8.7(b) shows that the value of k_{crit} is slightly lower for a beam spacing of 400mm. This is because k_{crit} is also dependent on the effective span of the beam. Hence, larger joist spacing leads to a shorter effective span, so a slightly lower value of k_{crit} is obtained.

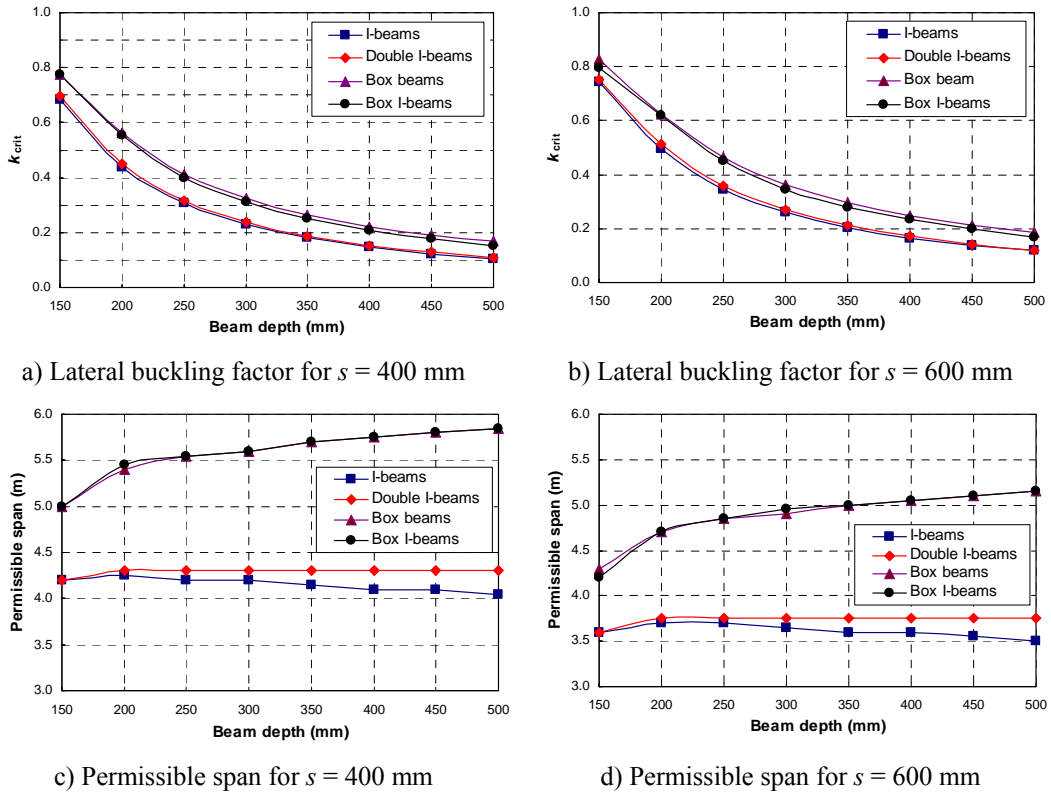


Figure 8.7 Permissible span and lateral buckling factor for engineered joists with C16 timber flanges

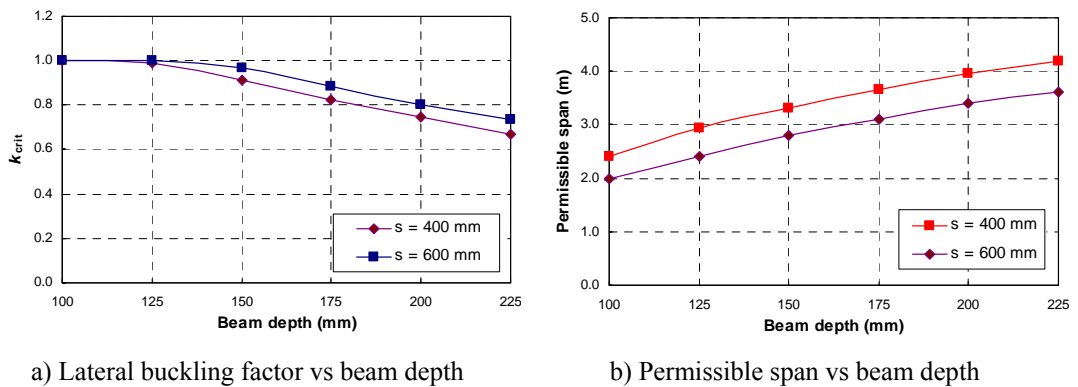


Figure 8.8 Permissible span and lateral buckling factor for C16 solid timber joists

Figures 8.7(c) and 8.7(d) show the relationship between the permissible span and the beam depth for composite beams spaced at 400 and 600mm centres in conditions where the lateral stability is the governing criterion. For I and double I-beams the permissible spans first increase slightly with the beam depth until the depth reaches 200mm. Thereafter, the span gradually decreases with beam depth for the I-beams but remains almost unchanged for the double I-beams. However, in the case of box and box I-beams the permissible spans first increase rapidly with increase in the beam depth until the depth reaches 200mm and thereafter the rate of increase slows down.

The comparison of Figures 8.7(c) and 8.7(d) also shows that as expected, the increase of the joist spacing will reduce the permissible spans for all the engineered beams. The maximum permissible spans for the I-beams, double I-beams, box beams and boxed I-beams are 4.25, 4.30, 5.85 and 5.85 metres respectively, for beams at 400mm centres, and are reduced to 3.70, 3.75, 5.15 and 5.15 metres respectively, when beams are spaced at 600mm centres.

Figure 8.8(a) shows the relationship between the lateral buckling factor and the beam depth for C16 solid timber joists spaced at 400 and 600mm centres. In general, the lateral buckling factor k_{crit} decreases with increase in the beam depth. The smaller joist spacing leads to a lower value of k_{crit} because it corresponds to a longer effective span. The relationships between the permissible span and the beam depth for the solid timber joists at spacing of 400 and 600mm are shown in figure 8.8(b). The permissible span generally increases with the increasing beam depth.

8.5 Beam depth

The main emphasis of this study was on investigating the effect of geometrical and material variability on the permissible span of beams; however, effects of variations in beam depths were also calculated. Permissible span results for I-beams and box I-beams of various depths are given in Table 8.3. A comparison of beam depth with the fixed span length for different profiles and materials, showed that by adopting a box I-beam profile made of Plywood web and with C24 timber flanges instead of an I-beam made of OSB with C16 timber flanges, the beam depth can be reduced by up to 100mm or 20%. For instance, to achieve a span of 7.45m with an I-beam made of

OSB with C16 timber flanges a beam depth of 500mm was required when spacing was 400mm (Table 8.3c), but a longer permissible span of 7.65m can be achieved with a 400mm deep box I-beam made of Plywood webs with C24 timber flanges (Table 8.3 b). In other words, geometrical and material variability of the fixed span length decreases, or increases, the beam depth by up to 20%. This finding could be used in construction of long span flooring systems when available depth of the section is restricted.

8.6 Summary and conclusions

This chapter presented and discussed the results of parametric studies on CIB beams of types double I, box and box I, together with I-beams and solid timber joists. The parametric studies were based on the model which was described in chapter 7. These studies investigated effects of varied geometry and materials on permissible spans of the beam/joists for timber flooring systems. Geometrical variability was considered, by making calculations for different beam cross-sections and for variations in their depth. Material variability was considered, by calculating the effects of two different flange types, C16 and C24, together with the effects of two different web types, F11 Plywood and OSB/3.

The following key points can be noted as the main outcomes of this chapter.

- The parametric study has shown that the requirements for serviceability limit states generally control the design of timber flooring systems. In most cases, for serviceability limit states, the deflection under unit point load governs the permissible spans of the composite beams studied. Using option B in the UK National Annex to EC5 leads to a less conservative permissible span compared to option A.
- Rolling shear and static deflection are the controlling criteria for the shallow I-beams but with increase in depth the unit point load deflection governs the design criteria.
- For the composite beams, adopting option B results in longer permissible spans than option A. The increase in permissible span is 6 to 7% for a spacing of 400mm and 3 to 4% for a spacing of 600mm. Using option B for the solid timber joists at a spacing of 400mm also leads to an increase in the permissible span by 3%.
- Comparison of the permissible spans of the solid timber joists calculated to EC5 with the permissible spans recommended in BS 5268-7.1 shows no significant difference.

- In terms of material variability, the influence of the flange material is more pronounced than that of the web material. The use of a box I-beam instead of an I-beam enhances the permissible span by up to 20%. The combined effects of using C24 timber flanges and plywood webs instead of OSB webs increase the permissible span by up to 29% under option A and 35% when option B of the UK National Annex is used.
- For a fixed span length adopting the different geometrical and material properties can lower the beam's depth up to 20%.

CHAPTER 9: PERFORMANCE OF BEAMS WITH INFILL OF POLYURETHANE (COMPOSITE INSULATED BEAMS, CIB)

9.1 Introduction

In this chapter research is focused on the effects of injected polyurethane on the performance of the composite beams by conducting a comparative study between beams with and without infill. Investigations were conducted to ascertain the effects of injected polyurethane on structural performance, long-term durability, thermal behaviour and dynamic response of beams with various cross sections.

Polyurethane is a thermosetting material that is unlike polystyrene, because polystyrene can be reformed by heating, but polyurethane can only be formed once. Polyurethane belongs to the family of rigid foams, which are known for providing efficient thermal insulation.

Beams were fabricated with different materials, as explained earlier in chapter 3. In stage two of the experimental work, beams were fabricated with F11 Plywood webs and Radiata Pine timber flanges, while in stage 3, beams were fabricated with OSB/3 webs and C16 and C24 timber flanges.

Long-term durability and thermal behaviour were investigated for the beams made in stage 2, while dynamic response was investigated using beams, which were fabricated in stage 3. But structural performance was investigated for both groups. Structural performance of beams with and without infill was examined to determine their bending, shear, and bearing capacities, together with possible effects of web openings. Accelerated ageing methods were used to study the long-term durability of the beams. Thermal transmittance of the beams was evaluated by simulating the horizontal heat flow. Natural frequency and damping ratio were evaluated using dynamic responses of beams and the effect of the support condition on natural frequency was also discussed.

This study shows that foam enhances the bearing capacity of the beams while its effect on bending, shear and stiffness is not significant. The acceptable performance

of the beams with OSB webs proved the suitability of OSB for web construction. Tests on long-term beam durability, showed that the loading capacity of the beam increased, whereas its stiffness decreased during the various weathering cycles. Foam significantly decreases the thermal transmittance of the beam and this has direct relation with overall thickness of the foam, which is sandwiched between the webs. Tests of dynamic response showed that the damping ratio of beams with infill increased in comparison to identical beam profiles without infill, but the effect of foam on the natural frequency of the beams is not significant.

9.2 Effect of the infill on structural performance

9.2.1 Bearing capacity and infill materials

The average bearing capacities of various profiles with and without infill material are given in Table 9.1. Comparing the two similar profiles with and without infill shows that there are 18 to 30% enhancements in bearing capacity depending on the profile.

Failure mode could explain this enhancement as reported in Chapter 7 and Bahadori et al., 2006. Bearing failure began with web buckling and tensional failure in the flange. Infill material improves the buckling resistance of the webs, which consequently enhances the bearing capacity of the profile. As a result CIBs can be fabricated without using any stiffeners or straps such as those used in traditional box beams to enhance the bearing capacity of each beam (Figure 9.1). A typical bearing failure of a Box I-beam with infill is illustrated in Figure 9.2.

Table 9.1 - Average maximum bearing capacity of the different designs with and without infill material.

Profiles	Bearing capacity test						
	No foam			foam			Enhancem ent (%)
	AVE (kN)	StD	C _v (%)	AVE (kN)	StD	C _v (%)	
I-Beam	25.91	4.94	19.07	---	---	---	---
Double I-Beam	49.35	6.52	13.20	63.69	2.17	3.41	29.06
Recessed beam	27.57	2.68	9.71	32.59	7.99	24.51	18.21
Box beam	31.86	6.28	19.69	39.97	9.57	23.94	25.43
Boxed I-Beam	53.61	6.51	12.15	68.94	14.78	21.44	28.61
Boxed double I-Beam	74.84	9.67	12.92	97.83	10.41	10.64	30.71
LVL I-Beam	26.44	3.31	12.51	---	---	---	---
LVL Double I-Beam	45.80	5.17	11.29	58.78	4.75	8.08	28.34
LVL Boxed I-Beam	62.23	6.60	10.61	79.81	16.85	21.12	28.25

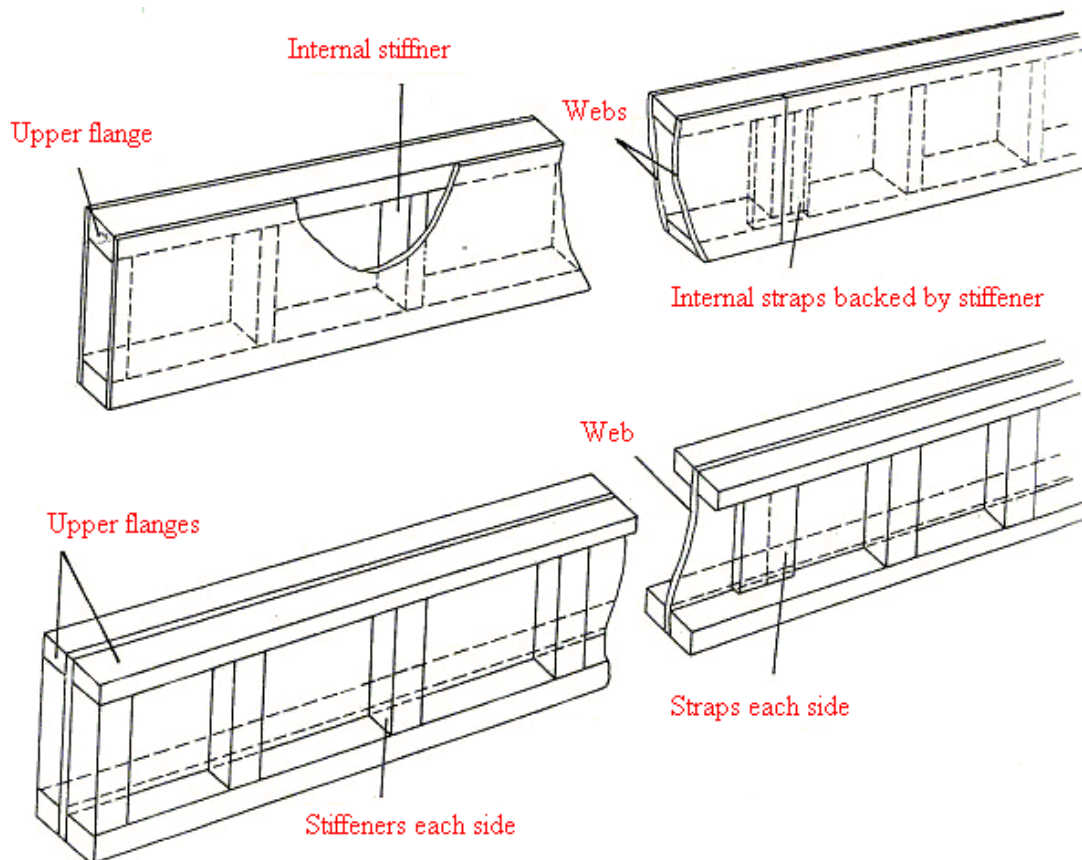


Figure 9.1 Traditional box and I-beams

(Reproduced from Mettem 1986)



Figure 9.2 Filled box I-beam before and after compression test

9.2.2 Infill material and stiffness

Three point bending tests were conducted on each beam before and after polyurethane injection and load-deflection results were recorded to ascertain the effect of the filling material on overall stiffness of the beam. Table B.1 in Appendix B presents the load-deflection results for the beam (K) over spans of 4500, 3000, 2100 and 1450mm.

NF and F subscripts mean no foam and foam respectively and the subsequent number shows the span length. For instance, $K_{NF,4500}$ means stiffness of the beam without foam over a span of 4500mm. As shown in Table B.1 in Appendix B infill material enhances the beam stiffness, but improvements vary from 1% to 10%. Variations in foam density could explain these results. Chapter 3 demonstrated that foam density has an inverse relation to distance between the webs and it varied from 53.67kg/m^3 for double I-beams to 35.22kg/m^3 for box beams. Foam density has a direct relation to its mechanical properties such as Young modulus, tensile, compressive and shear strength (Davies, 2001 & Oertel, 1996), therefore variation of the foam density results in variation of overall stiffness. The overall volume of foam effects stiffness, but that varies for different profiles and causes part of the variation of stiffness.

Results for the LVL double I-beam with and without infill are presented in Table 9.2. Comparison of results shows that infill material enhances the stiffness by a maximum of 4% (Table 9.2). From the results recorded in Tables 9.2 and D.1 in Appendix B it can be concluded that foam has a positive, but not significant, effect on overall stiffness of the beam and due to the variable nature of space and density of foam it is difficult to predict the amount of enhancement.

Table 9.2 Effect of infill on load deflection of the long span beams with LVL flanges

LVL Double I-beam	Long LVL Double I-beam without infill (No foam)				
	ID:347	ID:348	AVE	SD	C _v (%)
k_{NF,4500} (kN/mm)	0.528	0.574	0.55	0.03	5.90
k_{NF,3000} (kN/mm)	1.424	1.471	1.45	0.03	2.30
k_{NF,2100} (kN/mm)	3.124	3.104	3.11	0.01	0.45
k_{NF,1450} (kN/mm)	6.166	5.953	6.06	0.15	2.49
	Long LVL Double I-beam with infill (Foam)				
	ID:347	ID:348	AVE	SD	C _v (%)
k_{F,4500} (kN/mm)	0.553	0.556	0.55	0.00	0.38
k_{F,3000} (kN/mm)	1.502	1.509	1.51	0.00	0.33
k_{F,2100} (kN/mm)	3.266	3.141	3.20	0.09	2.76
k_{F,1450} (kN/mm)	6.437	6.113	6.28	0.23	3.65
Effect of the foam on load/deflection (k)					
k_{F,4500}/k_{NF,4500}	1.05	0.97	1.01	0.06	5.52
k_{F,3000}/k_{NF,3000}	1.05	1.03	1.04	0.02	1.97
k_{F,2100}/k_{NF,2100}	1.05	1.01	1.03	0.02	2.31
k_{F,1450}/k_{NF,1450}	1.04	1.03	1.04	0.01	1.17

The average result of the destructive tests for the empty and filled long span beam when tested under a four point bending are given in Table 9.3. Beams with infill typically show flexural failure patterns similar to those shown by the empty beams and in some cases neither could reach their maximum bending capacity as immature failure occurred in the knot area as explained in chapter 5. Nevertheless, by comparing unfilled and filled beams it could be concluded that the effect of the infill material on enhancement of the bending capacity is not significant.

Table 9.3 Result of destructive tests for beams of 4.35m span

Bending tests-long beam without infill								
Profile	I-beam	Double I-beam	Recess beam	Box beam	Box I-beam	Box Double I-beam	LVL Double I-beam	LVL Box I-beam
P_{max} (kN)	20.92	29.03	32.88	30.24	37.14	38.20	39.45	59.82
Δ_{max} (mm)	43.07	44.49	48.76	43.72	44.25	40.93	60.00	78.46
K_{4PNF} (kN/mm)	0.56	0.67	0.72	0.73	0.89	0.89	0.72	0.83
Bending tests-long beam with infill								
P_{max} (kN)	---	35.39	27.52	42.96	43.42	49.94	44.47	---
Δ_{max} (mm)	---	49.49	38.85	63.42	52.92	54.14	66.10	---
K_{4PF} (kN/mm)	---	0.76	0.72	0.75	0.88	0.93	0.68	---

9.2.3 Effect of a web opening in beams with and without infill

Empty and filled beams with circular web opening diameters of 0, 76, 102 and 152 mm were tested under a four point bending rig (Figure 9.3). For each profile twelve beams were tested. They were divided into four groups of three members and then loaded to destruction. The first group had no web opening, the second group had a web opening of 76mm, the third group had a web opening of 102mm and the last group had a web opening of 152mm.

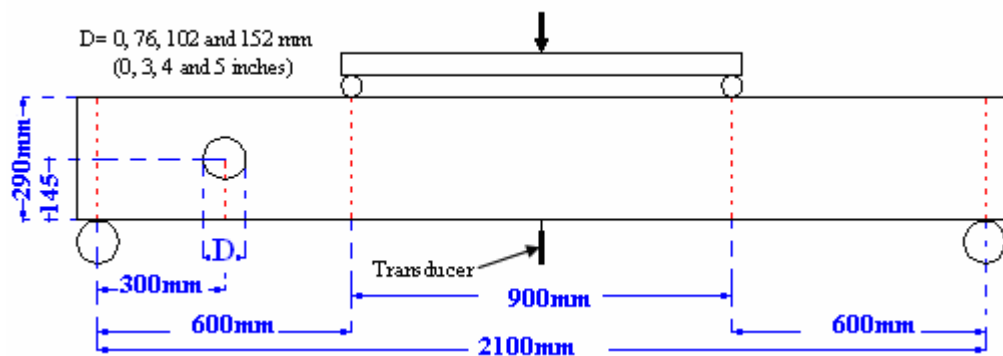


Figure 9.3 Test arrangement for measuring maximum loading capacity of the beams

The comparison of beams with and without infill shows that injecting the infill material enhances the stiffness and maximum loading capacity of beams with a web opening (Table 9.4). Experimental tests show that failure began from the web opening for both empty and filled beams (Figure 9.4), therefore the enhanced stiffness and loading capacity are due to the contribution of the foam to shear and tensile stress of the web.

When the circular web opening on the beam was created, it caused concentration of stress in the mid-point of each quarter as shown in the finite element model in Figure 9.5. A double I-beam with web opening of 152mm and under unit load of 1kN is presented in Figure 9.6. Elastic analysis shows that maximum principle stress occurred at the mid-point of the first and third quarters of the circular opening, which are the points where failure began in experimental work (Figure 9.4). Minimum principle stress occurring at mid-points of the second and fourth quarters.

Table 9.4 Effect of infill on performance of beams with various sizes of web opening

PROFILES / HOLE SIZES	Hole size (H.S) 0, 76, 102 and 152 mm								
		H.S=0 (mm)	C _v (%)	H.S=76(mm)	C _v (%)	H.S= 102 (mm)	C _v (%)	H.S= 152 (mm)	C _v (%)
	Without foam								
Double I-beam	P_{max} (kN)	62.83	12.66	56.77	19.59	56.94	16.72	50.66	50.66
	Δ_{max} (mm)	18.30	6.40	16.03	13.83	16.03	11.17	16.39	16.39
	K (kN/mm)	4.57	20.44	4.25	17.63	4.17	15.19	3.83	3.83
	With foam								
Double I-beam	P_{max} (kN)	62.08	3.84	62.40	2.81	---	---	45.73	4.25
	Δ_{max} (mm)	24.54	25.32	21.07	3.89	---	---	12.92	9.78
	K (kN/mm)	4.25	14.86	3.73	1.06	---	---	4.19	10.89
	Without foam								
Recessed beam	P_{max} (kN)	59.23	4.94	54.65	4.99	48.42	3.82	44.14	44.14
	Δ_{max} (mm)	18.16	29.34	17.42	18.69	13.93	10.94	14.03	14.03
	K (kN/mm)	4.27	14.53	3.89	20.32	3.93	6.18	3.72	3.72
	With foam								
Recessed beam	P_{max} (kN)	61.86	10.61	66.44	0.41	56.21	1.90	52.16	4.64
	Δ_{max} (mm)	19.45	19.09	19.18	0.29	16.99	14.71	15.40	7.10
	K (kN/mm)	4.02	20.99	4.51	0.08	4.17	11.25	4.02	4.65

Table 9.4 Effect of infill on performance of beams with various sizes of web opening (Continued)

PROFILES / HOLE SIZES	Hole size (H.S) 0, 76, 102 and 152 mm								
		H.S=0 (mm)	C _v (%)	H.S=76(mm)	C _v (%)	H.S= 102 (mm)	C _v (%)	H.S= 152 (mm)	C _v (%)
	Without foam								
Box I-beam	P_{max} (kN)	82.41	18.39	81.43	10.11	65.59	18.57	67.36	67.36
	Δ_{max} (mm)	20.11	23.87	20.12	15.34	16.61	13.64	16.39	16.39
	K (kN/mm)	5.51	16.86	5.57	14.48	5.18	12.70	4.99	4.99
	With foam								
Box I-beam	P_{max} (kN)	95.99	4.03	---	---	---	---	74.42	4.98
	Δ_{max} (mm)	24.24	15.77	---	---	---	---	18.25	20.85
	K (kN/mm)	5.39	14.07	---	---	---	---	5.48	7.37

Table 9.4 Effect of infill on performance of beams with various sizes of web opening (Continued)

PROFILES / HOLE SIZES	Hole size (H.S) 0, 76, 102 and 152 mm								
		H.S=0 (mm)	C _v (%)	H.S=76(mm)	C _v (%)	H.S= 102 (mm)	C _v (%)	H.S= 152 (mm)	C _v (%)
	Without foam								
LVL double I- beam	P _{max} (kN)	66.66	7.34	---	---	---	---	---	---
	Δ _{max} (mm)	22.24	21.62	---	---	---	---	---	---
	K (kN/mm)	4.23	7.09	---	---	---	---	---	---
	With foam								
LVL double I-beam	P _{max} (kN)	69.87	6.27	64.95	2.54	50.77	14.89	53.64	0.76
	Δ _{max} (mm)	25.56	22.10	20.40	1.74	15.07	18.12	17.26	13.70
	K (kN/mm)	4.63	5.05	4.17	0.21	3.88	4.96	4.01	3.29
	Without foam								
LVL Box I-beam	P _{max} (kN)	90.82	1.78	---	---	---	---	---	---
	Δ _{max} (mm)	25.08	8.93	---	---	---	---	---	---
	K (kN/mm)	4.56	9.80	---	---	---	---	---	---
	With foam								
LVL Box I- beam	P _{max} (kN)	98.07	3.11	---	---	---	---	70.47	6.33
	Δ _{max} (mm)	21.36	12.17	---	---	---	---	18.97	13.43
	K (kN/mm)	6.29	10.43	---	---	---	---	5.66	8.47



a) Double I-beam with 76mm web opening



b) Double I-beam with 102 mm web opening



c) Double I-beam with 152 mm web opening



d) Filled LVL Double I-beam with web opening of 76mm



e) Filled LVL Double I-beam with web opening of 76 mm



f) Filled LVL Double I-beam with web opening of 102 mm

Figure 9.4 Mode of failure in the double I-beam with various sizes of web opening

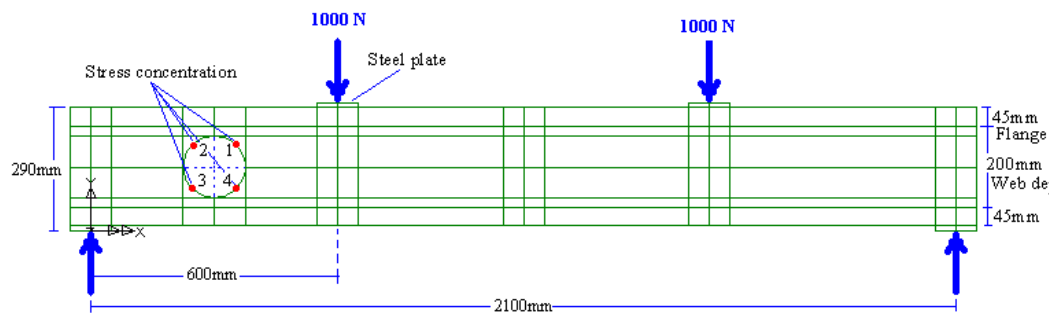
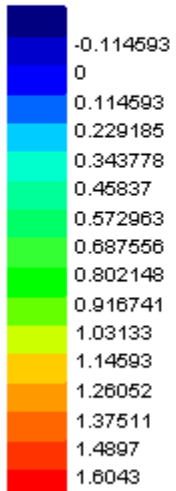


Figure 9.5 Modelling the beam

LOAD CASE = 1
Loadcase 1
RESULTS FILE = 1
STRESS
CONTOURS OF SMax



Max 1.626 at Node 4733
Min -0.2070 at Node 66

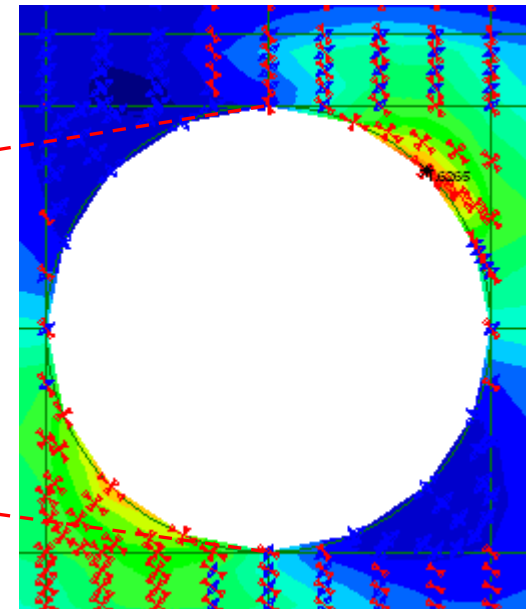
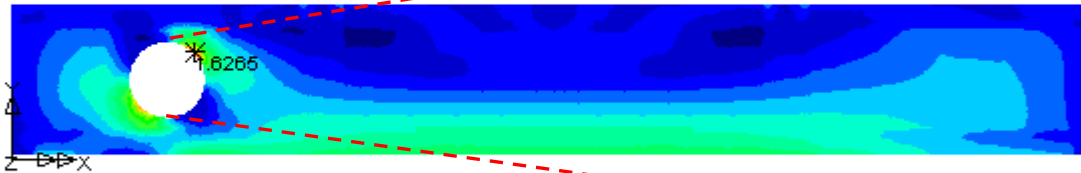


Figure 9.6 Maximum principal stresses in an empty double I-beam with 152mm web opening.
Red and blue arrows show the tension and compression vectors

9.3 Durability

Durability is defined as the maintenance of satisfactory functional, aesthetic and economic performance for the design life of a product. In structural engineering, durability is often examined by assessing the product performance under harsh weathering conditions over a short period. This accelerated aging method is used to magnify the environmental loads on the product of interest and then results are extrapolated to predict the lifespan of the product. The acceleration factor is the ratio between the test period needed to create material failure and the normal time until failure occurs and service would be required, therefore the theoretical design life of the material can be obtained by multiplying the exposure time until material failure by the acceleration factor (ASTM E632, 1996).

Even though such information would be very useful for predicting the durability of CIBs there are reservations about this method (Ratay, 2005).

1. The accelerated aging method may not consider effects of all the environmental factors such as pollution or biological attack.
2. The failure criteria are not defined in the standard testing procedures.
3. There is no agreement on the true value of the acceleration factor in industry.

ASTM E632, 1996 also describes how the reliable accelerated ageing method could be correlated with the laboratory test results by observing conditions in the field, or by exposing samples to the normal weathering situation where they are to be used. In addition, as it is mentioned in Chapter 4, there are no current standard testing procedures to evaluate durability of most construction materials. Therefore the testing procedures described in this thesis are based on a combination of personal experience and methods described in the published literature.

9.3.1 Durability testing procedures

In this study experiments were conducted on empty box beams and on others injected with polyurethane so that comparative performance could be assessed. The aim was to identify any effect of the foam on long term performance of the beams. The box beams 300mm deep, 106mm wide and 2.1m long were exposed to cyclic series of simulated extreme weathering conditions. As described in chapter 4, the accelerated

ageing procedure for the beams involved six cycles each comprising the following harsh environmental stages:

7. Immersion in a treatment tank in hot water (50 ° C) for one hour
8. Transference to the steam room, for 3 hours steaming at 100 ° C.
9. Storage in freezer at -20 ° C for 20 hours
10. Taken to kiln for 3 hours heating at 100 ° C
11. Steaming for another 3 hours at 100 ° C
12. Drying in the kiln at 100 ° C for 18 hours

Twelve empty and twelve filled box beams were exposed to severe weathering conditions. These beams were divided into four groups each having three members. As described in chapter 3, the beams were fabricated so that components with variant Young modulus values were distributed evenly among each groups. Thus the four groups of filled box beams are comparable with each other and those of the empty beams.

9.3.2 Discussion of durability results

A group of beams were loaded to destruction using a four point bending test rig in cycle 0, before they were exposed to weathering conditions so that control values were established. One of the other groups was then tested to destruction after the end of cycle 2, another after cycle 4 and the last after cycle 6 (Figure 9.7). Then the values for maximum loading capacity, P_{max} , deflection at maximum load, Δ_{max} and load over deflection value, k for each beam were recorded. Test results for the empty and filled beams are given in Tables 9.5(a) and 9.5(b) respectively. In those tables load over deflection, k , has a subscript of C which stands for cycle and is followed by the numbers 0, 2, 4 or 6 which stand for cycle number. For instance k_{C2} stands for load over deflection value at the end of cycle 2. As explained earlier in chapter 4, stiffness is proportional to load/ deflection value, therefore the value k could be considered to reflect stiffness. The load/ deflection ratio, or stiffness ratio, is another value which is presented in Tables 9.5(a) and 9.5(b). For instance k_{C2}/k_{C0} gives the stiffness ratio between cycle 2 and 0. This value could show reduction of stiffness between cycle 2 and cycle 0. Load/ deflection performance figures for the empty and filled beams are shown in Figure 9.8. The left side of the figure presents load-

deflection performance of the empty beams for cycles 0, 2, 4 and 6 whereas the right side shows the load-deflection graphs for the same cycles, but for the filled beams.

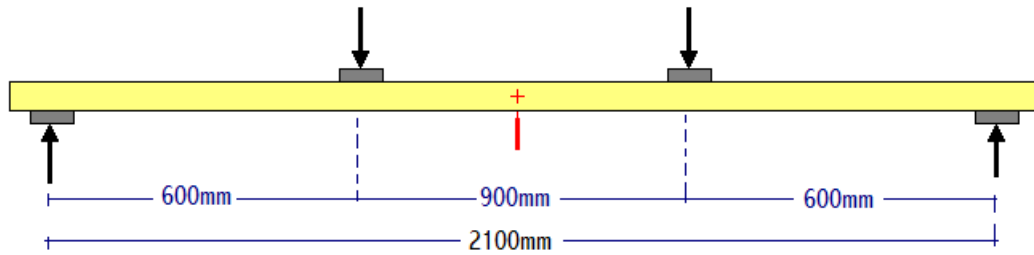


Figure 9.7 Measuring load deflection and shear capacity of short beam under four point bending

Table.9.5 Effect of the accelerated ageing method on structural performance of the box beams

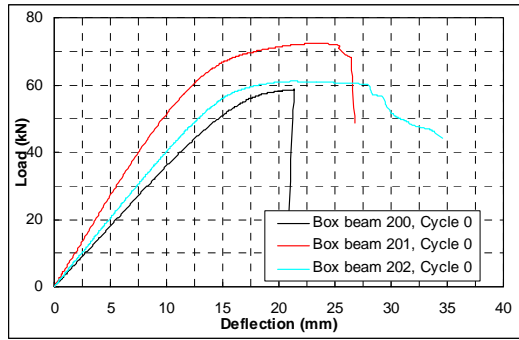
a) Without infill (empty)

Without infill (No foam)							
Box beam	Parameters for each beam				AVE	StD	C _v (%)
		I	II	III			
Cycle 0	P _{max,C0} (kN)	58.81	72.33	61.06	64.07	7.24	11.31
	Δ _{max,C0} (mm)	21.31	23.67	21.44	22.14	1.33	5.99
	K _{C0} (kN/mm)	3.612	5.418	4.07	4.37	0.94	21.50
Cycle 2	P _{max,C2} (kN)	---	51.82	55.08	53.45	2.31	4.31
	Δ _{max,C2} (mm)	---	12.75	26.87	19.81	9.98	50.40
	K _{C2} (kN/mm)	---	5.517	3.623	4.57	1.34	29.31
	P _{max,C2} / P _{max,C0}	---	0.72	0.90	0.83	0.13	15.73
	K _{C2} / K _{C0}	---	1.02	0.89	1.05	0.09	8.66
Cycle 4	P _{max,C4} (kN)	48.26	51.3	48.13	49.23	1.79	3.64
	Δ _{max,C4} (mm)	13.21	20.71	14.82	16.25	3.95	24.30
	K _{C4} (kN/mm)	4.971	4.025	5.186	4.73	0.62	13.07
	P _{max,C4} / P _{max,C0}	0.82	0.71	0.79	0.77	0.06	7.41
	K _{C4} / K _{C0}	1.38	0.74	1.27	1.13	0.34	30.06
Cycle 6	P _{max,C6} (kN)	41.8	39.26	32.85	37.97	4.61	12.15
	Δ _{max,C6} (mm)	14.71	10.94	7.4	11.02	3.66	33.18
	K _{C6} (kN/mm)	3.572	5.208	4.768	4.52	0.85	18.75
	P _{max,C6} / P _{max,C0}	0.71	0.54	0.54	0.60	0.10	16.48
	K _{C6} / K _{C0}	0.99	0.96	1.17	1.04	0.11	10.98

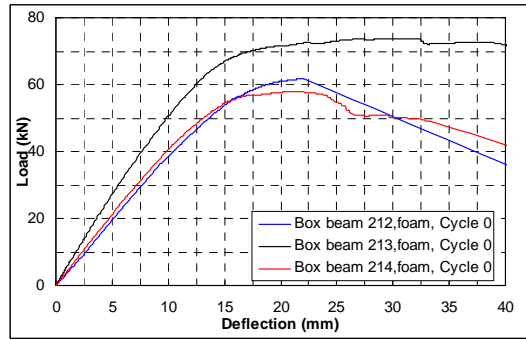
Table.9.5 Effect of the accelerated ageing method on structural performance of the box beams

b) With infill (filled)

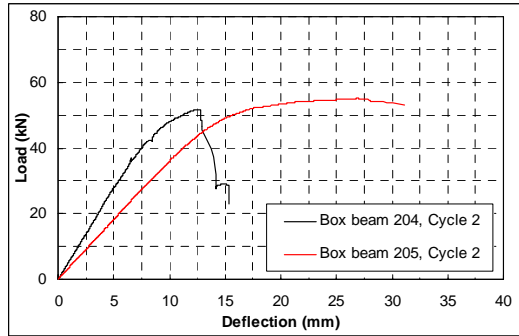
With infill (Foam)							
Box beam	Parameters for each beam			AVE	SD	C _v (%)	
		I	II				III
Cycle 0	P _{max,C0} (kN)	61.67	73.8	57.82	64.43	8.34	12.94
	Δ _{max,C0} (mm)	24.07	26.96	21.24	24.09	2.86	11.87
	K _{C0} (kN/mm)	3.37	5.603	4.251	4.41	1.12	25.52
Cycle 2	P _{max,C2} (kN)	51.64	60.2	49.12	53.65	5.81	10.82
	Δ _{max,C2} (mm)	22.65	23.35	22.66	22.89	0.40	1.75
	K _{C2} (kN/mm)	4.587	4.458	3.275	4.11	0.72	17.61
	P _{max,C2} / P _{max,C0}	0.84	0.82	0.85	0.83	0.02	2.05
Cycle 4	K _{C2} / K _{C0}	1.36	0.80	0.77	0.98	0.33	34.23
	P _{max,C4} (kN)	52.3	48.07	53.28	51.22	2.77	5.41
	Δ _{max,C4} (mm)	27.57	19.8	18.88	22.08	4.77	21.62
	K _{C4} (kN/mm)	3.334	3.675	4.574	3.86	0.64	16.59
	P _{max,C4} / P _{max,C0}	0.85	0.65	0.92	0.81	0.14	17.31
Cycle 6	K _{C4} / K _{C0}	0.99	0.66	1.08	0.91	0.22	24.45
	P _{max,C6} (kN)	47.72	46.12	47.17	47.00	0.81	1.73
	Δ _{max,C6} (mm)	24.83	25.32	23.26	24.47	1.08	4.40
	K _{C6} (kN/mm)	3.216	3.09	3.246	3.18	0.08	2.60
	P _{max,C6} / P _{max,C0}	0.77	0.62	0.82	0.74	0.10	13.59
	K _{C6} / K _{C0}	0.95	0.55	0.76	0.76	0.20	26.64



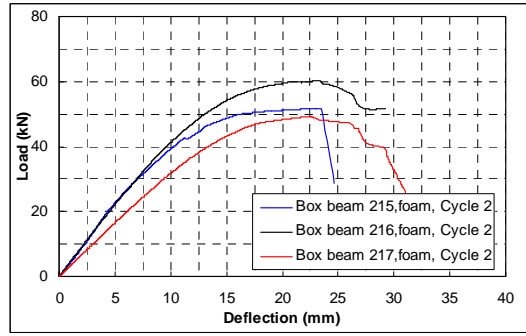
a) Box beam, without foam, cycle 0



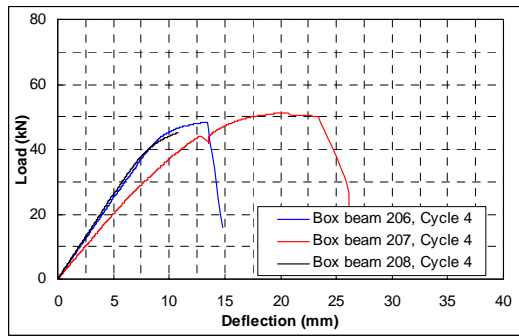
b) Box beam, with foam, cycle 0



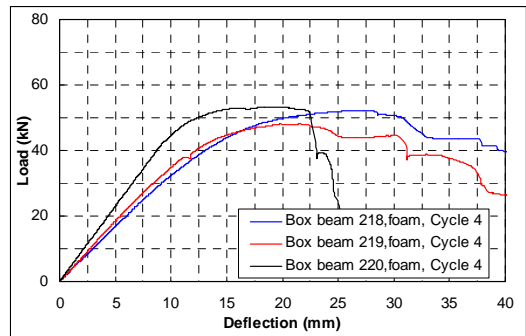
c) Box beam, without foam, cycle 2



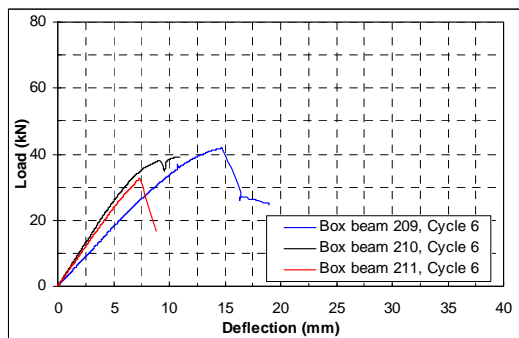
d) Box beam, with foam, cycle 2



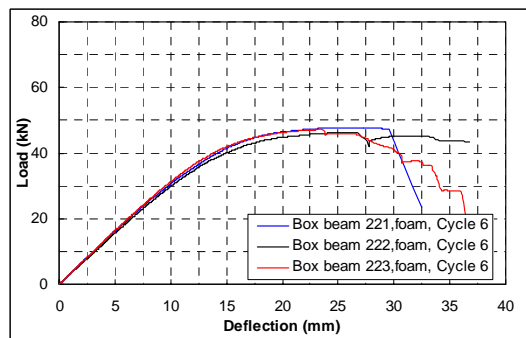
e) Box beam, without foam, cycle 4



f) Box beam, with foam, cycle 4



g) Box beam, without foam, cycle 6



h) Box beam, with foam, cycle 6

Figure 9.8 Comparing the load deflection of the box beams without and with foam at the end of different cycles

Table 9.6 Average results for the beams without and with infill

Parameters	Cycle	0	2	4	6
k(kN/mm)	No foam	4.37	4.57	4.73	4.52
	Foam	4.41	4.11	3.86	3.18
P_{max}(kN)	No foam	64.07	53.45	49.25	37.97
	Foam	64.43	53.65	51.22	47.00
	Ratio	C0/C0	C2/C0	C4/C0	C6/C0
k_{ratio}	No foam	1	1.05	1.13	1.04
	Foam	1	0.98	0.91	0.76
P_{ratio}	No foam	1	0.83	0.77	0.60
	Foam	1	0.83	0.81	0.74

In order to compare the durability performance of the empty and filled beams, average results from Tables 9.5(a) and 9.5(b) are presented in Table 9.6 above. The value of k for the beams without infill increased in cycles 2, 4 and 6 relative to the value in cycle 0, whereas the reverse trend can be seen for the beams with infill as the value of k decreased in cycles 2, 4 and 6 in comparison to their value in cycle 0. The value of P_{max} decreased for both empty and filled beams, but the reduction is more pronounced for the beams without infill. The percentage of enhancement or reduction for the k and P of empty or filled beams can be found from the k_{ratio} and P_{ratio} in Table 9.6. For the beams without infill there is 5%, 13% and 4% increase of stiffness by cycles 2, 4 and 6 respectively compared to their value in cycle 0. In contrast, for filled beams there is only 2%, 9% and 24% reduction of stiffness compared to their values in cycle 0. In terms of maximum loading capacity, beams without infill show 17%, 23% and 40% reduction by cycles 2, 4 and 6 in comparison to their values in cycle 0. Filled beams respond better than empty ones because their maximum loading capacities reduce by 17%, 19% and 26% at the end of cycles 2, 4 and 6.

Chapter 8 described how ultimate limit states criteria are needed to prevent loss of life and structural system collapse, whereas serviceability limit states are related to conditions of normal use and concern the functioning of structures or structural members, the comfort of people, the appearance and longevity of structures. The experimental results demonstrate that the filled beams perform well by carrying more load than unfilled ones under ultimate limit state criteria, but their performance under serviceability limit state criteria is poorer for stiffness decreases. This pattern is reversed for the beams without infill. Beams without infill perform better in terms of

serviceability limit state criteria, but their performance decreases under ultimate limit states criteria.

9.3.2.1 Explanation of different durability performance

As previously described, all the beams were exposed to similar testing procedures but the empty and filled types performed differently. The moisture content of the beams before and after testing, taken together with infill characteristics, could explain the differences in performance. Polyurethane foam is water permeable and absorbs low amounts of water. Moisture migrates through the foam and eventually reaches interfaces with the plywood webs and timber flanges. Moisture, once absorbed by Plywood/ timber, affects the overall stiffness of the beams. The more moisture absorbed, the more reduction in stiffness occurs.

The moisture content of the top and bottom flanges on the beams before and after the durability test is shown in Table 9.7. Reduction and increase of moisture content for the empty and filled beams was calculated from the average moisture content of the top and bottom flanges before and after durability tests (Table 9.8). That table shows moisture content of beams without infill reduces by 3.80%, 19.52 % and 23.90 % at the end of cycles 2, 4 and 6 respectively. Therefore the better performance in stiffness for the beams without infill can be explained knowing the reverse relation between moisture content and stiffness. Similarly, decrease of stiffness for the beams with infill is explained as moisture content of those beams at the end of cycles 2, 4 and 6 is raised by 96.07%, 67.72% and 108.10% respectively.

9.3.2.2 Explanation of reduction in ultimate load capacity

Figures 9.9 and 9.10 show the mode of failure in empty and filled box beams. The combination of absorbed moisture together with temperature fluctuations caused cracking on timber flanges and plywood webs. However, there was no de-lamination at either flange to web connections or between plywood veneers. It seems that components of the beams are weakened at the end of each cycle and naturally this is reflected in their decreased loading capacity. However, the weakening effect of the cycles is less pronounced on the beam with infill because one side of each beam is protected by the foam unlike the beams without infill where their components are exposed to weathering conditions from inside and outside.

Table 9.7 Moisture content of the box beam before and after testing

Beams without infill materials							
		Top flanges			Bottom flanges		
	Beam No	Density kg/m³	Moisture content		Density kg/m³	Moisture content	
			Before test AVE (%)	After test AVE (%)		Before test AVE (%)	After test AVE (%)
Cycle 0	200	404.24	11.53	13.85	368.14	11.97	14.00
	201	480.79	12.80	12.03	528.49	12.57	11.27
	202	391.68	12.77	13.64	419.83	11.67	13.29
AVE		425.57	12.37	13.17	438.82	12.07	12.85
Cycle 2	203	419.76	10.77	8.04	424.17	12.20	8.00
	204	548.36	12.43	7.95	569.68	12.80	19.71
	205	494.89	13.07	14.11	530.90	11.43	12.13
AVE		487.67	12.09	10.03	508.25	12.14	13.28
Cycle 4	206	476.91	12.17	10.71	495.41	12.60	10.41
	207	516.50	12.07	11.29	445.46	13.37	8.76
	208	542.77	11.40	11.73	448.15	12.77	6.96
AVE		512.06	11.88	11.24	463.01	12.91	8.71
Cycle 6	209	455.31	11.50	6.64	417.09	12.17	12.63
	210	475.08	12.07	9.14	456.04	11.63	5.83
	211	497.74	13.03	8.49	498.86	11.77	12.20
AVE		476.04	12.20	8.09	457.33	11.86	10.22
Beams with infill materials							
Cycle 0	212	445.40	12.20	12.19	365.94	11.47	12.76
	213	440.74	12.40	12.78	371.52	13.70	12.88
	214	525.83	12.10	10.58	423.92	10.93	13.24
AVE		470.66	12.23	11.85	387.12	12.03	12.96
Cycle 2	215	418.95	11.30	25.34	435.61	8.73	16.12
	216	524.45	12.07	16.25	532.88	12.03	13.64
	217	512.23	12.53	25.74	505.17	9.67	32.93
AVE		485.21	11.97	22.44	491.22	10.14	20.90
Cycle 4	218	539.33	11.33	18.98	640.72	13.17	17.39
	219	478.35	11.87	19.25	505.37	9.73	19.35
	220	478.44	11.53	17.53	539.60	11.97	24.21
AVE		498.71	11.58	18.59	561.90	11.62	20.32
Cycle 6	221	506.31	11.40	22.96	480.52	12.13	25.40
	222	536.38	11.20	23.20	490.58	12.67	28.99
	223	495.48	11.43	30.18	515.06	11.90	16.40
AVE		512.73	11.34	25.45	495.39	12.23	23.60

Table 9.8 Average moisture content and percentage difference before and after the durability tests.

		Beams without foam					
		Cycle	0	2	4	6	
Moisture content	Before test (%)		12.22	12.12	12.40	12.03	
	After test (%)		13.01	11.66	9.98	9.16	
	Reduction (%)		6.46	-3.80	-19.52	-23.90	
	Beams with foam						
			Cycle	0	2	4	6
	Before test (%)		12.13	11.06	11.60	11.79	
	After test (%)		12.41	21.67	19.46	24.53	
Increase (%)		2.27	96.02	67.72	108.10		



Figure 9.9 Box beam failed under four point bending test after exposure to 6 cycles of accelerated weathering conditions.



Figure 9.10 Box beam with infill is failed under four point bending after exposure to 6 accelerated weathering cycles

9.4 Thermal performance CIBs

Building energy consumption accounts for 45% of all energy consumed in the UK (Nicholls, 2002) and that fact highlights the importance of low energy designs in buildings. Reducing building energy consumption will protect the environment, produce better buildings and cut costs.

Adoption of appropriate new construction materials, such as polyurethane filled CIBs, should reduce the amount of the heat loss thus contributing to low energy designs. Perhaps the main advantage of injected polyurethane is its low thermal conductivity, $0.022\text{W/m}^2\text{K}^\circ$ on average, which should reduce heat loss through the beams and prevent cold bridge formation between the internal and external volumes.

9.4.1 Thermal transmittance

In order to investigate effect of the injected polyurethane on thermal properties of the CIB beams, the thermal transmittance, or U value, for the empty and filled beams was measured. The U value is a measure of the speed with which heat is moved through one square meter of the specimen with 1 K temperature difference across its faces: see Equation 9.1 (Graves and Zarr, 1997)

$$U_s = \frac{Q_s}{A_s(t_H - t_C)} \quad \text{Equation 9.1}$$

Where -

U_s : Thermal transmittance $\text{W/m}^2\text{K}$

Q_s : Heat flow through the test specimen, Watts, W

A_s : the projected area of the test specimen m^2

t_H : Warm side air temperature Kelvin, K

t_C : Cold side air temperature K

The U value of the specimen can be calculated from equation 9.2 where R_t is the thermal resistance of specimen $\text{m}^2\text{K/W}$.

$$U = \frac{1}{R_t} \quad \text{Equation 9.2}$$

Thermal resistance of the specimen can be calculated as

$$R_t = \frac{t}{k_c} \quad \text{Equation 9.3}$$

Where

t is the thickness of the material (m)

k_c is the thermal conductivity of the specimen (W/m K)

Cymap software was used to evaluate the thermal transmittance, U, of different beam cross-sections when empty and filled (Cymap, 2006). In principle, this software calculates the thermal resistance of each individual component and then combines them together to calculate the overall thermal resistance and thermal transmittance of a section.

This comparative study applied for weather conditions in Edinburgh as reported by BBC Weather, 2006 which recorded:

- Minimum average temperature outdoors is +1° c
- Average relative humidity outdoors during the year is 80 %

The following assumptions were also made:

- Indoor average temperature is +21° c
- Average indoor relative humidity during the year is 50%
- The gap between the webs for the beams without infill was defined as unventilated air, which means there is no express provision for air flow through beams (BSEN ISO 6946:1996).

The dimensions of the beam cross-section were chosen to be similar to the dimensions of fabricated beams which are shown in Figure 3.3 in Chapter 3.

Figures 9.11 and 9.12 present typical results for the U values of empty and filled box I-beams calculated by Cymap software. In addition, values of thermal transmittance, U, for the various beam cross-sections are summarised in Table 9.9. Symbols U_{NF} and U_F in Table 9.9 are defined as thermal transmittance without foam and with foam respectively.

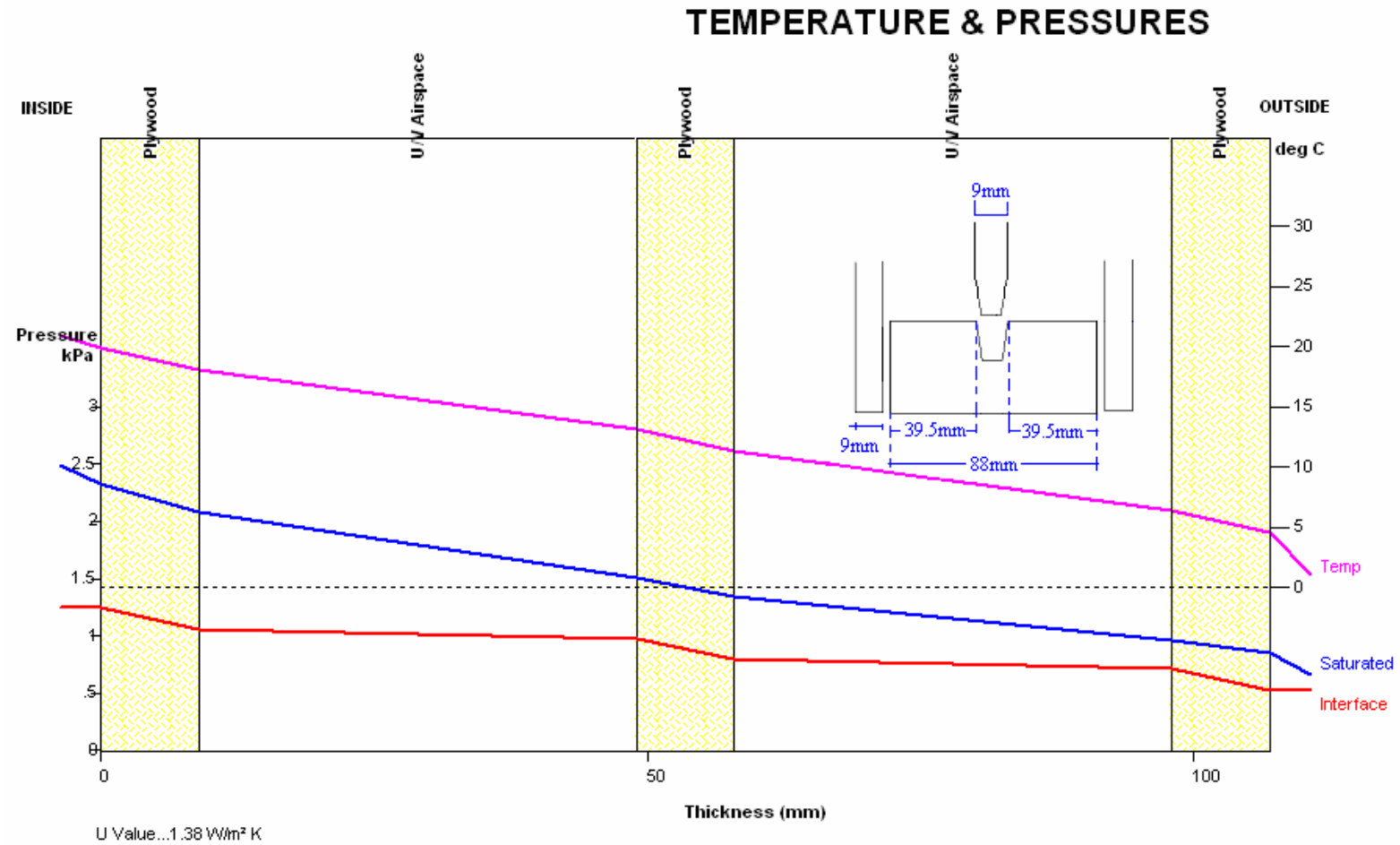


Figure 9.11 Thermal transmittance of box I-beam without insulation

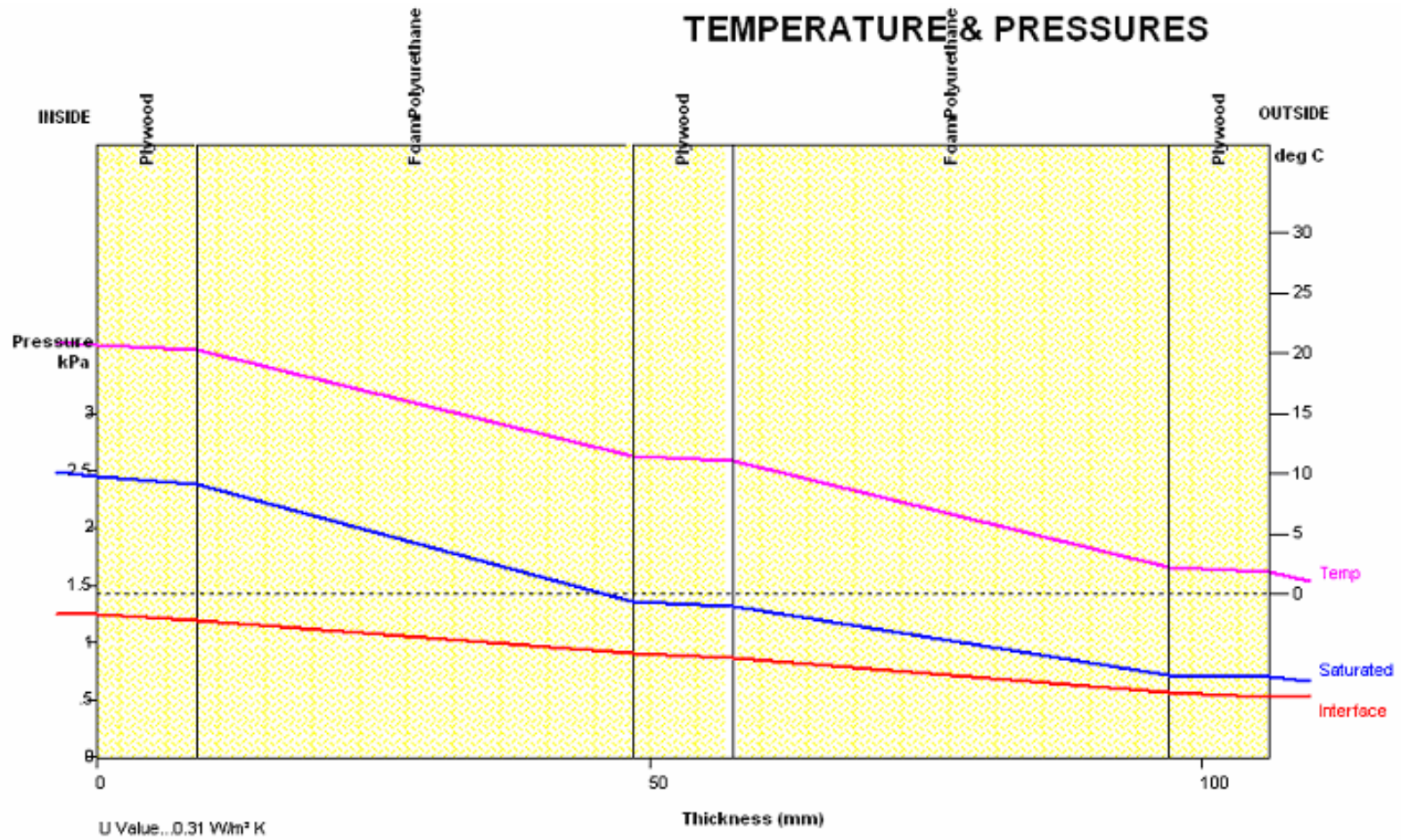


Figure 9.12 Thermal transmittance of box I-beam with insulation

Table 9.9 The U value of the beam cross-section without and with foam

Profiles	U_{NF}	U_F	$1-U_F/U_{NF}$
	(Without foam) (W/m ² K)	(With foam) (W/m ² K)	(%)
Timber section of 90mm width	1.23	---	---
I-beam	4.27	---	---
Double I-beam	2.10	0.92	56
Recessed beam	2.09	0.36	83
Box beam	2.09	0.29	86
Box I-beam	1.38	0.31	78
Box Double I-beam	1.04	0.34	67

9.4.2 Effect of the foam on thermal properties

Value of the U indicates amount of the heat loss through the web of the beams. The greater value shows the greater heat loss. Injected polyurethane reduces the heat loss by 56% for double I-beams, 83% for recessed beams, 86% for box beams, 78% for box I-beams and 67% for boxed double I-beams.

The Building Regulations, 2006 limit heat loss and gain through the fabric of the building by defining the limiting U values for elements and sub-elements as shown in Table 9.10. Column b of the table defines the maximum acceptable U value for the sub-element. Beams can be considered as sub-elements of walls, so in this case ideally the U value for beams should be lower than 0.35W/m²K and in any case should not exceed the 0.70W/m²K. Therefore, except for double I-beams all other profiles satisfy the conditions for they are much lower than the upper limit of 0.70 W/m²K, indeed some are lower than the specified ideal level.

Table 9.10 Limiting U-value standards (W/m²K)

Element	(a) Area-weighted dwelling average	(b) Worst individual sub-element
Wall	0.35	0.70
Floor	0.25	0.70
Roof	0.25	0.35
Windows, roof windows, roof-lights and doors	2.20	3.30

The U value for different profiles has a direct relation with thickness of the foam filling the gaps between the webs; therefore, the box beam provides the lowest U

value as it has the greatest gap between webs in any of the profiles. In the case of the double I-beam, increasing the web distance would accommodate a larger amount of foam to satisfy the building regulations on U value.

This study demonstrates the thermal efficiency of composite insulated beams, and it has shown that even solid sections of timber with 90mm width could not meet the U value limit set in Building Regulations, 2006.

9.5 Composite insulated beams with OSB webs

Chapters 3 and 4 described phase three of the experimental work, when I, double I, box and box I, beams were fabricated using OSB/3 webs instead of plywood webs and C16 or C24 timber flanges instead of MGP 10 Radiata pine timber. Performance of the beams, which were tested over 4.35 m span under 3-point and 4-point bending, is here used to demonstrate the viability of using OSB webs and also low grade C16 timber. This section presents the results of the tests and discusses the performance of the OSB/low grade timber beams.

Beams were loaded to destruction by a four point bending test-rig acting on 4.35m spans without and with infill. Load-deflection graphs for each individual beams are presented in Figure 9.13 and average result for each profile is given in Table 9.11 where:

- P_{max}**: Maximum load
- Δ_{max}**: Deflection at maximum load
- K_{4P}**: Value of the load over deflection under four point bending without foam
- K_{4PF}**: Value of the load over deflection under four point bending with foam

Tests on I-beams with C16 timber flange were used as a reference. The use of additional webs to create double I and box beams increased the loading capacity of the long span beams by 9% to 21% and peaked at 30% for boxed I-beams. Furthermore, double I beams show 14% higher stiffness in comparison to I-beams and increase in stiffness reached 25% and 31 % for box and boxed I-beams respectively (Table 9.11a).

Table 9.11 Average results of structural tests over a 4.35m span

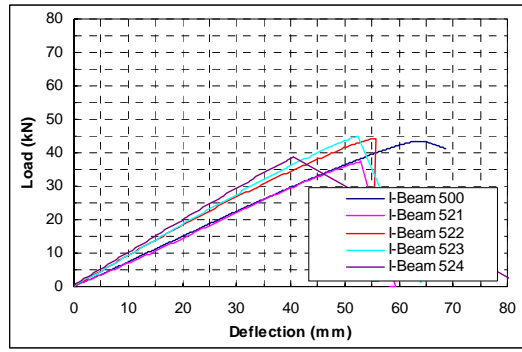
a) Beams made of C16 and C24 timber flanges and OSB webs without infill

Bending tests-Beams with C16 flanges without foam							
Profile	I-beam	Double I-beam	Box beam	Box I-beam	Double I beam v I-beam	Box beam v I-beam	Box I beam v I-beam
P_{max} (kN)	41.78	45.57	50.53	54.38	1.09	1.21	1.30
Δ_{max} (mm)	53.11	52.33	50.07	50.13	---	---	---
K_{4P} (kN/mm)	0.85	0.97	1.06	1.11	1.14	1.25	1.31
Bending tests-Beams with C24 flanges without foam							
P_{max} (kN)	40.70	46.74	46.07	48.27	1.15	1.13	1.19
Δ_{max} (mm)	55.08	50.32	46.38	44.36	---	---	---
K_{4P} (kN/mm)	0.79	1.00	1.05	1.16	1.27	1.33	1.47

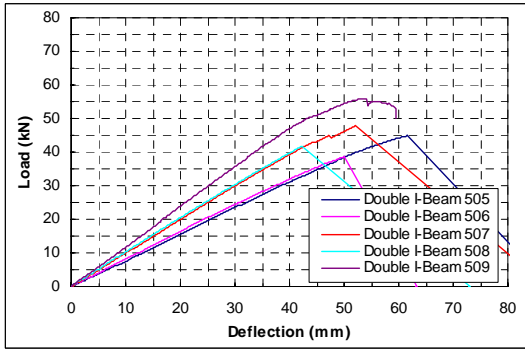
Table 9.11- Continued

b) Beams made of C16 and C24 timber flanges and OSB webs with infill

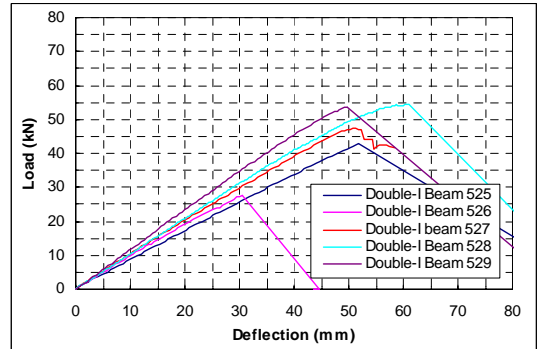
Bending tests-Beams with C16 flanges and infill							
Profile	I-beam	Double I-beam	Box beam	Box I-beam	Double I beam v I-beam	Box beam v I-beam	Box I beam v I-beam
P_{max} (kN)	41.78	45.23	50.90	61.11	1.08	1.22	1.46
Δ_{max} (mm)	53.11	48.92	50.12	54.38	---	---	---
K_{4PF} (kN/mm)	0.85	1.01	1.08	1.19	1.19	1.27	1.40
Bending tests-Beams with C24 flanges and infill							
P_{max} (kN)	40.70	46.11	43.80	57.65	1.13	1.08	1.42
Δ_{max} (mm)	55.08	46.33	40.91	47.67	---	---	---
K_{4PF} (kN/mm)	0.79	1.02	1.11	1.25	1.29	1.41	1.58



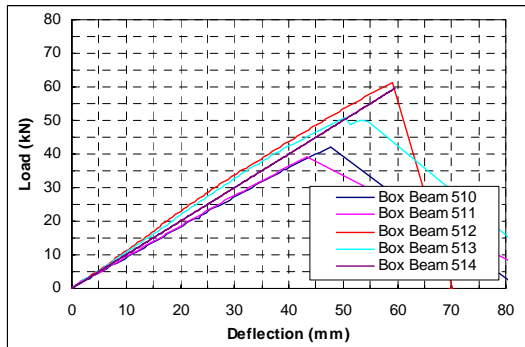
a) I-beam without infill



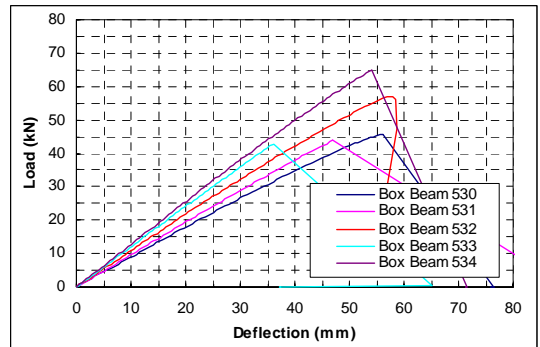
b) Double I-beam without infill



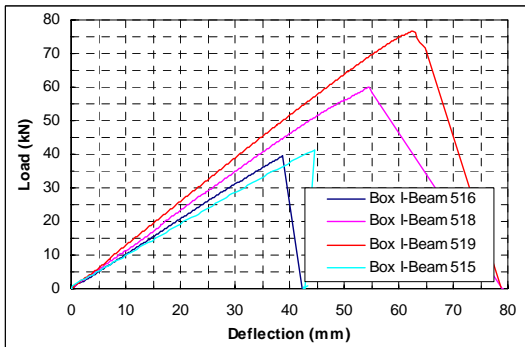
c) Double I-beam with infill



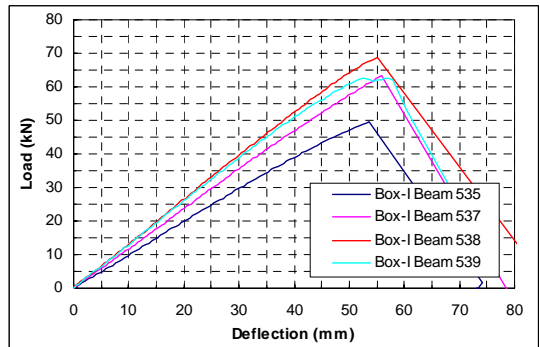
d) Box beam without infill



e) Box beam with infill



f) Box I-beam without infill



g) Box I-beam with infill

Figure 9.13(A) Comparison between the CIB made of C16 timber flanges without and with infill

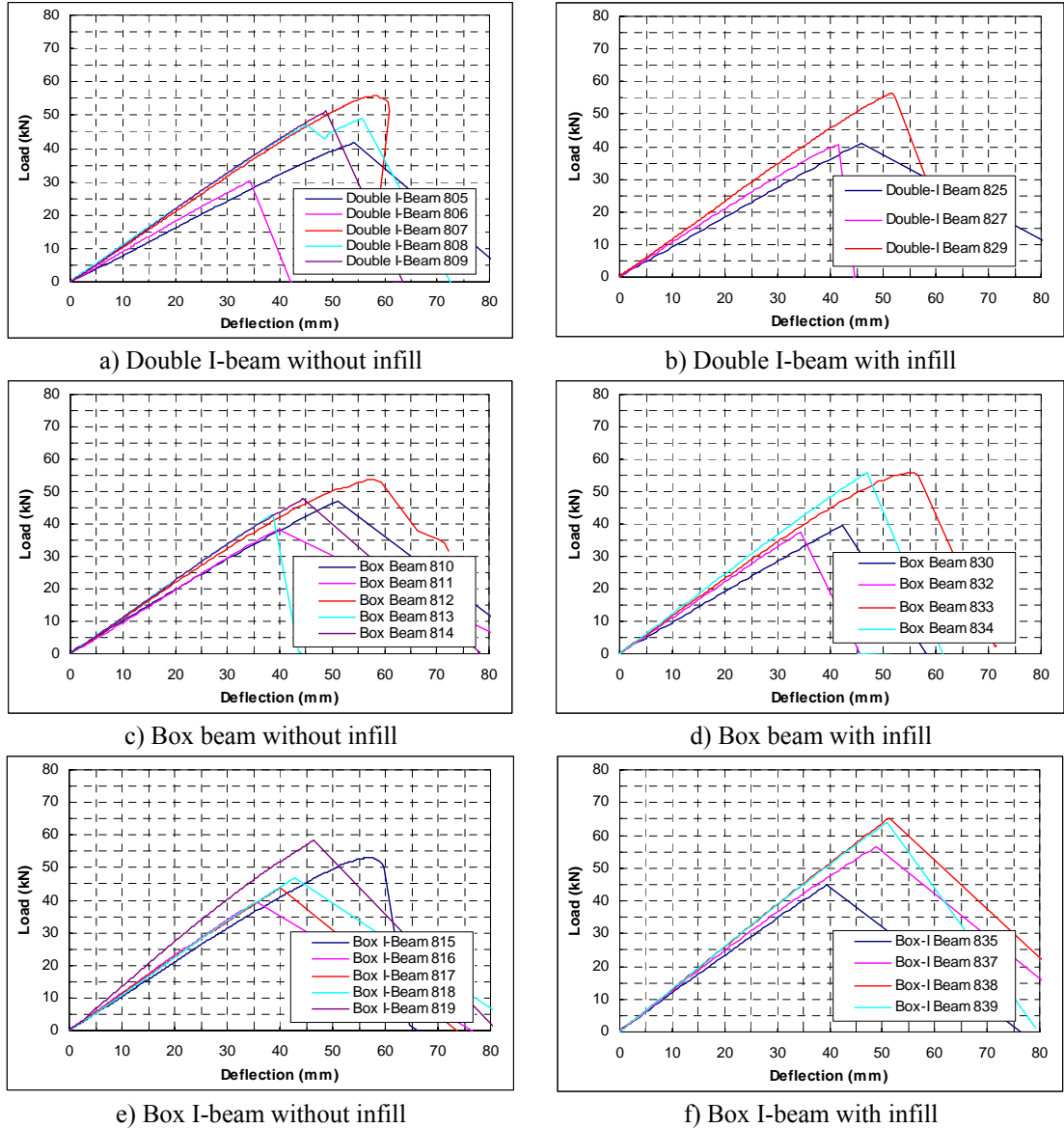


Figure 9.13(B) Comparison between the CIB made with C24 timber flanges without and with infill

However, as shown in Table B.2 in Appendix B there is large variation within the results, since the coefficient of variation reaches 33% for C16 boxed I-beams. More accurate comparisons could be made if a less variable material such as LVL was used as a flange option, or by conducting proof loading tests on timber flanges to eliminate the faulty ones before fabricating the beams.

Overall performance of the beams shows that OSB could be used as an alternative web material; moreover, performance of various profiles made with C16 timber flanges proved that it is possible to manufacture beams with that low grade timber.

Comparison between the beams with C16 and C24 timber in Table 9.11 shows that average P_{\max} and K_{4P} for both grades are very close. The Young modulus of the timber flanges, MoE, could explain that result. According to BS EN338, the average MoE for C16 timber is 8kN/mm^2 and for C24 timber MoE is 11kN/mm^2 , which means C24 timber 27% is stiffer than C16 timber. But results of laboratory tests in chapter 3 revealed that the average MoE of C16 timber was 11.77 kN/mm^2 and for C24 the MoE was 12.38 kN/mm^2 (Table 3.6). Evidently the C24 timber used in this study was only 5% stiffer than the C16 timber, therefore there was not much difference between performance of beams with C16 or C24 timber flanges.

Flexural failure was the dominant failure mode for double I, box and boxed I, beams (Figure 9.14) just as for beams with plywood webs, whereas shear failure was observed for I-beams (Figure 9.15). Some failures occurred in knotty areas, but this could easily be remedied by removing knots and finger-jointing from the sections.



a) Destructive test, four point bending



b) Flexural failure in Box I-beam

Figure 9.14 Test arrangement and failure mode



Figure 9.15 Failure in an I-beam

Comparison between the beams without and with infill in Tables 9.11(a) and 9.11(b) shows that infill material has a marginal effect on enhancement of the bending capacity, P_{max} , and stiffness K . The effect of the foam on stiffness of the beams was evaluated by testing the beams before and after injecting the polyurethane and the average results are given in Table 9.12 where:

$K_{3PNF,4350}$:	Load /deflection result under 3 point bending test for the beam without infill over 4.35 span
$K_{4PNF,4350}$:	Load /deflection result under 4 point bending test for the beam without infill over 4.35 span
$K_{3PF,4350}$:	Load /deflection result under 3 point bending test for the beam with infill over 4.35 span
$K_{4PF,4350}$:	Load /deflection result under 4 point bending test for the beam with infill over 4.35 span
$K_{3PF,4350}/K_{3PNF,4350}$:	Ratio of the load deflection under 3 point bending
$K_{4PF,4350}/K_{4PNF,4350}$:	Ratio of the load deflection under 4 point bending

Results in Table 9.12 show that foam enhances the overall stiffness by only 2 to 6% percent. As mentioned in section 9.2.2 this is caused by variation of foam density and also by total volume of the foam.

Table 9.12 Effect of the foam on stiffness of the beam

Profiles	Beams with C16 timber flanges		
	Double I-beam	Box beam	Box I-beam
$K_{3PNF,4350}$ (kN/mm)	0.71	0.76	0.85
$K_{4PNF,4350}$ (kN/mm)	0.99	1.04	1.12
$K_{3PF,4350}$ (kN/mm)	0.74	0.79	0.88
$K_{4PF,4350}$ (kN/mm)	1.01	1.08	1.19
$K_{3PF,4350}/K_{3PNF,4350}$	1.03	1.04	1.03
$K_{4PF,4350}/K_{4PNF,4350}$	1.02	1.04	1.06
	Beams with C24 timber flanges		
$K_{3PNF,4350}$ (kN/mm)	0.73	0.80	0.86
$K_{4PNF,4350}$ (kN/mm)	0.97	1.06	1.15
$K_{3PF,4350}$ (kN/mm)	0.77	0.82	0.93
$K_{4PF,4350}$ (kN/mm)	1.02	1.11	1.25
$K_{3PF,4350}/K_{3PNF,4350}$	1.04	1.03	1.08
$K_{4PF,4350}/K_{4PNF,4350}$	1.03	1.04	1.05

9.6 Dynamic performance of the beam

9.6.1 Experimental bending vibration of a beam

In order to investigate the possible effects of foam on dynamic performance of CIBs, the natural frequency and damping ratio was measured for each CIB profile with and without polyurethane. ARTeMIS Testor and Extractor, 2005 software was used along with a TEAC LX-10 data recorder (TEAC, 2006) to evaluate the natural frequency and damping ratio of the simply supported beams over a 4.5m span (Figure 9.16). The Danskin Reflex Bearer (Danskin, 2005) incorporating a double-density resilient fibre layer was used as the support material to prevent the beam wobbling (Figure 9.16 c).

The box beam was excited by using a brush along its upper flange where four vibration sensors record the output of the system (Figures 9.16 b and c). The vibration sensors are placed along the length no more than 1.5m apart (Figure 9.16 c). The Pinocchio Vibraphone A 150 sensors are capable of measuring structural vibrations from 0.01 Hz to 1 kHz (Pinocchio Data Systems, 2005).



a) TEAC hardware transfer the data to PC



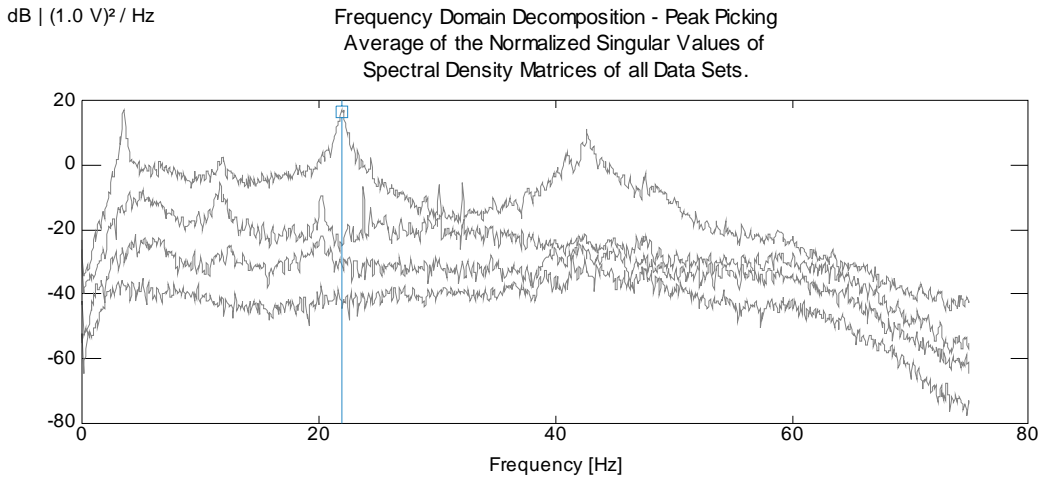
b) Vibration sensor



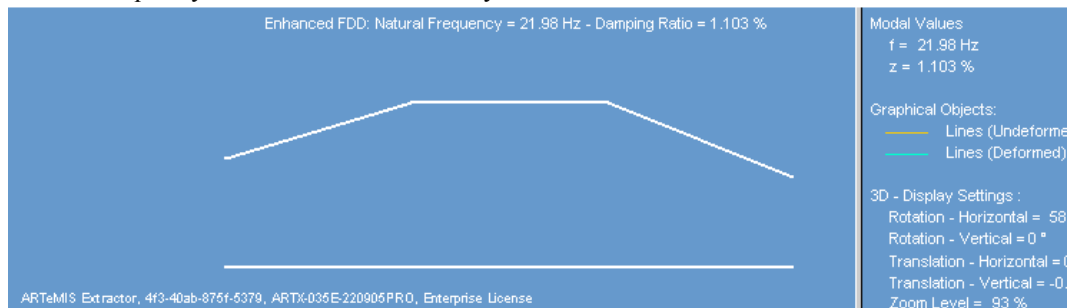
c) Typical dynamic test set up

Figure 9.16 Evaluating natural frequency and damping ratio of a beam

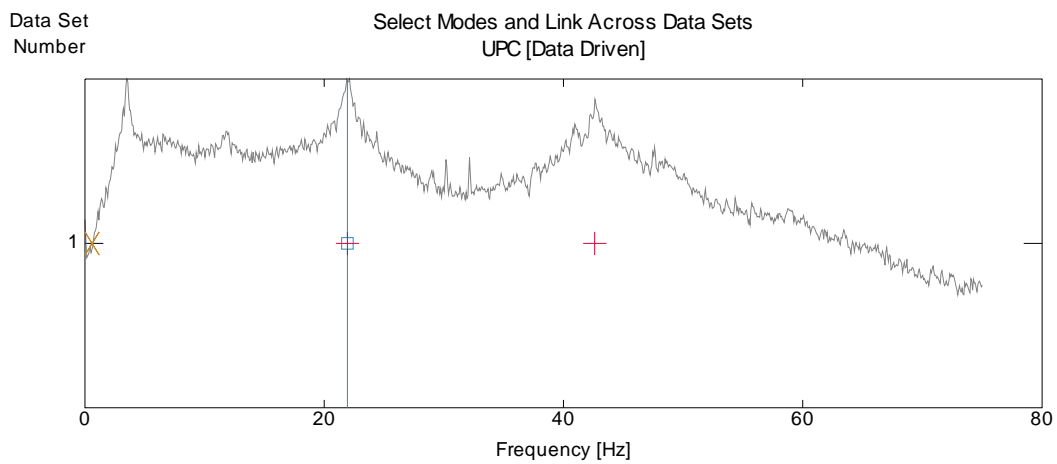
The natural frequency of the beams was calculated by three methods, namely: Frequency Domain Decomposition or FDD (Brincker ... et. al, 2000); Enhanced Frequency Domain Decomposition, EFDD; and Stochastic Subspace Identification, SSI, (Overschee and Moor, 1996) and (Peeters ... et. al, 1995). In addition, the damping ratio is estimated by using the EFDD and SSI methods. The natural frequency and damping ratio for double I-beam 825 was calculated with and without infill by the EFDD and SSI methods and results are illustrated in Figure 9.17. A summary of the results for different profiles without and with infill is presented in Table 9.13.



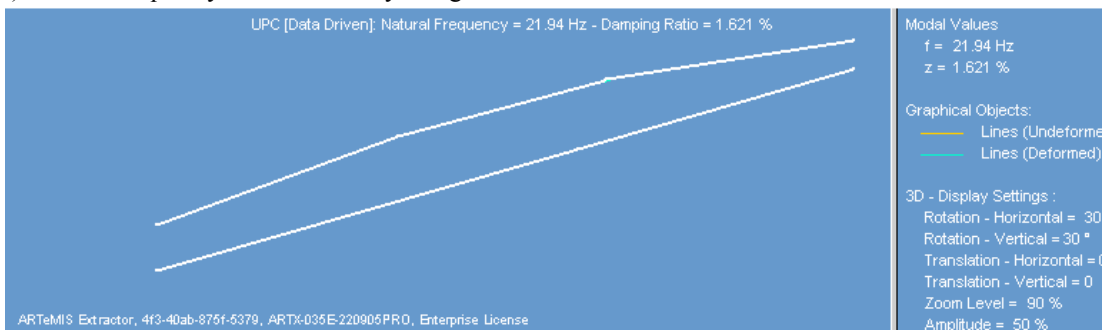
a) Natural frequency of first mode calculated by EFDD method



b) Damping ratio of first mode measured by EFDD method



c) Natural frequency of first mode by using SSI method



d) Damping ratio of first mode calculated by SSI method (1.621%)

Figure 9.17 Demonstration of dynamic characteristic for the Double I-beam 825 without infill

Table 9.13 Natural frequency and damping ratio of the beams without and with infill

a) Before filled by injected polyurethane

Profiles	Timber grade	Beam ID	Beams without infill				
			Natural frequency (f) Hz			Damping ratio (ζ)	
			FDD	EFDD	SSI	EFDD	SSI
I-beam	C24	803	22.71	22.75	22.76	1.883	1.460
		804	22.56	22.48	22.42	2.091	1.765
Double I-beam	C16	525	21.75	21.88	21.89	0.952	1.444
		527	22.05	22.16	22.56	0.848	1.138
	C24	825	21.97	21.98	21.94	1.103	1.621
		829	23.29	23.41	23.42	0.999	1.298
Box beam	C16	531	22.63	22.53	22.53	1.330	1.320
		534	22.71	22.69	22.65	1.683	1.780
	C24	830	21.94	21.78	21.77	1.150	1.280
		833	22.78	22.81	22.82	1.151	1.426
Box I-beam	C16	537	21.57	21.6	21.64	0.869	1.580
		539	22.49	22.2	22.24	0.933	1.414
	C24	836	21.35	21.44	21.49	1.664	1.893
		837	22.01	21.99	22.17	1.201	1.271

b) After filled by injected polyurethane

Profiles	Timber grade	Beam ID	Beams with infill				
			Natural frequency (f) Hz			Damping ratio (ζ)	
			FDD	EFDD	SSI	EFDD	SSI
Double I-beam	C16	525	22.34	22.05	22.11	1.589	1.773
		527	23.00	22.79	22.8	1.431	1.849
	C24	825	22.16	22.03	22.03	1.723	2.088
		829	23.14	23.07	23.08	1.371	1.278
Box beam	C16	531	21.35	21.25	21.27	1.228	1.597
		534	22.85	22.69	22.66	1.560	2.084
	C24	830	21.50	21.5	21.51	1.238	1.690
		833	21.86	21.88	21.86	1.123	1.443
Box I-beam	C16	537	21.02	21.17	21.18	0.925	1.590
		539	22.08	22.05	22.01	1.394	1.537
	C24	836	21.42	21.44	21.49	1.667	1.893
		837	22.01	21.97	21.97	0.986	1.337

Stochastic Subspace Identification, SSI is more accurate than FDD and EFDD, but it needs a longer analysing time (Andersen, 2005). Enhanced Frequency Domain Decomposition and Stochastic Subspace Identification methods can be used to calculate the damping ratio as well as the natural frequency, whereas the FDD method cannot do so.

The values of natural frequency calculated by the three different methods are close, but there is significant difference between the damping ratio calculated by the EFDD and SSI methods. Average results for dynamic characteristics of the beam without and with infill material were calculated by the SSI method and are given in Table 9.14 where:

f_{NF} is a natural frequency of the beam without foam for a first mode

ζ_{NF} is a damping ratio for the beam without foam

f_F is a natural frequency of the beam with foam for a first mode

ζ_F is a damping ratio for the beam with foam

Table 9.14 Average dynamic characteristic of the beam without and with infill

Profiles	Timber grade	No foam		Foam		Comparison	
		f_{NF}	ζ_{NF}	f_F	ζ_F	f_F/f_{NF}	ζ_F/ζ_{NF}
		(Hz)	(%)	(Hz)	(%)		
Double I-beam	C16	22.23	1.41	22.46	1.81	1.01	1.28
	C24	22.68	1.46	22.56	1.68	0.99	1.15
Box beam	C16	22.59	1.55	21.97	1.84	0.97	1.19
	C24	22.30	1.35	21.69	1.57	0.97	1.16
Box I-beam	C16	21.94	1.50	21.60	1.56	0.98	1.04
	C24	21.83	1.58	21.73	1.62	1.00	1.03

Average results in Table 9.14 show that the effect of the foam on natural frequency of beams is not considerable, whereas the effect of the foam is more pronounced on the damping ratio. For instance, the damping ratio of the double I-beam is enhanced by 28% and 15% respectively for beams with C16 and C24 timber flanges. In box beams the damping ratio is increased by 19% and 16% for beams with C16 and C24 flanges,

but enhancement of the damping ratio for the box I-beam is less pronounced than for double I and box beams. Indeed, the damping ratio increased by only 4% and 3% respectively for box I-beams with C16 and C24 timber flanges. Thus it can be concluded that injecting polyurethane foam enhances the dynamic characteristics of CIBs by increasing their damping ratios.

Comparing the average results for natural frequency, f , and damping ratio, ζ , of the double I-beam, box beam and box I-beam shows that the effect of geometrical variability, on natural frequency of the beams is not significant, but it is not possible to draw a conclusion on the effect of beam profile on damping ratio. In some cases damping ratio is significantly increased as for the C16 box beam in comparison to the C16 double I-beam, whereas there is a reduction in damping ratio for the C24 box beam in comparison to the C24 double I-beam (Table 9.14).

9.6.2 Theoretical bending vibration of the beam

9.6.2.1 Natural frequency

The experiments were designed to measure the first mode of natural frequency of each beam and that mode is defined as vibration of the beam perpendicular to its length, but the natural frequency of a beam can be also evaluated by theoretical methods. For a simply supported beam, the natural frequency can be calculated from the Euler-Bernoulli equation (Inman, 2003).

$$\omega_i = (\lambda_i L)^2 \sqrt{\frac{EI}{\rho AL^4}} \quad \text{Equation 9.4}$$

Where:

ω is a natural frequency (rad/s)

λ is a factor depending on support condition

E is the Young modulus of the beam (N/m²)

I is the second moment of area about the strong axis (m⁴)

L is the beam span (m)

ρ is the density of the beam (kg/m³)

A is the cross-section area (m²)

Factors for various boundary conditions are given in Table 9.15

Table 9.15 Lowest five frequency factors, $\lambda_i L$ for a single span beam

End condition	$\lambda_1 L$	$\lambda_2 L$	$\lambda_3 L$	$\lambda_4 L$	$\lambda_5 L$
Free- Free	4.730	7.853	10.996	14.137	17.279
Clamped-free	1.875	4.694	7.855	10.996	14.137
Clamped-pinned	3.927	7.069	10.210	13.352	16.493
Clamped-sliding	2.365	5.498	8.639	11.781	14.923
Clamped-Clamped	4.730	7.853	10.996	14.137	12.279
Pinned-Pinned	π	2π	3π	4π	5π

Density can be calculated as

$$\rho = \frac{m}{A} \quad \text{Equation 9.5}$$

Where:

m is mass of the beam per meter length, (kg/m)

A is cross section of the beam, (m^2)

Therefore Equation 9.4 can be rewritten as:

$$\omega_i = (\lambda_i L)^2 \sqrt{\frac{EI}{m L^4}} \quad \text{Equation 9.6}$$

Natural frequency in hertz is calculated as

$$f = \frac{\omega}{2\pi} \quad \text{Equation 9.7}$$

Therefore equation 9.6 can be written as:

$$f_i = \frac{(\lambda_i L)^2}{2\pi} \sqrt{\frac{EI}{m L^4}} \quad \text{Equation 9.8}$$

From Table 9.15, the value of boundary condition $\lambda_1 L = \pi$ for a simply supported beam, therefore equation 9.8 can be simplified as:

$$f_1 = \frac{\pi}{2L^2} \sqrt{\frac{EI}{m}} \quad \text{Equation 9.9}$$

Where

E is a young modulus of the beam (N/m^2)

I is the second moment of area about the strong axis, (m^4)

L is a beam span (m)

m is a mass of the beam per meter (kg/m)

This equation is also used in Eurocode 5 for calculating the fundamental frequency of the floor. More details for calculating natural frequency of the floor for the first mode are given in chapter 7.

The natural frequency of a box beam with 4.5 meter span can be calculated from Equation 9.9 when:

Beam span $L = 4.5$ m

Flange breadth, $b = 88$ mm

Flange depth, $h_f = 45$ mm

Depth of the beam $h = 290$ mm

Overall breadth of the web $b_w = 18$ mm

Young's modulus of the beam, $E = 11 \times 10^9$ (N/m²)

The box beam comprises C24 timber flanges and OSB/3 webs therefore weight per meter length of the Box beam can be calculated from Equation 9.10

$$m_{\text{Box beam}} = \frac{A_{\text{OSB}} \rho_{\text{OSB}} + A_{\text{timber}} \rho_{\text{timber}}}{10^6} \quad \text{Equation 9.10}$$

Where:

A_{OSB} is area of the web, $A_{\text{OSB}} = 5.22 \times 10^3$ (mm²)

A_{timber} is area of the flange, $A_{\text{timber}} = 7.92 \times 10^3$ (mm²)

ρ_{OSB} is density of the OSB, $\rho_{\text{OSB}} = 550$ kg/m³

ρ_{timber} is density of the timber flange, $\rho_{\text{timber}} = 420$ kg/m³

Hence $m_{\text{Box beam}} = 6.20$ kg/m

Second moment of area about the strong axis, $I = 1.366 \times 10^{-4}$ (m⁴)

Natural frequency of the first mode for the box beam is calculated by substituting the values in Equation 9.9.

$$f_1 = \frac{\pi}{2 \times 4.5^2} \sqrt{\frac{11 \times 10^9 \times 1.366 \times 10^{-4}}{6.20}}$$

Hence $f_i = 38.20$ Hz

Comparing the theoretical natural frequency ($f_i = 38.20$ Hz) to the experimental results in table 9.14 shows that theoretical method overestimates the natural frequency by 71%.

Boundary conditions could explain the difference. In reality, the beam support may not be a true simple support; therefore, factors for the boundary condition would be different. The support in the experiments done, may have acted as a spring, so shear force was resisted by spring stiffness.

In order to investigate this issue, the vibration tests were repeated for the I-beams 803 and 804 using solid concrete blocks instead of the reflex batten. The results for natural frequencies and damping ratios were calculated by FDD, EFDD and SSI methods and are presented in Table 9.16.

By comparing the results in Table 9.16 with those given in Table 9.13 it was shown that changing the boundary condition increased natural frequencies for beam 803 from 22.76 to 37.30 and for 804 from 22.42 to 37.89 Hz.

Table 9.16 Effect of the support condition on dynamic characteristics of I-beams

Profiles	Timber grade	Beam ID	Beams without infill				
			Natural frequency (f) Hz			Damping ratio (ζ)	
			FDD	EFDD	SSI	EFDD	SSI
I-beam	C24	803	37.65	37.52	37.30	1.838	1.605
		804	37.79	37.99	37.89	1.294	1.257

Theoretical natural frequency of the beam can be calculated from equation 9.9 as

$$f_i = 43.51 \text{ Hz}$$

When:

I-beam mass is $m = 4.392$ kg/m

First moment of area: $I = 1.256 \times 10^{-4}$

The average experimental natural frequency for I-beam is thus 14% lower than the theoretical one.

Result of this study highlights the importance of the support conditions in determining the natural frequency of a beam. The stiffness of the support is directly related to the natural frequency of the beam. This could be an important issue for timber flooring system where natural frequency is one of the criteria which should be satisfied under serviceability performance. Poor installation or changes in support condition of the beams used in a timber flooring system will reduce the natural frequency which in turn could cause failure in vibration criteria as discussed in chapters 7 and 8.

9.6.2.2 Damping factor, force and ratio

Dynamic behaviour can be written as a function of time thus:

$$m\ddot{x}(t) + c\dot{x}(t) + kx(t) = F(t) \quad \text{Equation 9.11}$$

Where:

m: Mass

c: Damping factor

k: Stiffness

$\ddot{x}(t), c\dot{x}(t), x(t)$: Functions of time for acceleration, velocity and displacement

F(t): External force

A damping force $c\dot{x}(t)$, is one that resists vibration and decay of energy, normally to heat. Damping force is proportional to velocity. A damping factor, C, reduces both duration of vibration and peak acceleration caused by dynamic force. The critical damping factor, C_C , is the value that returns the mass to its original place after disturbance. The damping ratio, ζ , is the ratio between the damping factor, C, and critical damping, C_C .

$$\zeta = C/C_C \quad \text{Equation 9.12}$$

However, it is worth mentioning that structural damping is unpredictable, so it can only be measured through experimental work (Sarafin and Larson, 1995). System damping is measured by exciting harmonic motion and then allowing the vibration to decompose in a damped sinusoidal function of time. Then the damping ratio can be obtained by measuring peak displacement at x_1 and x_2 for two vibration cycles.

9.7 Chapter summary and conclusions

This chapter described experiments on the effects of injected rigid polyurethane foam on the structural performance, durability and thermal performance of ply-webbed composite timber beams. This was followed by the investigation of the structural performance and dynamic response of the OSB-webbed composite timber beams. The key points obtained from the experimental and analytical procedures are summarised below.

Structural performance of the plywood webbed beams:

- Infill material improves the buckling resistance of the webs, which consequently enhances the bearing capacity of the profiles from 18% to 30% dependent upon the geometry of the profile. As a result CIBs can be fabricated without using any stiffeners or straps, which are used in traditional box beams to enhance the bearing capacity of the beams.
- Experimental tests show that foam has a positive but not significant effect, on overall stiffness of beams and increases vary from 1 to 10%. Variation of the results is due to variation of the foam density, which has a direct relation to its mechanical properties.
- Flexural failure is typical for the long span, 4.35m, beams with infill and that result is similar to the beam without infill. Comparison between the empty and filled beams showed that the effect of the infill material on enhancement of bending capacity is not significant.
- The comparison between the beams with and without infill shows that injecting the infill material enhances the stiffness and maximum loading capacity of beams with web openings. That enhancement is due to the contribution of foam to shear and tensile stress of the web. Experimental tests show that failure began from the web opening for both empty and filled beams.
- Creating a circular web opening in a beam, resulted in concentration of principle stress at the mid-point of each quarter, a fact identified by using a finite element model. Elastic analysis showed that the maximum principle stress occurred in the mid-points of the first and third quarters of a circular

opening, which are the points where failure initiated in experimental work. The minimum principle stress occurred at the mid-points of the other quarters.

Durability of the plywood webbed beams:

- Stiffness of the empty beams increased by 5%, 13% and 4% when they were tested at the end of cycles 2, 4 and 6 and compared to stiffness in cycle 0. In contrast, there is a reduction of stiffness of the filled beams by 2%, 9% and 24% at the end of cycles 2, 4 and 6 in compared to stiffness in cycle 0.
- Decreasing the moisture content is the reason for great enhancement of stiffness for the empty beams, whereas increasing moisture content much reduces stiffness in the filled beams. Moisture content of the empty beams reduced by 3.80%, 19.52% and 23.90% at the end of cycles 2, 4 and 6 respectively, while moisture content of the filled beams at the end of cycles 2, 4 and 6 increased by 96.07%, 67.72% and 108.10% respectively.
- Both empty and filled beams demonstrated reduction in ultimate load capacity when they were tested at end of cycles 2, 4 and 6 in comparison to their capacity in cycle 0, but reduction of ultimate load on empty beams was much more pronounced than on filled beams. At the end of cycle 6 empty beams displayed, 40% reduction of ultimate load in comparison to their capacity in cycle 0, whereas the figure was 26% for the filled beams.
- Reduction of the ultimate load capacity for both empty and filled beams is due to the weakening effect of the accelerated ageing procedures on components of the beams, but exposing the beams to severe weathering conditions did not cause any de-lamination between the flange-web connections nor between plywood veneers.

Thermal performance of plywood webbed beams:

- This study demonstrated the thermal efficiency of composite insulated beams, for it was shown that even a solid section of timber 90mm wide could not meet the thermal transmittance limit set in Building Regulations, 2006.
- The U value for different profiles has a direct relation to thickness of the foam that filled the gaps between the webs; therefore, box beams provide the lowest U value for they have the largest gap between webs in all the profiles.

- Comparison between the double I, recessed, box , box I and box double I, beams, empty and filled, showed that injected polyurethane reduced the heat loss by 56% , 83%, 86%, 78% and 67% respectively.

Structural performance of OSB webbed beams:

- These behaved similarly to plywood webbed beams. Flexural failure was a dominant failure mode for double I, box and boxed I beams which were fabricated with OSB/3 and C16 or C24 timber flanges, whereas shear failure was observed for I-beams.
- Comparison between the empty and filled beams proved that infill material marginally enhanced both the bending capacity and stiffness of the beams.
- The foam only enhanced stiffness by 2 to 6% for the beams made from OSB webs and that was caused by variation of foam density and total volume of foam present.
- Structural performance of beams with C16 timber flanges was similar to that of those made with C24 timber flanges. From this it seems likely that Scottish grown C16 timber could be used for manufacturing CIBs.

Dynamic performance of the OSB webbed beams:

- Average experimental results showed that the effect of foam on the natural frequency of beams is not considerable, but its effect is more pronounced on the damping ratio.
- Comparing the average results for natural frequency, f , and damping ratio, ζ , of I-beams, double I-beams, box beams and box I, beams shows that the effect of geometrical variability, on the natural frequency of beams is not significant.
- Results of this study highlight the influence of support conditions on natural frequency of beams. The stiffness of the support has a direct relation with the natural frequency of a beam. Analytical calculation showed that ignoring the support stiffness resulted in overestimating the natural frequency of a beam. It was also shown that similar equation could be used to estimate the natural frequency of a flooring system. It was observed that poor installation, or change in support conditions of a timber floor could lead to overestimation of

the natural frequency of the floor, which in turn could cause it to fail to meet specified vibration criteria.

CHAPTER 10 CONCLUSIONS AND RECOMMENDATIONS

10.1 Introduction

This research has developed and evaluated new types of engineered wood products namely double I-beams, recessed beams, box beams, box I-beams and boxed double I-beams which are here described as Composite Insulated Beams (CIBs) or multi-webbed composite beams. A summary of conclusions concerning fabrication and performance of CIBs is provided here.

10.2 Engineered wood products

A literature review revealed the various environmentally friendly engineered wood products and identified advantages and disadvantages of each, then introduced the novel CIB concept developed by the author and others at Napier who combined the structural efficiency of sandwich panels with that of existing EWPs.

10.3 Fabrication process

Beams were manufactured using three different combinations of materials. The following key findings were made:

- Fabricating the beam with SIPs was difficult, as it needed two different types of glue and it was not possible to taper the OSB faces.
- During manufacturing of the different profiles it was proved that mechanical fasteners were unnecessary, because proper bonding between web and flange was provided by using Resorcinol adhesive.
- The difficulty of clamping the long I and double I beams with timber and LVL flanges was discovered and overcome by making the roller clamp.
- Testing the flange stiffness revealed lower values than were claimed by the NZ timber manufacturer.
- A statistical method was explained and was used to distribute the timber flanges into profiles so that variation of Young Modulus could be evened and reduced in beams. The outcome was that comparable beams were obtained within each group of one profile and among different profiles.
- Injected polyurethane was proved to be a suitable alternative for the polystyrene sheets, which had been used in stage one. Using injected

polyurethane provided the possibility of assembling beam frames without the limitations imposed by SIPs and no glue was required to bond the polyurethane with webs and flanges.

- Measurements of foam density inside the beams showed that it is always higher than the level of 32kg/m^3 claimed in manufacturer's data sheets. Furthermore experimental results show an inverse relation between the foam density and the distance between the webs. As the web distance decreases polyurethane density increases.

10.4 Testing procedures

A series of full-scale testing methods were described for evaluating the structural characteristics and long term durability of the beams. The difficulty of testing non-isotropic material was addressed. Descriptions were given of stiffness, shear, bending and bearing tests on the empty and filled CIBs, together with ready made timber Glulam , LVL and I-beams. The following achievements and observations arose:

- A new pulling test was devised to assess the tensile resistance of I-beams and double I-beams exposed to a hanging load and a testing procedure was described.
- Testing procedures for evaluating the long term durability of the CIBs were developed and the testing process was described.
- Full-scale testing was expensive and time consuming, so proper planning and careful supervision was required; but full-scale testing was essential for evaluating the structural behaviour of the new structural elements.
- Failures in full-scale testing occur fast and sometimes one after the other, so recording the test provides an opportunity for reviewing the failure process and the chance to identify the exact mode of failure.
- Setting the uniaxial testing machine on constant rate of displacement or constant rate of loading creates different results unless testing is undertaken within the elastic limit of the test material. A constant rate of displacement was used in this study.

10.5 Geometrical variability and structural performance

Results from experiments to determine the effect of geometrical variability on structural performance of empty, CIBs, LVL and Glulam beams were discussed. An analytical procedure based on the energy method and Castigliano's theorem was developed for calculating the shear stress, shear factor and deflection of beams with different cross-sections. Key points arising are as follows:

- Experimental results showed that shear has a significant effect on the total deflection of CIBs and this also extends to solid sections such as LVL.
- The modulus of elasticity and shear modulus can be calculated by solving a pair of deflection/load equations, using results from a combination of two different tests; however, in order to achieve reliable results, it is necessary to use a number of different combinations.
- The mean value of the elastic modulus calculated for the fabricated beams is lower than those measured for their flanges.
- The bending capacity of lightweight beams made with LVL flanges is more consistent than that for similar beams made with timber flanges as in LVL the natural defects are dispersed.
- Creating the double I-beams or boxed I-beams by simply employing additional webs significantly enhanced the bending capacity of the beams as well as their shear capacity, while at the same time preserving the high strength to weight ratio.
- Boxed I-beams with plywood webs and timber or LVL flanges were found to be the optimum design among the fabricated beams in terms of structural performance and ease of manufacturing.
- It was shown that it is usually possible to predict the failure mode by comparing the theoretical stresses with the characteristic values of the components.

10.6 Investigating the structural performance of multi-webbed I-beams

The effect of circular web openings of different diameters on stiffness and strength of the nine different beam profiles was tested and compared. The bearing capacity of each profile was investigated together with the pulling resistance of the LVL/ timber I and double I-beams. A finite element model was also used to describe and predict

bearing and pulling failures. In addition, an analytical procedure based on Eurocode 5 was used to predict the buckling load limit of a beam profile exposed to compressive load. Key findings follow:

- It was shown that the diameter of the circular hole has a major effect on the reduction of the maximum loading capacity of the beams, whereas the effect of a large hole on load/deflection of the beams is less pronounced.
- The effect of the web opening on reduction of stiffness is more severe for I-beams or LVL I-beams than for double I or boxed I-beams. For instance, web openings of 76mm and 102mm have negligible effect on the stiffness reduction of the double, and boxed I beams, but it caused 6% and 10% stiffness reduction in I-beams respectively.
- The presence of additional webs significantly enhances structural performance of the I-beams. For instance, it is shown that shear loading capacity of double I-beams and box I-beams with 152mm web openings is 52% and 101% higher than for I-beams without a web opening.
- Poor performance of the recessed beams under compressive load highlights the importance of the web-flange connection method.
- The compressive stress test results proved that failure is caused by a combination of web buckling and flange cracking, where the sequence of failure is governed by cross-section of the profile and height of the beam.
- For pulling resistance, experimental results show that tension stress perpendicular to the grain direction of the flange is a controlling factor for evaluating the resistance of the beam under hanging loads.

10.7 Analytical model to assess the beams based on EC5

Chapter seven describes the analytical model, which was derived from Euro code 5 and formed the basis for a parametric study. The model was used to assess structural performance of timber flooring systems constructed with double I-beams, but it was also applied to evaluate performance of the other CIB profiles. Various conditions under ultimate limit states (ULS) and serviceability limit states (SLS) were introduced during examination of the double I-beam model. It was shown that:

- The described design model can predict the maximum permissible span and can also identify governing design criteria for all the beam profiles.

- In designing light timber floors, the straight forward option to avoid the excessive vibration is enhancement of the beam/ joist stiffness, because increasing the stiffness enabled CIB floors to meet Eurocode 5 vibration criteria.

10.8 Parametric evaluation of CIBs, I-beams and solid timber joists

The parametric study showed the influence of geometric and material variability of CIB beams, I-beams and solid joists on permissible spans for timber flooring systems. The parametric study used the analytical model described above. Different beam cross-sections were considered together with variations of the depth of each. The effect of different flange materials were analysed using the model together with effects of different web materials. Performance under both ultimate limit states and serviceability limit states was considered. Options A and B detailed in UK National Annex to BS EN 1995-1-1 (EC5) for vibrational performance of timber floors were applied and results were compared and assessed.

- The parametric study showed that the requirements for serviceability limit states generally control the design of timber flooring systems. In most cases, for serviceability limit states, the deflection under unit point load governs the permissible spans of the composite beam studied. Using Option B in the UK National Annex to EC5 leads to a less conservative permissible span compared to Option A.
- Rolling shear and static deflection are the controlling criteria for the shallow I-beams but with increase in depth the unit point load deflection became the governing design criterion.
- For composite beams, adopting option B resulted in a longer permissible span than option A. The increase in permissible span is 6 to 7% for a spacing of 400mm and 3 to 4% for a spacing of 600mm. Using Option B for solid timber joists at a spacing of 400mm also lead to an increase in the permissible span by 3%.
- Comparison of the permissible spans of solid timber joists calculated to EC5 with the permissible spans recommended in BS 5268-7.1 revealed no significant difference.

- In terms of material variability, the influence of the flange material is more pronounced than that of the web material. The use of a box I-beam instead of an I-beam enhances the permissible span by up to 20%. The combined effects of using C24 timber flanges and plywood webs instead of OSB webs increase the permissible span by up to 29% under option A and by 35% when Option B of the UK National Annex is used.

10.9 Effect of infill on performance of CIBs

The effect of the injected polyurethane on structural performance, long term durability, thermal behaviour and dynamic response of beams with various cross sections was investigated, so that a comparison could be made between performance of empty and filled beams. Long term durability and thermal behaviour were investigated for the beams made in stage 2, namely those with plywood web(s) and timber or LVL flanges, but dynamic response was investigated on beams which were fabricated in stage 3, namely those with OSB web(s) and C16 or C24 timber flanges. Structural performance was investigated for both the groups made in stages 2 and 3.

The key findings for each part of the work are summarised below.

10.9.1 Structural performance of the plywood webbed beams

- The presence of the infill material improved the buckling resistance of the webs, which consequently enhanced the bearing capacity of the profiles by 18% to 30% dependent on the geometry of the profile. As a result CIBs can be fabricated without using any stiffeners or straps like those used in traditional box beams to enhance their bearing capacity.
- Experimental tests showed that foam had a positive, but not significant effect, on overall stiffness of the beams which increased by 1 to 10%. Variation in the results is due to non-uniform foam density and that has a direct relation to mechanical properties of the foam.
- Flexural failure is the typical failure pattern for the 4.35m long-span filled beams, but a similar failure pattern occurs in empty beams. Comparison of filled and empty beams leads to the conclusion that the small enhancement in bending capacity of filled beams is not significant.

- Another comparison between empty and filled beams showed that applying the infill material enhanced the stiffness and maximum loading capacity of beams with a web opening.
- Experimental tests showed that failure began from the web opening for both empty and filled beams. From observed failure pattern it is evident that the foam contributed to the shear and tensile stresses of the webs.
- The presence of a circular web opening in a beam resulted in concentration of principle stress at the mid-point of each quarter, which is identified by the using finite element model. Elastic analysis showed that the maximum principle stress occurred at the mid-points of the first and third quarters of the circular opening which are the points where failure initiated in experimental work. Minimum principle stress occurring at the mid-point of the second and fourth quarters.

10.9.2 Durability of the plywood webbed beams

- For beams with no infill, stiffness increased by 5%, 13% and 4% when they were tested at the end of cycles 2, 4 and 6 in comparison to stiffness in cycle 0. In contrast there was a reduction of stiffness in filled beams by 2%, 9% and 24% at the end of cycles 2, 4 and 6 compared with beam stiffness in cycle 0.
- Decreasing the moisture content was the reason for enhancement of the stiffness for the empty beams, whereas increased moisture content in filled beams created reduction in stiffness. Moisture content of the empty beams reduced by 3.80%, 19.52 % and 23.90 % at the end of cycles 2, 4 and 6 respectively, but moisture content of the filled beams at the end of cycles 2, 4 and 6 rose by 96.07%, 67.72% and 108.10% respectively.
- Both empty and filled beams demonstrated reduction in ultimate load capacity when they were tested at end of cycles 2, 4 and 6 and compared to their cycle 0 values. Reduction of ultimate load on empty beams was much more pronounced than for filled beams. At the end of cycle 6 beams without infill showed 40% reduction of ultimate load in comparison to their cycle 0 value, whereas reduction was just 26% for the filled beams.
- Reduction of the ultimate load capacity for both beam states is due to the weakening effect of accelerated ageing procedures on beam components.

- Exposing the beams to severe weathering conditions did not cause any delamination between flange-web connections or between plywood veneers.

10.9.3 Thermal performance of plywood webbed beams

- The U value for different CIB profiles has a direct relation to thickness of the foam which filled the gaps between webs; thus, box beams provide the lowest U value for they have the widest gap among the profiles.
- Comparison between the empty and filled double I, recessed, box, box I and box double I beams showed that injected polyurethane reduces the heat loss by 56%, 83%, 86%, 78% and 67% respectively.

10.9.4 Structural performance of OSB webbed beams

- As in beams with plywood webs, flexural failure was the dominant failure mode for double I, box and boxed I beams which were fabricated with OSB/3 and C16 or C24 timber flanges, but in contrast with plywood webbed beams shear failure was observed in OSB I-beams.
- Comparison between empty and filled beams proved that infill material marginally enhanced the bending capacity and stiffness.
- The foam enhanced stiffness by 2 to 6% for the beam made of OSB webs because of variations of foam density and total volume of the foam.
- Structural performance of the beam with C16 timber flanges was similar to those made with C24 timber flanges, so it can be concluded that C16 timber grown in Britain could be used for manufacturing CIBs.

10.9.5 Dynamic performance of the OSB webbed beams

- Average results obtained from experimental work show that the effect of the foam on natural frequency of the beam is not considerable, but its effect is more pronounced on the damping ratio.
- By comparing the average result for natural frequency, f , and damping ratio, ζ , of the I-beams, double I-beams, box beams and box I beams it became clear that the natural frequency and damping ratio of the beams was not significantly affected by geometrical variability.

- From experimental data it was found that the support conditions had important effects on the natural frequency of beams. The stiffness of the support was found to be directly related to the natural frequency of a beam. Analytical calculations showed that ignoring the support stiffness resulted in overestimation of the natural frequency of the beam. Similar equations were also used to estimate natural frequency of a flooring system. It became apparent that poor installation or change in support conditions of a timber floor could also lead to overestimation of the natural frequency of the floor, so the floor could fail vibration criteria in Building Regulations, 2006.

10.10 Potential applications of findings:

The structural limitations and difficulties of timber are partially overcome by the new development of Composite Insulated Beams, which create more options for structural engineers in future. Low levels of technology, therefore low capital investment is required for fabrication of composite insulated beams.

Variations of material properties in timber are an important influence on the ultimate bending and shear capacity of CIBs. Experimental work proved that LVL flanges on CIBs increase uniformity of performance therefore CIBs should preferably have LVL flanges.

LVL box I-beams and box I-beams could be used in the construction industry instead of solid timber sections or glulam, because additional webs significantly raised the resistance to bending of the beams as well as increasing their shear capacity, whilst the beams maintain a high strength to weight ratio. CIBs could also be used instead of I-beams where they provide either longer span for a fixed depth, or lower depth for a fixed span, at identical loading conditions and spacing.

The parametric study of CIBs in floor systems showed that increasing web numbers and use of strong flange materials creates longer acceptable spans. Experimental work on the structural behaviour and dynamic responses of CIBs provided understanding of their engineering performance, which may enable engineers to build lighter structures than by using solid timber sections or I-beams. Experiments also showed that

incorporating infill material not only enhances the thermal insulation properties of CIBs, but also improves their long term durability, thus they have potential for use in energy efficient, long lasting structures. Finally, studies of dynamic performance of CIBs showed that stiffness of the support was directly related to the natural frequency of the beams.

10.10 Recommendations for future research

A selection of recommendations for continuation of this work is presented below.

10.10.1 Effects of long term loading

Like timber and wood based materials, CIBs experience a reduction in strength under sustained loading, and they also display a form of behaviour known as creep. The two effects are related. Creep is the increase of deflection with time, under the influence of variable loading and moisture content. Both effects should be thoroughly investigated before CIBs are utilised in industry.

10.10.2 Flooring system studies

Experimental work on full scale floor systems built using CIBs could be conducted for comparison with the parametric studies on similar flooring systems. Moreover, the performance of different CIB profiles against vibration criteria should be explored.

10.10.3 Evaluation of the fire resistance of CIBs

For fire safety in a building, it is not the fire resistance of an infill that is decisive, but rather the behaviour of the whole beam. In practical terms, the fire safety of a combustible material is not viewed in isolation for its interaction with ambient conditions must be taken into account. Polyurethane foam infill was chosen because it does not melt or form burning droplets; moreover, its combustion gases are similar to those of other combustible natural materials like wood and wool (IVPU, 1998). Nevertheless, further research is required on the fire resistance and safety of CIBs to ascertain whether they satisfy building regulations.

10.10.4 Environmental issues regarding CIBs

Different methods of recycling the CIBs should be investigated to ensure that the beams meet European requirements for reduced waste disposal (Council of the European Union, 1999). In that context, energy recovery and waste prevention in production should also be investigated. Polyurethane can be used for energy recovery and would create no critical increase in emissions between the old generation or new generation (Isopa, 1998) and (Weigand & Strobbe, 1998). In the late 1990s 272 municipal solid waste incinerators (MSW) with energy recovery systems were available in Europe (Juniper Consultancy Services, 1998) and they are capable of burning the filled beams.

REFERENCES

Advanced Building, (2002). Engineered wood products, website of Advanced Building Technologies & Practices.

http://www.advancedbuildings.org/_frames/fr_search.htm - Used 12 Apr. 04.

Aerodux, (2005). Aerodux 500 with Hardener 501, Technical data sheet, URL: <http://www.sky-craft.co.uk/>.

American Society for Testing and Materials (ASTM), (1993). D1037 - Standard methods of evaluating the properties of Wood base fibre and particle panel materials.

Andersen, P., (2005). ARTeMIS user training course. Data analysis & signal processing. URL <http://www.svibs.com>.

Arya, C., (2002). Design of structural elements. Spon. ISBN: 0415268451.

AS/NZS 2269, (1994). Australian/New Zealand standard: plywood structural. Published Jointly by: Standards Australia and Standards New Zealand. ISBN 0 7262 8908 6.

AS/NZS 4063, (1992). Australian/New Zealand standard: Timber stress graded, in grade and stiffness evaluation. Published Jointly by: Standards Australia and Standards New Zealand. ISBN 0 7262 7750 9.

ASTM C481-99, (1999). Standard test method for laboratory aging of sandwich constructions. USA PA, West Conshohocken: ASTM International.

ASTM E632, (1996). Standard practice for developing accelerated tests to aid prediction of the service life of building components and materials. IN - (*Annual Book of ASTM Standards. USA, PA, West Conshohocken: ASTM International.*)

Bahadori -Jahromi, A., Kermani, A., Zhang, B., Harte, A., Bayne, K., Turner, J., Walford, B., (2006). Influence of geometrical profiles on structural properties of engineered composite timber beams. *ICE Journal of Structures and Buildings. [In press.]*

Bahadori-Jahromi, A., (2005) Composite insulated beam. Innovation & Research Focus Issue, (61) May 2005. ISSN 0960 5185. Institution of Civil Engineers. <http://www.innovationandresearchfocus.org.uk>.

- BBC, Weather**, (2006).
http://www.bbc.co.uk/weather/world/city_guides/results.shtml?tt=TT003780.
- Bengtsson, C.**, (2000). Stiffness of Spruce wood- influence of moisture conditions. *Holz als Roh und Werkstoff*, 58:352.
- Blake, A.** (1985). Handbook of mechanics, materials and structures. John Wiley & Sons. ISBN: 0471862398.
- Blass, H.J. ... et.al (eds.)**, (1995). Timber Engineering Step 1: Basis of design, material properties, structural components and joints. Centrum Hout. ISBN: 9056450018.
- Bodge, J. & Jayne, B.A.**, 1982. Mechanics of wood and wood composites. New York: Van Nostrand Reinhold.
- Bodig, J. & Jayne, B.A.** (1993). Mechanics of wood and wood composites. Krieger Publishing. ISBN 0-89464-777-6.
- Brincker, R., Zhang, L., and Andersen, P.**, (2000). Modal identification from ambient responses using frequency domain decomposition, pp. 625–630. IN – (*Proceedings of IMAC 18, the International Modal Analysis Conference, San Antonio, TX, Feb.*)
- BS 4512**: 1969, Methods of test for clear plywood.
- BS 5268-2**: 2002. Structural use of timber- Part 2: Code of practice for permissible stress design, materials and workmanship. ISBN 0 580 333140.
- BS 5268-7.1**:1989. Structural use of timber. Recommendations for the calculation basis for span tables. Domestic floor joists. BSI.
- BS 5291**:1984 Specification for manufacture of finger joints of structural softwood.
- BS EN 12369-1**: 2001. Wood-Based panels- Characteristic values for structural design, Part 1: OSB, Particleboards and fibreboards. ISBN 0-580-36993-5.
- BS EN 1990**, 2002. Eurocode 0. Basis of structural design. BSI.

BS EN 1991-1-1, 2002. Eurocode 1. Actions on structures. General actions. Densities, self-weight, imposed loads for buildings. BSI.

BS EN 1995-1-1: 2004. Eurocode 5, Design of timber structures. Common rules and rules for buildings. British Standards Institution. ISBN 0 580 45147 X.

BS EN 301 (1992), Adhesives, phenolic and aminoplastic, for load-bearing timber structures: classification and performance requirements.

BS EN 302-2: 2004. Adhesives for load-bearing timber structures — Test methods — Part 2: Determination of resistance to delamination. ISBN 0 580 44144X.

BS EN 338:2003. Structural timber –Strength class. ISBN 0 580 41845 6. BSI.

BS EN 386- (2001) Glued laminated timber. Performance requirements and minimum production requirements.

BS EN 391 (2001) Glued laminated timber — Delamination test of glue lines.

BS EN 408: 1995. Timber structures- Structural timber and glued laminated timber: determination of some physical and mechanical properties. British Standards Institution. ISBN 0 580 24284 6.

BS EN ISO 6946:1997. Building components and building elements — Thermal resistance and thermal transmittance —Calculation method. ISBN 0 580 26881 0.

BSI, (2005). British Standards Institute. <http://www.bsi-global.com/Eurocodes>.

Building regulations, (2006). Conservation of fuel and power. Draft approved document, subject to amendment prior to final publication. L1A work in new dwellings. 2006 edition. UK: Office of the Deputy Prime Minister.

Canadian Wood Council, (2000). Green by design: wood the best choice for the environment. <http://www.cwc.ca/>.

Chui, Y.H. & Craft, S., (2002). Fastener head pull-through resistance of plywood and oriented strand board. Published on the NRC Research Press web

site at <http://cjce.nrc.ca> (On 22 May 2002).

Chui, Y.H., (2000). Strength of OSB scarf joints in tension. *Wood and Fibre Science*, 32 (1) : 7-10. ISSN: 0735-6161.

Chung, W. A., (1964). The manufacture of Glue laminated timber structures. ISBN: 0510456014.

Clinch, Robert W. and Halligan, Alan F., (1989). Particleboard webbed I-beams, IN - (Proceedings of the Second Pacific Timber Engineering Conference, August, Auckland , New Zealand).

Cymap, (2006). Version 10. Building services software. www.cymap.com.

Dagher, H. J., Shaler, S.M. and Lowry, C., (1999). FRP Reinforced LVL and Structural I-Joists. IN- (*Proceedings of First International Conference on Advanced Engineered Wood Composites, Bar Harbor, ME. 5-8 July 1999.*)

Dahlbom, O., Petersson, H. and Ormarsson, S., (2000). Stiffness and shape stability grading analysis of sawn timber based on experimentally found growth characteristics. IN- (*Proceedings of the World Conference on Timber Engineering, Whistler Resort, British Colombia, Canada.*)

Danskin, J., (2005). Flooring systems. <http://www.danskin.co.uk/flooring/default.asp?p=24>.

Davies J.M., (2001). Light weight sandwich construction. UK: Blackwell Science. ISBN: 0632040270.

ECO Link (2001). Engineered wood products. Publication of Temperate Forest Foundation, Volume 11, Number 4, 2001:

EN 12369-1:2001. Wood based panels-characteristic values for structural design. Part 1: OSB, particleboards and fibreboards. ISBN 0 580 36993 5. CEN.

Endurathane product data, (2000). NZ Polymer and Developments Group Ltd. URL <http://www.polymer.co.nz/> .

EOTA (2000) Test methods for light composite beams and columns, Technical report TR 002, October 2000. 8pp.

European Organisation for Technical Approvals, (2000). Test methods for light composite wood-based beams and columns. (EOTA Technical Report 002.).

Fell, D., (2002). Segmenting single family home builders on measure of innovativeness, *Forest Products Journal*, June 2002.

Fisette, P., (1997). Choosing between Oriented strand board and plywood. Website of Building Materials and Wood Technology - http://www.umass.edu/bmatwt/publications/articles/osb_vs_plywood.html (On 14 Apr. 04).

Forest Products Laboratory, (1987). *Wood Handbook: Wood as an Engineering material*. (Agriculture Handbook, No.72). Madison, Wisconsin: USDA, Forest Service Forest Product laboratory.

Gaylord, E. H., Gaylord, C. N., & Stallmeyer, J. E (1996). *Structural engineering handbook*. Publisher: McGraw-Hill Publishing Co. ISBN: 0070237247.

Goldstein, E. W., (1999). *Timber construction for architects and builders*. (Construction series). McGraw-Hill. ISBN: 0-07-024580-0.

Grandt, A.F. (2003). *Fundamentals of structural integrity: damage tolerant design and nondestructive evaluation*. John Wiley & Sons. ISBN: 0471214590.

Grantham, R. & Enjily, V., (2003). *Multi-storey timber frame buildings – a designguide*, BR 454. London: BRE.

Graves, R.S. & Zarr, R.R., (1997). *Insulation materials: testing and applications (STP)*. American Society for Testing & Materials, (ASTM). ISBN: 0803124090.

Gulvanessian, H.; Calgaro, J-A. & Holicky, M., (2002). *Designers guide to EN 1990. Eurocode: Basis of structural design*. Published by Thomas Telford. ISBN 0-7277-3011-8.

Henriksen, K. & Frank, F. C., (1999). *Building construction- Timber bridges: guideline for wood protection by design*, Nordic wood, timber project, phase 2. Danish Technological Institute.

Hiles, L., (2002). APA. USA. *Forest Products Journal*, 52(10-15). Tacoma, Washington: The Engineered Wood Association. ISSN: 0015-7473
<http://www.wooduniversity.org> .

Hilson, B.O., Rodd, P.D., (1984) The effect of web Holes on the Behaviour and ultimate shearing strength of timber I-beams with hardboard webs. *Journal of the Institution of Structural Engineers*. pp. 69-78 and 90.

Hoffmeyer, P (1995) , Wood as a building material, Lecture A4. In Timber Engineering Step 1: Basis of design, material properties, structural components and joints, Ed. By Blass, H.J., Aune, P., Choo, B.S., Grolacher, R., Griffith, D.R., Hison, B.O., Racher, P. and Steck, G., Centrum Hout, Almere, The Netherlands: A4/1-A4/21, ISBN 90-5645-001-8.

Hoffmeyer, P., Brauner, L., Bostrom, L. & Solli, K.H., (1999). Tensile strength of Glulam laminations of Nordic Spruce. IN- (*Proceeding Pacific Timber Engineering Conference, Rotorua, New Zealand. March 14-18, 1999.*)

Inman , J. D., (2003). Engineering vibration. Prentice Hall. ISBN: 0130174483.

ISOPA, (1998). Fact sheet: recycling polyurethanes. Belgium, Brussels: European Isocyanate Producers Association.

IVPU, (1988). Eigenschaften von PUR-harschaum-warme-dammstoffen. 11th fully revised edition, June 1998. URL: <http://www.ivpu.de/>.

Jain, V. K., (2004). Evaluation of physical and mechanical properties and end-use classification for joinery, door and window shutters and frames and poles by conducting tests on strength properties. Dehra Dun: Indian Council of Forestry Research and Education.

Johansson, C.-J., Brundin, J. & Gruber, R., (1992). Stress grading of Swedish and German timber. A comparison of machine stress grading and three visual grading systems. Swedish National Testing and Research Institute, SP Report 1998:38.

Johansson. Carl-Johan, (2003). Grading of timber with respect to mechanical properties: pp 23-43. IN- (*Timber engineering. Edited by Thelandersson, S. & Larsen, H. ISBN 0 470 84469 8.*)

Juniper Consultancy Services, (1998). List of incinerators in Europe with a

capacity greater than 30kTpa with or without energy recovery and excluding co-combustion facilities. United Kingdom: Sheppards.

Kent, A & Williams, J. G., (1999). Encyclopaedia of microcomputers: Vol.23. Marcel Dekker. ISBN: 0824727215.

Kermani, A. & Bahadori-Jahromi, A., (2003). Composite insulated beams. British patent application, number 0319999172.3. UK: Patent Office.

Kermani, A., (1996). Influence of grain direction on in-plane strength properties of plywood. IN- (*Proceedings of the International Wood Engineering Conference, Oct. 28-31, 1996, New Orleans, USA. Vol. 3, pp 499-504.*)

Kermani, A., (1999). Structural Timber Design. Blackwell Science (UK)

ISBN: 0-632-05091-8.

Koschade, R., (2002). Sandwich panel construction. John Wiley and Sons. Ltd ISBN: 3-433-01617-8.

Lackner, R. & Foslie, M., (1988). Gran fra Vestlandet Styrke och sortering. Norwegian Institute of Wood Technology, Report. 74 pp.

Lam, F. & Prion, H.G.L., (2003). Engineered wood products for structural purposes Timber Engineering. Edited by Sven Thelandersson and Hans J. Larsen. ISBN: 0-470-84469-8.

Leicester, R. (2000). Why the stampede to engineered wood? *Building Innovation and Construction Technology*, (11) Feb. 2000.

Leichti, Robert J., Falk, Robert H. & Laufenberg, Theodore L., (1990). Prefabricated wood composite I-Beams. *Wood and Fiber Science*, 22 (1), 1990: 62-79.

Lewis, W.C. & Dawley, E.R. (1943 Reaffirm.1958). Design of plywood webs in box beams: stiffeners in box beam and details of design. USDA Forest Serv. No. 1318-A. Madison, WI.: Forest Prod.Lab. 12pp.

Lewis, W.C., Heebink, T.B. & Cottingham, W.S. (1944a, Reaffirm.1965). Design of plywood webs in box beams: buckling and ultimate strengths of shear webs of box beams having plywood face grain direction parallel or perpendicular to the axis of the beams. USDA Forest Serv., No.1318-D.

Madison, WI: Forest Prod.Lab. 34pp.

Lewis, W.C., Heebink, T.B. & Cottingham, W.S. (1944a, Reaffirm.1959) . Design of plywood box beams: the effect of repeated buckling on the ultimate strength of box beams with shear webs in the inelastic buckle range. USDA Forest Serv. No. 1318-E. Madison, WI: Forest Prod.Lab. 30pp.

Lowood, John P.E., (1997). Oriented strand board and waferboard. Engineered wood products. Willowdale, Ontario., Canada: Structural Board Association. ISBN: 0-9656736-0-X.

LUSAS finite element analysis software, Version 13.4. (2004)
<http://www.lusas.com>.

LUSAS-13.5, (2005). Finite Element software. <http://www.lusas.com>.

Mckenzie, W.M.C., (2000). Design of structural timber. Palgrave Macmillan. ISBN: 0-333-79236-X.

Mettem, C. J., (1986). Structural timber design and technology. Longman Higher Education. ISBN: 0582494850.

Morley, M., (2000). Building with structural insulated panels (SIPs). Taunton press. ISBN: 1-56158-351-0.

Nelson, Sherman P.E (1997), Structural composite lumber, IN – (*Trus Joist MacMillan. Engineered wood product: a guide for specifiers, designers and users. Ed. by Stephen Smulski. ISBN: 0-9656736-0-X.*)

New Zealand. Scion Research Centre. SCION website. Rotorua: SCION.
<http://www.scionresearch.com/>.

NHBC, (2000). Timber and concrete upper floors. National House Building Council. Chapter 6.4: Timber and concrete upper floors.

Nicholls, R., (2002). Low energy design. Action energy. Interface publishing. ISBN: 0-9539409-2-6.

NZS 3603, (1993). New Zealand standard. Timber structures standard.

- Oertel, G.**, (1996). Polyurethane Handbook: Chemistry - Raw Materials – Processing- Application – Properties. Hanser Gardner Publications. ISBN: 1569901570.
- Ohlsson, S.**, 1982. Floor vibrations and human discomfort. Doctoral thesis. Gothenburg, Sweden: Chalmers University of Technology.
- Ohlsson, S.**, 1988. Springiness and human-induced floor vibrations, Document D12:1988. Stockholm: Swedish Council for Building Research.
- ORICA, (2002).** Adhesives and resins, (2002). Sylvic R15/ Sylvic L5, technical data sheet. URL [http:// www.orica-adhesives.co.nz](http://www.orica-adhesives.co.nz).
- Overschee, Peter van & Moor, Bart L.R.De**, (1996). Subspace identification for linear systems: theory-implementation-applications. Kluwer Academic. ISBN: 0792397177.
- Ozelton, E.C. & Baird, J.A.** (2002). Timber designers' manual. 3rd ed. Blackwell. ISBN: 0-632-03978-7.
- Peeters, B., De Roeck , G., Pollet, T. & Schueremans, L.**, (1995). Stochastic subspace techniques applied to parameter identification of civil engineering structures, pp. 151-162. IN – (*Proceedings of new advances in modal synthesis of large structures: nonlinear, damped and nondeterministic cases, Lyon, France, 5-6 October 1995. Ed. by L. Jezequel.*)
- Pellicane, P.J. & Franco, N.** (1994). Modelling wood pole failure, Part 2: material and geometric considerations. *Wood Science and Technology*, 28 (4): 261-274.
- Persson, K.**, (2000). Micro mechanical modelling of wood and fibre properties. PhD thesis. Lund University: Department of Mechanics and materials.
- Pinocchio Data Systems.**, (2005). Pinocchio Data Systems. <http://www.pidats.com>.
- Product approval** (1996). Wisconsin Department of Commerce, Safety and Building Division, Approval 200024-W, SBD-5863 (R. 08/96).
- Pye, P.W. & Harrison, H.W.**, (2003). Building elements: floors and flooring, performance, diagnosis, maintenance, repair and the avoidance of defects. BR

460. 2nd ed. BRE. ISBN 1 86081 631 2.

Ranai, A., (2003) [Private communication: meeting with director of Fletcher Challenge Forests held in Origin plywood factory.] URL <http://www.origin.co.uk>.

Ratay, R., (2005). Structural condition assessment for serviceability: code compliance, rehabilitation, retrofitting, and adaptive reuse. John Wiley & Sons. ISBN: 0-471-64719-5.

Roark, J.R., (2003). Formulas for stress and strain. McGraw-Hill International. ISBN 0071210598.

Sandberg, D. & Stehr, M. (1997). Bending strength of I-beams with webs of wood fibre board and flanges of star-sawn triangular profiles. *Holz als Roh- und Werkstoff* 55(5):292.

Sarafin, T.P. & Larson, W.J. (eds), (1995). Spacecraft structures and mechanisms: from concept to launch. (Space Technology Library). Kluwer Academic. ISBN: 0792334760.

Schrieve, W. R. (1980). Full scale load testing of structures. Astm Intl. ISBN: 0686760204 .

SCION research institute, (ex New Zealand Forest Research Institute). SCION web page. URL: <http://www.scionresearch.com/home.aspx>.

Scottish Enterprise, (July 2004). Proof of Concept Programme. Projects underway. Composite insulated beams (CIB): a new engineered timber concept of potential use in the construction industry. <http://www.scottishenterprise.com>.

Shames, Irving H., & Pitarresi, James M., (1999). Introduction to solid mechanics. Pearson US Imports & PHIPEs. ISBN 013267758X.

Sherman, Nelson P.E., (1997). Engineered wood products: a guide for specifiers, designers & users, structural composite lumber, pp. 147-154. PFS Research Foundation. ISBN 0-9656736-0-X.

Smith, I., Landis, E. & Gong, M., (2003). Fracture and fatigue in wood. John Wiley and Sons. ISBN: 0-471-48708-2.

Smulski, S., (1997). Wood science specialists. Shutesbury, Massachusetts: Engineered Wood Products. ISBN: 0-9656736-0-X.

SNCCBLC, (2004), Website of French National Glued Laminated Structural Timber Contractors and Suppliers Trade Organisation
<http://www.glulam.org/Telecharge/Europe.pdf> (Used in Apr 04).

Spelter, H., (1997). Plywood niche narrows but producers still have ample opportunities. *PanelWorld*, 38 (5) September 1997: pp 28-31.

Steffen, A., Johansson, C. J., & Wormuth, E-W., (1997). Study of the relationship between flat-wise and edge-wise moduli of elasticity of sawn timber as a means to improve mechanical strength grading technology. *Holz als Roh und Werkstoff*, 55: 245-253.

TEAC, (2006). TEAC Instruments corporation. URL
<http://www.tic.teac.co.jp/en/products/recorder/recordingunit-det.html>.

The Council of the European Union, (1999). Landfill of waste. IN- (*Official Journal of the European Communities*, OJ L 182 (16.07.1999)).
<http://europa.eu.int/scadplus/leg/en/lvb/l21208.htm>.

Tingley, D., (1999). High-strength fiber reinforced plastic as reinforcement for wood flange I-beams. IN- (*Proceedings of First International Conference on Advanced Engineered Wood Composites, Bar Harbor, ME. 5-8 July 1999.*)

TRADA Timber I-joists 2003: application and design. TRADA Technology Ltd. URL: www.asktrada.co.uk .

TRADA, (1994). Eurocode design aid I. TRADA. ISBN: 1 899615083.

TRADA, (2001). Timber frame construction. 3rd ed. TRADA Technology ISBN: 1900510 32 4.

U.K. Office of Deputy Prime Minister, 2003. Implementation of structural Eurocodes in the UK. U.K. Office of the Deputy Prime Minister, February 2003. Product code 02BR00877.
<http://www.safety.odpm.gov.uk/bregs/index.htm>.

U.S., Office of Energy Efficiency and Renewable Energy, (2004). EREC reference Briefs: structural insulated panels. Web site of U.S., Department of

Energy at <http://www.eere.energy.gov/consumerinfo/refbriefs/bd1.html> (Used in 04/2004).

U.S.A., Department of Agriculture, Forest Service, Forest Products Laboratory, (1999). Wood handbook: wood as an engineering material. (General Technical Report FPL–GTR–113.) Madison, WI., USA.: Department of Agriculture, Forest Service, Forest Products Laboratory. 463p. ISBN: B0000EHVED.

Ugural, Ansel C. & Fenster, Saul K., (2003). Advanced strength and applied elasticity. 4th ed. ISBN: 0-13-047392-8. Pp.252-256.

UK National Annex to EN1995-1-1., (May 2004). Design of timber structures common rules and rules for buildings. Draft for public comment. BSI.

United Nations Economic Commission for Europe - UNECE, (2003). Forest products annual market analysis 2002-2004. *Timber Bulletin, LVI (3)* United Nations, Food and Agriculture Organization (FAO).

Waiariki Institute of Technology. (Home page.) <http://www.waiariki.ac.nz>.

Walker, J.C.F. (1993). Primary wood processing: Principle and practice. London: Chapman & Hall.

Weigand, E. & Strobbe, G., (1998). Recycling Polyurethanes: achievements in Europe. (Paper presented at the R'99 Congress (Recovery, Recycling, Re-integration), February 1998.)

URL: <http://www.environmental-center.com/articles/article426/WEI197C.htm>

Williamson, Thomas G. editor, (2002). APA Engineered wood handbook 2002. McGraw-Hill. ISBN: 0-07-136029-8.

Wood Wisdom, (2005). WoodWisdom-Net. <http://www.woodwisdom.net>.

Xu, P., (2000). The mechanical properties and stability of radiata pine structural timber. PhD thesis. New Zealand: University of Canterbury.

Yeh, B., (2002). APA engineered wood handbook, Thomas G. Williamson, editor. ISBN: 0-07-136029-8.

APPENDICES

Appendix A: Material properties of CIB beams

Table A.1. Young modulus of the CIB flange over a 2.1 m span

Span	Flange No	Width	Depth	E	Span	Flange No	Width	Depth	E
(mm)		(mm)	(mm)	(kN/mm ²)	(mm)		(mm)	(mm)	(kN/mm ²)
2100	1	89.67	45.38	5.36	2100	40	89.18	45.04	6.98
	2	89.35	45.17	5.41		41	87.31	44.4	7.02
	3	90.22	44.91	5.76		42	88.47	44.45	7.04
	4	90.41	45.66	5.78		43	87.82	44.79	7.07
	5	90.81	45.09	5.79		44	90.47	45.68	7.12
	6	89.14	44.76	5.94		45	90.33	45.43	7.14
	7	89.79	44.96	6.02		46	89.01	43.93	7.19
	8	90.15	45.29	6.14		47	90.79	45.59	7.19
	9	90.44	46.15	6.16		48	87.72	44.32	7.22
	10	89.65	45.22	6.17		49	89.29	44.41	7.28
	11	88.31	44.87	6.18		50	88.34	44.42	7.32
	12	89.45	44.51	6.24		51	89.75	45.12	7.33
	13	90.44	45.38	6.25		52	90.22	44.99	7.33
	14	89.79	44.58	6.27		53	89.83	45.18	7.35
	15	88.95	45.08	6.34		54	89.32	44.75	7.4
	16	90.86	46.11	6.34		55	88.65	44.87	7.46
	17	90.11	44.92	6.35		56	90.37	45.21	7.47
	18	89.95	44.62	6.36		57	88.6	44.24	7.48
	19	89.73	44.99	6.36		58	90.57	44.42	7.56
	20	90.24	44.79	6.36		59	89.01	44.73	7.57
	21	90.65	45.61	6.37		60	88.13	44.7	7.58
	22	90.46	45.18	6.38		61	91.04	45.79	7.61
	23	90.54	45.16	6.42		62	87.84	44.84	7.7
	24	89.87	44.85	6.53		63	88.5	44.8	7.72
	25	89.49	43.82	6.58		64	88.87	44.74	7.73
	26	89.66	44.82	6.59		65	88.36	44.38	7.74
	27	89.93	44.97	6.59		66	90.56	45.46	7.74
	28	88.21	44.48	6.74		67	90.26	44.88	7.76
	29	89.56	44.32	6.74		68	87.01	44.38	7.8
	30	89.92	45.11	6.77		69	90.5	45.58	7.83
	31	89.88	45.05	6.81		70	90.33	45.21	7.86
	32	89.41	45.21	6.83		71	88.36	44.6	7.89
	33	89.36	44.92	6.84		72	90.52	44.95	7.91
	34	89.28	44.73	6.9		73	90.31	45.07	7.96
	35	89.16	44.66	6.92		74	89.06	45.14	8
	36	90.53	45.43	6.95		75	91.59	45.47	8.01
	37	88.92	45.02	6.96		76	88.54	44.6	8.03
	38	87.52	43.89	6.96		77	90.29	44.73	8.06
	39	90.6	45.74	6.97		78	90.44	45.94	8.06

Table A.1 Continued

Span	Flange No	Width	Depth	E	Span	Flange No	Width	Depth	E
(mm)		(mm)	(mm)	(kN/mm ²)	(mm)		(mm)	(mm)	(kN/mm ²)
2100	79	88.67	44.84	8.09	2100	118	89.4	45	8.64
	80	91.55	45.32	8.09		119	87.72	44.43	8.67
	81	88.27	44.54	8.11		120	89.03	44.42	8.7
	82	87.9	44.13	8.14		121	90.49	45.33	8.79
	83	89.34	45.37	8.14		122	90.43	45.47	8.84
	84	87.98	44.58	8.15		123	89.13	44.11	8.85
	85	90.4	45.3	8.15		124	90.73	44.98	8.86
	86	89.52	45.18	8.16		125	90.34	45.26	8.86
	87	90.64	45.53	8.17		126	88.91	44.53	8.89
	88	88.58	44.27	8.19		127	90.07	45.27	8.89
	89	90.04	45.35	8.19		128	90.37	45.35	8.89
	90	89.08	44.49	8.19		129	90.18	44.66	8.89
	91	88.23	44.53	8.21		130	90.56	46.06	8.94
	92	90.08	45.44	8.21		131	89.33	44.65	8.99
	93	87.86	44.22	8.23		132	90.5	46.12	8.99
	94	89.32	44.12	8.28		133	88.87	44.11	9.02
	95	90.23	45.54	8.28		134	88.76	44.9	9.04
	96	89.99	46.12	8.29		135	88.67	44.66	9.1
	97	90.17	45.42	8.36		136	90.44	45.65	9.16
	98	90.28	44.81	8.36		137	90.59	46.1	9.17
	99	89.11	44.63	8.37		138	89.75	44.99	9.21
	100	88.56	44.61	8.38		139	90.26	45.19	9.21
	101	87.78	44.22	8.39		140	90.64	45.37	9.23
	102	88.11	44.11	8.43		141	90.58	45.36	9.33
	103	88.06	44.3	8.45		142	89	43.89	9.34
	104	89.65	45.31	8.48		143	88.13	44.77	9.39
	105	88.09	44.49	8.5		144	89.1	44.7	9.42
	106	89.31	45.29	8.5		145	89.32	45.02	9.43
	107	88.64	44.18	8.52		146	90.34	45.38	9.45
	108	90.62	45.32	8.52		147	87.65	44.08	9.46
109	88.06	43.36	8.53	148	88.23	44.46	9.46		
110	86.87	43.44	8.56	149	90.71	45.67	9.47		
111	90.49	45.84	8.58	150	88.96	43.84	9.5		
112	88.1	44.56	8.59	151	88.42	44.44	9.51		
113	90	44.67	8.59	152	90.36	44.96	9.51		
114	88.76	44.43	8.6	153	88.11	43.59	9.58		
115	90.35	45.32	8.6	154	89.19	43.74	9.6		
116	90.63	45.25	8.6	155	87.68	44.63	9.62		
117	89.29	44.31	8.63	156	89.01	44.14	9.73		

Table A.1 Continued

Span	Flange No	Width	Depth	E	Span	Flange No	Width	Depth	E
(mm)		(mm)	(mm)	(kN/mm ²)	(mm)		(mm)	(mm)	(kN/mm ²)
2100	157	90.41	45.88	9.81	2100	196	88.71	45.04	10.7
	158	90.61	45.33	9.82		197	89.91	45.32	10.71
	159	90.40	45.17	9.86		198	90.42	45.23	10.77
	160	88.97	45.03	9.86		199	90.27	45.66	10.78
	161	86.52	43.03	9.87		200	90.39	46.22	10.84
	162	90.52	45.4	9.89		201	90.71	46.02	10.85
	163	90.34	45.89	9.9		202	87.57	44.2	10.86
	164	89.70	44.91	9.91		203	90.45	45.44	10.86
	165	90.55	45.38	9.92		204	88.22	43.61	10.87
	166	88.36	43.44	9.94		205	86.57	44.33	10.9
	167	90.26	45.44	9.97		206	87.88	44.19	10.95
	168	90.47	45.39	9.98		207	90.41	44.9	11.03
	169	90.6	46.58	10.04		208	90.55	45.33	11.04
	170	88.01	44.45	10.05		209	88.92	44.78	11.07
	171	91.02	46.28	10.06		210	87.4	44.33	11.12
	172	88.9	44.93	10.13		211	87.78	43.71	11.12
	173	88.78	43.81	10.16		212	90.49	45.52	11.14
	174	90.44	45.56	10.17		213	90.71	46.44	11.17
	175	88.27	44.84	10.19		214	88.90	45.07	11.2
	176	90.35	45.55	10.2		215	86.99	44.56	11.23
177	87.62	44.65	10.21	216	89.85	44.19	11.24		
178	90.60	45.09	10.23	217	90.56	45.23	11.24		
179	88.69	44.51	10.26	218	90.45	45.35	11.26		
180	90.50	45.82	10.32	219	90.66	45.42	11.34		
181	88.30	44.32	10.34	220	89.86	44.98	11.37		
182	86.01	44	10.38	221	90.71	46.45	11.4		
183	90.51	45.27	10.38	222	90.5	45.64	11.49		
184	90.36	44.84	10.42	223	90.57	45.15	11.52		
185	87.65	44.35	10.46	224	87.24	43.76	11.54		
186	87.83	44.47	10.51	225	87.00	43.73	11.59		
187	89.39	44.25	10.52	226	87.91	44.49	11.66		
188	90.63	45.17	10.52	227	89.85	45.03	11.68		
189	90.31	45.33	10.57	228	90.34	45.24	11.75		
190	90.62	46.15	10.57	229	90.51	45.75	11.75		
191	90.68	45.33	10.57	230	90.77	45.22	11.88		
192	89.60	45.19	10.64	231	90.71	45.97	11.9		
193	90.75	45.5	10.64	232	90.57	45.45	12.12		
194	90.45	45.41	10.65	233	90.65	45.77	12.13		
195	90.67	45.72	10.69	234	90.81	45.56	12.14		

Table A.1 Continued

Span	Flange No	Width	Depth	E	Span	Flange No	Width	Depth	E
(mm)		(mm)	(mm)	(kN/mm ²)	(mm)		(mm)	(mm)	(kN/mm ²)
2100	235	90.64	45.42	12.18	2100	252	90.55	45.3	12.85
	236	90.8	45.34	12.23		253	90.29	45.23	12.91
	237	90.55	45.48	12.31		254	90.61	44.34	12.92
	238	90.45	45.14	12.32		255	90.45	45.13	12.95
	239	90.83	45.49	12.36		256	86.87	44.24	13.03
	240	90.2	45.34	12.38		257	90.59	44.34	13.2
	241	90	44.94	12.39		258	85.87	44.32	13.22
	242	90.63	45.77	12.45		259	90.15	45.21	13.25
	243	87.84	44.81	12.47		260	89.49	44.67	13.32
	244	90.06	45.02	12.47		261	90.1	45.24	13.54
	245	90.51	45.78	12.51		262	90.7	45.26	13.72
	246	90.36	45.14	12.53		263	87.99	44.47	13.92
	247	90.1	45.3	12.54		264	90.46	45.31	14.23
	248	89.56	46.18	12.66		265	90.35	45.11	14.42
	249	89.87	45.17	12.67		266	90.29	45.36	14.59
250	90.17	44.98	12.71	267	90.37	45.28	15.07		
251	88.31	44.62	12.76						

Table A.2 Timber flanges for short CIBs grouped by their E values

Profile No	(6)	(13)	(3)	(10)	(7)	(14)	(5)	(12)	(1)
Colour code	Half orange	Orange	Half Red	Red	Half yellow	Yellow	Half blue	Blue	No colour
Flange ID	41-50	42-51	43-52	44-53	45-54	46-55	47-56	48-57	49-58
	59-68	60-69	61-70	62-71	63-72	64-73	65-74	66-75	67-76
	77-86	78-87	79-88	80-89	81-90	82-91	83-92	84-93	85-94
	95-104	96-105	97-106	98-107	99-108	100-109	101-110	102-111	103-112
	113-122	114-123	115-124	116-125	117-126	118-127	119-128	120-129	121-130
	131-140	132-141	133-142	134-143	135-144	136-145	137-146	138-147	139-148
	149-158	150-159	151-160	152-161	153-162	154-163	155-164	156-165	157-166
	167-176	168-177	169-178	170-179	171-180	172-181	173-182	174-183	175-184
	185-194	186-195	187-196	188-197	189-198	190-199	191-200	192-201	193-202
	203-212	204-213	205-214	206-215	207-216	208-217	209-218	210-219	211-220
	221-230	222-231	223-232	224-233	225-234	226-235	227-236	228-237	229-238
	239-248	240-249	241-250	242-251	243-252	244-253	245-254	246-255	247-256

Table A 3 Young modulus of the timber flanges tested over a 4.5 m span

Span	Flange No	Width	Depth	E	Span	Flange No	Width	Depth	E
(mm)		(mm)	(mm)	(kN/mm ²)	(mm)		(mm)	(mm)	(kN/mm ²)
4500	1	90.53	45.58	5.45	4500	29	90.13	44.98	9.65
	2	90.98	45.93	5.67		30	90.50	45.92	9.79
	3	90.50	45.11	5.75		31	90.34	45.30	9.83
	4	90.43	45.19	6.05		32	90.54	44.61	9.87
	5	90.58	45.76	6.75		33	90.67	45.16	10.23
	6	90.81	45.41	6.80		34	90.93	45.28	10.28
	7	90.55	45.08	7.04		35	90.40	45.10	10.42
	8	90.21	45.26	7.04		36	90.22	45.48	10.48
	9	90.26	45.56	7.14		37	90.46	45.40	10.49
	10	90.25	45.45	7.17		38	90.94	45.20	10.50
	11	90.50	46.76	7.24		39	89.53	45.18	10.55
	12	90.39	45.09	7.31		40	90.22	44.89	10.96
	13	90.77	45.21	7.56		41	90.22	45.17	11.00
	14	90.94	46.92	7.71		42	89.79	45.20	11.09
	15	90.37	45.18	7.91		43	90.25	45.10	11.22
	16	90.50	45.95	8.24		44	90.31	46.32	11.50
	17	90.29	45.48	8.64		45	90.09	45.23	11.84
	18	90.27	45.43	8.65		46	90.40	45.11	11.85
	19	90.65	45.36	8.71		47	90.40	45.22	12.56
	20	90.38	45.24	8.72		48	90.34	45.04	13.35
	21	90.33	45.24	8.93		49	89.85	44.95	13.62
	22	90.59	45.15	8.96		50	90.63	45.33	13.84
	23	90.25	45.46	9.09		51	90.41	45.32	14.29
	24	90.63	45.32	9.16		52	90.71	45.23	14.54
	25	90.45	44.27	9.23		53	90.78	45.04	14.81
	26	90.23	45.30	9.26		54	90.49	45.35	16.03
	27	90.79	45.36	9.31		55	90.10	45.25	16.73
	28	90.63	45.24	9.54		----	----	----	----

Table A 4. Timber flanges for Long CIB beams grouped by their E values

Profile No	(6)	(13)	(3)	(10)	(7)	(14)	(5)	(12)
Colour code	Half orange	orange	Half Red	Red	Half yellow	yellow	Half blue	blue
Flange ID	7-15	8-16	9-17	10-18	11-19	12-20	13-21	14-22
	23-31	24-32	25-33	26-34	27-35	28-36	29-37	30-38
	39-47	40-48	41-49	42-50	43-51	44-52	45-53	46-54

Table A 5. Young modulus of 20 randomly selected LVL flanges over a 2.1 m span

Span	Flange No	Width	Depth	E	Span	Flange No	Width	Depth	E
(mm)		(mm)	(mm)	(kN/mm ²)	(mm)		(mm)	(mm)	(kN/mm ²)
2100	100	90.3	45.69	12.87	2100	110	90.2	45.56	10.68
	101	90.57	46.23	11.78		111	90.3	45.64	11.34
	102	90.36	45.81	11.77		112	90.25	45.79	12.22
	103	90.26	45.77	11.15		113	90.53	45.37	11.64
	104	90.21	45.82	12.11		114	90.25	45.62	11.90
	105	90.36	45.58	10.32		115	90.37	46.11	11.88
	106	90.46	45.53	10.20		116	90.33	45.15	11.89
	107	90.57	46.07	11.85		117	90.17	46.00	12.57
	108	90.15	45.81	12.39		118	90.34	45.53	10.51
	109	90.23	45.92	12.32		119	90.4	45.51	12.42

Table A.6 Young modulus of 6 randomly selected LVL flanges over a 4.5 m span

Span	Flange No	Width	Depth	E	Span	Flange No	Width	Depth	E
(mm)		(mm)	(mm)	(kN/mm ²)	(mm)		(mm)	(mm)	(kN/mm ²)
4500	500	90	45	12.70	4500	503	90	45	10.75
	501	90	45	11.36		504	90	45	10.24
	502	90	45	10.73		505	90	45	10.56

Table A.7 Young modulus of the additional timber flanges tested over a 4.5 m span

Span	Flange No	Width	Depth	E	Span	Flange No	Width	Depth	E
(mm)		(mm)	(mm)	(kN/mm ²)	(mm)		(mm)	(mm)	(kN/mm ²)
4500	600	90.54	45.14	7.59	4500	613	90.39	45.31	10.39
	601	90.20	45.26	7.73		614	90.21	44.26	10.57
	602	90.25	45.08	8.05		615	90.45	45.29	10.70
	603	90.24	45.46	8.05		616	90.42	46.91	10.72
	604	90.93	45.38	8.11		617	90.57	45.17	11.04
	605	89.52	45.18	8.14		618	90.80	45.94	11.78
	606	90.21	45.16	8.15		619	90.53	45.42	11.95
	607	90.36	44.87	8.55		620	90.66	45.35	11.95
	608	90.39	45.15	8.93		621	90.49	45.23	12.06
	609	90.45	45.18	9.52		622	90.46	45.23	12.21
	610	90.57	45.08	9.64		623	90.92	45.14	12.43
	611	90.80	46.30	9.85		624	90.39	45.47	13.15
	612	90.92	45.45	10.23		625	90.21	45.45	14.10

Table A.8 Timber flanges for additional CIBs grouped by their E values

Flanges for short beams			Flanges for long beams			
Profile No	(9)	(16)	Profile No	(1)	(9)	(16)
Colour code	Half red	Red	Colour code	No colour	Half red	Red
Flange ID	603-603	604-604	Flange ID	600-605	601-606	602-607
	608-608	609-609		610-615	611-616	612-617
	613-613	614-614		618-621	619-622	620-623
				624-625		

Table A.9 Material properties of the Plywood

Table A.9(a) Modulus of rigidity, moisture content and density of plywood

Sample No	Size	Thickness	Modulus of rigidity	Moisture content	Density
	(mm ²)	(mm)	(N/mm ²)	(%)	(kg/m ³)
1	289 × 289	8.96	761.27	7.71	439.03
2		8.89	788.91	8.00	450.95
3		8.89	936.76	7.75	445.95
4		9.06	832.08	8.09	468.28
5		8.92	588.89	9.02	476.37
6		9.01	610.60	8.87	456.80
Ave value			8.96	753.09	8.24

Table A.9(b) MoE of the Plywood with the face grain parallel to the span

Sample No	Width	Depth	Slop	Max load
	(mm)	(mm)	(N/mm)	(N)
1	300.73	9.32	117.65	3706
2	300.36	9.38	178.57	3866
3	300.32	9.12	204.08	5650
4	300.46	9.03	163.93	5008
5	299.03	9.19	166.67	5852
Ave value	300.18	9.21	166.18	4816.4

Table A.9(c) MoE of the Plywood with the face grain perpendicular to the span

Sample No	Width	Depth	Slop	Max load
	(mm)	(mm)	(N/mm)	(N)
1	300.56	9.44	17.24	914
2	300.70	9.34	16.67	856
3	300.21	9.51	15.63	935
4	300.41	9.21	17.24	----
5	300.10	9.22	20.83	902
Ave value	300.40	9.34	17.52	902

Table A.10 Statistical method for sorting and numbering the beams

Set	Initial matching			Final matching			
	Profile 6			Profile 6			
	S.No	Flanges ID	E (kN/mm ²)	S.No	Flanges ID	Beam ID	E (kN/mm ²)
1	1	41-50	7.02-7.32	1	41-50	200	7.02-7.32
	2	59-68	7.57-7.80	12	239-248	201	12.36-12.66
	3	77-86	8.06-8.16	5	113-122	202	8.59-8.84
			AVE 7.66				AVE 9.47
2	4	95-104	8.28-8.48	2	59-68	203	7.57-7.80
	5	113-122	8.59-8.84	11	221-230	204	11.40-11.88
	6	131-140	8.99-9.23	6	131-140	205	8.99-9.23
			AVE 8.74				AVE 9.48
3	7	149-158	9.47-9.82	3	77-86	206	8.06-8.16
	8	167-176	9.97-10.20	10	203-212	207	10.86-11.14
	9	185-194	10.46-10.65	7	149-158	208	9.47-9.82
			AVE 10.1				AVE 9.59
4	10	203-212	10.86-11.14	4	95-104	209	8.28-8.48
	11	221-230	11.40-11.88	9	185-194	210	10.46-10.65
	12	239-248	12.36-12.66	8	167-176	211	9.97-10.20
			AVE 11.72				AVE 9.67

*S.No: Sorting number

Table A.11 Short CIB profiles and ID, sorted by their MoEs
A.11(a) I-beam Profile

Initial matching			Final matching		
Profile (1)			Profile (1)-I-beam		
S.No	Top-Bottom Flanges ID	Top-Bottom MoE	S.No	Top-Bottom Flanges ID	BEAM ID
		GPa			
1	49-58	7.28-7.56	1	49-58	302
2	67-76	7.76-8.03	12	247-256	303
3	85-94	8.15-8.28	5	121-130	304
4	103-112	8.45-8.59	2	67-76	305
5	121-130	8.79-8.94	11	229-238	306
6	139-148	9.21-9.46	6	139-148	307
7	157-166	9.81-9.94	3	85-94	308
8	175-184	10.19-10.42	10	211-220	309
9	193-202	10.64-10.86	7	157-166	310
10	211-220	11.12-11.37	4	103-112	311
11	229-238	11.75-12.32	9	193-202	312
12	247-256	12.54-13.03	8	175-184	313

A.11(b) Double I-beam profile

Initial matching			Final matching		
Profile 3			Profile 3-Double I-beam		
S.No	Top-Bottom Flanges ID	MoE	S.No	Top-Bottom Flanges ID	BEAM ID
		GPa			
1	43-52	7.07-7.33	1	43-52	224
2	61-70	7.61-7.86	12	241-250	225
3	79-88	8.09-8.19	5	115-124	226
4	97-106	8.36-8.50	2	61-70	227
5	115-124	8.60-8.86	11	223-232	228
6	133-142	9.02-9.34	6	133-142	229
7	151-160	9.51-9.86	3	79-88	230
8	169-178	10.04-10.23	10	205-214	231
9	187-196	10.52-10.70	7	151-160	232
10	205-214	10.90-11.20	4	97-106	233
11	223-232	11.52-12.12	9	187-196	234
12	241-250	12.39-12.71	8	169-178	235

A.11(c) Filled Double I-beam profile

Initial matching			Final matching		
Profile 10			Profile 10- Filled Double I-beam		
S.No	Top-Bottom Flanges ID	Top-Bottom MoE	S.No	Top-Bottom Flanges ID	BEAM ID
		GPa			
1	44-53	7.12-7.35	1	44-53	236
2	62-71	7.70-7.89	12	242-251	237
3	80-89	8.09-8.19	5	116-125	238
4	98-107	8.36-8.52	2	62-71	239
5	116-125	8.60-8.86	11	224-233	240
6	134-143	9.04-9.39	6	134-143	241
7	152-161	9.51-9.87	3	80-89	242
8	170-179	10.05-10.26	10	206-215	243
9	188-197	10.52-10.71	7	152-161	244
10	206-215	10.95-11.23	4	98-107	245
11	224-233	11.54-12.13	9	188-197	246
12	242-251	12.45-12.76	8	170-179	247

A.11(d) Recessed beam Profile

Initial matching			Final matching		
Profile 5			Profile 5- Recessed beam		
S.No	Top-Bottom Flanges ID	Top-Bottom MoE	S.No	Top-Bottom Flanges ID	BEAM ID
		GPa			
1	47-56	7.19-7.47	1	47-56	272
2	65-74	7.74-8	12	245-254	273
3	83-92	8.14-8.21	5	119-128	274
4	101-110	8.39-8.56	2	65-74	275
5	119-128	8.67-8.89	11	227-236	276
6	137-146	9.17-9.45	6	137-146	277
7	155-164	9.62-9.91	3	83-92	278
8	173-182	10.16-10.38	10	209-218	279
9	191-200	10.57-10.84	7	155-164	280
10	209-218	11.07-11.26	4	101-110	281
11	227-236	11.68-12.23	9	191-200	282
12	245-254	12.51-12.92	8	173-182	283

A.11(e) Filled Recessed beam Profile

Initial matching			Final matching		
Profile 12			Profile 12- Filled Recessed Beam		
S.No	Top-Bottom Flanges ID	Top-Bottom MoE	S.No	Top-Bottom Flanges ID	BEAM ID
		GPa			
1	48-57	7.22-7.48	1	48-57	284
2	66-75	7.74-8.01	12	246-255	285
3	84-93	8.15-8.23	5	120-129	286
4	102-111	8.43-8.58	2	66-75	287
5	120-129	8.70-8.89	11	228-237	288
6	138-147	9.21-9.46	6	138-147	289
7	156-165	9.73-9.92	3	84-93	290
8	174-183	10.17-10.38	10	210-219	291
9	192-201	10.64-10.85	7	156-165	292
10	210-219	11.12-11.34	4	102-111	293
11	228-237	11.75-12.31	9	192-201	294
12	246-255	12.53-12.95	8	174-183	295

C.11(f) Box beam Profile

Initial matching			Final matching		
Profile 6			Profile 6- Box beam		
S.No	Top-Bottom Flanges ID	Top-Bottom MoE	S.No	Top-Bottom Flanges ID	BEAM ID
		GPa			
1	41-50	7.02-7.32	1	41-50	200
2	59-68	7.57-7.80	12	239-248	201
3	77-86	8.06-8.16	5	113-122	202
4	95-104	8.28-8.48	2	59-68	203
5	113-122	8.59-8.84	11	221-230	204
6	131-140	8.99-9.23	6	131-140	205
7	149-158	9.47-9.82	3	77-86	206
8	167-176	9.97-10.20	10	203-212	207
9	185-194	10.46-10.65	7	149-158	208
10	203-212	10.86-11.14	4	95-104	209
11	221-230	11.40-11.88	9	185-194	210
12	239-248	12.36-12.66	8	167-176	211

* Each group has 12 members which are divided within four sets (Table A 12)

**MoE: Apparent modulus of Elasticity

A.11(g) Filled Box beam Profile

Initial matching			Final matching		
Profile 13			Profile 13- Filled Box beam		
S.No	Top-Bottom Flanges ID	Top-Bottom MoE	S.No	Top-Bottom Flanges ID	BEAM ID
		GPa			
1	42-51	7.04-7.33	1	42-51	212
2	60-69	7.58-7.83	12	240-249	213
3	78-87	8.06-8.17	5	114-123	214
4	96-105	8.29-8.50	2	60-69	215
5	114-123	8.60-8.85	11	222-231	216
6	132-141	8.99-9.33	6	132-141	217
7	150-159	9.5-9.86	3	78-87	218
8	168-177	9.98-10.21	10	204-213	219
9	186-195	10.51-10.69	7	150-159	220
10	204-213	10.87-11.17	4	96-105	221
11	222-231	11.49-11.90	9	186-195	222
12	240-249	12.38-12.67	8	168-177	223

A.11(h) Boxed I-beam Profile

Initial matching			Final matching		
Profile 7			Profile 7- Boxed I-beam		
S.No	Top-Bottom Flanges ID	Top-Bottom MoE	S.No	Top-Bottom Flanges ID	BEAM ID
		GPa			
1	45-54	7.14-7.40	1	45-54	248
2	63-72	7.72-7.91	12	243-252	249
3	81-90	8.11-8.19	5	117-126	250
4	99-108	8.37-8.52	2	63-72	251
5	117-126	8.63-8.89	11	225-234	252
6	135-144	9.10-9.42	6	135-144	253
7	153-162	9.58-9.89	3	81-90	254
8	171-180	10.06-10.32	10	207-216	255
9	189-198	10.57-10.77	7	153-162	256
10	207-216	11.03-11.24	4	99-108	257
11	225-234	11.59-12.14	9	189-198	258
12	243-252	12.47-12.85	8	171-180	259

A.11(i) Filled Boxed I-beam Profile

Initial matching			Final matching		
Profile 14			Profile 14- Filled Boxed I-beam		
S.No	Top-Bottom Flanges ID	Top-Bottom MoE	S.No	Top-Bottom Flanges ID	BEAM ID
		GPa			
1	46-55	7.19-7.46	1	46-55	260
2	64-73	7.73-7.96	12	244-253	261
3	82-91	8.14-8.21	5	118-127	262
4	100-109	8.38-8.53	2	64-73	263
5	118-127	8.64-8.89	11	226-235	264
6	136-145	9.16-9.43	6	136-145	265
7	154-163	9.6-9.90	3	82-91	266
8	172-181	10.13-10.34	10	208-217	267
9	190-199	10.57-10.78	7	154-163	268
10	208-217	11.04-11.24	4	100-109	269
11	226-235	11.66-12.18	9	190-199	270
12	244-253	12.47-12.91	8	172-181	271

A.11(j) Boxed Double I-beam Profile

Initial matching			Final matching		
Profile 9			Profile 9- Boxed Double I-beam		
S.No	Top-Bottom Flanges ID	Top-Bottom MoE	S.No	Top-Bottom Flanges ID	BEAM ID
		GPa			
1	603-603	8.05-8.05	1	603-603	296
2	608-608	8.93-8.93	2	608-608	297
3	613-613	10.39-10.39	3	613-613	298

A.11(k) Filled Boxed Double I-beam Profile

Initial matching			Final matching		
Profile 16			Profile 16-Filled Boxed Double I-beam		
S.No	Top-Bottom Flanges ID	Top-Bottom MoE	S.No	Top-Bottom Flanges ID	BEAM ID
		GPa			
1	604-604	8.11-8.11	1	604-604	299
2	609-609	9.52-9.52	2	609-609	300
3	614-614	10.57-10.57	3	614-614	301

Table A.12 Long CIB profiles and ID sorted by their MoEs

Profile 1-I-Beam							
S.No	Top-Bottom Flanges ID	Top-Bottom MoE	BEAM ID	S.No	Top-Bottom Flanges ID	Top-Bottom MoE	BEAM ID
		GPa					
1	600-605	7.59-8.14	344				
2	610-615	9.64-10.7	345				
3	618-621	11.78-12.06	346				
Profile 3-Double I-beam				Profile 10-Filled Double I-beam			
1	9-17	7.14-8.64	320	1	10-18	7.17-8.65	323
2	25-33	9.23-10.23	321	2	26-34	9.26-10.28	324
3	41-49	11-13.62	322	3	42-50	11.09-13.84	325
Profile 5- Recessed beam				Profile 12- Filled Recessed beam			
1	13-21	7.56-8.93	332	1	13-21	7.71-8.96	335
2	29-37	9.65-10.49	333	2	29-37	9.79-10.50	336
3	45-53	11.84-14.81	334	3	45-53	11.85-16.03	337
Profile 6- Box Beam				Profile 13- Filled Box beam			
1	7-15	7.04-7.91	314	1	7-15	7.04-8.24	317
2	23-31	9.09-9.83	315	2	23-31	9.16-9.87	318
3	39-47	10.55-12.56	316	3	39-47	10.96-13.35	319
Profile 7-Boxed I-beam				Profile 14-Filled Boxed I-beam			
1	11-19	7.24-8.71	326	1	12-20	7.31-8.72	329
2	27-35	9.31-10.42	327	2	28-36	9.54-10.48	330
3	43-51	11.22-14.29	328	3	44-52	11.50-14.54	331
Profile 9-Boxed Double I-beam				Profile 16- Filled Boxed Double I-beam			
1	601-606	7.73-8.15	338	1	602-607	8.05-8.55	341
2	611-616	9.85-10.72	339	2	612-617	10.23-11.04	342
3	619-622	11.95-12.21	340	3	620-623	11.95-12.43	343

Table A.13 Short CIBs IDs for those made with LVL flanges

CIB beams with LVL flanges			
Profile 2-LVL I-Beam	Beam ID	N/A	Beam ID
	390		---
	391		---
	392		---
	393		---
	394		---
	395		---
	396		---
	397		---
	398		---
Profile 4-LVL Double I-Beam	368	Filled LVL Double I-Beam	355
	369		356
	370		357
	371		358
	372		359
	---		360
	---		361
	---		362
	---		363
	---		364
	---		365
	---		366
	---		367
	---		373
	---		374
---	375		
---	376		
LVL Boxed I-Beam	377	Filled LVL Boxed I-Beam	382
	378		383
	379		384
	380		385
	381		386
	---		387
	---		388
	---		389

Table A.14 Long CIBs IDs for those made with LVL flanges

Long CIB beams with LVL flanges			
Profile 2-LVL I-beam	Beam ID	N/A	Beam ID
	353		----
	354		----
Profile 4-LVL Double I-beam	349	Profile 11-Filled LVL Double I-	347
	350		348
Profile 8-LVL Boxed I-beam	351	N/A	----
	352		----

Table A 15. Moisture content of the top and bottom timber flanges of CIBs

Beam ID	Flange ID	Moisture content %			AVE	Flange ID	Moisture content %			AVE
		I*	II	III			I	II	III	
199	266	12.5	12.5	13.9	13.0	257	11.0	11.3	11.3	11.2
200	41	11.6	11.4	11.6	11.5	50	11.6	12.1	12.2	12.0
201	239	12.6	12.4	13.4	12.8	248	11.6	12.4	13.7	12.6
202	113	12.4	12.6	13.3	12.8	122	11.4	11.6	12	11.7
203	59	10.9	10.9	10.5	10.8	68	12.1	11.9	12.6	12.2
204	221	12.5	12.7	12.1	12.4	230	12.2	11.9	14.3	12.8
205	131	13.0	13.8	12.4	13.1	140	10.9	11	12.4	11.4
206	77	12.4	12.2	11.9	12.2	86	13.0	12.2	12.6	12.6
207	203	13.4	11.6	11.2	12.1	212	14.1	13.2	12.8	13.4
208	149	11.0	11.6	11.6	11.4	158	12.2	12.8	13.3	12.8
209	95	11.4	11.5	11.6	11.5	104	10.6	11.6	14.3	12.2
210	185	12.6	12.6	11	12.1	194	11.6	11.5	11.8	11.6
211	167	13.4	13.2	12.5	13.0	176	12.2	12.6	10.5	11.8
		Average			12.2		Average			12.2
212	42	11.9	12.1	12.6	12.2	51	10.9	13.3	10.2	11.5
213	240	12.1	12.5	12.6	12.4	249	13.8	13.7	13.6	13.7
214	114	13.2	11.5	11.6	12.1	123	10.5	11	11.3	10.9
215	60	10.3	12.7	10.9	11.3	69	9.2	8.5	8.5	8.7
216	222	12.2	11.9	12.1	12.1	231	12.5	11.4	12.2	12.0
217	132	12.7	12.8	12.1	12.5	141	9.9	9.6	9.5	9.7
218	78	11.4	10.7	11.9	11.3	87	13.7	13.4	12.4	13.2
219	204	12.5	11.9	11.2	11.9	213	10.2	10	9	9.7
220	150	11.4	11.6	11.6	11.5	159	12	11.9	12	12.0
221	96	11.5	11.2	11.5	11.4	105	12	11.9	12.5	12.1
222	186	11.5	10.7	11.4	11.2	195	13.3	11.6	13.1	12.7
223	168	11.4	11.4	11.5	11.4	177	11.6	12.1	12	11.9
		Average			11.8		Average			11.5

Table A.15. Continued

Beam ID	Flange ID	Moisture content %			AVE	Flange ID	Moisture content %			AVE
		I	II	III			I	II	III	
224	43	11.4	11.5	9.6	10.8	52	11.3	11.6	11.2	11.4
225	241	14.8	14.3	12.6	13.9	250	14.5	14	14.5	14.3
226	115	11.6	11.4	11.6	11.5	124	13.8	13	12.4	13.1
227	61	11.5	9.6	11.3	10.8	70	11.9	12.8	12.7	12.5
228	223	11.9	12	12.8	12.2	232	11.6	11.6	12.2	11.8
229	133	11.6	11.3	11.6	11.5	142	10.6	11.5	11.6	11.2
230	79	9.3	9.5	9.6	9.5	88	10	11	10.6	10.5
231	205	12.2	12.6	13	12.6	214	12.2	12.4	12.8	12.5
232	151	13.1	13.8	12.6	13.2	160	12.1	12.2	12.6	12.3
233	97	11.9	12.8	11.6	12.1	106	10.5	10.9	11.4	10.9
234	187	11.6	11.6	13.9	12.4	196	12	12.8	13.6	12.8
235	169	12.4	14	13.1	13.2	178	12.5	11.6	11.8	12.0
		Average			12.0		Average			12.1

*I,II and III : Results of readings one, two and three relevant to beginning ,middle and end of the beam respectively

Table A.15 Continued

Beam ID	Flange ID	Moisture content %			AVE	Flange ID	Moisture content %			AVE
		I	II	III			I	II	III	
236	44	14.3	12.7	12.4	13.1	53	12.2	12.2	12.1	12.2
237	242	13.9	13.8	12.6	13.4	251	11.6	11.3	11.5	11.5
238	116	12.4	11.5	11.6	11.8	125	11.1	11.2	12.4	11.6
239	62	13.2	12.7	12.5	12.8	71	10.7	10.2	11	10.6
240	224	12.2	11.6	12.1	12.0	233	13.7	11.6	11.5	12.3
241	134	11.6	12.4	11.6	11.9	143	10.3	11.2	12.1	11.2
242	80	12.2	11.5	11.6	11.8	89	12.1	12.1	14.1	12.8
243	206	12.7	12.8	12.7	12.7	215	10.7	11.6	12	11.4
244	152	12.2	11.3	11	11.5	161	11.6	11.5	12.1	11.7
245	98	13.2	12.7	13.1	13.0	107	12.1	11.8	12.2	12.0
246	188	12	13.1	13.9	13.0	197	14.1	11.8	14.4	13.4
247	170	11.8	10.9	10.9	11.2	179	11.6	12.4	12.2	12.1
		Average			12.4		Average			11.9
		I	II	III			I	II	III	
248	45	11.9	12.5	12.2	12.2	54	12.2	11.5	11.2	11.6
249	243	13.3	13.6	13.8	13.6	252	11.6	13.4	13.1	12.7
250	117	11.5	11.3	11.7	11.5	126	12.7	13.6	12.8	13.0
251	63	11.5	11.4	10.2	11.0	72	10.7	10.2	11	10.6
252	225	12.4	12.8	12.5	12.6	234	13.2	12.3	12.8	12.8
253	135	13.1	12.2	13.6	13.0	144	12.5	12.7	12.7	12.6
254	81	13.2	13.3	12.3	12.9	90	11	9.8	9.8	10.2
255	207	11.9	12.1	11.4	11.8	216	11.3	12.2	11.5	11.7
256	153	10.5	11	11.2	10.9	162	12.1	12.6	11.3	12.0
257	99	10.7	11.3	11.6	11.2	108	9.9	10.7	11.4	10.7
258	189	12.6	11.4	11.6	11.9	198	12.5	11.5	11.4	11.8
259	171	10.5	11.1	10.8	10.8	180	10.6	12.1	11.6	11.4
		Average			11.9		Average			11.8
260	46	10.2	11.2	11.6	11.0	55	11	11.6	12.4	11.7
261	244	13.6	14	13.4	13.7	253	11.6	11.4	11.7	11.6
262	118	12.6	12.6	12.1	12.4	127	9.6	11.9	11.8	11.1
263	64	11.2	11.4	11.2	11.3	73	12.1	11.4	12.4	12.0
264	226	13.1	13.1	12.7	13.0	235	12	13.2	12.4	12.5
265	136	12.6	12.2	11.4	12.1	145	11.6	14.1	12.5	12.7
266	82	12.2	12.8	12.3	12.4	91	12.5	12.7	12.5	12.6
267	208	11	12.3	10.7	11.3	217	12	11.2	11.4	11.5
268	154	11.6	11.8	12.7	12.0	163	13	13.2	13.4	13.2
269	100	13.6	11	10.3	11.6	109	10.3	11.3	10.3	10.6
270	190	10.9	11.6	12.5	11.7	199	13.3	12.6	13.1	13.0
271	172	12.1	10.6	11	11.2	181	11.5	12.9	10.6	11.7
		Average			12.0		Average			12.0

Table A.15 Continued

Beam ID	Flange ID	Moisture content %			AVE	Flange ID	Moisture content %			AVE
		I	II	III			I	II	III	
272	47	11.5	11.6	11.6	11.6	56	13.3	13.7	12.2	13.1
273	245	15.1	14.3	13	14.1	254	12.8	12.5	13.6	13.0
274	119	11.2	12.1	12.1	11.8	128	12.2	11	11.4	11.5
275	65	10.9	11.6	12.4	11.6	74	9	11.6	10.6	10.4
276	227	16	15.5	12.5	14.7	236	13.8	13.1	13.9	13.6
277	137	13.2	13	12.1	12.8	146	13.2	12.6	13.4	13.1
278	83	12.7	11.9	11.5	12.0	92	11.9	13.8	12.6	12.8
279	209	11.6	11.9	11.9	11.8	218	11.6	12	13.1	12.2
280	155	12.5	12.5	12.4	12.5	164	11.9	11.3	11.8	11.7
281	101	13.7	12.1	12.5	12.8	110	11.9	12.6	11.4	12.0
282	191	12.5	13.3	13	12.9	200	9.8	10.5	11.9	10.7
283	173	11.3	12.1	11.2	11.5	182	12.2	12.6	13.6	12.8
		Average			12.5		Average			12.2
284	48	9.2	11	10.6	10.3	57	11	11.6	11.9	11.5
285	246	12.7	13.4	13.6	13.2	255	13.1	13.2	13.6	13.3
286	120	11.4	11.6	12	11.7	129	12	11.2	10.5	11.2
287	66	11.5	12.5	12.5	12.2	75	9.8	10	10.5	10.1
288	228	12.7	14	13	13.2	237	12.2	12.5	12.4	12.4
289	138	11	11.2	12.2	11.5	147	11.6	12.5	12.2	12.1
290	84	12.4	12.1	11.6	12.0	93	11.9	11.8	11.8	11.8
291	210	11.9	12	12.1	12.0	219	9.9	10.9	10.6	10.5
292	156	10.3	10.6	11.6	10.8	165	11.4	11.6	11.8	11.6
293	102	10.9	11	11.4	11.1	111	9.8	9.8	11.3	10.3
294	192	13.3	13.1	12.8	13.1	201	13.2	15	12.2	13.5
295	174	10.9	11.6	12.1	11.5	183	12.4	12.1	11.4	12.0
		Average			11.9		Average			11.7
296	603	12.1	12.2	11.9	12.1	603	11.4	11.6	10.9	11.3
297	608	13.3	11.4	11.2	12.0	608	9.8	10.7	11.3	10.6
298	613	9.9	13.2	13.3	12.1	613	10.8	12.2	11.5	11.5
		Average			12.1		Average			11.1
299	604	11.3	13.8	13.2	12.8	604	13.4	14.3	13.4	13.7
300	609	13.7	14	14.5	14.1	609	13.3	12.4	12.5	12.7
301	614	12.8	13.1	13	13.0	614	13	12.7	13.4	13.0
		Average			13.3		Average			13.2

Table A.15 Continued

Beam ID	Flange ID	Moisture content %			AVE	Flange ID	Moisture content %			AVE
		I	II	III			I	II	III	
302	49	12.2	10.6	11	11.3	58	12	11.6	11.6	11.7
303	247	15.4	13.7	14.3	14.5	256	13	13.7	13.2	13.3
304	121	13.2	13.3	12.6	13.0	130	14.4	14.4	12.8	13.9
305	67	9.8	10	9.6	9.8	76	11.7	13.4	11.4	12.2
306	229	10.2	10.2	11	10.5	238	12.5	13.2	13.1	12.9
307	139	14	13	12.8	13.3	148	12.8	12.5	12.2	12.5
308	85	9.8	9.1	10	9.6	94	12.2	13	13.1	12.8
309	211	11.5	11.8	11.4	11.6	220	13.4	13.7	13.3	13.5
310	157	11.8	11.6	11.6	11.7	166	11.6	11.4	11.6	11.5
311	103	11	12.7	11.6	11.8	112	14.4	11.6	12.6	12.9
312	193	10.9	11.5	11.6	11.3	202	12.6	13	12	12.5
313	175	12	12.6	12.5	12.4	184	11	11.6	13	11.9
		Average			11.7		Average			12.6
314	7	9.5	10.5	11.5	10.5	15	12.5	13.7	13.3	13.2
315	23	13.4	13.1	13.5	13.3	31	12.8	11.5	10.7	11.7
316	39	12.6	12.5	12.1	12.4	47	11.6	11.5	11.3	11.5
		Average			12.1		Average			12.1
317	8	11.4	12	12.6	12.0	16	12.5	13.2	13.6	13.1
318	24	10.2	11.7	10.8	10.9	32	11.3	13	13.9	12.7
319	40	12.7	10.7	13.1	12.2	48	14.1	11.3	11	12.1
		Average			11.7		Average			12.6
320	9	10.3	9.2	11.5	10.3	17	11.8	11	11.3	11.4
321	25	11.9	12.4	11.6	12.0	33	11	11.6	12.1	11.6
322	41	12.7	14.3	14.4	13.8	49	12.2	11.6	9.8	11.2
		Average			12.0		Average			11.4
323	10	9.9	11	12.5	11.1	18	12.3	11.6	12.8	12.2
324	26	13.3	12.8	13.1	13.1	34	14.6	13	13.6	13.7
325	42	14.3	13.8	13.3	13.8	50	13.3	12.2	14.1	13.2
		Average			12.7		Average			13.1
326	11	12.2	10.2	11.3	11.2	19	12.5	11.6	12.1	12.1
327	27	11.8	11.6	12.7	12.0	35	12.6	12.6	12.3	12.5
328	43	11.4	12.6	13.9	12.6	51	13.3	13.4	13.8	13.5
		Average			12.0		Average			12.7
329	12	11.8	11.5	10.6	11.3	20	11.9	11.6	12.5	12.0
330	28	9.8	11.6	11.3	10.9	36	11.6	9.8	10	10.5
331	44	12.6	12.5	11.5	12.2	52	13.3	14.2	13.1	13.5
		Average			11.5		Average			12.0

Table A.15 Continued

Beam ID	Flange ID	Moisture content %			AVE	Flange ID	Moisture content %			AVE
		I	II	III			I	II	III	
332	13	14.3	10.6	12.5	12.5	21	9.4	9.6	9.5	9.5
333	29	11.6	12.5	12.2	12.1	37	11.4	12.3	12.8	12.2
334	45	13.9	12.7	11.6	12.7	53	13.4	14.1	13.9	13.8
		Average			12.4		Average			11.8
335	14	13.4	11.9	11.9	12.4	22	13.1	11.6	10.9	11.9
336	30	13.4	12.8	13.1	13.1	38	9.6	10.7	11	10.4
337	46	14.4	14.3	13.6	14.1	54	13.5	11.2	14.8	13.2
		Average			13.2		Average			11.8
338	601	11.6	11.4	11.9	11.6	606	10.2	13.1	10.8	11.4
339	611	12	11.9	10.6	11.5	616	12.7	12.2	11.5	12.1
340	619	12.5	12.6	11.3	12.1	622	11.5	12.4	13.3	12.4
		Average			11.8		Average			12.0
341	602	12	11.4	11.6	11.7	607	11	11.2	11.5	11.2
342	612	13.7	12.8	14.1	13.5	617	12.5	12.6	12.7	12.6
343	620	12.3	11.4	11.4	11.7	623	12.3	11.8	12.4	12.2
		Average			12.3		Average			12.0
344	600	11.4	11.3	10.9	11.2	605	10.6	9.9	12	10.8
345	610	11.2	11.9	13	12.0	615	11.2	11.2	11.1	11.2
346	618	12.6	12.1	11.9	12.2	621	12.7	12.7	12.6	12.7
		Average			11.8		Average			11.6

Table A.16 Moisture content of the top and bottom LVL flanges of CIBs

Beam ID	Flange ID	Moisture content %			AVE	Flange ID	Moisture content %			AVE
		I	II	III			I	II	III	
347	LVL top flange	13.7	14.5	15	14.4	LVL bottom flange	14	13.4	14.1	13.8
348		12.7	13.7	13.4	13.3		13.4	14.3	13.9	13.9
349		13.2	14.1	12.8	13.4		13.7	14.2	14.3	14.1
350		13.7	13.4	11.5	12.9		13.9	14.1	13.9	14.0
		Average			13.5		Average			13.9
351	LVL top flange	13.8	13.4	13.2	13.5	LVL bottom flange	14.1	14.1	14	14.1
352		14.3	12.4	13.8	13.5		12	12.4	13.2	12.5
		Average			13.5		Average			13.3
353	LVL top flange	13.9	14.3	13.7	14.0	LVL bottom flange	12.8	14.3	13	13.4
354		13.8	15.2	14.1	14.4		13	13.4	12.4	12.9
		Average			14.2		Average			13.2
355	LVL top flange	16.6	15.6	16.2	16.1	LVL bottom flange	16.6	15.7	15.6	16.0
356		16.7	16.9	15.7	16.4		15	14.9	13.2	14.4
357		17.6	16	15.1	16.2		15.3	15.4	15.7	15.5
358		15.8	15.4	14.1	15.1		16.2	15.2	15.7	15.7
359		15.2	15.4	16	15.5		14.9	14	13.9	14.3
360		16.5	15.9	16.2	16.2		14.8	15.5	15.2	15.2
361		16.7	17.1	16.6	16.8		14.4	14.5	14.6	14.5
362		16	16.2	15.7	16.0		12.8	12.8	13.3	13.0
363		16.6	15.1	14.7	15.5		14.2	13.9	14.5	14.2
364		17.3	17	17.6	17.3		14.4	13.5	12.9	13.6
365		17.2	16	16	16.4		15.9	15.5	15.2	15.5
366		15.4	14.9	16.2	15.5		16.1	16.2	14.8	15.7
367		15.3	14.8	14	14.7		14.4	15.4	14.3	14.7
368		14.4	11.6	13.3	13.1		16.4	16.1	16	16.2
369		13.5	13.3	13.9	13.6		16	15.5	14.5	15.3
370		14.4	15.5	16.1	15.3		15.7	15.5	16.3	15.8
371		14.6	14.3	14.8	14.6		15.6	16.6	15	15.7
372	15.4	14.8	14.5	14.9	15.7	14.5	15.5	15.2		
373	14.6	14.3	14.5	14.5	15.5	15.2	15.6	15.4		
374	15.6	15.1	15.7	15.5	15.4	15.7	15.4	15.5		
375	13.8	15.2	14.8	14.6	16.2	16.6	17.4	16.7		
376	17.4	17.6	16.7	17.2	14.9	14.3	14.3	14.5		
		Average			15.5		Average			15.1

Table A 16 Continued

Beam ID	Flange's ID	Moisture content %			AVE	Flange ID	Moisture content %			AVE
		I	II	III			I	II	III	
377	LVL top flange	16.6	16.7	16.6	16.6	LVL bottom flange	15.8	15.4	15.7	15.6
378		13.2	13	13.4	13.2		13.9	13.4	13.1	13.5
379		15.2	16.7	15.8	15.9		15.1	14.8	13.8	14.6
380		13.6	14.8	15.5	14.6		12.7	13.1	14.3	13.4
381		16.2	16.6	15.5	16.1		17	16.2	16.4	16.5
382		15.4	15.8	16.2	15.8		14.3	13.3	14.4	14.0
383		13.2	14	15.5	14.2		16.7	16.6	16.2	16.5
384		14.3	16.9	14	15.1		14.3	14.9	14.8	14.7
385		16.9	16.9	15	16.3		14.4	14.3	16.2	15.0
386		15.4	14.6	15.6	15.2		15.5	14.6	15.4	15.2
387		16.9	14.9	16.7	16.2		15	16.1	16.3	15.8
388		17.1	15.7	15	15.9		15.8	14.4	14.9	15.0
389		13.9	14.5	13.9	14.1		16.2	15.4	14.3	15.3
		Average			15.3		Average			15.0
390	LVL top flange	16	16.1	16.6	16.2	LVL bottom flange	16.5	16.8	16.9	16.7
391		16.2	15.6	17.7	16.5		17.2	16.7	16.4	16.8
392		17	16.2	16.8	16.7		15.7	16.2	16.2	16.0
393		14.5	14.4	14.5	14.5		16.1	16.3	16.3	16.2
394		16.7	15.9	16.3	16.3		14	14.6	14.4	14.3
395		16.8	17.1	15.9	16.6		16.7	16.3	18.2	17.1
396		15.1	15.7	15.1	15.3		17.7	17	17.2	17.3
397		15.1	15.5	15.6	15.4		15.2	14.4	15.8	15.1
398		16.1	16.1	16.9	16.4		17.1	15.5	16.2	16.3
		Average			16.0		Average			16.2

Table A.17. Weight of the manufactured beams with timber flanges

C.17(a) I-beam Profile

I-Beam				
Beam	Weight without foam	Length	Flanges	Weight per meter
ID	(Kg)	(m)	ID	(Kg/m)
302	10.6	2.3	49-58	4.6
303	12.5	2.4	247-256	5.3
304	13.0	2.4	121-130	5.4
305	11.3	2.4	67-76	4.8
306	12.1	2.4	229-238	5.0
307	11.5	2.3	139-148	4.9
308	12.0	2.4	85-94	5.0
309	11.3	2.3	211-220	4.8
310	11.4	2.3	157-166	4.9
311	11.3	2.4	103-112	4.8
312	12.1	2.4	193-202	5.0
313	11.2	2.4	175-184	4.8
344	22.0	4.9	600-605	4.5
345	24.0	4.8	610-615	5.0
346	25.8	4.9	618-621	5.3

A.17(b) Double I-beam Profile

Double I-Beam									
Beam	Weight without foam	Length	Flanges	Weight per meter	Beam	Weight with foam	Length	Weight per meter	Foam weight
ID	(Kg)	(m)	ID	(Kg/m)	ID	(Kg)	(m)	(Kg/m)	(Kg)
224	12.6	2.3	43-52	5.4					
225	15.0	2.4	241-250	6.2					
226	13.7	2.4	115-124	5.8					
227	14.2	2.4	61-70	5.9					
228	15.0	2.4	223-232	6.2					
229	12.6	2.3	133-142	5.4					
230	11.9	2.3	79-88	5.1					
231	13.5	2.4	205-214	5.8					
232	13.6	2.4	151-160	5.8					
233	13.1	2.3	97-106	5.6					
234	13.9	2.4	187-196	5.9					
235	14.9	2.4	169-178	6.2					
236	14.0	2.4	44-53	5.9	236	14.5	2.4	6.16	0.5
237	14.9	2.4	242-251	6.3	237	15.5	2.4	6.58	0.6
238	14.7	2.4	116-125	6.1	238	15.2	2.4	6.30	0.5
239	13.2	2.4	62-71	5.6	239	13.7	2.4	5.84	0.5
240	14.7	2.4	224-233	6.1	240	15.3	2.4	6.39	0.6
241	13.4	2.4	134-143	5.6	241	14.0	2.4	5.88	0.6
242	13.7	2.4	80-89	5.8	242	14.3	2.4	6.07	0.6
243	13.3	2.3	206-215	5.8	243	13.9	2.3	6.01	0.5
244	13.3	2.4	152-161	5.7	244	13.8	2.4	5.88	0.5
245	15.0	2.4	98-107	6.2	245	15.6	2.4	6.44	0.6
246	15.7	2.4	188-197	6.5	246	16.2	2.4	6.73	0.5
247	13.4	2.4	170-179	5.7	247	14.0	2.4	5.94	0.6
320	28.1	4.8	9 & 17	5.8					
321	29.7	4.8	25-33	6.1					
322	29.2	4.9	41-49	6.0					
323	28.6	4.8	10-18	5.9	323	29.6	4.8	6.12	1.1
324	30.9	4.8	26-34	6.4	324	32.0	4.8	6.60	1.1
325	31.2	4.8	42-50	6.4	325	32.2	4.8	6.65	1.0

A.17(c) Recessed beam Profile

Recessed beam									
Beam	Weight without foam	Length	Flanges	Weight per meter	Beam	Weight with foam	Length	Weight per meter	Foam weight
ID	(Kg)	(m)	ID	(Kg/m)	ID	(Kg)	(m)	(Kg/m)	(Kg)
272	14.2	2.4	47-56	5.9					
273	15.4	2.4	245-254	6.4					
274	12.5	2.3	119-128	5.4					
275	12.0	2.3	65-74	5.1					
276	16.2	2.4	227-236	6.7					
277	14.7	2.4	137-146	6.1					
278	12.9	2.4	83-92	5.5					
279	13.7	2.4	209-218	5.8					
280	13.9	2.4	155-164	5.8					
281	13.0	2.3	101-110	5.5					
282	15.2	2.4	191-200	6.3					
283	13.1	2.3	173-182	5.6					
284	13.0	2.4	48-57	5.5	284	14.2	2.4	6.04	1.2
285	15.6	2.4	246-255	6.4	285	16.8	2.4	6.94	1.2
286	13.0	2.4	120-129	5.5	286	14.2	2.4	6.02	1.1
287	14.6	2.4	66-75	6.1	287	15.8	2.4	6.60	1.2
288	15.2	2.4	228-237	6.3	288	16.3	2.4	6.76	1.1
289	13.7	2.4	138-147	5.8	289	14.9	2.3	6.34	1.2
290	14.0	2.4	84-93	6.0	290	15.3	2.4	6.49	1.2
291	13.2	2.4	210-219	5.6	291	14.4	2.4	6.12	1.2
292	13.7	2.4	156-165	5.8	292	14.9	2.4	6.33	1.2
293	13.5	2.4	102-111	5.6	293	14.6	2.4	6.09	1.1
294	14.9	2.4	192-201	6.3	294	16.1	2.4	6.85	1.2
295	14.6	2.4	174-183	6.0	295	15.9	2.4	6.56	1.2
332	27.7	4.8	13-21	5.7					
333	28.7	4.9	29-37	5.9					
334	30.9	4.9	45-53	6.4					
335	28.6	4.8	14-22	5.9	335	31.1	4.8	6.42	2.5
336	28.7	4.8	30-38	5.9	336	31.2	4.8	6.45	2.5
337	32.1	4.8	46-54	6.6	337	34.6	4.8	7.13	2.5

A.17(d) Box beam Profile

Box Beam									
Beam	Weight without foam	Length	Flanges	Weight per meter	Beam	Weight with foam	Length	Weight per meter	Foam weight
ID	(Kg)	(m)	ID	(Kg/m)	ID	(Kg)	(m)	(Kg/m)	(Kg)
199	16.4	2.4		6.8					
200	14.8	2.4	41-50	6.3					
201	17.6	2.4	239-248	7.3					
202	15.0	2.3	113-122	6.4					
203	14.1	2.3	59-68	6.0					
204	17.8	2.4	221-230	7.4					
205	16.9	2.4	131-140	7.0					
206	16.0	2.4	77-86	6.8					
207	16.1	2.4	203-212	6.8					
208	16.5	2.4	149-158	6.8					
209	15.0	2.3	95-104	6.4					
210	15.7	2.3	185-194	6.7					
211	16.4	2.4	167-176	6.8					
212	15.4	2.3	42-51	6.7	212	16.8	2.3	7.36	1.4
213	17.7	2.4	240-249	7.4	213	19.2	2.4	8.00	1.5
214	15.9	2.3	114-123	6.8	214	17.3	2.3	7.43	1.4
215	14.5	2.3	60-69	6.2	215	15.9	2.3	6.78	1.4
216	17.0	2.4	222-231	7.0	216	18.4	2.4	7.63	1.4
217	15.3	2.3	132-141	6.5	217	16.6	2.3	7.09	1.3
218	18.1	2.4	78-87	7.5	218	19.6	2.4	8.16	1.5
219	15.7	2.3	204-213	6.7	219	17.1	2.3	7.34	1.4
220	15.2	2.3	150-159	6.5	220	16.6	2.3	7.15	1.4
221	14.9	2.3	96-105	6.4	221	16.3	2.3	7.02	1.4
222	15.7	2.3	186-195	6.7	222	17.2	2.3	7.34	1.5
223	15.7	2.3	168-177	6.7	223	17.1	2.3	7.35	1.5
314	30.9	4.8	7 - 15	6.4					
315	33.9	4.8	23-31	7.0					
316	32.7	4.8	39-47	6.8					
317	30.7	4.9	8 - 16	6.3	317	33.5	4.9	6.91	2.8
318	31.6	4.9	24-32	6.5	318	34.5	4.9	7.11	3.0
319	34.2	4.9	40-48	7.0	319	37.5	4.9	7.72	3.3

Table A.17(e) Boxed I-beam profile

Boxed I-Beam									
Beam	Weight without foam	Length	Flanges	Weight per meter	Beam	Weight with foam	Length	Weight per meter	Foam weight
ID	(Kg)	(m)	ID	(Kg/m)	ID	(Kg)	(m)	(Kg/m)	(Kg)
248	17.6	2.3	45-54	7.5					
249	19.0	2.3	243-252	8.2					
250	17.8	2.3	117-126	7.6					
251	17.0	2.3	63-72	7.2					
252	18.5	2.4	225-234	7.9					
253	17.7	2.3	135-144	7.5					
254	16.7	2.4	81-90	7.1					
255	18.4	2.4	207-216	7.6					
256	17.1	2.3	153-162	7.3					
257	16.5	2.3	99-108	7.1					
258	19.3	2.4	189-198	8.0					
259	18.3	2.4	171-180	7.6					
260	17.2	2.3	46-55	7.3	260	19.0	2.3	8.09	1.7
261	19.0	2.4	244-253	7.9	261	20.6	2.4	8.58	1.6
262	17.9	2.3	118-127	7.6	262	19.5	2.3	8.35	1.6
263	17.7	2.3	64-73	7.5	263	19.2	2.3	8.17	1.5
264	19.7	2.4	226-235	8.2	264	21.3	2.4	8.90	1.6
265	18.5	2.4	136-145	7.8	265	20.0	2.4	8.40	1.5
266	18.5	2.3	82-91	7.9	266	19.9	2.3	8.48	1.4
267	19.2	2.4	208-217	8.1	267	20.8	2.4	8.74	1.6
268	18.6	2.4	154-163	7.9	268	20.2	2.4	8.59	1.6
269	16.9	2.3	100-109	7.2	269	18.3	2.3	7.83	1.4
270	18.9	2.4	190-199	7.9	270	20.4	2.4	8.59	1.6
271	17.5	2.3	172-181	7.4	271	19.2	2.4	8.15	1.7
326	35.3	4.8	11 & 19	7.3					
327	38.2	4.8	27-35	7.9					
328	38.9	4.8	43-51	8.0					
329	36.9	4.8	12 & 20	7.6	329	39.9	4.8	8.24	3.1
330	36.5	4.9	28-36	7.5	330	39.8	4.9	8.20	3.3
331	39.2	4.8	44-52	8.1	331	42.4	4.8	8.80	3.2

Table A 17(f) Boxed Double I-beam profile

Boxed double I-Beam									
Beam	Weight without foam	Length	Flanges	Weight per meter	Beam	Weight with foam	Length	Weight per meter	Foam weight
ID	(Kg)	(m)	ID	(Kg/m)	ID	(Kg)	(m)	(Kg/m)	(Kg)
296	20.3	2.4	603-603	8.5					
297	20.4	2.4	608-608	8.4					
298	20.7	2.4	613-613	8.6					
299	21.3	2.4	604-604	9.1	299	22.9	2.4	9.74	1.6
300	21.7	2.4	609-609	9.1	300	23.5	2.4	9.86	1.8
301	21.4	2.4	614-614	8.9	301	23.1	2.4	9.62	1.7
338	40.5	4.8	601-606	8.4					
339	40.2	4.8	611-616	8.3					
340	42.5	4.8	619-622	8.8					
341	40.2	4.9	602-607	8.3	341	43.8	4.9	9.04	3.6
342	43.4	4.8	612-617	9.0	342	47.3	4.8	9.84	3.9
343	40.9	4.8	620-623	8.4	343	44.6	4.8	9.21	3.7

Table A.18 Weight of the manufactured beams with LVL flanges

A.18(a) LVL I-beam profile

LVL I-Beam				
Beam	Weight without foam	Length	Flanges	Weight per meter
ID	(Kg)	(m)	ID	(Kg/m)
390	13.4	2.4	LVL	5.5
391	13.2	2.4	LVL	5.5
392	13.4	2.4	LVL	5.6
393	12.9	2.4	LVL	5.3
394	13.2	2.4	LVL	5.4
395	13.6	2.4	LVL	5.6
396	13.4	2.4	LVL	5.5
397	12.6	2.4	LVL	5.2
398	13.3	2.4	LVL	5.6
353	26.4	4.8	LVL	5.5
354	26.4	4.8	LVL	5.4

A.18(b) LVL Double I-beam profile

LVL double I-Beam										
Beam	Weight without foam	Length	Flanges	Weight per meter		Beam	Weight with foam	Length	Weight per meter	Foam weight
ID	(Kg)	(m)	ID	(Kg/m)		ID	(Kg)	(m)	(Kg/m)	(Kg)
355	15.4	2.4	LVL	6.4		355	16.3	2.4	6.74	0.8
356	15.7	2.4		6.5		356	16.6	2.4	6.86	0.9
357	15.7	2.4		6.5		357	16.4	2.4	6.81	0.8
358	15.3	2.4		6.3		358	16.1	2.4	6.68	0.8
359	15.1	2.4		6.3		359	15.9	2.4	6.62	0.9
360	15.3	2.4		6.4		360	16.1	2.4	6.70	0.8
361	15.1	2.4		6.3		361	15.8	2.4	6.60	0.7
362	15.4	2.4		6.4		362	16.2	2.4	6.71	0.8
363	15.2	2.4		6.3		363	16.0	2.4	6.63	0.8
364	15.4	2.4		6.4		364	15.9	2.4	6.63	0.5
365	15.7	2.4		6.5		365	16.5	2.4	6.82	0.8
366	15.2	2.4		6.3		366	16.1	2.4	6.67	0.9
367	15.5	2.4		6.4		367	16.4	2.4	6.79	0.9
368	15.4	2.4		6.4						
369	14.7	2.4		6.2						
370	15.5	2.4		6.5						
371	15.3	2.4		6.4						
372	15.4	2.4		6.4						
373	15.3	2.4		6.4		373	16.1	2.4	6.72	0.8
374	15.4	2.4		6.4		374	16.1	2.4	6.73	0.7
375	16.0	2.4		6.6		375	16.7	2.4	6.92	0.7
376	15.8	2.4		6.5		376	16.5	2.4	6.84	0.7
347	31.2	4.8		6.4		347	32.6	4.8	6.72	1.4
348	30.8	4.8		6.4		348	32.1	4.8	6.63	1.4
349	31.2	4.8		6.4						
350	31.0	4.9		6.4						

A.18(c) LVL Boxed I-beam profile

LVL Boxed I-Beam										
Beam	Weight without foam	Length	Flanges	Weight per meter		Beam	Weight with foam	Length	Weight per meter	Foam weight
ID	(Kg)	(m)	ID	(Kg/m)		ID	(Kg)	(m)	(Kg/m)	(Kg)
377	19.4	2.4	LVL	8.1						
378	19.0	2.4	LVL	7.9						
380	19.4	2.4	LVL	8.1						
381	19.8	2.4	LVL	8.2						
382	19.8	2.4	LVL	8.3		382	21.7	2.4	9.06	1.9
383	19.4	2.4	LVL	8.1		383	21.2	2.4	8.82	1.8
384	19.1	2.4	LVL	8.0		384	20.9	2.4	8.72	1.7
385	19.7	2.4	LVL	8.2		385	21.3	2.4	8.95	1.7
386	19.6	2.4	LVL	8.2		386	21.3	2.4	8.92	1.7
387	19.9	2.4	LVL	8.3		387	21.9	2.4	9.18	2.0
388	19.2	2.4	LVL	8.0		388	21.2	2.4	8.81	2.0
389	19.9	2.4	LVL	8.3		389	21.9	2.4	9.12	2.0
351	39.7	4.8	LVL	8.2						
352	38.8	4.8	LVL	8.0						

Table A.19 Young modulus of the CIB flanges of C16 grade over 4.5 m span

Timber grade C16									
Span	Timber ID	Width	Height	E	Span	Timber ID	Width	Height	E
4500		(mm)	(mm)	(kN/mm ²)	4500		(mm)	(mm)	(kN/mm ²)
	1	90.30	44.41	8.85		49	90.02	44.14	18.74
	2	89.66	44.08	14.66		50	90.26	44.29	11.59
	3	89.46	44.06	9.87		51	90.27	44.08	11.85
	4	89.35	43.72	12.85		52	89.91	43.99	12.78
	5	90.14	44.18	9.37		53	89.50	44.42	11.23
	6	88.85	43.83	15.28		54	90.27	44.48	15.05
	7	88.94	43.93	13.11		55	89.57	44.10	9.99
	8	89.53	44.06	9.27		56	89.52	44.16	14.92
	9	89.92	43.95	10.39		60	89.39	44.11	14.27
	10	89.90	43.97	15.08		61	89.00	44.22	14.84
	11	89.43	44.29	14.37		62	89.52	44.17	10.15
	12	89.68	44.41	10.03		63	89.56	44.40	11.11
	13	89.84	43.86	12.70		64	89.09	44.40	12.75
	14	89.98	44.34	12.93		65	89.58	44.17	10.52
	15	89.58	44.06	15.53		66	89.89	44.11	14.27
	16	90.02	44.22	14.32		67	89.51	44.05	12.56
	17	89.11	44.06	12.98		68	89.95	44.20	14.32
	18	89.52	44.17	15.47		69	89.82	44.61	11.61
	19	89.18	44.05	12.10		70	89.61	44.39	14.48
	20	90.09	44.23	14.38		71	89.92	44.31	13.17
	21	89.39	44.02	16.39		72	89.63	44.13	20.30
	22	90.21	44.24	12.87		73	89.87	44.61	11.69
	23	90.31	44.17	12.28		74	89.59	43.70	12.74
	24	90.24	44.18	10.47		75	89.90	44.78	11.95
	25	89.71	44.62	12.06		136	89.31	44.71	13.01
	29	89.74	44.35	13.46		137	98.49	44.86	10.48
	30	89.84	44.23	14.21		138	89.25	45.08	13.57
	31	89.50	44.17	12.13		139	89.62	44.76	12.40
	32	89.57	44.12	15.75		140	90.07	45.01	11.21
	33	89.89	44.85	9.57		141	89.71	44.52	12.12
	34	90.17	44.56	8.56		142	89.62	44.65	12.62
	35	90.28	44.45	11.25		143	90.13	44.94	13.25
	36	90.52	44.39	10.37		144	87.39	41.94	17.73
	37	90.31	44.26	8.53		145	87.40	41.76	17.80
	38	90.22	44.53	14.75		182	90.42	44.37	8.86
	40	89.95	44.21	12.48		183	90.66	45.88	7.20
	41	89.93	44.08	9.29		184	90.22	44.27	9.00
	42	90.17	44.22	11.74		185	89.38	44.55	7.59
	43	90.20	43.96	14.27		186	89.34	44.39	7.84
	44	89.37	44.11	12.06		187	90.11	44.93	10.08
	45	89.94	44.15	13.84		188	89.54	44.79	11.96
	46	90.52	44.03	10.73		189	89.51	44.76	7.94
	47	89.36	44.42	13.18		190	90.54	46.09	5.75
	48	90.18	44.46	16.82		191	89.89	45.61	4.84

Table 19. Continued

Timber grade C16									
Span	Timber ID	Width	Height	E	Span	Timber ID	Width	Height	E
4500		(mm)	(mm)	(kN/mm ²)	4500		(mm)	(mm)	(kN/mm ²)
	192	89.47	44.00	11.84		202	89.80	43.93	11.79
	193	89.75	44.50	10.36		203	90.04	44.51	7.39
	194	90.22	45.06	9.38		204	90.47	45.07	11.51
	195	90.26	45.03	6.41		205	90.36	44.94	8.41
	196	90.73	44.08	10.52		206	89.04	44.32	7.60
	197	89.87	44.38	10.23		207	89.48	44.39	10.85
	198	89.54	44.10	10.84		208	89.70	44.25	14.16
	199	89.42	44.71	7.13		209	90.51	44.75	5.95
	200	89.60	44.47	10.70		210	89.99	44.80	8.87
	201	89.68	44.03	6.77		211	90.10	44.55	8.00

Table A.20 Young modulus of the CIB flanges of C24 grade over 4.5 m span

Timber grade C24									
Span	Timber ID	Width	Height	E	Span	Timber ID	Width	Height	E
4500		(mm)	(mm)	(kN/mm ²)	4500		(mm)	(mm)	(kN/mm ²)
	26	90.02	44.17	9.47		114	89.17	43.97	12.83
	27	89.81	44.36	9.90		115	89.20	43.88	11.62
	28	90.36	44.73	10.43		116	89.34	43.90	14.90
	39	89.91	44.31	15.80		117	88.44	43.88	15.23
	57	89.81	44.30	14.92		118	89.21	43.87	9.34
	58	89.45	43.87	15.09		119	88.50	44.14	13.73
	59	89.01	44.03	13.18		120	88.48	43.83	12.80
	76	89.64	43.98	15.11		121	88.17	43.92	10.18
	77	89.96	44.35	10.79		122	89.56	44.01	12.31
	78	89.89	44.22	12.85		123	89.69	43.54	13.40
	79	89.49	44.31	13.65		124	89.60	43.93	13.35
	80	88.06	44.29	16.76		125	89.40	43.83	11.43
	81	89.04	44.03	12.52		126	89.70	44.19	11.96
	82	89.09	44.23	12.55		127	89.60	44.49	10.08
	83	89.14	44.15	12.29		128	89.13	43.97	11.01
	84	89.87	43.73	12.22		129	89.60	44.17	12.71
	85	89.15	44.22	16.29		130	89.59	44.15	13.16
	86	89.26	43.98	11.96		131	89.33	44.02	8.23
	87	89.66	44.67	12.66		132	90.46	44.21	13.75
	88	89.84	44.54	12.73		133	89.65	44.13	12.55
	89	89.52	44.37	13.94		134	89.52	44.11	14.87
	90	89.76	44.41	15.73		135	89.10	44.36	14.92
	91	89.69	44.73	10.25		146	90.21	45.30	14.78
	92	89.94	44.66	13.64		147	89.66	44.81	11.99
	93	89.64	44.06	12.05		148	88.91	44.54	12.03
	94	89.76	44.08	11.83		149	90.58	45.04	14.86
	95	90.08	44.35	9.91		150	89.93	45.04	10.33
	96	89.89	44.23	7.14		151	89.36	45.10	8.42
	97	89.96	44.36	13.18		152	89.58	44.56	10.35
	98	88.31	43.95	15.75		153	90.10	44.78	14.16
	99	88.74	43.82	15.40		154	90.28	44.83	13.78
100	89.21	44.13	14.67	155	90.04	44.89	7.08		
101	88.86	43.99	10.84	156	90.10	44.95	8.80		
102	89.16	43.96	17.61	157	89.90	45.84	10.56		
103	89.66	44.00	16.73	158	90.70	45.02	11.59		
104	89.18	43.82	11.34	159	90.33	45.50	12.66		
105	89.27	43.57	13.99	160	89.99	44.93	11.72		
106	88.80	43.98	11.20	161	89.78	44.87	9.40		
107	89.35	43.71	13.46	162	89.98	45.10	10.35		
108	89.28	43.80	12.47	163	90.20	45.03	8.70		
109	89.57	43.97	10.85	164	90.33	44.75	11.55		
110	89.32	43.78	8.77	165	90.47	44.93	11.49		
111	89.36	44.09	12.26	166	90.71	45.27	10.76		
112	88.74	43.99	12.05	167	90.17	44.97	17.79		
113	89.33	44.03	14.31	168	90.36	45.40	9.93		

Table A.20 Continued

Timber grade C24									
Span	Timber ID	Width	Height	E	Span	Timber ID	Width	Height	E
4500		(mm)	(mm)	(kN/mm ²)	4500		(mm)	(mm)	(kN/mm ²)
	169	90.14	45.27	7.41		176	90.03	44.69	12.07
	170	90.78	45.08	18.33		177	89.78	45.27	13.42
	171	90.18	45.09	13.38		178	90.30	44.94	11.68
	172	90.50	45.00	10.14		179	90.07	44.84	10.91
	173	91.00	44.71	11.29		180	90.08	45.04	13.15
	174	89.77	44.99	15.01		181	89.81	44.81	9.32
	175	89.89	44.66	11.10					

Table A.21 Long CIBs profiles and ID sorted by their MoEs

A.21(a) CIB beams with C16 flanges and OSB3 webs

Long beam with C16 timber flanges							
Profile 1-I-Beam							
S.No	Top-Bottom Flanges ID	Top-Bottom MoE	BEAM ID	S.No	Top-Bottom Flanges ID	Top-Bottom MoE	BEAM ID
		GPa					
1	211-8	8.00-9.27	500	1	1-33	8.85-9.57	520
2	187-196	10.08-10.52	501	2	36-198	10.37-10.84	521
3	53-192	11.84-11.23	502	3	69-141	11.61-12.12	522
4	40-22	12.48-12.87	503	4	74-7	12.74-13.11	523
5	29-16	13.46-14.32	504	5	30-70	14.21-14.48	524
Profile 3-Double I-beam				Profile 10-Filled Double I-beam			
1	205-41	8.41-9.29	505	1	182-3	8.86-9.87	525
2	62-65	10.15-10.52	506	2	9-207	10.39-10.85	526
3	35-51	11.25-11.85	507	3	73-31	11.69-12.13	527
4	67-14	12.56-12.93	508	4	64-71	12.75-13.17	528
5	138-68	13.57-14.32	509	5	66-2	14.27-14.66	529
Profile 6- Box Beam				Profile 13- Filled Box beam			
1	37-5	8.53-9.37	510	1	210-55	8.87-9.99	530
2	197-200	10.23-10.70	511	2	24-63	10.47-11.11	531
3	204-75	11.51-11.95	512	3	42-23	11.74-12.28	532
4	142-17	12.62-12.98	513	4	52-47	12.78-13.18	533
5	45-11	13.84-14.37	514	5	43-38	14.27-14.75	534
Profile 7-Boxed I-beam				Profile 14-Filled Boxed I-beam			
1	34-194	8.56-9.38	515	1	184-12	9.00-10.03	535
2	193-46	10.36-10.73	516	2	137-140	10.48-11.21	536
3	50-44	11.59-12.06	517	3	202-139	11.79-12.40	537
4	13-136	12.70-13.01	518	4	4-143	12.85-13.25	538
5	208-20	14.16-14.38	519	5	60-54	14.27-15.05	539

A.21(b) CIB beams with C24 flanges and OSB3 webs

Long beam with C24 timber flanges							
Profile 1-I-Beam							
S.No	Top-Bottom Flanges ID	Top-Bottom MoE	BEAM ID	S.No	Top-Bottom Flanges ID	Top-Bottom MoE	BEAM ID
		GPa					
1	181-172	9.32-10.14	800	1	27-152	9.90-10.35	820
2	166-173	10.76-11.29	801	2	179-164	10.91-11.55	821
3	160-176	11.72-12.07	802	3	147-122	11.99-12.31	822
4	82-180	12.55-13.15	803	4	88-124	12.73-13.35	823
5	107-153	13.46-14.16	804	5	132-149	13.75-14.86	824
Profile 3-Double I-beam				Profile 10-Filled Double I-beam			
1	118-121	9.34-10.18	805	1	95-162	9.91-10.35	825
2	77-104	10.79-11.34	806	2	128-158	10.01-11.59	826
3	94-84	11.83-12.22	807	3	148-108	12.03-12.47	827
4	159-130	12.66-13.16	808	4	120-171	12.80-13.38	828
5	92-113	13.64-14.31	809	5	154-134	13.78-14.87	829
Profile 6- Box Beam				Profile 13- Filled Box beam			
1	161-91	9.40-10.25	810	1	168-28	9.93-10.43	830
2	101-125	10.84-11.43	811	2	175-115	11.10-11.62	831
3	86-111	11.96-12.26	812	3	112-81	12.05-12.52	832
4	87-59	12.66-13.18	813	4	114-123	12.83-13.40	833
5	79-100	13.65-14.67	814	5	89-116	13.94-14.90	834
Profile 7-Boxed I-beam				Profile 14-Filled Boxed I-beam			
1	26-150	9.47-10.33	815	1	127-157	10.08-10.56	835
2	109-165	10.85-11.49	816	2	106-178	11.20-11.68	836
3	126-83	11.96-12.29	817	3	93-133	12.05-12.55	837
4	129-97	12.71-13.18	818	4	78-177	12.85-13.42	838
5	119-146	13.73-14.78	819	5	105-57	13.99-14.92	839

Appendix B: Effect of the foam on CIB beams

Table B.1 Effect of the infill on load deflection of the long span beams

Double I-beam	Long Double I-beam without infill (No foam)					
	ID:323	ID:324	ID:325	AVE	SD	C _v (%)
k _{NF,4500} (kN/mm)	0.461	0.454	0.659	0.525	0.12	22.18
k _{NF,3000} (kN/mm)	1.220	1.414	1.656	1.430	0.22	15.28
k _{NF,2100} (kN/mm)	2.644	3.128	3.594	3.122	0.48	15.22
k _{NF,1450} (kN/mm)	5.967	6.454	6.506	6.309	0.30	4.71
Double I-beam	Long Double I-beam with infill (Foam)					
	ID:323	ID:324	ID:325	AVE	SD	C _v (%)
k _{F,4500} (kN/mm)	0.484	0.539	0.68	0.568	0.10	17.81
k _{F,3000} (kN/mm)	1.387	1.513	1.750	1.550	0.18	11.89
k _{F,2100} (kN/mm)	3.190	3.323	3.663	3.392	0.24	7.19
k _{F,1450} (kN/mm)	6.103	6.605	6.950	6.553	0.43	6.50
Effect of the foam on load/deflection (k)						
k _{F,4500} /k _{NF,4500}	1.05	1.19	1.03	1.08	0.08	7.85
k _{F,3000} /k _{NF,3000}	1.14	1.07	1.06	1.08	0.04	3.96
k _{F,2100} /k _{NF,2100}	1.21	1.06	1.02	1.09	0.10	9.03
k _{F,1450} /k _{NF,1450}	1.02	1.02	1.07	1.04	0.03	2.51

Recessed beam	Long Recessed beam without infill (No foam)					
	ID:335	ID:336	ID:337	AVE	SD	C _v (%)
k _{NF,4500} (kN/mm)	0.457	0.541	0.624	0.541	0.08	15.44
k _{NF,3000} (kN/mm)	1.221	1.371	1.461	1.351	0.12	8.97
k _{NF,2100} (kN/mm)	2.594	2.947	3.109	2.883	0.26	9.13
k _{NF,1450} (kN/mm)	5.361	5.762	6.04	5.721	0.34	5.97
Recessed beam	Long Recessed beam with infill (Foam)					
	ID:335	ID:336	ID:337	AVE	SD	C _v (%)
k _{F,4500} (kN/mm)	0.480	0.544	0.624	0.549	0.07	13.13
k _{F,3000} (kN/mm)	1.281	1.447	1.617	1.448	0.17	11.60
k _{F,2100} (kN/mm)	2.815	3.045	3.367	3.076	0.28	9.02
k _{F,1450} (kN/mm)	5.334	5.823	6.262	5.806	0.46	8.00
Effect of the foam on load/deflection (k)						
k _{F,4500} /k _{NF,4500}	1.05	1.01	1.00	1.02	0.03	2.72
k _{F,3000} /k _{NF,3000}	1.05	1.06	1.11	1.07	0.03	2.95
k _{F,2100} /k _{NF,2100}	1.09	1.03	1.08	1.07	0.03	2.75
k _{F,1450} /k _{NF,1450}	0.99	1.01	1.04	1.01	0.02	2.08

Table B.1 Effect of the infill on load deflection of the long span beams (Continued)

Box beam	Long Box beam without infill (No foam)					
	ID:317	ID:318	ID:319	AVE	SD	C _v (%)
k _{NF,4500} (kN/mm)	0.501	0.555	0.662	0.57	0.08	14.31
k _{NF,3000} (kN/mm)	1.300	1.493	1.616	1.47	0.16	10.84
k _{NF,2100} (kN/mm)	2.776	3.143	3.318	3.08	0.28	8.98
k _{NF,1450} (kN/mm)	5.662	5.693	6.330	5.90	0.38	6.40
Long Box beam with infill (Foam)						
Box beam	ID:317	ID:318	ID:319	AVE	SD	C _v (%)
k _{F,4500} (kN/mm)	0.518	0.583	0.572	0.56	0.03	6.24
k _{F,3000} (kN/mm)	1.392	1.581	1.714	1.56	0.16	10.36
k _{F,2100} (kN/mm)	3.024	3.138	3.403	3.19	0.19	6.10
k _{F,1450} (kN/mm)	---	5.939	6.523	6.23	0.41	6.63
Effect of the foam on load/deflection (k)						
k _{F,4500} /k _{NF,4500}	1.03	1.05	0.86	0.97	0.10	10.60
k _{F,3000} /k _{NF,3000}	1.07	1.06	1.06	1.06	0.01	0.60
k _{F,2100} /k _{NF,2100}	1.09	1.00	1.03	1.04	0.05	4.51
k _{F,1450} /k _{NF,1450}	---	1.04	1.03	1.06	0.01	0.85

Box I-beam	Long Box I-beam without infill (No foam)					
	ID:329	ID:330	ID:331	AVE	SD	C _v (%)
k _{NF,4500} (kN/mm)	0.520	0.644	0.762	0.64	0.12	18.85
k _{NF,3000} (kN/mm)	1.518	1.801	1.997	1.77	0.24	13.59
k _{NF,2100} (kN/mm)	3.498	4.046	4.333	3.96	0.42	10.72
k _{NF,1450} (kN/mm)	6.606	8.653	9.465	8.24	1.47	17.88
Long Box I-beam with infill (Foam)						
Box I-beam	ID:329	ID:330	ID:331	AVE	SD	C _v (%)
k _{F,4500} (kN/mm)	0.542	0.645	0.776	0.65	0.12	17.92
k _{F,3000} (kN/mm)	1.578	1.808	2.192	1.86	0.31	16.68
k _{F,2100} (kN/mm)	3.678	4.137	4.608	4.14	0.47	11.23
k _{F,1450} (kN/mm)	7.595	8.228	9.346	8.39	0.89	10.57
Effect of the foam on load/deflection (k)						
k _{F,4500} /k _{NF,4500}	1.04	1.00	1.02	1.02	0.02	2.01
k _{F,3000} /k _{NF,3000}	1.04	1.00	1.10	1.05	0.05	4.51
k _{F,2100} /k _{NF,2100}	1.05	1.02	1.06	1.05	0.02	2.01
k _{F,1450} /k _{NF,1450}	1.15	0.95	0.99	1.02	0.11	10.40

Table B.1 Effect of the infill on load deflection of the long span beams (Continued)

Box Double I-beam	Long Box Double I-beam without infill (No foam)					
	ID:341	ID:342	ID:343	AVE	SD	C_v (%)
k_{NF,4500} (kN/mm)	0.595	0.674	0.733	0.67	0.07	10.38
k_{NF,3000} (kN/mm)	1.721	1.684	2.110	1.84	0.24	12.84
k_{NF,2100} (kN/mm)	3.987	4.231	4.816	4.34	0.43	9.81
k_{NF,1450} (kN/mm)	7.671	9.382	9.817	8.96	1.13	12.67
Box Double I-beam	Long Box Double I-beam with infill (Foam)					
	ID:341	ID:342	ID:343	AVE	SD	C_v (%)
k_{F,4500} (kN/mm)	0.609	0.684	0.761	0.68	0.08	11.10
k_{F,3000} (kN/mm)	1.774	2.030	2.256	2.02	0.24	11.94
k_{F,2100} (kN/mm)	4.275	4.556	5.085	4.64	0.41	8.87
k_{F,1450} (kN/mm)	9.157	9.897	10.378	9.81	0.62	6.27
Effect of the foam on load/deflection (k)						
k_{F,4500}/k_{NF,4500}	1.02	1.01	1.04	1.03	0.01	1.15
k_{F,3000}/k_{NF,3000}	1.03	1.21	1.07	1.10	0.09	8.35
k_{F,2100}/k_{NF,2100}	1.07	1.08	1.06	1.07	0.01	1.03
k_{F,1450}/k_{NF,1450}	1.19	1.05	1.06	1.10	0.00	0.15